The Handbook of Environmental Chemistry 50
Series Editors: Damià Barceló · Andrey G. Kostianoy

Liudmila L. Demina
Sergey V. Galkin *Editors*

Trace Metal Biogeochemistry and Ecology of Deep-Sea Hydrothermal Vent Systems

Springer

The Handbook of Environmental Chemistry

Founded by Otto Hutzinger

Volume 50

More information about this series at http://www.springer.com/series/698

Trace Metal Biogeochemistry and Ecology of Deep-Sea Hydrothermal Vent Systems

Volume Editors: Liudmila L. Demina · Sergey V. Galkin

With contributions by

L.L. Demina · S.V. Galkin · N.G. Holm · M. Ivarsson · A. Koschinsky · A. Neubeck · A.M. Sagalevich · S.G. Sander

Springer

Editors
Liudmila L. Demina
P.P. Shirshov Institute of Oceanology
Russian Academy of Sciences
Moscow
Russia

Sergey V. Galkin
P.P. Shirshov Institute of Oceanology
Russian Academy of Sciences
Moscow
Russia

ISSN 1867-979X ISSN 1616-864X (electronic)
The Handbook of Environmental Chemistry
ISBN 978-3-319-41338-9 ISBN 978-3-319-41340-2 (eBook)
DOI 10.1007/978-3-319-41340-2

Library of Congress Control Number: 2016946030

Printed on acid-free paper

This Springer imprint is published by Springer Nature
The registered company is Springer International Publishing AG Switzerland

The Handbook of Environmental Chemistry Also Available Electronically

The Handbook of Environmental Chemistry is included in Springer's eBook package *Earth and Environmental Science*. If a library does not opt for the whole package, the book series may be bought on a subscription basis.

For all customers who have a standing order to the print version of *The Handbook of Environmental Chemistry,* we offer free access to the electronic volumes of the Series published in the current year via SpringerLink. If you do not have access, you can still view the table of contents of each volume and the abstract of each article on SpringerLink (www.springerlink.com/content/110354/).

You will find information about the

– Editorial Board
– Aims and Scope
– Instructions for Authors
– Sample Contribution

at springer.com (www.springer.com/series/698).

All figures submitted in color are published in full color in the electronic version on SpringerLink.

Aims and Scope

Since 1980, *The Handbook of Environmental Chemistry* has provided sound and solid knowledge about environmental topics from a chemical perspective. Presenting a wide spectrum of viewpoints and approaches, the series now covers topics such as local and global changes of natural environment and climate; anthropogenic impact on the environment; water, air and soil pollution; remediation and waste characterization; environmental contaminants; biogeochemistry; geoecology; chemical reactions and processes; chemical and biological transformations as well as physical transport of chemicals in the environment; or environmental modeling. A particular focus of the series lies on methodological advances in environmental analytical chemistry.

Series Preface

With remarkable vision, Prof. Otto Hutzinger initiated *The Handbook of Environmental Chemistry* in 1980 and became the founding Editor-in-Chief. At that time, environmental chemistry was an emerging field, aiming at a complete description of the Earth's environment, encompassing the physical, chemical, biological, and geological transformations of chemical substances occurring on a local as well as a global scale. Environmental chemistry was intended to provide an account of the impact of man's activities on the natural environment by describing observed changes.

While a considerable amount of knowledge has been accumulated over the last three decades, as reflected in the more than 70 volumes of *The Handbook of Environmental Chemistry,* there are still many scientific and policy challenges ahead due to the complexity and interdisciplinary nature of the field. The series will therefore continue to provide compilations of current knowledge. Contributions are written by leading experts with practical experience in their fields. *The Handbook of Environmental Chemistry* grows with the increases in our scientific understanding, and provides a valuable source not only for scientists but also for environmental managers and decision-makers. Today, the series covers a broad range of environmental topics from a chemical perspective, including methodological advances in environmental analytical chemistry.

In recent years, there has been a growing tendency to include subject matter of societal relevance in the broad view of environmental chemistry. Topics include life cycle analysis, environmental management, sustainable development, and socio-economic, legal and even political problems, among others. While these topics are of great importance for the development and acceptance of *The Handbook of Environmental Chemistry,* the publisher and Editors-in-Chief have decided to keep the handbook essentially a source of information on "hard sciences" with a particular emphasis on chemistry, but also covering biology, geology, hydrology and engineering as applied to environmental sciences.

The volumes of the series are written at an advanced level, addressing the needs of both researchers and graduate students, as well as of people outside the field of

"pure" chemistry, including those in industry, business, government, research establishments, and public interest groups. It would be very satisfying to see these volumes used as a basis for graduate courses in environmental chemistry. With its high standards of scientific quality and clarity, *The Handbook of Environmental Chemistry* provides a solid basis from which scientists can share their knowledge on the different aspects of environmental problems, presenting a wide spectrum of viewpoints and approaches.

The Handbook of Environmental Chemistry is available both in print and online via www.springerlink.com/content/110354/. Articles are published online as soon as they have been approved for publication. Authors, Volume Editors and Editors-in-Chief are rewarded by the broad acceptance of *The Handbook of Environmental Chemistry* by the scientific community, from whom suggestions for new topics to the Editors-in-Chief are always very welcome.

Damià Barceló
Andrey G. Kostianoy
Editors-in-Chief

Contents

Introduction

Sergey V. Galkin and Liudmila L. Demina

Abstract Over a period of time after discovery in 1977 of the extraordinary abundant faunal assemblages functioning at the deep-sea hydrothermal vent systems, a new knowledge has been gained of highly dynamic and extreme conditions in their habitats. Hydrothermal vent communities have to survive in habitats which are exposed to high heavy metal load, emitting from vents and dispersing into ambient water and changing physicochemical parameters. All these processes are reflected in the distribution pattern of bottom communities along the gradients of reduced substances that serve a basement for chemosynthetic primary productivity. In the book we aimed to summarize available data, which are of fundamental interest for understanding the trace metal biogeochemistry and ecology of biological communities of deep-sea vent systems. Along with, some interesting aspects of the subseafloor biosphere are considered.

This book is addressed to the specialists working in various fields of environmental problems, especially in marine biogeochemistry and ecology.

Keywords Deep-sea hydrothermal vent systems, Subseafloor biosphere, Trace metals

Content

S.V. Galkin (✉) and L.L. Demina
P.P. Shirshov Institute of Oceanology, Russian Academy of Sciences (IO RAS), Nakhimovsky pr., 36, 117997 Moscow, Russia
e-mail: galkin@ocean.ru; l_demina@mail.ru

L.L. Demina, S.V. Galkin (eds.), *Trace Metal Biogeochemistry and Ecology of Deep-Sea Hydrothermal Vent Systems*, Hdb Env Chem (2016) 50: 1–8,
DOI 10.1007/698_2016_7,
Published online: 5 May 2016

In the beginning of the twentieth century Alfred Wegener suggested the idea of the drift of continents. A symmetry of magnetic anomalies on either side of the mid-ocean ridges and the correspondence of the anomaly patterns with the pattern of magnetic reversals on Earth confirmed the process of seafloor spreading and led to general acceptance of global plate tectonic theory [1]. It was shown that the ocean floor is young, in geological terms; its age is about 160 million years. During this period, basalt foundation of the bottom was formed along the mid-ocean ridges that girdle the globe. In the middle 1960s and early 1970s geologists hypothesized the presence of hot springs on the seafloor with temperatures as great as 300°C [2–4]. The first unequivocal evidence of warm water, buoyant plumes was collected by May 1976 using the Scripps Institution of Oceanography Deep-Tow vehicle. On May 29, 1976 in the area of Galapagos Spreading Center (0°48′N, 86°09′W) large white clam shells lying within cracks of basalt lava at the depth about 2500 m were photographed by the Deep-Tow camera system "Angus" [5]. In 1977 during deep-sea submersible "Alvin" dives at the Galapagos Spreading Center, dense settlements of large clams, mussels, giant tube worms, crabs, sea anemones, and other animals were detected. The discovery of extraordinary faunal assemblages associated with hot vents [6] is one of the most significant events in the Earth Science of the last 40 years.

Hydrothermal vent communities function under extreme conditions of high hydrostatic pressure and high-temperature gradients, low oxygen, high acidity, anomalous concentrations of the reduced compounds (H_2S, H_2, CH_4, Fe^{2+}, etc.), and heavy metals. Such features of hydrothermal environment make this habitat unfavorable for most deep-sea animals. However, despite this, the biomass of benthic communities associated with deep-sea vents amounted to $n \cdot 10$ kg/m^2, that is 3–4 orders of magnitude higher than that of surrounding background benthic community. Due to this, hydrothermal fauna can evidently participate in the trace metal biogeochemical cycling in the ocean.

The main distinctive feature of hydrothermal vent ecosystems is their orientation on chemosynthetic primary production contrary to most of other ecosystems of our planet driven by photosynthesis [7–9]. Dominant animals of vent communities (vestimentiferans and bivalves) are symbiotrophs that feed due to intracellular bacterial symbionts. Free living bacteria provide nutrition for different taxa of grazers, deposit- and filter feeders. Stable isotope analyses evidenced that many animals consume as well photosynthetic organic matter transported from photic zone of the ocean [7, 10]. The trophic structure of hydrothermal communities is also unusual that causes taxonomical originality of the deep-sea vent fauna. To date, in areas of hydrothermal activity more than 700 species are known. Most species and many taxa of higher rank are obligate (=endemic) for hydrothermal biotopes, i.e., they are not found in any other habitats [11].

Geological age of vent ecosystems amounts 430 million years (Silurian), while bacterial communities exist at least 3 billion years. Although the taxonomic composition of hydrothermal communities have changed over time, their ecological structure remains unchanged at least 200 million years [12]. In the course of evolution biocommunities have developed an adaptation strategy, including both

biochemical and physiological mechanisms that contribute to natural detoxification of heavy metals.

Hydrothermal manifestations are of particular interest to geologists, because in the sites of high-temperature vents massive polymetallic sulfide ores are formed. The estimated mass of hydrothermal sulfides reaches 100 million tons [13, 14]. Maximal ore reserves are discovered at the TAG hydrothermal field where they account for up to 3–5 million tons. According to [13] only 5% of the fluid trace metal load is concentrated in the form of ore deposits, while the major portion of metals is being dissipated into the ambient environment and/or deposited out beyond the vent mounds.

In the 1990s, there was a resurgent interest in extraction of cooper, zinc, silver, and gold from seafloor massive sulfide deposits. The United Nations Convention on the Low of the Sea and the 1994 Agreement on the regime of seafloor mining established the International Seabed Authority (ISA) with jurisdiction over all seafloor resources in the area beyond national jurisdiction. At the part of its business, the ISA began to convene annual workshops on scientific and technical aspects of deep seafloor mining of minerals and the environmental impacts associated with mining [15]. Presently hydrothermal vents are targeted for exploitation of massive sulfide deposits planned for 2017 in Papua New Guinea. The strong association of vent ecosystems with the target high-grade ores has focused attention on the risks and the lack of management frameworks to assess potential impacts. Conservation of hydrothermal vent ecosystems is a growing concern as exploitation of massive sulfide deposits [15]. To date, there are about 300 areas of high-temperature hydrothermal polymetallic sulfide deposits, 62% of which were located on mid-ocean ridges, 25% in back-arc basins, and 13% on submarine volcanic arcs [16].

Despite the worldwide distribution in the oceans, hydrothermal ecosystems are extremely difficult to study. Such their features as small linear sizes of the individual fields, the discontinuous distribution and, as a rule, very complicated topography with a predominance of hard substrate make the most of the traditional methods of environmental research not applicable. The discovery of hydrothermal vent ecosystems itself became possible only with the reduction to practice of oceanographic studies of deep-sea manned submersibles. At the initial stages of the study of hydrothermal systems the investigations were conducted essentially from the board of manned submersibles. The greatest contribution to the study of hydrothermal systems has made American submersibles “Alvin” (operating depth up to 4000 m) and “Sea Cliff” (6000 m), Canadian “Pisces” (2000 m), French “Nautile” (6000 m) and “Cyana” (3000 m), Russian “Mir” (6000 m), and the Japanese “Shinkai” (6500 m). The contribution of manned submersibles to the study of hydrothermal ecosystems environments cannot be overstated. Most initial discoveries in this area were made using this method. In particular, all the materials for biogeochemical analyses used in this book as well as images of hydrothermal landscapes were obtained at different hydrothermal areas using DSRV “Mir-1” and “Mir-2”.

However, despite the effectiveness of the deep-sea manned submersibles, their use has certain limitations. This is primarily due to the fact that this method is extremely technically difficult, costly, and time consuming. The dependence of autonomous manned submersibles on batteries charge limits the useful operating time at bottom for a few hours. Therefore, in recent decades other methods of research of hydrothermal systems were actively developed. This is primarily due to widespread use of unmanned underwater vehicles (remotely operated underwater vehicle, ROV) receiving power supply and controlled from mothership. It makes the time they stay active on the bottom is almost unlimited. Furthermore these devices are relatively inexpensive and many countries have already established their mass production. For today, the investigations of ROVs "Victor," "Kaikō," "Isis" in the Atlantic, Indian, and Southern Oceans are widely known [17–19]. The use of remotely operated vehicles to study hydrothermal ecosystems undoubtedly has great potential.

In recent years, for studies of hydrothermal ecosystems also conceptually new methods were applied. In December 2009 after a decade of work the Canadian project, called NEPTUNE (North-East Pacific Time-Series Undersea Networked Experiments) was launched. This project has laid 800 km of cable to transmit power and data, and established five "nodes" that act like giant, 13-ton plug-in points for scientific instrumentation, lying up to 2.6 km beneath the ocean surface. The network spans the Juan de Fuca Plate, which hosts earthquakes and tsunamis, along with hydrothermal vents and frozen methane deposits [20]. It has allowed scientists to run deep-water experiments from labs and universities around the world. Taking advantage of this platform, scientists collaborating with NEPTUNE are expected to conduct thousands of unique experiments.

Recent studies have shown that hydrothermal fluids are a significant source for bioactive trace metals in their dissolved form in the global deep-ocean. It has become evident thanks to numerous GEOTRACES ocean basin transects and other studies [21–26]. For instance, data from the GEOTRACES Eastern Pacific Zonal Transect (EPZT, GP16) demonstrated unexpected magnitude of the hydrothermal iron inputs in the deep Pacific. The lateral transport of hydrothermal iron, manganese, and aluminum is extending up to 4000 km west of the southern East Pacific Ridge, therefore crossing a significant part of the deep Pacific Ocean. The dissolved iron behaves conservatively, the resulting flux is more than four times what was assumed before. A coupled ocean circulation/biogeochemical modelling demonstrates that this hydrothermal iron input is sustaining a large fraction of the Southern Ocean export production [26].

Deep-sea hydrothermal fields are of particular interest from the point of view of biogeochemistry since there exist the processes of both scattering of chemical elements, that are brought by the hydrothermal fluids, and concentration, carried out as in mineral formation, and as a result of the activities of the biota. The total length of the rift zones in the ocean is about 70,000 km, i.e., we can talk about the global nature of biogeochemical processes here. Taking into account the global nature of the hydrothermal manifestations and high biomass of hydrothermal fauna, we can assume that it plays a significant role in the processes of biodifferentiation of

matter originating from hydrothermal vents. The term "biodifferentiation" refers to the modifications in migration of chemical elements as a result of vital activity of living organisms [27, 28].

Hydrothermal vent systems were proposed as plausible environments for the origin of life based on the research of abiotic synthesis of various amino acids and other organic substances at 150°C under reducing hydrothermal conditions [29, 30].

Today the subseafloor biosphere is considered to be widespread at both ocean ridges and off-axis, the ocean crust has a potential to harbor life [31–33].

After almost 40 years of investigations, an evaluation of the ecological and geochemical role of hydrothermal benthic communities and our knowledge of the deep subseafloor biosphere is still incomplete due to insufficiency of data resulted from complexity of hydrothermal systems and difficulties related mainly to sampling problems.

To reveal the factors that may influence the trace metal bioaccumulation by vent organisms, there is a need to estimate both the environmental parameters (depth, temperature, chemical composition of fluids, and mineralogy of the substrate) and biological characteristics (taxonomic position, ontogenetic stage, trophic level, type of food, and metabolic activity). At the same time, data on the distribution, abundance, and biomass of hydrothermal vent fauna are of fundamental interest for understanding the ecology of communities and biological productivity of deep-sea vent systems [34–37].

The book contains ten chapters including Introduction and Conclusions written by the Volume Editors.

In the first chapter (S. Sander and A. Koschinsky) the importance of deep-sea hydrothermal vents for the biogeochemical cycling of iron and other trace metals in the global ocean is highlighted, as well as a fact that the role of hydrothermal processes as a source for certain trace metals was evidenced to a great extent through GEOTRACES ocean basin transects. The second chapter (S. Galkin, L. Demina) is devoted to geologic-geochemical and ecological characteristics of selected hydrothermal vent areas located at the Mid-Atlantic Ridge, East Pacific Ridge, and in the Guaymas Basin (Gulf of California). The third chapter (L. Demina) is focused on the trace metal distribution in water of biotopes of these vent fields. In the fourth chapter (S. Galkin) the structure of hydrothermal vent communities at the same vent areas is considered. The fifth chapter (A. Koschinsky) analyzes the sources and forms of trace metals taken up by hydrothermal vent mussels, as well as their adaptation and mediation strategies. The sixth chapter (L. Demina, S. Galkin) summarizes the available data on both the environmental parameters (temperature, chemical composition of fluids, and mineralogical features) and the biological characteristics (taxonomic position, ontogenetic stage, trophic level, and type of food), that may influence the trace metal bioaccumulation by vent organisms, inhabiting the same vent fields.

The seventh chapter (M. Ivarsson, N. Holm, and A. Neubeck) covers gained knowledge so far and discusses future prospects in the search for life in the deep ocean floors.

The eighth chapter (A. Sagalevich) describes methodology of research of hydrothermal vents using manned submersibles *Mir*.

The book ends with our conclusions, where the above-mentioned aspects are summarized and further research frontier is outlined in the scope of biogeochemical, geological, and oceanological sciences.

The book is addressed to specialists working in different fields of marine environmental sciences, including ecologists, geochemists, biologists, as well as astrobiologists. The understanding of biological-geological interactions in metal-rich hydrothermal environments can also be of interest for a larger community, including researchers interested in understanding the possible evolution of life on early Earth, which may have taken place in an environment very similar to today's submarine hydrothermal systems.

Graduate and undergraduate students in marine and environmental sciences will find this book as a valuable resource of knowledge, information, and references on the deep-sea hydrothermal vent systems.

Acknowledgements We are very thankful to Springer-Verlag (The Handbook of Environmental Chemistry book series) and one of the Series Editor Prof. Andrey Kostianoy for the idea to publish this book. We wish to thank our colleagues who contributed the chapters, as well as those who helped us in the expeditions, treatment, and analysis of the unique specimens of hydrothermal organisms. Data obtained earlier were generalized with support of Russian Scientific Foundation (Project No 14-50-00095 "World Ocean in XXI century: climate, ecosystems, mineral resources and disasters").

References

1. Vine FJ, Matthews DH (1963) Magnetic anomalies over oceanic ridges. Nature 199:947–949
2. Elder JW (1965) Physical processes in geothermal areas. AGU Monogr 8:211–239
3. Talwani M, Windish CC, Langseth ML (1971) Reykjanes ridge crest: a detailed geographical study. J Geophys Res 76:473–517
4. Lister CRB (1972) On the thermal balance of a mid-oceanic ridge. Geophys J Roy Astron Soc 426(26):515–535
5. Lonsdale P (1977) Clustering of suspension-feeding macrobenthos near abyssal hydrothermal vents at oceanic spreading centres. Deep-Sea Res 24:857–863
6. Corliss JB, Ballard RD (1977) Oases of life in the cold abyss. Nat Geogr 152:440–453
7. Jannasch HW, Wirsen GO (1979) Chemosynthetic primary production at East Pacific sea floor spreading centers. Bioscience 79:592–598
8. Karl DM, Wirsen CO, Jannasch HW et al (1980) Deep-sea primary production at the Galapagos hydrothermal vents. Science 207:1345–1347
9. Fisher CR (1990) Chemoautotrophic and methanotrophic symbioses in marine invertebrates. Rev Aquat Sci 2:399–436
10. Van Dover CL, Fry B (1994) Microorganisms as food resources at deep-sea hydrothermal vents. Limnol Oceanogr 39:51–57
11. Galkin SV (2016) Structure of hydrothermal vent communities. Hdb Env Chem. doi:10.1007/698_2015_5018

12. Little C (2005) Deep-time perspectives on chemosynthetic communities (vents, seeps and wale-falls). In: Abstract of the 3rd International Symposium on hydrothermal vent and seep biology, Scripps Institute of Oceanography, La Jolla, USA: 2
13. Rona PA (1984) Hydrothermal mineralization at seafloor spreading centers. Earth Sci Rev 20:1–104
14. Lisitzyn AP (1993) Hydrothermal vent systems of the world ocean – supply of endogenous matter. In: Lisitzyn AP (ed) Hydrothermal systems and sedimentary formations of the mid-ocean ridges of the Atlantic Ocean. Nauka, Moscow, pp 147–246
15. Van Dover CL (2010) Mining seafloor massive sulphides and biodiversity: what is at risk? ICES J Mar Sci. doi:10.1093/icesjms/fsq086
16. Petersen S (2007) Hydrothermal systems of the modern ocean floor as a perspective mineral resource of the XXI Century. In: Silantiev SA, Bortnikov NS (eds) Materials of the Workshop of the Intern Project InterRidge, IGEM RAS, Moscow, pp 44–46, 1–3 June 2011
17. Fabri M-C, Bargain A, Briand P, Gebruk A, Fouquet Y, Morineaux M, Desbruyères D (2010) The hydrothermal vent community of a new deep-sea field, Ashadze-1, 12858′N on the Mid-Atlantic Ridge. J Mar Biol Assoc U K, doi:10.1017/S0025315410000731
18. Hashimoto J, Ohta S, Gamo T, Chiba H, Yamaguchi T, Tsuchida S, Okudaira T, Watabe H, Yamanaka H, Kitazwara M (2001) First hydrothermal vent communities from the Indian Ocean discovered. Zoolog Sci 18(5):717–721
19. Marsh L, Copley JT, Huvenne VAI, Linse K, Reid WDK et al (2012) Microdistribution of faunal assemblages at deep-sea hydrothermal vents in the Southern Ocean. PLoS One 7(10), e48348. doi:10.1371/journal.pone.0048348
20. Jones N (2010) Undersea project delivers data flood. Nature 464:1115. doi:10.1038/4641115a
21. Bennett SA, Achterberg EP, Connelly DP, Statharn PJ, Fones GR, German CR (2008) The distribution and stabilisation of dissolved Fe in deep-sea hydrothermal plumes. Earth Planet Sci Lett 270(3–4):157–167. doi:10.1016/j.epsl.2008.01.048
22. German CR, Thurnherr AM, Knoery J, Charlou J-L, Jean-Baptiste P, Edmonds HN (2010) Heat, volume and chemical fluxes from submarine venting: a synthesis of results from the Rainbow hydrothermal field, 36°N MAR. Deep Sea Res I 57:518–527
23. Yücel M, Gartman A, Chan CS, Luther GW (2011) Hydrothermal vents as a kinetically stable pyrite (FeS_2) nanoparticle source to the ocean. Nat Geosci 4:367–371
24. Nishioka J, Obata H, Tsumune D (2013) Evidence of an extensive spread of hydrothermal dissolved iron in the Indian Ocean. Earth Planet Sci Lett 361:26–33. doi:10.1016/j.epsl.2012.11.040
25. Schlitzer R (2004) Ocean data view. http://odv.awi-bremerhaven.de
26. Fitzsimmons JN, Boyle EA, Jenkins WJ (2014) Distal transport of dissolved hydrothermal iron in the deep South Pacific Ocean. Proc Natl Acad Sci 111(47):16654–16661. doi:10.1073/pnas.1418778111
27. Lisitzyn AP, Vinogradov ME (1983) Global patterns of living matter distribution in the ocean. In: Monin AS, Lisitzyn AP (eds) Biogeochemistry of the ocean. Nauka, Moscow, pp 279–368 (in Russian)
28. Lisitzyn AP (2014) Current views on the sedimentation in oceans and seas. The ocean as a natural recorder of the interaction of geospheres of the Earth. In: The world ocean, vol 2. Scientific World, pp 331–553 (in Russian)
29. Holm NG (1992) Why are hydrothermal systems proposed as plausible environments for the origin of life? In: Holm NG (ed) Marine hydrothermal systems and origin of life, vol 22, Special issue of origins of life and evolution of the biosphere. Kluwer, Dordrecht, pp 5–14
30. Holm NG, Neubeck A (2009) Reduction of nitrogen compounds in oceanic basement and its implications for HCN formation and organic synthesis. Geochem Trans 10:1467–1486
31. Edwards KJ, Bach W, McCollom T (2005) Geomicrobiology in oceanography: microbe-mineral interactions at and below the seafloor. TRENDS Microbiol 13:449–456
32. Schrenk MO, Huber JA, Edwards KJ (2009) Microbial provinces in the subseafloor. Ann Rev Mar Sci 2:279–304

33. Orcutt BN, Sylvan JB, Knab NJ, Edwards KJ (2011) Microbial ecology of the dark ocean above, at, and below the sea-floor. Microbiol Mol Biol Rev 75:361–422
34. Desbruyères D, Almeida A, Biscoito M et al (2000) A review of the distribution of hydrothermal vent communities along the northern Mid-Atlantic Ridge: dispersal vs. environmental controls. Hydrobiologia 440:201–216
35. Gebruk AV, Chevaldonné P, Shank T, Lutz RA, Vrienhoek RC (2000) Deep-sea hydrothermal vent communities of the Logatchev area (14°45′N, Mid-Atlantic Ridge): diverse biotope and high biomass. J Mar Biol Assoc U K 80:383–394
36. Galkin SV (2002) Hydrothermal vent communities of the World Ocean. Structure, typology, biogeography. GEOS, Moscow, p 99 (in Russian)
37. Van Dover CL (2000) The ecology of deep-sea hydrothermal vents. Princeton University Press, Princeton, p 415

The Export of Iron and Other Trace Metals from Hydrothermal Vents and the Impact on Their Marine Biogeochemical Cycle

S.G. Sander and A. Koschinsky

Abstract Recently the role of hydrothermalism as a significant source for several bioactive trace metals in their dissolved form has become evident through numerous GEOTRACES ocean basin transects and other studies. Especially iron (Fe) has found much attention due to its important role as a limiting micronutrient in about 40% of the global surface ocean. Organic complexation has been confirmed as one of the processes stabilizing the dissolved phase of Fe and other trace metals from forming insoluble (oxy)hydroxides or being scavenged on these surface active particulate phases. Small colloidal metal phases can also enhance transport of dissolved metals from vents into the ocean. However, hydrothermalism is not only a source for dissolved trace metals into the ocean basins but for some it is also a sink. Particulates forming in hydrothermal plumes, especially Fe and Mn ox (yhydrox)ides, are very efficient scavengers of other trace metals and were found to bind PO_4^{3-}, V, As, REE (rare earth elements), Th, plus other elements from seawater. The linkage between the hydrothermal dissolved, soluble and colloidal phases, as well as the particulate phase in the non-buoyant plume is not a simple thermodynamic equilibrium and our knowledge about biological processes involved is still in its infancy. The oceanic iron and carbon cycles are inseparable from each other and observations as well as modeling approaches have shown that in some areas hydrothermal iron input is needed to balance the iron required to explain global marine primary productivity. On the other hand it has also been

S.G. Sander (✉)
Department of Chemistry, and NIWA/University of Otago Research Centre for Oceanography, University of Otago, PO BOX 56, Dunedin 9094, New Zealand
e-mail: sylvia.sander@otago.ac.nz

A. Koschinsky
Department of Physics and Earth Sciences, Jacobs University Bremen, Campus Ring 1, Bremen 28759, Germany
e-mail: a.koschinsky@jacobs-university.de

L.L. Demina, S.V. Galkin (eds.), *Trace Metal Biogeochemistry and Ecology of Deep-Sea Hydrothermal Vent Systems*, Hdb Env Chem (2016) 50: 9–24,
DOI 10.1007/698_2016_4, © Springer International Publishing Switzerland 2016,
Published online: 23 April 2016

demonstrated that the precipitation of iron (oxy)hydroxides will coprecipitate organic carbon causing a removal flux of dissolved organic carbon not only from the hydrothermal vent but also from the deep-ocean water. This particulate organic carbon flux is a significant source of organic carbon in the basin sediments. After a long period of underestimating the importance of deep-sea hydrothermal vents for the biogeochemical cycling of iron and other trace metals in the global ocean today much effort is put into this emerging field of research. Especially the role of shallow island arcs for direct hydrothermal trace metal input into the productive zone promises to become an exciting field of studies.

Keywords Biogeochemical cycle, Flux, Hydrothermal, Iron, Trace metals, Organic carbon

Contents

1 Introduction

Although it has been known for quite some time that hydrothermal vents are ubiquitous along mid-ocean ridges, in back-arc basins, oceanic island arcs and at intraplate volcanoes. They emit fluids into the water column with concentrations of up to millimolar for Fe and Mn, and in the micromolar range for other trace metals such as Cu, Zn, and others (e.g., [1]), the magnitude of these fluxes and their impact on the chemical composition of seawater and biogeochemical cycles in the ocean have not been well defined. Until recently it was assumed that because of the relatively fast precipitation of Fe^{2+} as sulfide minerals in the vicinity of the vents, and its fast oxidation to Fe^{3+} during mixing with ambient oxic seawater, nearly all of the discharged Fe would precipitate at some distance from the vents. The occurrence of hydrothermal sediments and encrustations enriched in Fe, Mn, and other trace metals of hydrothermal origin were seen as evidence for this. Although the oxidation of Mn is kinetically slower than that of Fe, Mn was also considered to be largely scavenged and precipitated as Mn oxides in the hydrothermal plume that form hydrothermal sediments and crusts at some distance from the source

[2]. However, it could already be speculated, based on early data on sediment geochemistry in the Pacific [3], that hydrothermal Fe apparently can escape further away from the vents than thermodynamics based on simple inorganic oxidation would allow, since Fe-rich sediments were observed hundreds of kilometers away from the mid-ocean ridge axes. Also, the fact that oxidation rates of Fe(II) in plumes of the East Pacific Rise (EPR) were slower than in other areas of the World oceans [4] could have been seen as an indicator for possible escape of dissolved Fe from hydrothermal vent sites into the ocean. However, the true order of magnitude of the impact of hydrothermal fluxes on metal biogeochemical cycles in the ocean has only recently become obvious, partly thanks to better trace metal clean sampling techniques, more precise analytical methods with lower detection limits, and the systematic sampling campaigns as part of the international GEOTRACES program. The results and implications of these new studies will be highlighted in this chapter.

2 Hydrothermal Flux of Trace Metals into the Ocean

2.1 Stabilization of Dissolved Trace Metals in Hydrothermal Vent Plumes

The view of hydrothermal vent environments as being largely isolated trace metal reactors was challenged in the past decade by several modeling and field studies demonstrating that hydrothermal fluxes of Fe, and probably also of other metals, into the ocean have been significantly underestimated in the past. This is because many metals behave less reactive during transport away from the vents than assumed. First evidence for an important role of organic complexation stabilizing metals in soluble form came from studies on chromium species in hydrothermal plumes and surrounding seawater [5]. It was shown that Cr(III) discharged from hydrothermal vents in the North Fiji Basin, which in the oxic water column was assumed to be quickly oxidized to Cr(IV), was apparently stabilized by organic ligands and was hence detectable at significant distance away from the anoxic discharge source. This finding was later confirmed in a study in the Lesser Antilles island arc where indications for hydrothermal venting were found based on maxima of dissolved Cr (III) in the water column [6]. Since then, several studies have demonstrated the presence of other stable soluble organic complexes of Fe and Cu in hydrothermal vent fluids and plumes that allow significant quantities of hydrothermal Fe and Cu to remain in solution even after continued mixing with seawater. In the surrounding of different vent sites on the Mid-Atlantic Ridge (MAR) Cu–organic complexes were found to dominate Cu speciation in hydrothermal fluids, with a wide concentration range of organic copper-binding ligands, up to 4,000 nM, with very high conditional stability constants [7]. It was shown that dissolved Cu concentrations increase again in the mixing zone of the vents when the water becomes more oxic, which was related to the dissolution of Cu sulfide particles [8]. If this re-dissolved Cu would

then be stabilized by organic complexation, this process could also enhance hydrothermal Cu fluxes into the ocean. Geochemical modeling based on field data indicated that up to 4.2% of hydrothermal Cu could be stabilized in soluble form by organic complexation, which would account for about 14% of the deep-ocean Cu budget to be of hydrothermal origin [9]. Later, a similar study at three volcanically active areas with shallow hydrothermal vents confirmed that although here Cu and ligand concentrations were significantly lower than a deep-sea hot vent sites, strong organic complexation of Cu in the vent environment was also the dominant form of Cu speciation and kept Cu in soluble form [10]. This can be seen as compelling evidence for the importance of organic ligands, forming complexes strong enough to play an important role in controlling the bioavailability and geochemical behavior of Cu and other metal ions around hydrothermal vents.

Measurements of dissolved Fe concentrations about 2.5 km away from a vent site at the MAR were much higher than would be predicted for plume dilution and dissolved Fe(II) oxidation rates, but confirmed that also Fe is stabilized in hydrothermal vent environments by organic Fe complexation and Fe colloids [11]. Fe-binding ligand concentrations accounted for stabilization of ~4% of the total Fe emitted from the vent sites. Extrapolation to the global ocean would mean that 12–22% of the deep-ocean dissolved Fe budget could be of hydrothermal origin. In hydrothermal plumes in the Southern Ocean, about 7.5% of all hydrothermal Fe was found to be stabilized by complexation with ligands, which would be sufficient for an important impact on deep-ocean Fe distribution, and 47% in the plume existed in colloidal phases (<0.2 μm) [12]. These field data agree in their order of magnitude with thermodynamic calculations of hydrothermal Fe fluxes from hydrothermal vents into the ocean, which resulted in 0.33% of hydrothermal Fe to remain dissolved, accounting for 9% of the deep-ocean Fe budget [9]. In an ocean model calculating the various sources and fluxes of Fe to the Southern Ocean an agreement of the model with observations of the distribution of dissolved Fe could only be replicated if a significant hydrothermal Fe flux was included [13]. In the model simulations, especially the deep water in the Southern Ocean was significantly affected by hydrothermal input, which is an important finding because this region is strongly Fe-limited and thus hydrothermal Fe could play an important role in the biogeochemical cycle of this area. The authors suggested that hydrothermal Fe fluxes, which are relatively constant over longer timescales, could buffer the oceanic Fe inventory against fluctuations of Fe on shorter timescales, e.g., from dust deposition. All these findings led to the "leaky vent hypothesis" [14], arguing that some hydrothermal Fe persists in dissolved form in hydrothermal plumes and represents a significant part of the dissolved Fe fluxes to the global oceans.

While nearly all recent studies on hydrothermal trace metal input have focused on Fe, because of its very important role in ocean biogeochemistry, it can be speculated that hydrothermal metal fluxes can also be important for other metals such as Mn and Zn, which are also important micronutrients. While oxidation of Mn^{2+} is assumed to be microbially mediated in hydrothermal plumes, and Mn oxide particles would subsequentially deposit on the seafloor, there is evidence from several sides that also hydrothermal Mn can escape the hydrothermal vent

environments for hundreds of kilometers and might significantly contribute to the global oceanic Mn cycle. Soluble forms of Mn(III) have been measured in the oxic–suboxic boundaries, e.g., in the Black Sea, Chesapeake Bay, and North Atlantic [15–17], that were stabilized by organic complexation; similarly, the presence of such soluble Mn(III) can be predicted to exist in hydrothermal plumes and might travel long distances away from the source. This could explain field observations in the South Pacific Ocean where a hydrothermal Mn plume was detected over large distances towards the west from the East Pacific Rise, correlating with the far-reaching extension of Fe and ^{3}He in the plume [18]. While Mn was removed from the dissolved phase until a certain point, it finally behaved conservatively with respect to ^{3}He, which requires a physico-chemical stabilization in solution.

While very few other studies investigated the stabilization and transport of hydrothermally derived Zn or other trace metals other than Fe and Cu so far, the generally similar behavior of Zn compared to Cu, both being divalent cations in seawater, representing important micronutrients and showing pronounced organic complexation in seawater [19], implies that organic complexation may also enhance hydrothermal fluxes of Zn into the ocean. Data for Zn and Zn isotopes in the North Atlantic showed a specific hydrothermal isotopic signature of Zn close to the Mid-Atlantic Ridge but it was assumed that Zn is not transported far from the vents [20]. However, theoretically, all trace metals forming strong soluble organic complexes in seawater, including Co and Ni [21, 22], could be affected by such stabilization processes enhancing hydrothermal metal fluxes. However, compared to Cu and Zn the total concentrations of Co, Ni, and other trace metals in most hydrothermal fluids are much lower than for Cu and Zn and hence the corresponding hydrothermal flux of these elements would also be smaller.

In addition to the established role of organic complexation, transport of hydrothermal metals into the ocean may also be enhanced by the formation of nanoparticles containing Fe and other metals in the vent environment. Closer to the vents sulfide nanoparticles will be important [23]; e.g., pyrite nanoparticles with a size of 4–200 nm have been shown to account for 5–25% of the dissolved Fe in vent fluids [24, 25]. With increasing distance from the vent sites, oxyhydroxide colloids, e.g., of Fe, will become dominant. Nanoparticles behave physically like dissolved components since they do not sink and settle; nevertheless chemically they can act like particles with active surfaces which may be occupied, e.g., by organic molecules that may stabilize these nanoparticles and could protect sulfide nanoparticles from oxidation. However, at some point these sulfides oxidize, and seawater organic ligands, being ubiquitous in ambient seawater, may bind to the released metals and keep them in solution. Hence, it was suggested that organic complexation and metal clusters, or nanoparticles, act in concert in enhancing hydrothermal metal fluxes into the oceanic water column [9].

A third option for solubilizing hydrothermal Fe was recently suggested by Li et al. (2014): a microbial Fe pump that converts the hydrothermal Fe from the vent fluids into dissolved Fe/organic C complexes and so could represent another important pathway of converting hydrothermal iron into bioavailable forms that can be dispersed throughout the oceans [26].

2.2 Far-Field Transport of Hydrothermally Derived Metals into the Ocean

How exactly the stabilized chemical components enter the water column via the hydrothermal plume and become distributed with the laterally dispersing plume is a question of the mixing and transport processes above the vents and in the water column. Simplified models of geochemistry and microbial activity constructed based on near vent physical conditions showed that parameters such as chimney height, and fluid exit velocity exert a strong kinetic influence on the chemical reactions occurring in the initial particle-forming zone of hydrothermal plumes [27]. Turbulent mixing continuously entrains seawater, further diluting the hydrothermal signature of the mixture [28]. While these physical processes within the buoyant rising plume are largely responsible for the initial chemical transformations of the plume components, e.g., from reduced to oxidized species, or from labile to stable dissolved forms, once neutral buoyancy is reached at the maximum plume height, regular ocean currents disperse the hydrothermal signatures over long distances away from its source site. While the signals of reactive components such as methane disappear at some distance from the vent sites, because the components disappear from the water column (e.g., by chemical reaction or biological uptake), conservative components such as ^{3}He, which is a primordial gas exhaled from the magma below the vent fields, only become progressively diluted by ambient seawater and can often be traced thousands of kilometers away from the vent, such as on the EPR [29]. The unexpected new discovery of the past years was that hydrothermal Fe, previously assumed to be extremely reactive, can also be detected in hydrothermal plumes far away from the vents. A GEOTRACES study in the Indian Ocean found hydrothermal Fe from the Central Indian Ridge to be distributed over 3,000 km distance at a depth of about 3,000 m [30]. Size fractionation revealed that a large part of Fe was in soluble form, supporting the idea of stabilization in the form of organic colloids and explaining the long distance travel of hydrothermal Fe. The data of the GEOTRACES intermediate data product 2014 demonstrate the existence of striking plumes of elevated Fe concentrations centering along the Mid-Atlantic Ridge [31]. Similar observations were made in the Pacific; dissolved Fe concentrations significantly above background concentrations were measured in the SE and SW Pacific in the depth range of the hydrothermal plume and could be related to hydrothermal sources thousands of kilometers away [32]. The authors of this investigation also observed increases in the proportion and absolute concentration of soluble Fe (in contrast to colloidal Fe) at greater distance from the active vent sites, which they interpreted as an active exchange between these Fe pools during the transit with the neutral plume. Comparison with the most conservative element in hydrothermal plumes, ^{3}He, showed a strong decrease of scavenging loss of Fe from the station closest to the EPR compared to the farthest stations, where Fe behaved more conservative. Based on their data they calculated a flux of 7×10^{8} mol Fe/year as the overall global hydrothermal Fe flux, which is in the range of previous estimates [13]. A nearly conservative behavior of

hydrothermal Fe in the westward spreading plume of the southern EPR was confirmed during another GEOTRACES cruise [18]. While in the near field only about 20% of the total dissolvable Fe was soluble, indicating rapid oxidation and loss of hydrothermal Fe close to the vent site, linear correlation of Fe with ^{3}He at stations further away from the ridge axis indicated conservative behavior and stabilization of the dissolved phase over a distance of 4,300 km. Based on these observations, a global hydrothermal input of dissolved Fe of about 4 Gmol/year was estimated, which is about fourfold higher than previous estimates.

Far-field transportation of hydrothermal manganese was already described long before the discovery of the far-spreading hydrothermal Fe- plumes [33, 34]. This, however, was more in agreement with expectations that oxidation and precipitation would limit the impact of hydrothermal metal fluxes into the ocean, since Mn oxidation kinetics were known to be much slower than for Fe, allowing for a more far-ranging hydrothermal Mn signal in the ocean. Resing et al. (2015) demonstrated that the dissolved Mn plume west of the southern EPR also stretched over thousands of kilometers, although somewhat less than the Fe plume [18]. The relationship between Mn and ^{3}He indicated that close to the source hydrothermal Mn showed loss due to precipitation or scavenging but beyond a certain point Mn behaved conservatively, similar to Fe. This again points to a physico-chemical stabilization of dissolved Mn, as discussed above, possibly as an Mn(III) organic complex [18].

Far-field transport of hydrothermal plumes was also confirmed in a study on dissolved and particulate Th isotopes in the Central Equatorial Pacific; lower concentrations of ^{230}Th in the water interval, which has high concentrations of ^{3}He and dissolved Fe and had been traced to hydrothermal plumes from the EPR, thousands of kilometers away [35]. Apparently, ^{230}Th had been scavenged by hydrothermally derived Fe–Mn particles closer to the sources.

2.3 Hydrothermal Plumes as Sinks for Trace Metals

While in the previous paragraphs evidence was presented that hydrothermal plumes are important sources of many trace metals into the ocean there is another process in plumes that also has important implications for the trace metal budget of seawater [36]. Particulates forming in hydrothermal plumes, especially Fe and Mn (oxy)hydroxides, are very efficient scavengers of other trace metals, due to their very high active surface area and surface charge, and were found to bind PO_4^{3-}, V, As, REE (rare earth elements), Th, and other elements. Calculations of hydrothermal input fluxes and plume removal fluxes [37] resulted in negative fluxes for many elements including anionic species of Cr, V, As, P, U, Mo, Be, and REE, since the removal in plumes was larger than the input from the vents. This makes hydrothermal plumes efficient sinks for reactive trace metals that strongly bind on Fe or Mn oxide particles in hydrothermal plumes. Based on high concentrations of oxyanions (P, V, and As) in hydrothermal FeOOH particles of a shallow island

arc system it was calculated that hydrothermal island arcs alone may be responsible for >50% of global hydrothermal P and >40% V scavenging [38]. A study of particulate matter in a plume above the MAR revealed that some metals were co-precipitated when the plume particles formed, while others were scavenged on the particles from entrained seawater [39–41]. For some elements scavenging appeared to be largely restricted to the buoyant plume (As, and Cr), for other elements including Y and Be scavenging from seawater appeared to be ongoing. For REE, a similar plume study indicated that in addition to initial coprecipitation and uptake on plume Fe oxide particles, scavenging of REE continues during dispersion of the particles through the neutral plume, with the consequence that the seawater experiences a net depletion of REE because of the scavenging on hydrothermally derived particulate matter [42].

However, while at the time of the earlier studies based on metal–Fe ratios in the particles and fluids it was concluded that for many dissolved trace metals hydrothermal activity is not a source to the ocean, this view might have to be revised based on the new picture of the hydrothermal Fe fluxes. This may especially be the case for those metals such as Cu, Zn, and Co, that are known to be potentially stabilized in dissolved form by organic complexation.

3 The Coupling of the Iron and Carbon Cycling in the Deep Ocean Near Hydrothermal Vents

3.1 Hydrothermal Organic Carbon Sources

Hydrothermal vents are oases in the deep dark ocean but the biosphere is extending into the subseafloor as well. Figure 1 shows an image from a diffuse hydrothermal vent field at the 5°S field at the Mid-Atlantic Ridge (MAR) where the sampling with the ROV Quest removed the top layer exposing fresh subseafloor microbial community being flushed from below, seen as white snow-like flakes. This is characteristic of the large amount of organic matter and of the intense biological activity and high biomass in hydrothermal vent environments.

While the dissolved organic carbon (DOC) in hot hydrothermal vent fluids is usually considerably lower than that in ambient seawater of around 10^{-5} mol C kg^{-1}, the DOC in diffuse hydrothermal vent fluids is highly variable and can range from 39×10^{-6} mol C kg^{-1} at the 9°50′N field on the East Pacific Rise to as much as $1{,}180 \times 10^{-6}$ mol C kg^{-1} at the Woody vent at the Menez Gwen hydrothermal field [43–46]. Dissolved free amino acids (DFAA) were determined in samples from the Logatchev field at 15°N and hydrothermal vent fields between 4° and 9°S on the Mid-Atlantic, which included black smoker fluids with endmember temperatures between 350 and 407°C, and diffuse fluids with temperatures of up to 10°C. DFAA concentrations between <50 and 24,878 nmol kg^{-1} were found, with the lowest concentrations found in hot focused vent fluids and the highest in diffuse

Fig. 1 High density of organic material observed at vent site "Golden Valley at Twin Peaks," 5°S MAR (4°48.13 S/12°22.35′W). Photo courtesy of MARUM

vent samples [47]. Dissolved free amino acids are readily available as micronutrients, and some are also known to be potential organic ligands, i.e., sulfur containing cysteine and cysteine [7].

The particulate organic carbon (POC) concentrations measured in vents as well as in the buoyant plume are around $1–4 \times 10^{-6}$ mol kg^{-1}. Compared to surrounding seawater with a POC of only 0.16×10^{-6} mol kg^{-1} this is still two orders of magnitude lower than the DOC in the same sample [14].

While organic compounds can be produced abiotically under deep-sea hydrothermal conditions [48] it is more likely that the majority of organic compounds would be biogenic as they resemble the composition of DOM found elsewhere known to be degradation products of terrestrial and marine organic material [49]. Recently it was also shown that DOM in diffuse hydrothermal vents is highly biologically available, as opposed to background deep-sea DOM, which is considered recalcitrant [46]. However, hydrothermal circulation at high temperatures is, at the same time, efficiently removing recalcitrant deep-ocean DOM, based on field data and experiments in which samples were heated under hydrothermal conditions [50].

3.2 Forms of Iron Coupled With Organic Carbon

Hydrothermal venting is responsible for much of the dissolved iron flux into the deep ocean, as discussed above [9, 11, 13, 18, 32]. By contrast the impact of

hydrothermal venting on the marine carbon cycle has been largely overlooked [1, 51].

Dissolved organic matter (DOM) is removed by coprecipitation with hydrous ferric oxides upon oxidation and it has been shown recently that this process is a selective one. While DOM containing nitrogen and phosphorus preferentially remained in solution, DOM only containing carbon, hydrogen, and oxygen and sulfur containing DOM were preferentially found in the precipitates [49]. Spectroscopic measurements in plume particles from the East Pacific Rise mid-ocean ridge have shown that Fe(II) is dispersed evenly in organic carbon rich hydrothermal plume particles. Discrete Fe(II) particles were not present, suggesting organic carbon is stabilizing Fe(II) released from the vents, retarding or even preventing its oxidation and precipitation in the near field [14, 45].

3.3 *Hydrothermal Fe Flux Coupling With Deep-Ocean Organic Carbon Scavenging*

An important question of the linkage between the iron and carbon cycling was addressed recently [44]. Site-specific field data from the East Pacific Rise 9°50′N hydrothermal field as well as global estimates for dissolved Fe were used to synthesize the first coherent model of all hydrothermal Fe-sources, sinks and fluxes (see Fig. 2 top panel). After receiving realistic values for all Fe-Flows as detailed in the model structure (see bottom panel of Fig. 2) the model was then used to link global hydrothermal iron and carbon fluxes. That is, setting the global dissolved Fe flux (Fe-Flow 4.2) required to support the worldwide Fe distribution [13] a priori to 4 ± 1 Gmol Fe yr^{-1} as estimated recently [18, 32]. Details of the model equations are described in German et al. 2015 [44]. As a result of this model it was demonstrated that the diffuse vent Fe-Flow 2 must play a major role in the supply of stabilized dissolved Fe transported into the deep ocean. Dissolved Fe concentrations calculated for diffuse venting using this approach ranged from 7 to 965 μmol kg^{-1}, which is within the range of reported values [9, 52, 53]. The model also showed that a ratio of Fe-Flow 4.2/Fe-Flow 4 between 0.0033 and 0.075 that had been predicted earlier is all reasonable to match the Fe budget [9, 12, 45]. Most importantly linking these water volume and Fe-Flows with carbon flows and DOC concentrations, as found in hydrothermal fluids [43, 45], an excess DOC flow resulting from hydrothermal input would only be between 0.04 and 2.81×10^9 kgC yr^{-1}. An enrichment of 0–10% over ambient deep-ocean seawater of DOC entering hydrothermal plumes also agrees with observed values [45, 46].

Close relationships had previously been observed between Fe flux in the oxyhydroxide fraction and particulate organic matter (POC) in hydrothermal plumes [14, 45]. Using the reverse model described above we estimated a global removal flux for POC in the sinking particulates of the non-buoyant plume (C-Flow 4.1) using the C:Fe stoichiometry found in particles collected in sediment traps

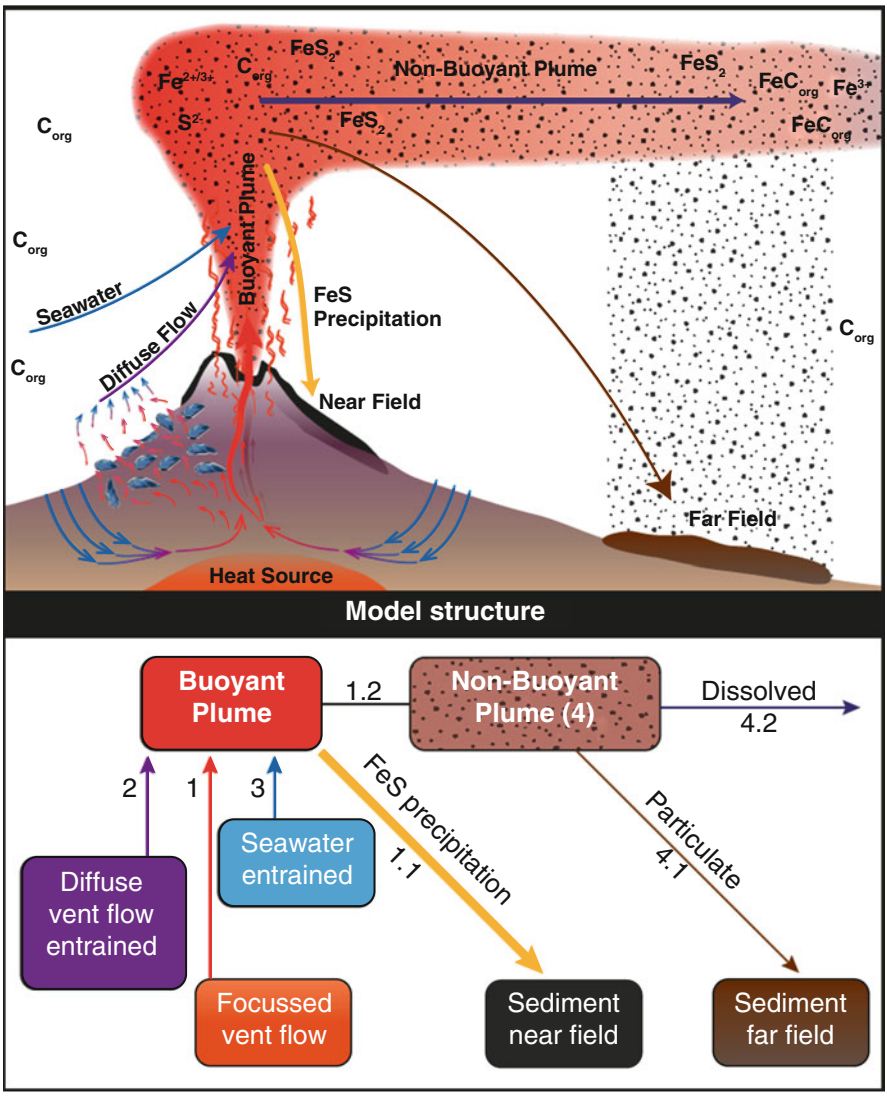

Fig. 2 *Top panel*: Schematic of iron sources and sinks in a submarine hydrothermal system and linkage with organic carbon. Focused and diffuse vent flow as well as ambient seawater are being entrained into the buoyant plume, which rises until neutral buoyancy is reached. Much of the hydrothermal iron is precipitated in form of polymetallic sulfides in the near field, while other precipitation processes occur during the plume rise which will form sinking particles depositing as sediments in the far field. Much of the iron present in the non-buoyant plume will be dispersed laterally in the form of nanoparticulate pyrite, organic complexes, and colloids with organic carbon. *Bottom panel*: Conceptual structure used in the inverse model to quantify the iron fluxes (*labeled arrows*) which was then used to calculate associated carbon fluxes as shown in A. Fe-Flow 1, 2, and 3 represent the three primary inputs into the buoyant plume. The focused vent Flow 1 is subdivided into immediate removal flux 1.1 of sulfide precipitation in the near field. Fe-flow 1.2 is the remainder of Fe-Flow 1 that rises together with Fe-Flow 2 (Diffuse vent) and 3 (entrained

close to the East Pacific Rise 9°50′N vent field [14]. Values are in the range of 7.8 to 206.8×10^9 kgCyr^{-1}, which are two orders of magnitudes higher than the DOC input flux. While these values are small compared to upper ocean POC fluxes it provides evidence that processes in and around hydrothermal plumes are an important and so far ignored source of POC to sediments in the deep ocean, not only around hydrothermal vents but also on a global scale.

4 Concluding Remarks and Outlook to Future Research

Recent research has shown that there is a link between the soluble, colloidal, and particulate distributions of Fe in the basin scale plume being distributed laterally from the East Pacific Rise. This distribution is different than that of Mn, indicating that processes for different trace metals even with similar chemistry are not the same [32]. The linkage with the organic carbon via complexation or the formation of iron containing particulate organic matter may play the key difference. The microbial uptake of iron from deep-sea hydrothermal vents has likewise been shown to play an important role in the processes underlying the iron transport [26]. The focus of these investigations has been mainly on the biogeochemically important element iron, with little interest being devoted to other metals known or assumed to be transported beyond the near field of the hydrothermal vents. Manganese, Zn, Cu, and Co would be logical candidates for future studies on trace metal export from hydrothermal vent systems into the open ocean.

While most knowledge of today on hydrothermal metal export from hydrothermal vents comes from studies on mid-ocean ridges, such as the EPR and MAR, a few recent investigations focused on shallow hydrothermal systems, e.g., on island arcs (Dominica, Caribbean) [10, 38, 49, 54]. While generally shallow vent systems have lower trace metal concentrations, due to the lower fluid temperatures, some of them have been shown to be quite rich in Fe and other metals and Fe–DOM interactions and the role of organic complexation and nanoparticles for metal export have been indicated. Since these shallow vents discharge their metals directly into the photic zone of high bioproductivity and both chemosynthetic and photosynthetic processes may play a role in mediating metal speciation and transport, their role in the biogeochemical cycle of metals and bioproductivity in the shallow ocean may have been underestimated so far. We foresee some exciting new results from upcoming investigations in island arc vent systems in different parts of the world's oceans and suggest that transects over a range of water depths from shallow to deep

Fig. 2 (continued) seawater) where it is incorporated into the non-buoyant plume flow 4. The laterally dispersing Fe-Flow 4 is subdivided again into the removal flux 4.1 of precipitating iron (oxy)hydroxy particles and the actual Fe-Flow 4.2 that stays in solution and is incorporated in the dissolved deep-sea iron cycle. Adopted from [44]

in such systems may be very useful in assessing the impact of water depth (as well as pressure and temperature of the fluids, which are closely related to water depth) on hydrothermal trace metal input into the bioproductive zone.

Isotope analysis has recently been proven to be a powerful tool to distinguish between different sources and processes relevant for the distribution and biogeochemical cycling of elements. Again Fe was in the focus of several studies and while the non-phase separated hydrothermal endmember fluid does not show much of a fractionation compared to mid-ocean ridge basalt (MORB), phase separation, redox reactions, pyrite formation, and microbial processes can cause significant isotopic shifts [55, 56]. Another study indicated that hydrothermal vents in the North Atlantic are a source of isotopically light iron, which travels thousands of kilometers from vent sites, potentially influencing surface productivity [57]. Dissolved stable iron isotope ratios (δ^{56}Fe) revealed that hydrothermal venting at the Mid-Atlantic Ridge contributed about 2–6% of dissolved Fe along a transect in the North Atlantic Ocean. More research is needed to constrain all processes responsible for the isotopic fingerprints of Fe and other metals in the ocean to elucidate the role of hydrothermal metal contributions in the ocean.

Last but not least, better knowledge about the hydrothermal input of iron and iron-stabilizing processes is important for the input parameters of global climate models and can help to improve predictions on the role of Fe and possibly also other metals in buffering ocean productivity and carbon cycling [13].

References

1. German CR, Von Damm KL (2003) Hydrothermal processes. In: Holland HD, Turekian KK (eds) Treatise on geochemistry, vol 6, 1st edn. Elsevier-Pergamon, Oxford, pp 181–222
2. Mandernack KW, Tebo BM (1993) Manganese scavenging and oxidation at hydrothermal vents and in vent plumes. Geochim Cosmochim Acta 57:3907–3923
3. Boström P (1969) The origin of aluminium-poor ferro-manganoan sediments in areas of high heat flow on the East Pacific Rise. Mar Geol 7:427–447
4. Field MP, Sherrell RM (2000) Dissolved and particulate Fe in a hydrothermal plume at 9°45′N, East Pacific Rise: slow Fe (II) oxidation kinetics in Pacific plumes. Geochim Cosmochim Acta 64:619–628
5. Sander S, Koschinsky A (2000) Onboard-ship redox speciation of chromium in diffuse hydrothermal fluids from the North Fiji Basin. Mar Chem 71(1–2):83–102
6. Sander S, Koschinsky A, Halbach P (2003) Redox speciation of chromium in the oceanic water column of the Lesser Antilles and offshore Otago Peninsula, New Zealand. Mar Freshw Res 54 (6):745–754
7. Sander SG, Koschinsky A, Massoth GJ, Stott M, Hunter KA (2007) Organic complexation of copper in deep-sea hydrothermal vent systems. Environ Chem 4:81–89. doi:10.1071/EN06086
8. Sarradin PM, Waeles M, Bernagout S, Le Gall C, Sarrazin J, Riso R (2009) Speciation of dissolved copper within an active hydrothermal edifice on the Lucky Strike vent field (MAR, 37 degrees N). Sci Total Environ 407(2):869–878. doi:10.1016/j.scitotenv.2008.09.056
9. Sander SG, Koschinsky A (2011) Metal flux from hydrothermal vents increased by organic complexation. Nat Geosci 4(3):145–150

10. Kleint C, Kuzmanovski S, Powell Z, Bühring SI, Sander SG, Koschinsky A (2015) Organic Cu-complexation at the shallow marine hydrothermal vent fields off the coast of Milos (Greece), Dominica (Lesser Antilles) and the Bay of Plenty (New Zealand). Mar Chem 173:244–252. doi:10.1016/j.marchem.2014.10.012
11. Bennett SA, Achterberg EP, Connelly DP, Statharn PJ, Fones GR, German CR (2008) The distribution and stabilisation of dissolved Fe in deep-sea hydrothermal plumes. Earth Planet Sci Lett 270(3–4):157–167. doi:10.1016/j.epsl.2008.01.048
12. Hawkes JA, Connelly DP, Gledhill M, Achterberg EP (2013) The stabilisation and transportation of dissolved iron from high temperature hydrothermal vent systems. Earth Planet Sci Lett 375:280–290
13. Tagliabue A, Bopp L, Dutay JC, Bowie AR, Chever F, Jean-Babtiste P, Bucciarelli E, Lannuzel D, Remenyi T, Sarthou G, Aumont O, Gehlen M, Jeandel C (2010) Hydrothermal contribution to the oceanic dissolved iron inventory. Nat Geosci 3:252–256. doi:10.1038/NGEO818
14. Toner BM, Marcus MA, Edwards KJ, Rouxel O, German CR (2012) Measuring the form of iron in hydrothermal plume particles. Oceanography 25(1):209–212. doi:10.5670/oceanog.2012.19
15. Trouwborst RE, Clement BG, Tebo BM, Glazer BT, Luther GW III (2006) Soluble Mn(III) in suboxic zones. Science 313:1955–1957
16. Oldham VE, Owings SM, Jones MR, Tebo BM, Luther GW (2015) Evidence for the presence of strong Mn(III)-binding ligands in the water column of the Chesapeake Bay. Mar Chem 171:58–66. doi:10.1016/j.marchem.2015.02.008
17. Wu JF, Roshan S, Chen G (2014) The distribution of dissolved manganese in the tropical-subtropical North Atlantic during US GEOTRACES 2010 and 2011 cruises. Mar Chem 166:9–24. doi:10.1016/j.marchem.2014.08.007
18. Resing JA, Sedwick PN, German CR, Jenkins WJ, Moffett JW, Sohst BM, Tagliabue A (2015) Basin-scale transport of hydrothermal dissolved metals across the South Pacific Ocean. Nature 523(7559):200–203. doi:10.1038/nature14577
19. Bruland KW (1989) Complexation of zinc by natural organic ligands in the central north Pacific. Limnol Oceanogr 32:269–285
20. Conway TM, John SG (2014) The biogeochemical cycling of zinc and zinc isotopes in the North Atlantic Ocean. Global Biogeochem Cycles 28(10):1111–1128. doi:10.1002/2014gb004862
21. Saito MA, Moffett JW (2001) Complexation of cobalt by natural organic ligands in the Sargasso Sea as determined by a new high-sensitivity electrochemical cobalt speciation method suitable for open ocean work. Mar Chem 75(1–2):49–68
22. Achterberg EP, van den Berg CMG (1997) Chemical speciation of chromium and nickel in the western Mediterranean. Deep-Sea Res II Top Stud Oceanogr 44(3–4):693–720. doi:10.1016/s0967-0645(96)00086-0
23. Hsu-Kim H, Mullaugh KM, Tsang JJ, Yucel M, Luther GW (2008) Formation of Zn- and Fe-sulfides near hydrothermal vents at the Eastern Lau spreading center: implications for sulfide bioavailability to chemoautotrophs. Geochem Trans 9:6. doi:10.1186/1467-4866-9-6
24. Yucel M, Gartman A, Chan CS, Luther GW (2011) Hydrothermal vents as a kinetically stable source of iron-sulphide-bearing nanoparticles to the ocean. Nature Geosci 4(6):367–371, http://www.nature.com/ngeo/journal/v4/n6/abs/ngeo1148.html#supplementary-information
25. Gartman A, Findlay AJ, Luther GW III (2014) Nanoparticulate pyrite and other nanoparticles are a widespread component of hydrothermal vent black smoker emissions. Chem Geol 366:32–41
26. Li M, Toner BM, Baker BJ, Breier JA, Sheik CS, Dick GJ (2014) Microbial iron uptake as a mechanism for dispersing iron from deep-sea hydrothermal vents. Nat Commun 5:3192. doi:10.1038/ncomms4192

27. Jiang HS, Breier JA (2014) Physical controls on mixing and transport within rising submarine hydrothermal plumes: A numerical simulation study. Deep-Sea Res I Oceanogr Res Pap 92:41–55. doi:10.1016/j.dsr.2014.06.006
28. McDuff RE (2013) Physical dynamics of deep-sea hydrothermal plumes. In: Seafloor hydrothermal systems: physical, chemical, biological, and geological interactions. American Geophysical Union, Washington, DC, pp 357–368. doi:10.1029/GM091p0357
29. Lupton JE, Craig H (1981) A major Helium-3 source at 15 degrees S on the east pacific rise. Science 214:13–18
30. Nishioka J, Obata H, Tsumune D (2013) Evidence of an extensive spread of hydrothermal dissolved iron in the Indian Ocean. Earth Planet Sci Lett 361:26–33. doi:10.1016/j.epsl.2012.11.040
31. Schlitzer R (2004) Ocean data view. http://odv.awi-bremerhaven.de
32. Fitzsimmons JN, Boyle EA, Jenkins WJ (2014) Distal transport of dissolved hydrothermal iron in the deep South Pacific Ocean. Proc Natl Acad Sci USA 111(47):16654–16661. doi:10.1073/pnas.1418778111
33. Klinkhammer G, Hudson A (1986) Dispersal patterns for hydrothermal plumes in the south-pacific using manganese as a tracer. Earth Planet Sci Lett 79(3–4):241–249. doi:10.1016/0012-821x(86)90182-2
34. Middag R, de Baar HJW, Laan P, Klunder MB (2011) Fluvial and hydrothermal input of manganese into the Arctic Ocean. Geochim Cosmochim Acta 75(9):2393–2408. doi:10.1016/j.gca.2011.02.011
35. Lopez GI, Marcantonio F, Lyle M, Lynch-Stieglitz J (2015) Dissolved and particulate ^{230}Th–^{232}Th in the central equatorial pacific ocean: evidence for far-field transport of the East Pacific rise hydrothermal plume. Earth Planet Sci Lett 431:87–95. doi:10.1016/j.epsl.2015.09.019
36. Lilley MD, Feely RA, Trefry JH (1995) Chemical and biochemical transformations in hydrothermal plumes. In: Humphris SE, Zierenberg RA, Mullineaux LS, Thomson RE (eds) Seafloor hydrothermal systems: physical, chemical, biological, and geological interactions, vol 91, Geophysical Monograph. American Geophysical Union, Washington, pp 369–391
37. Elderfield H, Schulz A (1996) Mid-ocean ridge hydrothermal fluxes and the chemical composition of the ocean. Annu Rev Earth Planet Sci 24:191–224
38. Hawkes JA, Connelly DP, Rijkenberg MJA, Achterberg EP (2014) The importance of shallow hydrothermal island arc systems in ocean biogeochemistry. Geophys Res Lett 41(3):942–947. doi:10.1002/2013gl058817
39. German CR, Campbell AC, Edmond JM (1991) Hydrothermal scavenging at the Mid-Atlantic Ridge: modification of trace element dissolved fluxes. Earth Planet Sci Lett 107(1):101–114. doi:10.1016/0012-821X(91)90047-L
40. Edmonds HN, German CR (2004) Particle geochemistry in the Rainbow hydrothermal plume, Mid-Atlantic Ridge. Geochim Cosmo Acta 68(4):759–772. doi:10.1016/s0016-7037(03)00498-8
41. Feely RA, Trefry JH, Lebon GT, German CR (1998) The relationship between P/Fe and V/Fe ratios in hydrothermal precipitates and dissolved phosphate in seawater. Geophys Res Lett 25(13):2253–2256. doi:10.1029/98gl01546
42. Mitra A, Elderfield H, Greaves MJ (1994) Rare earth elements in submarine hydrothermal fluids and plumes from the Mid-Atlantic Ridge. Mar Chem 46(3):217–235. doi:10.1016/0304-4203(94)90079-5
43. Lang SQ, Butterfield DA, Lilley MD, Johnson HP, Hedges JI (2006) Dissolved organic carbon in ridge-axes and ridge-flank hydrothermal systems. Geochim Cosmochim Acta 70:3830–3842
44. German CR, Legendre LL, Sander SG, Niquil N, Luther Iii GW, Bharati L, Han X, Le Bris N (2015) Hydrothermal Fe cycling and deep ocean organic carbon scavenging: model-based evidence for significant POC supply to seafloor sediments. Earth Planet Sci Lett 419:143–153. doi:10.1016/j.epsl.2015.03.012
45. Bennett SA, Statham PJ, Green DRH, Le Bris N, McDermott JM, Prado F, Rouxel OJ, Von Damm K, German CR (2011) Dissolved and particulate organic carbon in hydrothermal

plumes from the East Pacific Rise, 9 degrees 50′N. Deep-Sea Res I Oceanogr Res Pap 58 (9):922–931. doi:10.1016/j.dsr.2011.06.010
46. Rossel PE, Stubbins A, Hach PF, Dittmar T (2015) Bioavailability and molecular composition of dissolved organic matter from a diffuse hydrothermal system. Mar Chem 177:257–266. doi:10.1016/j.marchem.2015.07.002
47. Klevenz V, Sumoondur A, Ostertag-Henning C, Koschinsky A (2010) Concentrations and distributions of dissolved amino acids in fluids from Mid-Atlantic Ridge hydrothermal vents., Geochemical Journal accepted
48. McCollom TM, Seewald JS (2007) Abiotic synthesis of organic compounds in deep-sea hydrothermal environments. Chem Rev 107(2):382–401
49. Gomez-Saez GV, Riedel T, Niggemann J, Pichler T, Dittmar T, Bühring SI (2015) Interaction between iron and dissolved organic matter in a marine shallow hydrothermal system off Dominica Island (Lesser Antilles). Mar Chem 177, part 4:677–686. doi:10.1016/j.marchem.2015.10.003
50. Hawkes JA, Rossel PE, Stubbins A, Butterfield D, Connelly DP, Achterberg EP, Koschinsky A, Chavagnac V, Hansen CT, Bach W, Dittmar T (2015) Efficient removal of recalcitrant deep-ocean dissolved organic matter during hydrothermal circulation. Nat Geosci 8(11):856–860. doi:10.1038/ngeo2543
51. German CR, Campbell AC, Edmond JM (1991) Hydrothermal scavenging at the Mid-Atlantic Ridge – modification of trace-element dissolved fluxes. Earth Planet Sci Lett 107(1):101–114. doi:10.1016/0012-821x(91)90047-l
52. Koschinsky A, Seifert R, Halbach P, Bau M, Brasse S, De Carvalho LM, Fonseca NM (2002) Geochemistry of diffuse low-temperature hydrothermal fluids in the North Fiji Basin. Geochim Cosmochim Acta 66:1409–1427
53. GW L lll, Rozan TF, Taillefert M, Nuzzio DB, Meo CD, Schank TM, Lutz RA, Cary SC (2001) Chemical speciation drives hydrothermal vent ecology. Nature 410:813–816
54. Kleint C, Hawkes JA, Sander SG, Koschinsky A (2016) Voltammetric investigation of hydrothermal iron speciation. Frontiers, submitted
55. Ellwood MJ, Hutchins DA, Lohan MC, Milne A, Nasemann P, Nodder SD, Sander SG, Strzepek R, Wilhelm SW, Boyd PW (2015) Iron stable isotopes track pelagic iron cycling during a subtropical phytoplankton bloom. Proc Natl Acad Sci USA 112(1):E15–E20. doi:10.1073/pnas.1421576112
56. Nasemann P, Gault-Ringold M, Stirling CH, Ellwood M, Schmidt K, Koschinsky A, Garbe-Schönberg D, Häckel F, Sander SG (2016) Iron isotope study of the Nifonea vent field, Vanuatu (in preparation)
57. Conway TM, John SG (2014) Quantification of dissolved iron sources to the North Atlantic Ocean. Nature 511(7508):212–215. doi:10.1038/nature13482

Geologic-Geochemical and Ecological Characteristics of Selected Hydrothermal Areas

Sergey V. Galkin and Liudmila L. Demina

Abstract In this paper we consider geologic-geochemical and ecological characteristics of the areas where the material for biogeochemical study (Demina, Trace metals in water in the hydrothermal biotope. Hdb Env Chem. doi:10.1007/698_2016_1; Demina, Galkin, Factors controlling the trace metal distribution in hydrothermal vent. Hdb Env Chem. doi:10.1007/698_2016_5) has been collected. In the Atlantic Ocean five hydrothermal areas (Menez Gwen, Rainbow, Lost City, Broken Spur, and Snake Pit) have been investigated. In the Pacific Ocean the 9°50′N vent area at the East Pacific Rise and hydrothermal manifestations in Guaymas Basin (Gulf of California) were studied. Observations and sampling were provided in 1996–2005 during numerous cruises of RV "Akademik Mstislav Keldysh" using deep-sea manned submersibles "Mir." Explored vent areas exhibit a wide range of environmental conditions, including great variation in depth (particularly on the MAR), associated physical parameters, and different geologic setting and underlying rocks. Faunal communities also vary greatly in taxonomic composition and spatial structure. Short characteristic of abiotic environment and structure of benthic communities is given for each explored area. With all the variety of hydrothermal manifestations, in the spatial structure of communities a number of general patterns can be revealed. At the analysis of bioaccumulation function of vent organisms in the case of each area particular habitat conditions and characteristics of spatial structure of communities (microdistribution of animal's populations, their association with a specific temperature zone and a particular type of substrate) must be taken into account.

Keywords Abiotic environment, East Pacific Rise, Guaymas Basin, Hydrothermal vents, Microdistribution, Mid-Atlantic Ridge, Taxonomic composition

S.V. Galkin (✉) and L.L. Demina
P.P. Shirshov Institute of Oceanology Russian Academy of Sciences (IORAN), Nakhimovsky pr., 36, 117997 Moscow, Russia
e-mail: galkin@ocean.ru; l_demina@mail.ru

L.L. Demina, S.V. Galkin (eds.), *Trace Metal Biogeochemistry and Ecology of Deep-Sea Hydrothermal Vent Systems*, Hdb Env Chem (2016) 50: 25–52,
DOI 10.1007/698_2016_3,
Published online: 30 April 2016

Contents

1 Introduction

The vent zone is the most chemically and spatially heterogeneous environment of a hydrothermal field.

In the hydrothermal ecosystem there is a strong relationship between abiotic and biotic components. Bottom fauna is able to influence the basic chemical environmental parameters: aggregated settlement of hydrothermal fauna, in particular symbiotrophic mussels and shrimps, redistribute chemical components of habitat, consuming from water hydrogen sulfide, sulfide ion, nitrates, and nitrites, followed by excreting ammonium ion and dissolved organic carbon into the water of biotope [1]

Obviously, at the analysis of bioaccumulation function of vent organisms in the case of each area particular habitat conditions and characteristics of spatial structure of communities (microdistribution of animal's populations, their association with a specific temperature zone and a particular type of substrate) must be taken into account.

Hydrothermal vent areas exhibit a wide range of environmental conditions, including great variation in depth (particularly on the MAR), associated physical parameters, and different geologic setting and underlying rocks. All these factors together with geographical distance determine taxonomic composition and spatial structure of associated vent communities.

In this chapter we consider geologic-geochemical and ecological characteristics of the areas where the material for our biogeochemical study [2, 3] has been collected (Table 1). Principal geologic-geochemical characteristics describe abiotic environment. Ecological characteristics include mean by taxonomic composition and spatial structure of hydrothermal vent communities. In all cases concentrations of metals in water over the fauna habitats are much higher than in the reference ocean water where trace metal concentrations are to 3 orders of magnitude less for Fe, Co, and Pb in comparison with biotope water [4]. All underwater deep-sea

Table 1 Basic characteristics of selected deep-sea hydrothermal vent areas

Vent Area	Locality	Maximal depth (m)	Fluid maximal temperature (°C)	pH of fluids
Menez Gwen	37°51′N, 30°31′W	875	284	4.2–4.8
Rainbow	36°14′N, 33°54′W	2,350	365	2.8–3.1
Lost City	30°15′N, 42°24′W	900	90	9–11
Broken Spur	29°10′N, 43°10′W	3,875	364	2.9–3.2
Snake Pit	23°22′N, 43°10′W	3,480	356	3.0–3.3
9°50′N EPR	9°48–51′N, 104°17′W	2,580	300	3.0–3.4
Guaymas Basin	27°00′N, 111°24′W	2,050	315	5.4

images of hydrothermal landscapes used in present paper were taken in situ with submersibles "Mir" cameras.

2 Mid-Atlantic Ridge (MAR)

By now, at MAR at least 10 hydrothermal areas to the north equator are more or less studied. The most areas are located between 37°N and 12°N. The depth of areas generally increases from north to south from 850 m (Menez Gwen) to 4,100 m (Ashadze). The investigations of hydrothermal vents at southern part of MAR were initiated relatively recently. Now several areas between 4°N and 10°S have been described [5].

In the present chapter we consider five hydrothermal areas at the MAR: Menez Gwen, Rainbow, Lost City, Broken Spur, and Snake Pit.

2.1 Menez Gwen

Locality: 37°51′N; 31°31′W. Depth: 840–875 m.

2.1.1 Abiotic Environment

Menez Gwen is the active, shallowest, and youngest (with an age less than 100 years) of all the fields of the MAR [6]. It is located on a volcanic segment, small chimneys (less than 5 m height) grow on the fresh pillows and are mainly composed of white anhydrite [1, 7]. The active area occupies approximately 200 m^2. Vent field is situated near the base of volcano and associated with axial magma chambers. Fluid temperature ranges from 8°C to 30°C [8]. Diffuse low-temperature

hydrothermal vents dominate over focused ones, the black smokers are rare and there are no plumes. Rather low values of temperature and hydrostatic pressure determine relative lower (compared with other MAR vent areas) salinity of hydrothermal fluids [9]. The concentration of metals generally correlated with the salinity. Therefore, we anticipate lower concentrations of heavy metals in Menez Gwen fluids compared with other fields. Menez Gwen hydrothermal fluids ($pH > 4$) are enriched in gas (mainly CO_2 (75 %) and H_2S (10–20 %) [1]).

A characteristic feature of the landscape at Menez-Gwen is the presence of unconsolidated hydrothermal deposits of light gray, white or dark gray in most parts of the field. The most common type of fluid discharge within the area is the temperature diffuse flow through the sediments. Diffuse outflows run temperature of 10–40°C, pH 4.2–4.8. Emergence of relatively hot transparent fluid occurs at low (up to 0.5 m) edifices. The maximal recorded temperature of the fluid amounts up 284°C. The predominate substrates for the fauna are basaltic lavas, as well as white chimneys, consisting of anhydrite and barite. Fluids at Menez-Gwen are characterized by a number of features distinct from the fluids deep-water areas. It is connected with the process of subsurface phase separation [9–11]. Fluids at Menez Gwen showed low chlorinity, low salinity, low content of H_2S, low concentration of metals and silicon, the enrichment by gases and a high content of methane.

2.1.2 Taxonomic Composition and Spatial Structure of Community

Compared to communities of deeper areas, Menez-Gwen faunal community is impoverished in both abundance and diversity of vent fauna. Predominant macrofaunal group within the active zone of the field are mussels *Bathymodiolus azoricus* (Fig. 1). Population of the living mytilids seems quite small. The dimensions of continuous clusters never exceed a few tens of centimeters in diameter. According to [8], this may be due to a deficit of hard substrate appropriate for colonization by mytilids. Significant accumulations of large bivalves were observed on the ledges of solid rock, in the immediate vicinity of the most intensive vents, often in the shimmering water. Compared with other MAR vent areas, Menez Gwen characterized by very sparse population of the commensal polychaete *Branchipolynoe seepensis*. This peculiarity was mentioned by many authors [1].

From among bresilioid shrimps only *Mirocaris fortunata* has been recorded (in the initial version *Chorocaris* sp.), which also do not form clusters. Characteristic for deeper areas *Rimicaris exoculata* as well as carnivorous *Segonzacia mesatlantica* and *Phymorhynchus* are absent.

The most numerous forms within the hydrothermal community are limpets (*Lepetodrilus atlanticus*, *Protolyra thorvaldsoni* and *P. valvatoides*). These small (<0.5 cm) animals form aggregations on the surface of the mytilid shells, as well as on any hard substrate, including basalts. The density of their settlements reaches tens ind./dm^2. In these clusters other limpet species (in particular, *Shinkailepas briandi*) were recorded, but in single specimens. As the predominant form in the

Fig. 1 Menez Gwen hydrothermal area, Flores site. Depth 885 m. Settlement of mussels *Bathymodiolus azoricus*

inactive areas of the field the bresilioid shrimps *Mirocaris fortunata* and *Chorocaris chacei* were indicated in a number of papers (see, for example, [1]). However, during our observations, the first of these species was met only once, and the second was not marked at all, just as carnivorous crabs *Segonzacia mesatlantica*. The most notable carnivorous form within hydrothermal field was large geryonid crab *Chaceon affinis* (their number on the field at the moment of our observation was not less than 5).

The periphery of hydrothermal field is almost devoid of sedimentary cover. Background community is rather sparse. Dominating macrofauna is presented by gorgonian corals, hydroids, small sponges (including many encrusting forms) and alcyonarians. Peculiar element of the background landscape represent the accumulations of dead corals *Lophelia prolifera*, which form aggregates up to several square meters, mainly in the crevices of lava formations. These dead "reefs" are richly inhabited by diverse fauna, both attached forms (serpulids, hydroids, sponges, bryozoans, alcyonarians), and many mobile animals (Munidae crabs, errantia polychaetes, tanaids, amphipods (Stenothoidea), large Harpacticoida, brittle stars, gastropods Trochidae, Bursidae, and Opistobranchia). On the dead

colonies are willing to settle live corals of different species (including numerous *Caryophyllia sarsiae*). The most abundant animals at the periphery of active vent field are the different species of hydroids (dominated by *Eudendrium* sp. and *Grammaria abietina*), sometimes completely covering the rocks. Both species are representatives of widespread boreal taxa and are known in a wide range of depths. Their presence in the hydrothermal community may be related to increased dynamics of the bottom water, due to thermal circulation.

2.2 Rainbow

Locality: 36°14′N, 33°54′W. Depth 2,260–2,350 m.

2.2.1 Abiotic Environment

The Rainbow vent area (36°14′N) discovered in 1997 [12] is located at a depth of 2,300 m and associated with ultramafic rocks; high-temperature serpentinization processes cause the highly acidic character (pH 2.8) of fluids enriched in methane up to 2.5 mmol kg^{-1} [13, 14]. There are many black smokers at the Rainbow vent field with high-temperature fluids enriched with sulfide particles; according to [1], this leads to very high total particle flux (up to 6.9 g m^{-2} day^{-1}) compared with other MAR vent fields (0.26–0.64 g m^{-2} day^{-1}). The Rainbow fluids that have passed phase separation [9] are enriched with chloride ions and associated with them heavy metals, most of which show here the maximal concentrations [14]. The fluids enriched with finely dispersed sulfides (black solutions) are common.

The area itself is a field about the size of 80 × 300 m, on which active sulfide buildings alternate with inactive ones. Black smokers are usually confined to the tops of buildings; diffuse outflows occur through the walls of buildings and through fractured basalts at the bottom of them.

The temperature of the outgoing fluid reaches 364°C. The content of H_2S, Si, Li is significantly lower, while that of Ca and Rb is higher than in the areas associated with basalts. Anomalously high concentrations of gases, primarily hydrogen and methane, are also associated with the process of serpentinization. Sharp fluid enrichment by Fe, Mn, Co, Ni, Cu, Zn, and other metals and increased amount of chlorine compared with the fluids of other hydrothermal areas are also associated with phase separation [10, 11, 15].

2.2.2 Taxonomic Composition and Spatial Structure of Community

The benthic community of the Rainbow hydrothermal area was explored by Russian expeditions in 1995, 1998, 1999, 2002, and 2005. Repeated studies have shown that faunal zonation at Rainbow area is very complex and subject to

significant changes in a short time. During our 2005 expedition, we concentrated on researching specific structures, with the purpose of carrying out complete geological and biological surveys. One mature active structure in the central part of the field (mark AMKII) was investigated in great detail. During the dive of Mir-2 (St.4819) ten passes from base to top were carried out with continuous video-recording. The documentation of the ore-facial profile of the structure was carried out. At the same time, biological surveys were conducted and distribution of fauna was documented with reference to the rock facies. Faunal assemblages associated with different geo-morphological facies were described.

1. The basis of the structure (depth 2,317–2,313 m) is underlain by serpentinites and covered by metalliferous sediments and serves as a habitat for numerous Chaetopterids and hydroids (*Stegopoma plicatile*, *Candelabrum phrigium* a.o.). Settlements of the branchy xenophyophores *Luffamina* are characteristic for this zone. Numerous Nematoda, Harpacticoida, Tanaidacea, Foraminifera, and other small animals were found in the sediment.
2. Chaetopterids, hydroids, and xenophiophores are abundant and also present in an overlying zone (2,313–2,308 m), on a cone composed of fragments of tubes and massive blocks of sphalerite-pyrite ore. In this zone rare shrimps *Mirocaris fortunata* and rather abundant *Alvinocaris* sp. were observed. Gastropods *Protolyra thorvaldsoni*, *Pseudorimula mesatlantica*, *Peltospira smaragdina* and *Phymorhynchus* sp. are abundant. Polynoid polychaetes and picnogonids were recorded. Tanaids living in small houses constructed from particles of deposit material amounted to up to 200 individuals per several cm^2.
3. At a depth range of 2,309–2,303 m, the prevailing substratum consists of upright inactive pipes with a brown or dark surface. Shimmering water emissions are observed locally in this zone. The amount of dark rocks increases towards the top part of the structure. Shrimps *(Mirocaris fortunata;* up to 100 ind./m^2*)* are associated with these rocks. On a surface of the tubes, individual mollusks, *Bathymodiolus,* were observed that appear to be lifeless.
4. At a depth range of 2,303–2,301 m the vent structure consists of fused pipes of dark or orange color (Fig. 2). In this zone, shimmering water emissions and black smokes are most distinctive compared to the other zones. These water emission sites are marked by swarming shrimps *Rimicaris exoculata* (the swarm sizes are up to 0.5 m in diameter). The top of the structure (2,300 m) represents a multichannel, ramified smoker with no visible fauna.

Thus the spatial distribution of the fauna at Rainbow shows a similarity to that found at other MAR vent areas. There are an abundance of the *Rimicaris exoculata* adjacent to hot black smokes; predominance of *Mirocaris fortunata* in moderate temperature zone (sometimes also in shimmering water). The *Bathymodiolus* mussels mostly colonize the base of edifices, where the low temperature diffusors are located.

Mussel beds are inhabited by rather diverse fauna. There are polychaetes (Ampharetidae, Spionidae, Polynoidae, Capitellidae), fairly large picnogonids and limpets (*Peltospira smaragdina, Pseudorimula mesatlantica*).

Fig. 2 Rainbow hydrothermal area, depth 2,303 m. *Upper part* of the edifice AMKII. Dense swarms of bresilioid shrimps *Rimicaris exoculata* (*right*) and more sparse *Mirocaris fortunata* (*in center*)

2.3 Lost City

Locality: 30°15′N, 42°24′W. Depth 750–900 m.

2.3.1 Abiotic Environment

In Lost City hydrothermal area about 30 carbonate buildings with height from 30 to 70 m was described with a large number of smaller edifices [16, 17]. This field is distinctly different from all other known hydrothermal fields in that it is underlain by ultramatic rocks and is dominated by spectacular, steep-sided carbonate chimneys (Fig. 3) Weakly shimmering water with alkaline pH (up to 9.8) is found on the tops of and sometimes between the columns.

The slopes of the buildings are composed of white porous minerals: calcite, aragonite and brucite, and are often covered with bacterial mats [18]. ^{86}Sr isotope data, ^{12}C/^{13}C, ^{16}O/^{18}O, and ^{14}C isotope data suggest the approximate age of the hydrothermal activity equal to about 30,000 years. Thus this area is older than the

Fig. 3 Lost City hydrothermal area, depth ca. 760 m. Carbonate spires in the vicinity of the top of Poseidon edifice

areas with black smokers [16]. The unusual chemical composition of the fluids is controlled by the processes of serpentinization of ultramafic rocks. These subsurface reactions create fluids rich in hydrogen and methane [16, 17]. Although the influence of subsurface biosphere also could not to be excluded [15, 18].

2.3.2 Taxonomic Composition and Spatial Structure of Community

The fluid composition is controlled by the interaction between seawater and mantle peridotite. These subsurface reactions create fluids rich in hydrogen and methane, which are important energy sources for the primary producers of the Lost City ecosystem. These producers are represented by Archaea and eubacteria, their concentration reaches 10^7–10^8 cells per gram of wet carbonate. At the same time, communities of typical hydrothermal vent animals were not found at this field and it was originally thought that vent obligate (i.e., occurring only in hydrothermal vent environment) fauna at Lost City is absent.

In July 2002 Lost City was revisited on the 47th cruise of the RV "Akademik Mstislav Keldysh." During the dives with Mir submersibles several samples of

bottom fauna were recovered including obligate (occurring only in hydrothermal vent environment) hydrothermal species (limpets Peltospiridae, amphipods, archinomid polychaetes, etc.) inhabiting porous interiors of the carbonate edifices. Two subfossil valves and six fragments of bivalve shells presumably belonging to *Bathymodiolus* were collected at the base of the tower complex at a depth of 830 m [19, 20]. In 2003 during 19 dives with the submersible Alvin [17] ten discrete, active vent sites were sampled. Recovered samples revealed that over 65 morphospecies were present, and >90 % of these fauna were in the order of hundreds of micrometers or less in size.

The task of our 2005 expedition was to make comprehensive observations of and take samples from the different biotopes. Active chimneys, inactive tower flanges, and the base of the complex were explored. Initial analysis of recovered samples revealed the presence of at least 55 species. Of the most abundant taxa, polychaetes are most diverse (>14 species). Coelenterates (11 species) and small crustaceans (not less 7 species) are also abundant.

Our observations reveal qualitative differences in species abundance and composition relative to substrate type.

Active Tower Tops and Walls

White friable carbonate prevails; thermal discharges are often visible by characteristic shimmering of the water. Temperatures of up to 50°C were measured. Bacterial mats are often visible on the surface. Porous channels and crevices of carbonate that is rich in bacterial mats provide habitat for many small animals including typical vent species. The most characteristic fauna in this biotope are amphipods *Bouvierella curtirama*, limpets *Protolyra valvatoides*, harpacticids, ostracods, tanaids, giant (up to 1 cm long) nematodes, and representatives of several families of polychaetes (*Ophriotrocha* sp. and Ceratulidae were observed only in this zone). Bivalves Cuspidariidae and Thyasiridae were recorded. Sessile animals are almost absent. Numerous euphasiids *Nematoscelis* and hyperiids *Paraphronima* and *Streetsia* swarms were present in the water.

Inactive Chimneys and Tower Walls

These are made up of relatively hard, glaucous or yellowish rocks. There is no visual evidence for current hydrothermal activity. Non-vent animals are fairly abundant, corals *Lophelia* sp. and *Cariophyllia sarsiae* are often observed. *Lophelia* forms bushes of up to 2 m in diameter. Gorgonian corals, alcionarians (*Stolonifera*) and actinians *Sideractis glacialis* and *Amphianthus* sp. are common. Diverse hydroids associated with corals and rocks were collected and include *Halecium tenellum, Sertularella gayi, Zanclea costata, Mirocomella polydiademata,* and other species. Also common in this zone were the sponges Demospongia and Hexactinellida (*Farrea*). Polychaete fauna is also rich in species: representatives

of Serpulidae (two species) and Spirorbidae are common. Polynoidae, Eunicidae, Spionidae, Dorvilleidae, Sabellidae, Phyllodocidae, *Archinome rosacea* were observed, often in association with corals. Among larger mobile animals, gerionid crabs, galateids (*Munidopsis scabra*), *Agononida* and *Munida,* the swimming crab *Bathynectes maravigna*, echinoids *Araeosoma fenestratum* and Cidaridae, asteroids resembling *Ceramaster*, and brittle stars are common.

The Complex Base at 850–900 m

At the base of the tower complex, carbonate structures and hard rocks are locally covered with sediment. Macrofaunal composition and appearance in this zone is similar to the previous one. Analyses of our sediment samples revealed that fauna of this sediment are similar to ordinary background fauna and typically represented by meiobenthic taxa: Nematoda, Harpacticoida, small Polychaeta, and numerous diverse foraminifera.

Observations and sampling show that there is a well-defined boundary between vent and non-vent habitats at Lost City. This is generally true for all small, in particular vent-typical, animals. However we repeatedly observed large crabs, fishes, and echinoderms in active zones near the tops of the central complex. In the stomach of a sea-urchin *Araeosoma fenestratum* bacterial clots were found. The question which remains unclear is how far chemosynthetically derived production can be consumed by non-vent fauna and to what degree hydrothermal processes can influence the surrounding background community.

The most remarkable find on our 2005 expedition was the discovery of an extinct hydrothermal community which we named Lost Village [21]. Having discovered this community, we now know that Lost City area hosts (at least from time to time) large populations of *Bathymodiolus azoricus*, which may be compared (in terms of biomass and abundance) with dense populations of the same species living at other fields along the mid-Atlantic Ridge.

2.4 Broken Spur

Locality: 29°10′N, 43°10′W. Depth 3,050–3,875 m.

2.4.1 The Abiotic Environment

Hydrothermal area Broken Spur, discovered in 1993 [22, 23], is situated on a basaltic substrate and consists of massive sulfide structures. Broken Spur is one of the youngest MAR hydrothermal areas. Active hydrothermal manifestations are observed in the western part of the rift valley on about 6,000 m^2. Hydrothermal edifices with different morphology and activity are located at the bottom of the axial graben and marginal

terraces. There are five buildings with active black smokers and seven inactive buildings. The height of buildings varies from 5 to 40 m. Several main morphological types of hydrothermal edifices include high, column-like (Triple Chimney, Judy's Tower, Spire), high massive (Saracen's Head, Bogdanov Site), and relatively low, platform structures with fattened tops (White Mushroom, White Button, point "K"). Most high-temperature outflows in the form of black smokers and intense shimmering water are observed in the upper part and especially on the tops of columnar and massive buildings. Fungiform edifices are less active, dominant form of hydrothermal discharge – shimmering water expiration through the cracks in a flat surface.

Predominate forms of hydrothermal discharges are the focused high- and low-temperature vents. The main feature of the fluids is an extremely high hydrogen sulfide content (up to 11 mmol kg^{-1}) [24]. The fluids are characterized by high temperature: 56–364°C. Presence of high-temperature hydrothermal sulfide deposits indicates that in this area emerges almost not modified primary fluid. It is characterized by a high content of H_2S, Fe, and Mn. On the contrary, the enrichment in methane and chlorine is low [9, 10].

2.4.2 Taxonomic Composition and Spatial Structure of Community

Initial observations made in 1993 at Broken Spur [22] suggested a low biomass relative to other deep-water Mid-Atlantic vent communities (e.g., TAG, Snake Pit, Logachev).

Vent fauna at Broken Spur is associated with isolated chimney structures of various morphologies. During the expedition of RV "Akademik Mstislav Keldysh" in 2005, attention was focused on detailed research of spatial distributions of animals associated with the different types of vent structures. Communities were studied at seven sites: White Mushroom, Saracen's Head, Bogdanov Site, Triple Chimney, Judy's Tower, White Button, and Spire.

Several spatial faunal assemblages associated with discrete biotopes were identified:

1. "Swarms" of shrimps *Rimicaris exoculata* were concentrated near relatively high-temperature vents that discharge characteristic black smoke or turbid shimmering water. The continuous, extremely dense swarms of shrimps usually did not exceed a distribution zone of 1 m around, and commonly stayed within a limit of a few tens of centimeters of the vents. As analysis of the recovered samples from this zone shows, fauna other than shrimps was rare and represented by sporadic individuals of polychaetes (fam. Spionidae). The most dense aggregations of *Rimicaris exoculata* were observed on massive structures and sometimes in the upper part of column-like structures. In all cases, dense aggregations of *Rimicaris exoculata* were found where the topography of vent structures provided enough substrate that was washed over with warm shimmering water.
2. The second dominant shrimp, *Mirocaris fortunata,* was common in weakly shimmering water and formed aggregations of hundreds of individuals per m^2. Slow-flow areas were covered with bacterial mats (Fig. 4). Crabs *Segonzacia*

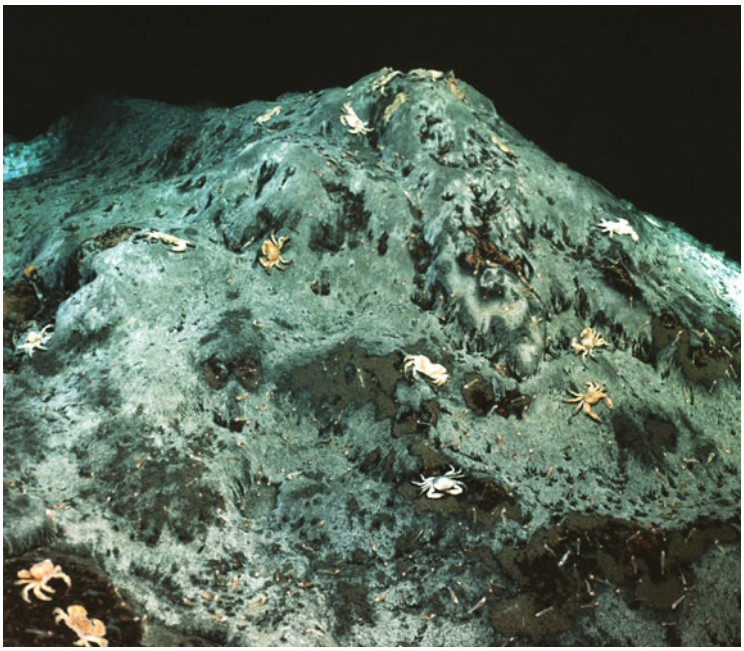

Fig. 4 Broken Spur hydrothermal area, depth 3,036 m. The *central part* of the White Mushroom edifice. Bythograeid crabs *Segonzacia mesatlantica*, shrimps *Mirocaris fortunata,* and bacterial mats

mesatlantica, gastropods *Phymorhynchus*, brittle stars *Ophioctinella acies* (tens of individuals per dm^2), and *Alvinocaris sp.* were all common in this area. Gastropods Peltospiridae (especially *Peltospira smaragdina*) and Fissurelidae formed patches of very dense aggregations. In samples recovered in this zone a number of polychaets (Polynoidae, Spionidae, Capitellidae, Hesionidae, *Archinome rosacea)* were recorded. The low-temperature discharge biotope marked by weakly shimmering water was sometimes inhabited by small aggregations of *Bathymodiolus puteoserpentis*. Single picnogonids were observed together with mussels. This assemblage was topographically associated with horizontal flanges of column-like structures and was especially common when associated with low and mushroom-like structures that had flat tops. A few meiofaunal taxa (Nematoda, Harpacticoida, Foraminifera) were collected in sediment from this habitat.

3. Settlements of actinostolid actinians *Maractis rimicarivora* (originally incorrectly identified as *Parasicyonis ingolfi*) occupied the closest peripheral zones of vents. These settlements are characteristic for the inactive base of all types of vent structures. In this zone chaetopterid polychaetes and *Phymorhynchus* are also abundant. Spionid and archinomid polychaetes, and *Ophioctinella acies* were recorded on friable hydrothermal deposit material near the base of chimneys. More or less dense populations of actinians and chaetopterids are also distributed throughout the field between venting structures.

Remarkable features of the Broken Spur hydrothermal community compared to other MAR areas are reduced total biomass of benthos and relatively high biomass of crabs *Munidopsis* and *Segonzacia* relatively with shrimps. According to [25], unusual quantitative predominance of carnivorous forms compared with symbiotrophs indicates that the community is not in a mature state. At the same time, the large size of the edifices and the abundance of dead shells do not allow to consider Broken Spur hydrothermal system as a "young." It is possible that the observed pattern is related to short-term decrease of hydrothermal activity in the recent past, which resulted in the extinction or emigration of mobile obligate symbiotrophs and gradual extinction of populations of *Bathymodiolus*, a few of which mixotrophic mode of feeding allowed to survive unfavorable conditions [25].

2.5 Snake Pit

Locality: 23°22′N, 44°57′W. Depth 3,420–3,480 m.

2.5.1 The Abiotic Environment

Snake Pit hydrothermal area was discovered in 1985 [26]. It is located in the most deep central part of the rift valley. Within the area there are three active hydrothermal hills, separated from each other by 50–100 m. Every hill is 20–60 m in diameter and from 20 to 26 m high. Snake Pit characterized by the focused high-temperature fluids outflowing from pipes of black smokers and diffusers. The surface of the rift valley is composed of basalts typical for ocean ridges. According to the classification of Y. A. Bogdanov, fluids of the Snake Pit represent the primary hydrothermal solutions which were not subject to phase separation. Black smokers are concentrated at the tops of hills [25, 27, 28]. The maximal measured temperature of the fluid is 356°C. Characteristic hydrothermal formations at Snake Pit area present also so-called diffusers (edifices up to 80 cm in diameter, with porous walls) emerging fluids with the temperature up to 70°C. Hydrothermal fluid of the Snake Pit area is slightly modified compared with the primary solution. The fluid is characterized by a high concentration of chlorine, H_2S, metals, and relatively low concentrations of gases and methane [9]. Researches performed by Russian expedition in 2002 have allowed to describe the landscape-ecological structure of the area. Active sites Beehive and Moose in the eastern part of the hydrothermal field were investigated especially in detail. The bottom at Beehive site is composed of sulfide deposits of different degree of fragmentation. Central part of the site on an area a diameter 20 m at a depth of 3,471 m is occupied by the complex of active smokers (diffusers and pipes) on a single base. Its basis is fused sulfide chimneys and honeycomb structures (diffusers) with a diameter of 1 m. The main forms of hydrothermal discharge within a site – diffuse outflows, visible on the shimmering water, warm black smoke emanating from cracks in the edifice, the hot discharge

from the diffusers (sometimes with black smoke in the upper half) and hot black smoke coming out of the vertical chimneys to 1.5 m high.

The active site of Moose is located approximately 40 m east-northeast of the Beehive. The site itself presents a hydrothermal building of about 12 m high (Fig. 5). Measured in our dive diameter of the building at a depth of 3,488 m is about 6 m, the top reaches approximately 3,476 m. The basement of the building is composed of brown cemented sulfide blocks. The edifice in the lower part consists of overlapping each other cornices from a few centimeters to almost a meter in thickness and sometimes protruding more than 1 m. The main forms of hydrothermal discharge within a site are: diffuse outflows through cracks in the basement and walls of edifice, between the cornices on the upper surface of the cornices rods and diffusers; warm black fumes escaping from cracks in the buildings and some diffusers; as well as the thick black smoke flowing from a vertical chimneys. The most active hydrothermal manifestations were observed in the upper third of the building, especially the top, where shimmering water is visible almost everywhere, and black smoke from numerous pipes merge together in the cloud.

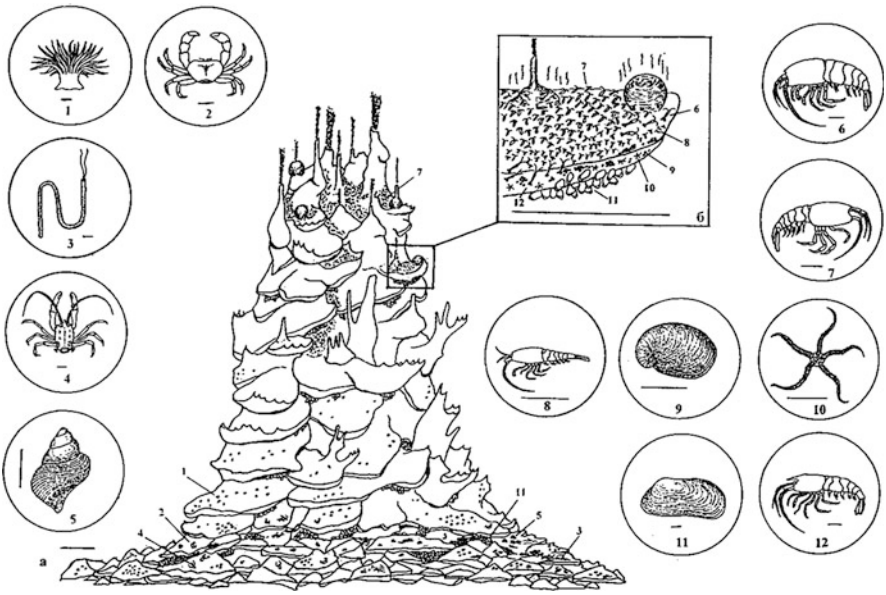

Fig. 5 The distribution of fauna on the edifice of Moose, Snake Pit hydrothermal area according to observations in the 47th cruise of RV "Akademik Mstislav Keldysh" (2002). (a) General view of the building from the south-west side, (**b**) the cornice at the top of the building. The main representatives of macrofauna: *1 Maractis rimicarivora*, *2 Segonzacia mesatlantica*, *3* Polychaeta: Chaetopteridae, *4 Munidopsis crassa, 5 Phymorhynchus* sp., *6 Chorocaris chacei*, *7 Rimicaris exoculata* (adult), *8 R. exoculata* (juvenile), *9* Gastropoda: Peltospiridae, *10 Ophioctinella acies*, *11 Bathymodiolus puteoserpentis*, *12 Alvinocaris markensis*. Scale: a, **b** – 1 m; animals – 1 cm (Peltospiridae – 0.5 cm). Depth of the base of edifice 3,490 m

2.5.2 Taxonomic Composition and Spatial Structure of Community

The distribution of fauna in the immediate vicinity of black smokers of the Snake Pit hydrothermal area was first described by Segonzac [29], they also made the first landscape reconstruction. The total number of species of invertebrates recorded in the area, according to different sources, is at least 50. Taxa marking the zone directly adjacent to the hot vents are the Alvinocarididae shrimps. *Chorocaris chacei* and *Alvinocaris markensis* are more than *Rimicaris exoculata* confined to the base of edifices, away from the vent. Sea anemones *Maractis rimicarivora*, gastropods *Phymorhynchus* sp., galatheid crabs *Munidopsis crassa,* and the brittle stars *Ophioctinella acies* are common at the foot of the active buildings. In the same habitat the aggregations of the tubes of chaetopterid polychaetes were recorded [25]. Bivalves *Bathymodiolus puteoserpentis* form clusters on the active sites of the edifices not occupied by shrimps [30]. According to the data of Fornari et al. [31], the temperature in the area of mussels habitat reaches approximately 5°C.

Summarizing all the available data, on the distribution of the main representatives of the macrofauna one can identify the following patterns. The indicator species of the far periphery of the hydrothermal field are galatheid crabs *Munidopsis crassa* whose abundance is apparently increasing in 50–100 m from the edifices, and the chaetopterid polychaetes, single tubes of which are starting to occur on the surface of the lava pillows at about the same distance. Sharp increase of the abundance of chaetopterids and the appearance of sparse sea anemones approximately coincide with the advent of hydrothermal incrustation on basalts and sulfide crusts. The outlook of the nearest peripheral zone of the field in the studied area determines the mass settlements of *Maractis rimicarivora*, clusters of Chaetopteridae and gastropods *Phymorhynchus* sp. (probably represented by two species: *P. carinatus* и *P. ovatus*). At the basement of edifice the abundance of gastropods amounts up to 3–10 specimens per m^2. In the same zone crabs *Munidopsis crassa* and *Segonzacia mesatlantica* are common. The shrimps *Alvinocaris*, *Chorocaris,* and sparse *Rimicaris* (especially juveniles of the last) were also observed in this area.

The biotope of low-temperature outflows is occupied by the mussels *Bathymodiolus puteoserpentis*, whose existence required at least a weak inflow of fluid. Mytilids are most abundant at the base on Moose edifice and on the surfaces of the building outside settlements of shrimps. Mussels form dense aggregations (several hundred individuals per m^2) in the places of low-temperature fluid discharge, sometimes in weakly shimmering water. Generally they are confined to cracks and depressions of relief. Mussel beds are inhabited by diverse small animals. Numerous limpets, polychaetes Hesionidae and Ampharetidae, brittle stars Ophioctinella acies, small Bryozoa, nematodes, Harpacticoida (fam. Ectinosomatidae), ostracods and copepods were found associated with mussels.

The appearance of the zone of intense shimmering water and warm black smokes determine dense swarms of *Rimicaris exoculata* that occupy the largest area in the upper third of the building. Juveniles of *Rimicaris* generally gravitate to

the external less temperature zone, although single specimens occur also in the clusters of adult forms. Carnivorous shrimps *Chorocaris* and *Alvinocaris* are found at all hydrothermal field, but there are most abundant at the surfaces of active edifices, free from accumulations of *Rimicaris*.

Limpet gastropods *Peltospira smaragdina* (fam. Peltospiridae) were often observed in dense aggregations (several hundred individuals) on cornices close to shimmering water zone. They are also abundant on sulfide surfaces occupied by shrimp's populations. As against, limpets *Pseudorimula mesatlantica* (also fairly abundant) are obviously associated with mussels.

Overall an exceptionally complex morphology of the Moose edifice, a variety of forms of the fluid discharge, and a complex picture of the local convective flows exclude simplified version of zonation. Diverse microhabitats within the active site are used by different groups of organisms (Fig. 6). Besides some aggregations (as,

Fig. 6 Snake Pit hydrothermal area, depth 3,485 m. Microdistribution of animals at Moose hydrothermal edifice. *On the left center* is a white smoker. *At the top* – the settlement of bivalves *Bathymodiolus puteoserpentis* and clusters of adult shrimps *Rimicaris exoculata*. On the walls of the smoker *Rimicaris exoculata* juveniles. *Below* – an accumulation of carnivorous gastropods *Phymorhinchus* sp. *Centre right* – gastropod's egg masses attached to sulfide formations

for example, clusters of mobile *Alvinocaris* or clusters of different age stages of *Rimicaris*) are obviously ephemerous.

However in general terms the zonation of hydrothermal fields of Snake Pit quite fit into the scheme, known in other deep-sea MAR vent areas. The main feature is the dominance of sea anemones, gastropods, and chaetopterids in the peripheral part of the field and at inactive sites and domination of bresilioid shrimps (primarily, *Rimicaris exoculata*) in the zones of shimmering water and black smokes. Bathymodiolin mussels occupy in some sense an intermediate biotope of low-temperature seeps. Mussels don't occur outside the active zone as well as in the accumulation of shrimps (although sometimes live side by side with them).

It should be noted that in quantitative terms the population of shrimps on the Beehive site is, apparently, one of the largest in the Atlantic. The complete absence of mytilids on the Beehive site (in the presence of abundant clearly independent population on the nearby Moose) remains a fact requiring explanation.

3 East Pacific Rise (EPR)

Hydrothermal areas of the northern part of EPR are characterized by sulfide edifices, black smokers and diffuse emissions through the sulfide and fractures in the basalts. The temperature of the fluids amounts up to 340°C. Hydrothermal fluid at EPR is weakly modified in comparison with primary solution. The fluid is characterized by a high concentration of chlorine, H_2S, metals, and methane [4, 10, 32, 33]. The surface of the rift valley is composed of basalt. Hydrothermal ecosystems of the East Pacific rise (ECP) have a high species diversity, complex, and changeable structure of hydrothermal communities.

At the East Pacific Rise we studied one hydrothermal area: 9°50′N.

3.1 9°50′N EPR

Locality: 9°48′–51′N; 104°17′W. Depth 2,480–2,580 m.

3.1.1 Abiotic Environment

The 9°50′N vent field at the EPR is interesting primarily for two reasons. First, it is located in the axial rift zone of the most fast-spreading basalt ridge (>11 cm $year^{-1}$). Second, repeated volcano eruptions periodically happened during the last 15 years and destroyed most of the living communities, resulting in evolutionary changes of the geochemical medium and recovery of the biotopes [34]. Two types of hydrothermal vents are developed at this field: low-temperature diffuse seeps and high-temperature vents with sulfide mounds and black smokers. Examined in our

expeditions active hydrothermal sites are located along the deep canyon (axial cracks), stretching from North to South. The bottom and walls of the canyon are composed of very young pillow lavas. A characteristic element of background landscape are high lava columns with ribbed surface. During the recent eruptions these columns served as channels for molten lava. Later some of them became part of the hydrothermal circulation system.

3.1.2 Taxonomic Composition and Spatial Structure of Community

The distribution of fauna at the sites of 9°N EPR was studied in detail during the expedition of RV "Akademik Mstislav Keldysh" in 2003.

Most high-temperature hydrothermal faunal assemblage is confined to diffuse seeps on the walls of active sulfide structures adjacent to places of discharge of the hot fluid (black and white smokers) (Fig. 7). The greatest tolerance to high temperature demonstrates "Pompeii worms" – polychaetes *Alvinella pompejana*. These animals are able to withstand temperatures of over 40°C. Tubes of polychaetes densely covered with bacterial owergrow. With Pompeii worms are associated *Alvinella caudata*, and motile polychaetes (Nereidae and Polynoidae).

The most characteristic representatives of the hydrothermal fauna of the immediate environment of the field are the giant vestimentiferans *Riftia pachyptila*. Tubes of this species reach over a meter in length. The requirement of vestimentiferans of high enough concentrations of fluids causes their localized distribution on hydrothermal field. They usually occur in groups, in places of warm outflows marked by shimmering water. At a relatively young hydrothermal sites vestimentiferans dominate. In the older sites mature tubes of vestimentiferans are often hidden under mussel beds (*Bathymodiolus thermophylus*). Vestimentiferan clusters and mussel beds are inhabited by numerous and diverse fauna [35]. On mytilid shells small limpets (fam. Lepetodrilidae) were abundant. Among them, *Lepetodrilus ovalis*, *L. elevatus,* and *L. cristatus* are most numerous. Small gastropods from the family Trochidae (*Bathymargarites* sp.) were common in this zone. In the water column above the clumps of vestimentiferans, and sometimes above mussel beds, in places of diffuse outflows dense clusters of obligate (endemic) amphipods *Halice hesmonectes* (fam. Pardaliscidae) were observed. These "swarms" represent a rare example of purely pelagic hydrothermal assemblage. According to the estimation of Van Dover et al. [36], the density of amphipods reaches more than 1,000 ind./L and represent the most massive accumulations of pelagic animals at great depths.

The areas devoid of mytilids, in the zone of low-temperature seeps are inhabited by large vesicomyid bivalves *Calyptogena magnifica* (see Figure 10 in the Chapter Galkin S.V. "Structure of hydrothermal vent communities"). They reach a length of 20 cm and usually are imbedded in crevices of basalt. Near the clam's settlements gastropods, serpulid polychaetes and barnacles are common. Near the accumulations of bivalves and outside of the active sites is quite common giant picnogonids *Collosendeis colossea*. On the active sites large mobile carnivorous

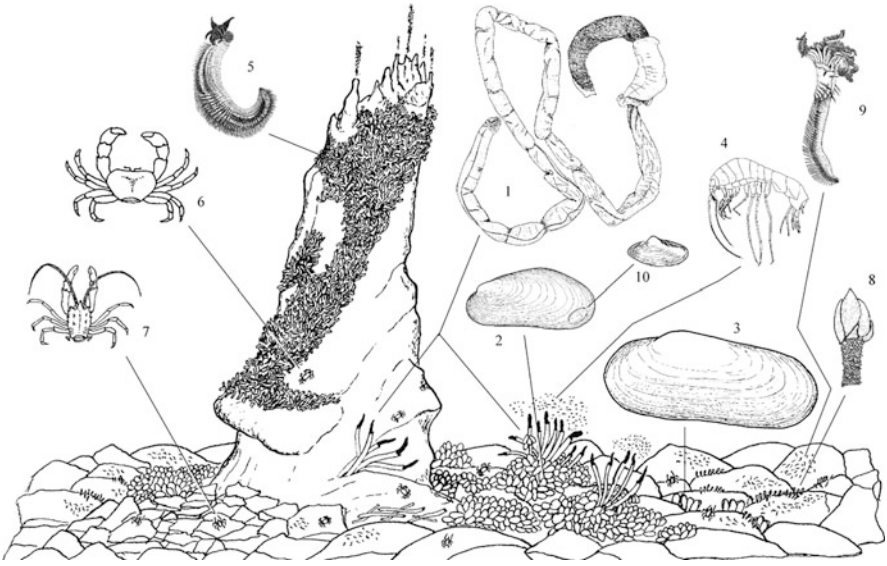

Fig. 7 9°N EPR hydrothermal area. Distribution of animals at the site BV (9°50,97′N; 104°17,59′W; depth 2,517 m). The hydrothermal edifice is 5 m high, diameter at base about 2 m. The view from the North-East. The reconstruction is performed on the basis of direct observations, analysis of videos and photographs obtained in the DSRV "Mir-2" (dive #22/360). Dominant fauna: *1 Riftia pachyptila, 2 Bathymodiolus thermophilus*, *3 Calyptogena magnifica, 4 Halice hesmonectes*, *5 Alvinella pompejana, 6 Bythograea thermidron, 7 Munidopsis subsqamosa, 8 Neolepas zevinae, 9 Laminatubus alvinae, 10 Lepetodrilus* aff. *elevatus*

crabs *Bythograea thermidron* are quite numerous. They eat live mussels and (or) their remains. Similar type of feeding is characterized the large gastropods *Phymorhynchus*, also common in the settlements of mytilids.

At the periphery of hydrothermal sites the aggregations of serpulid polychaetes of two obligate (endemic) hydrothermal species *Laminatubus alvinae* and *Protis hydrothermica* are common. According to our estimates, the number of polychaetes reaches up to 180–220 ind./m^2. Other typical inhabitants of the nearest periphery of the field were lepadomorph barnacles of the genus *Neolepas*. These sessile suspension-feeding animals sometimes form a thick "brush" on the rocks. Food for suspension-feeding assemblages of the peripheral zone provides the bacterial suspension, which is present in abundance in water surrounding the vent field. At the base of the basalt columns in crevices of lava pillows a small white octopuses *Vulcanoctopus hydrothermalis* (obligate hydrothermal genus) were repeatedly observed. At inactive sites of the canyon red and white shrimps (fam. Nematocarcinidae) and galatheid crabs *Munidopsis subsquamosa* are common. These animals do not belong to a specific hydrothermal taxa, however, the number of them markedly increases when approaching the active sites.

4 Guaymas Basin

Locality: 27°00′N, 111°24′W. Depth: 1,950–2,050 m.

4.1 Abiotic Environment

The vent area of the Guaymas Basin in the Gulf of California has some differences from other fields. The intense tectonic activity in this area is caused by the displacement of the Baja California peninsula towards the NW at a spreading rate of about 6 cm per year [37, 38]. An exceptional feature of the semi-enclosed Guaymas Basin (Gulf of California) hydrothermal vent area is the thick (>500 m) organic-rich sedimentary cover on the seafloor. This cover is a result of high (1–2 mm/year) sedimentation rates due to Colorado River sediment input directly before dam construction or tidal resuspension of previously supplied terrigenous sediments in the Upper Gulf of California [39, 40] and biogenic particles from the highly productive euphotic zone (>500 mg/m^2 per day) [41, 42]. High-temperature fluids are discharged to the surrounding seawater through the vents and by ascending through the overlying sediments, which are rich in Mn. This leads to the enrichment of fluids for Mn relative to Fe [43], which is a characteristic feature of Guaymas Basin fluids compared to other vent fields. This differs from the hydrothermal vent fluids of the Mid-Atlantic Ridge and 9°50′N of the East Pacific Rise, where Fe is found in higher concentrations than Mn [14, 44]. The surface sediments of the Guaymas Basin also have a Mn-oxide-rich and (relatively) Fe-oxide-rich turbidite layer that affects the distribution of C, Fe, Mn, S, and some trace metals [45]. Iron is mainly pyritized in the sediments, while Mn is found predominantly in carbonates (41 ± 12 %) and is associated with pyrite to a much lesser degree; Co, Cr, Cu, Ni, and Zn were highly pyritized (>80 %) in the sediments of the Guaymas Basin [45]. The low-temperature hydrothermal mineral associations on the floor of the Guaymas Basin are represented by opal and barite, while pyrrhotite, sphalerite, and chalcopyrite are the dominant ore minerals in high-temperature areas [46]. It is interesting to note that both mineral formations contain oil hydrocarbons, with a content of Corg in the surface sediments ranging from 0.15% (high-temperature area) to 2.23% (low-temperature area) [46] and reaching up to 6.21% in some deposits saturated with hydrocarbons. More than a hundred high-temperature hydrothermal mounds (black smokers) in an area of 30 km^2 were discovered and described by [41]. Sulfide chimneys commonly grow through overlying sediments and can reach heights of more than 25 m. High-temperature fluids (maximum temperatures of up to 315°C) are emitted from the vents into the surrounding water. Warm fluids flow through the chimney walls and ascend past the sedimentary cover, which is enriched with organic matter. This leads to a complicated transformation of organic matter into hydrocarbons and methane [43] that is characteristic of the Guaymas Basin fluids compared to other

known vent fields. A characteristic element of the Guaymas Basin landscape are extensive bacterial mats of white, cream, and orange, reaching a few centimeters in thickness and covering the space of hundreds of square meters.

4.2 Taxonomic Composition and Spatial Structure of Community

In 1986 and 1990, hydrothermal communities of the Guaymas Basin were studied by Russian expeditions using the submersibles "Pisces" and "Mir." In the area of hydrothermal activity around 40 species of macrofauna were recorded, their distribution was visually studied in a series of dives.

Abundant settlements of vestimentifera *Riftia pachyptila*, reaching up to 1 m length and occupying areas of up to hundreds m^2, were detected in the shimmering water at the hydrothermal chimney surfaces. These thickets are inhabited by numerous organisms, most notable of which are polynoid polychaetes, limpets, and bythograeid crabs. All vestimentiferans tubes are covered with bacterial fouling, obviously used as food by grayzers and deposit feeders. In areas free of vestimentiferans, but covered with bacterial mats, the settlements of alvinellid polychaetes *Paralvinella bactericola* were observed. The population of small (1–2 cm) anemones is located on the surface of the edifices often in shimmering water. At the basement of the buildings accumulate dead vestimentiferans tubes. Here carnivorous galatheids *Munidopsis* and some gastropods are most numerous. Large crabs Lithodidae were often observed near the edifices but also noted in the settlements of vestimentifera. On sediments, in areas of diffuse seepage, thick bacterial mats are developed (Fig. 8), under which the polychaetes *Ophryotrocha* are abundant.

The basic group of fauna inhabiting the soft sedimentary cover is the vesicomyid clam *Archivesica gigas* whose settlements can accumulate up to hundreds specimens per m^2. These communities of organisms are nutritionally dependent on the chemosynthetic bacterial community and are typically surrounded by accumulations of the bivalve mollusks *Nuculana grasslei* [47]. Sediments soaked with hydrocarbons serve as a substratum for these organisms. Chimney walls and bases are inhabited by *Munidopsis alvisca* crabs (predator), *Spongia* (filter-feeder), and *Phelliactis pabista* (filter-feeder and predator). The latter were often attached to the shells of the vesicomyid clam *Archivesica gigas*. Thick bacterial mats (with a thickness of up to a few cm) cover significant areas (hundreds of m^2).

Complex configuration of edifices (overhanging eaves, ledges, secondary chimneys) increases habitat diversity and strongly masks the zonal distribution of animals. However, a few prominent zones can be identified in the Guaymas Basin's hydrothermal vent field, each of which is dominated by certain megafaunal groups: (1) the euthermal or shimmering water zone (ambient temperature of about 25–30°C), where vestimentiferans commonly live; (2) the oligothermal zone

Fig. 8 Guaymas Basin hydrothermal area, depth ca. 2,000 m. Bright bacterial mats with thickness up to several centimeters on loose sediment at the foot of the sulfide structures – a characteristic element of the landscape of the Southern Trough

(temperatures of 3–6°C to 25°C), which is populated by vesicomyid clams; (3) the periphery of the vent zone (near-field, with very low or absent temperature anomalies), where specialized suspension-feeders consuming bacteria are the predominant taxa; and (4) the periphery of the vent zone (far-field, without temperature anomalies), which is occupied by non-vent suspension-feeders and carnivores and deposit feeders [32].

5 Concluding Remarks

The discussed above hydrothermal vent areas exhibit a wide range of environmental conditions, including great variation in depth (particularly on the MAR), associated physical parameters, and different geologic setting and underlying rocks. The MAR is a slow spreading ridge (spreading rate <6 cm/year), and the EPR is a fast-spreading ridge (>6 cm/year). In addition, the hydrothermal fields differ in depth, geologic structure, and rock composition, which results in different maximum fluid

temperatures, pH, and concentration levels of reduced compounds and metals. The youngest (less than 100 year) and shallowest (850 m deep) Menez Gwen field is located at the base of a volcano and associates with axial basaltic magma chambers. Low-temperature diffuse vents with T° up to 274°C are dominant in this field. Other fields comprise mainly high temperature (highest temperature of 405°C) vents (black smokers). In contrast to other sites considered in this paper, hydrothermal circulation at the Rainbow field is confined to ultrabasic rocks, the interaction of which with seawater penetrating along fractures results in anomalously high contents of hydrogen (low pH) in the fluids and extensive abiogenic methane formation. A distinctive feature of the hydrothermal field of the Guaymas Basin (Gulf of California) is the presence of a thick sedimentary cover enriched in organic matter owing to the very high sedimentation rates and the high productivity of the photic zone. At this site, high temperature fluids discharge into the bottom water through vents and also percolate through the overlying reduced sediments enriched in Mn. This results in the enrichment of fluids in Mn relative to Fe which is a characteristic feature of fluids from the Guaymas Basin, distinguishing them from the fluids of other fields. Faunal communities of studied areas also vary greatly in taxonomic composition and spatial structure. Especially strongly differences in taxonomic composition exhibit the communities of the Pacific and Atlantic Oceans. Between these two regions there are practically no shared species. The shallowest Atlantic area Menez Gwen has a lot of differences from deeper areas of the MAR. Herewith the depth was suggested as the main factor determining the differences between MAR hydrothermal vent communities [48]. Besides landscape circumstances, type of substrate, morphology of hydrothermal edifices, etc. are also important factors determining microdistribution of animals. Of the variety of factors determining fauna distribution, temperature and substratum characteristics are the easiest to estimate during bottom observation. Precise data is lacking in most cases, but numerous visual observations accompanied by temperature estimations have found that black smokers have a temperature in the range 275–400°C, while white smoker temperature varies from 100°C to 250°C [49]. Diffuse outflows of different types have a lower temperature, and are marked by a characteristic "shimmer" of water (the optical effect appearing by mixing of fluids of different density). This effect is clearly observed in the temperature anomalies in 3–6°C and more [50]. The heat extreme for most vent zone inhabitants seems to be about 25–40°C. Along with all the variety of hydrothermal manifestations, in the spatial structure of communities a number of general patterns can be revealed. Thus, the high temperature zone directly adjacent to black and white smokers is occupied in the Atlantic by the assemblage of shrimps *Rimicaris exoculata* while in the Pacific – by the assemblage of alvinellid polychaetes (*Alvinella pompejana* and *A.caudata*). Shrimps and alvinellids inhabit warmer zones with temperatures ranging from 20°C to 40°C. The bathymodiolin mussels under investigation reside in the zone of warm diffuse outflows at temperatures from 2°C to 20°C. Due to mixotrophic mode of feeding, bathymodiolins are widely distributed within the field and occur not only in shimmering water zone but also outside them. Siboglinids (vestimentiferans) may occur together with mytilids, but more often they settle closer to hydrothermal

vent emissions and live at temperatures exceeding 20°C. On the contrary, vesicomyid clams are confined to weak outflows and practically never were recorded in shimmering water. Mobile predators and scavengers (mostly crustaceans, large gastropods) are distributed all over the field. The scavengers are especially abundant at the periphery of vent sites and at the foot of high edifices where organic remains accumulate. Filter feeders using advective currents of water are characteristic for the periphery of the fields. Their distribution is largely determined by the availability of suitable substrate.

At the analysis of bioaccumulation function of vent organisms in the case of each area particular habitat conditions and characteristics of spatial structure of communities (microdistribution of animal's populations, their association with a specific temperature zone and a particular type of substrate) must be taken into account.

Acknowledgements The authors are grateful to Captain Yuri Gorbach of the R/V *Akademik Mstislav Keldysh* and his crew for their essential collaboration during the cruises. We also acknowledge Dr. A. Sagalevich and the *MIR* pilots and team for their constant support. We thank all submersible observers for sharing observations and samples and a great many of experts for identification of animals. This work was funded by the Russian Science Foundation (Grant No. 14-50-00095) (analyses and generalization of the material). The research has also received funding from the European Union Seventh Framework Programme (FP7/2007-2013) under the MIDAS project, grant agreement Nr 603418.

References

1. Desbruyères D, Biscoito M, Caprais J-C et al (2001) Variations in the deep-sea hydrothermal vent communities on the Mid-Atlantic Ridge near the Azores Plateau. Deep-Sea Res 48:1325–1346
2. Demina LL. Trace metals in water in the hydrothermal biotope. Hdb Env Chem. doi:10.1007/698_2016_1
3. Demina LL, Galkin SV. Factors controlling the trace metal distribution in hydrothermal vent organisms. Hdb Env Chem. doi:10.1007/698_2016_5
4. Demina LL, Holm NG, Galkin SV, Lein AY (2013) Some features of the trace metal biogeochemistry in the deep-sea hydrothermal vent fields (Menez Gwen, Rainbow, Broken Spur at the MAR and 9°50′N at the EPR): a synthesis. J Mar Syst 126:94–105
5. Haase KM, Petersen S, Koschinsky A et al (2007) Young volcanism and related hydrothermal activity at 5°S on the slow-spreading southern Mid-Atlantic Ridge. Geochem Geophys Geosyst 8(11):1–17
6. Desbruyères D, Almeida A, Biscoito M et al (2000) A review of the distribution of hydrothermal vent communities along the northern Mid-Atlantic Ridge: dispersal vs. environmental controls. Hydrobiologia 440:201–216
7. Charlou JL, Donval JP, Douville E et al (2000) Compared geochemical signatures and the evolution of Menez Gwen (37°50′N) and Lucky Strike (37°17′N) hydrothermal fluids, south of the Azores Triple Junction on the Mid-Atlantic Ridge. Chem Geol 171:49–75
8. von Cosel R, Comtet T, Krylova E (1999) *Bathymodiolus* (Bivalvia, Mytilidae) from hydrothermal vents on the Azores triple junction and the Logachev hydrothermal field, Mid-Atlantic Ridge. Veliger 42(3):218–248
9. Bogdanov YA (1997) Hydrothermal ore manifistations of rifts of the Mid-Atlantic Ridge. Nauchnii Mir, Moscow, 166 p. (in Russian)

10. Lein AY (2006) Geochemistry and biogeochemistry of hydrothermal fluids. Bacterial production on active hydrothermal fields. In: Vinogradov M.V., Vereschaka A.L. (eds) Hydrothermal ecosystems of the Mid-Atlantic Ridge. Nauka, Moscow, pp 68–94 (in Russian)
11. Gebruk AV, Mironov AN (2006) Biogeography of Mid-Atlantic Ridge hydrotherms. In: Hydrothermal ecosystems of the Mid-Atlantic Ridge. Nauka, Moscow, pp 119–162 (in Russian)
12. Fouquet Y, Charlou JL, Ondreas H et al (1997) Discovery and first submersible investigations on the Rainbow hydrothermal field on the MAR (36°14′N). EOS Trans AGU 78(46):F832
13. Holm NG, Charlou JL (2001) Initial indications of abiotic formation of hydrocarbons in the Rainbow ultramafic hydrothermal system, Mid-Atlantic Ridge. Earth Planet Sci Lett 191:1–8
14. Douville E, Charlou JL, Oelkers EH et al (2002) The Rainbow vent fluids (36°14′N, MAR): the influence of utramaphic rocks and phase separation on trace metals content in Mid-Atlantic Ridge hydrothermal fluids. Chem Geol 184(1):37–48
15. Bogdanov YA (2006) Geological preconditions of the diversity of Mid-Atlantic Ridge hydrothermal fauna. Hydrothermal ecosystems of the Mid-Atlantic Ridge, Nauka, Moscow, pp 19–36 (in Russian)
16. Kelley DS, Karson JA, Blackman DK, Frűh-Green GL, Butterfield DA, Lilley MD, Olson EJ, Schrenk MO, Roe KK, Lebon GT, Rivizzigno P, The AT3-60 Shipboard Party (2001) An off-axis hydrothermal vent field near the Mid-Atlantic Ridge at 30°N. Nature 412:145–149
17. Kelley DS, Karson JA, Früh-Green GL, Yoerger DR, Shank TM, Butterfield DA, Hayes JM, Schrenk MO, Olson EJ, Proskurowski G, Jakuba M, Bradley A, Larson B, Ludwig K, Glickson D, Buckman K, Bradley AS, Brazerlton WJ, Roe K, Elend MJ, Delacour A, Bernasconi SM, Lilley MD, Baross JA, Summons RE, Sylva SP (2005) A serpentinite-hosted ecosystem: the Lost City hydrothermal field. Science 307(5714):1428–1434
18. Lein AY (2004) Role of bacterial chemosynthesis and metanotrophy in ocean biogeochemistry. In: New idea in oceanology I. Physics, chemistry, biology. Nauka, Moscow, pp 280–324
19. Gebruk AV, Galkin SV, Krylova EM, Vereshchaka AL, Vinogradov GM (2002) Hydrothermal fauna discovered at Lost City (30°N, Mid-Atlantic Ridge). InterRidge News 11(2):18–19
20. Vereshchaka AL, Galkin SV, Gebruk AV, Krylova EM, Vinogradov GM, Borowski C, The "Mir" submersibles team (2002) Biological studies using Mir submersibles at six North Atlantic hydrothermal sites in 2002. InterRidge News 11(2):23–28
21. Galkin SV (2006) Lost Village – a "faubourg" of Lost City: benthic studies using Mir submersibles at North Atlantic hydrothermal sites in 2005. InterRidge News 15:18–24
22. Murton BJ, Klinkhammer G et al (1993) Direct measurements of the distribution and occurrence of hydrothermal activity between 27°N and 37°N on the Mid-Atlantic Ridge. EOS 74:99
23. Murton BJ, Van Dover C (1993) Alvin dives on the Broken Spur hydrothermal vent field at 29°10′N on the Mid-Atlantic Ridge. BRIDGE Newsl 5:11–14
24. James RH, Elderfield H, Palmer MR (1995) The chemistry of hydrothermal fluids from the Broken Spur site, 29°N Mid-Atlantic Ridge. Geochim Cosmochim Acta 59(4):651–659
25. Van Dover CL (1995) Ecology of Mid-Atlantic Ridge hydrothermal vents. In: Parson LM, Walker CL, Dixon DR (eds) Hydrothermal vents and processes, vol 87, Geological Society special publication. Geological Society, London, pp 257–294
26. Kong L, Solomon LC, Pudry GM (1985) Microearthquake characteristics of a mid-ocean ridge along axis high. J Geophys Res 97:1659–1685
27. Mevel C, Auzende J-M, Cannat M, Donval J-P, Dubois J, Fouquet Y, Gente P, Crimand D, Karson JA, Segonzac M, Stievenard M (1989) La ride du Snake Pit (dorsale medio-Atlantique, 23°22′N): resultats preliminaires de la compagne HYDROSNAKE. C R Acad Sci Paris Ser II 308(6):545–552
28. Fouquet J, Wafik A, Cambon P, Mevel C, Meyer G, Gente P (1993) Tectonic setting and mineralogical and geochemical zonation in the Snake Pit sulfide deposit (Mid-Atlantic Ridge at 23°N). Econ Geol 88:1018–1036
29. Segonzac M (1992) Les peuplements associes a l'hydrothermalisme oceanique du Snake Pit (dorsal Medio-Atlantique; 23°N, 3480 m): composition et microdistribution de la megafaune. C R Acad Sci Paris 314(III):593–600

30. von Cosel R, Metivier B, Hashimoto J (1994) Three new species of *Bathymodiolus* (Bivalvia: Mytilidae) from the hydrothermal vents in the Lau Basin and the North Fiji Basin, Western Pacific, and the Snake Pit area, Mid Atlantic Ridge. Veliger 37(4):374–392
31. Fornari DJ, Van Dover SL, Shank T, Lutz R, Olsson MA (1994) Versatile, low-cost temperature sensing device for time-series measurements at deep-sea hydrothermal vents. BRIDGE Newsl 6:40–47
32. Galkin SV (2002) Hydrothermal vent communities of the World Ocean. Structure, typology, biogeography. GEOS, Moscow, 99 p (in Russian)
33. Demina LL, Galkin SV, Lein AY, Lisitzin AP (2007) First data on microelements composition of benthic organisms of the hydrothermal field 9°50′N (East-Pacific Rise) Dokladi Akademii Nauk 415(4):528–531 (in Russian)
34. Von Damm KL, Lilley MD (2004) Diffusive from hydrothermal fluids from 9°50′N East Pacific Rise: origin, evolution and biogeochemical controls. In: Wilcock WSO (ed) The subseafloor biosphere at midoceanic ridges, vol 144, Geophysical monograph. American Geophysical Union, Washington, DC, pp 245–269
35. Goroslavskaya EI, Galkin SV (2010) Composition and structure of mytilid and alvinellid assemblages at 9°N East Pacific Rise: comparative analysis. Cah Biol Mar 51:389–392
36. Van Dover CL, Kaartwedt S, Bollens S et al (1992) Deep-sea amphipod shwarms. Nature 6381:25–26
37. Klitgord KD, Mudie JD, Bischoff JL, Henyey TL (1974) Magnetic anomalies in the northern and central Gulf of California. Geol Soc Am Bull 85:815–820
38. Lonsdale P (1984) Hot vents and hydrocarbon seeps in the Sea of Cortez. Oceanus 27(3):21–24
39. Calvert SE (1966) Accumulation of diatomaceous silica in the silica sediments of the Gulf of California. Geol Soc Am Bull 77:569–596
40. Carriquiry JD, Sánchez A (1999) Sedimentation in the Colorado River delta and Upper Gulf of California after nearly a century of discharge loss. Mar Geol 158:125–145
41. Lonsdale PF, Bischoff JL, Burns VM, Kastner M, Sweeney RE (1980) A high-temperature hydrothermal deposit on the sea bed at Gulf of California spreading center. Earth Planet Sci Lett 49:8–20
42. De la Lanza-Espino G, Soto LA (1999) Sedimentary geochemistry of hydrothermal vents in Guaymas Basin, Gulf of California, Mexico. Appl Geochem 14:499–510
43. Von Damm KL, Edmond JM, Measures CI, Grant B (1985) Chemistry of submarine hydrothermal solutions at Guaymas Basin, Gulf of California. Geochim Cosmochim Acta 49:2221–2237
44. Von Damm KL (2000) Chemistry of hydrothermal vent fluids from 9-10°N, East Pacific Rise: "Time zero", the immediate posteruptive period. J Geophys Res 105:11203–11222
45. Otero XL, Huerta-Diaz MA, Macías F (2003) Influence of a turbidite deposit on the extent of pyritization of iron, manganese and trace metals in sediments from the Guaymas Basin, Gulf of California (Mexico). Appl Geochem 18:1149–1163
46. Bogdanov YA, Lisitzin AP, Sagalevitch AM, Gurvich EG (2004) Hydrothermal ore formation at the ocean floor. Nauka, Moscow, 528 p (in Russian)
47. Allen JA (1993) A new deep-water hydrothermal species of *Nuculana* (Bivalvia: Protobranchia) from the Guaymas Basin. Malacologia 35:141–151
48. Rybakova (Goroslavskaya) E, Galkin S (2015) Hydrothermal assemblages associated with different foundation species on the East Pacific Rise and Mid-Atlantic Ridge, with a special focus on mytilids. Mar Ecol 36:45–61
49. BRIDGE (1994) Workshop report no. 4. Diversity of vent ecosystems (DOVE), Marine Biological Association, Plymouth
50. Desbruyeres D, Alayse-Danet AM, Ohta S et al (1994) Deep-Sea hydrothermal communities in Southwestern Pacific Back-Arc Basins (the North Fiji and Lau Basins): composition, microdistribution and food-web. Mar Geol 116(1–2):227–242

Trace Metals in the Water of the Hydrothermal Biotopes

Liudmila L. Demina

Abstract Hydrothermal vents on the ocean floor are surrounded by geochemical barriers that have been caused by extreme gradients of water temperature and concentrations of reduced compounds as well as trace metals. Now it is known that water of the faunal hydrothermal biotopes consists mostly of the diluted hydrothermal fluids while the biological communities concentrate many trace metals due to bioaccumulation processes. Thus the deep-sea hydrothermal vent fields represent geochemically interesting areas where processes of trace metal dispersion and concentration coexist. In spite of the numerous publications on hydrothermal fluid biogeochemistry, some unsolved problems caused by the complexity of hydrothermal systems still remain. In this chapter, an attempt is made to summarize the available data on the trace metal distribution in the water of hydrothermal vent community habitats. These data allow us to understand that there is a difference in trace metal concentration in the water of biotopes of the different vent sites. Here a trace metal chemical speciation in the water of biotope is considered briefly as soon as it influences the ability of hydrothermal organisms to accumulate trace metals.

Keywords Biological communities, Biotope water, Hydrothermal vent fluids, Trace metals

Contents

L.L. Demina (✉)
P.P. Shirshov Institute of Oceanology Russian Academy of Sciences (IO RAS), 117997, Nakhimovsky pr., 36, Moscow, Russia
e-mail: l_demina@mail.ru

L.L. Demina, S.V. Galkin (eds.), *Trace Metal Biogeochemistry and Ecology of Deep-Sea Hydrothermal Vent Systems*, Hdb Env Chem (2016) 50: 53–76,
DOI 10.1007/698_2016_1,
Published online: 27 February 2016

1 Introduction

The hydrothermal environments are characterized by high concentrations of many trace metals originating from discharge of hydrogen sulfide-rich vent waters [1, 2]. While mixing hydrothermal vent fluids with near-bottom ocean waters, a simple (conservative) dilution of fluid with seawater takes place, and the main tracer of this process was found to be temperature [3]. However, the relative importance of different factors (other than temperature) is still not fully accepted as direct "in situ" observations confirm the high variability of parameters within the same animal populations. Physical–chemical conditions of the habitat of organisms are generally considered as the main factors determining the distribution of organisms within the limit of hydrothermal vent field [4–7].

The goal of this chapter is to present distinctive features of the trace metal biogeochemistry in the water of biotope of some deep-sea hydrothermal ecosystems: the Menez Gwen, Rainbow, Lost City, Broken Spur, and Rainbow at the Mid-Atlantic Ridge (MAR), as well as the 9°50′N at the East Pacific Rise (EPR) and the Guaymas Basin (Gulf of California). These hydrothermal fields differ in temperature of fluids discharging from the vents; depth; spreading velocity of the ocean crust from the ridge crest, slow spreading (<6 cm year^{-1} at the MAR) versus fast spreading (>11 cm year^{-1} at the EPR); geological structure; basement composition (basaltic or ultramafic rocks), etc. (See Table 1 in Galkin and Demina [8]).

The biotope water samples ($n = 46$) were taken from the macrozoobenthos settlements. These were a relatively high-temperature shimmering water with shrimp colonies at the Rainbow and Broken Spur vent sites [9, 10], alvinellids and vestimentiferans inhabitants at the 9°50′N [11] and Guaymas Basin [12] vent sites, as well as mussel accumulations near the low- and high-temperature diffusers at the Menez Gwen and Rainbow vent sites, respectively [9]. The water samples were collected during the 49th and 50th cruises of the Russian research vessel "Akademik Mstislav Keldysh" (June–October, 2003, and July–August, 2005, respectively) using the "Mir-1" and "Mir-2" manned submersibles. Water samples were taken using 700 ml titanium syringes designed for sampling of hot fluids and Niskin bottles manipulated by the "Mir" submersibles. Aboard the ship the samples were transferred into the acid-washed flasks and acidified with nitric acid (super pure Merck, 69% v/v) to pH 2. Water samples were stored in a refrigerator until analysis of total dissolvable chemical elements. Concentrations of the chemical elements in the samples of biotope water were determined by methods of atomic

absorption spectroscopy (AAS flame and flameless) at the P.P. Shirshov Institute of Oceanology, Moscow, Russia, and inductively coupled plasma atomic emission spectroscopy (ICP-AES) at Stockholm University, Sweden. The analysis accuracy was controlled by the use of the international reference materials SLEW NRC-CNRC Estuarine Water Reference Material for Trace Metals. A comparison of metal contents in certified standard reference materials with the measured values has revealed that percentage recovery was 90–95% for Fe, Zn, Mn, Cu; 85–90% for Pb, Ag, Co, Cd, Cr; and 82–85% for Sb and Hg.

2 Hydrothermal Fluid-Bottom Ocean Water Geochemical Barrier and Alteration of Basic Characteristics of Fluids

In the heady early days of hydrothermal discovery, many scientists believed that the chemistry of hydrothermal solutions was simply a function of exit temperature [13]. Further discoveries demonstrated a much more complex universe of chemical variations [2]. The vent zone is known as the most chemically and spatially heterogeneous environment of a hydrothermal field. Turbulent outflow of the acid hot fluids, where concentration of trace elements is 10^2–10^6 times greater compared to the relatively cold near-bottom water, results in formation of a geochemical barrier with steep gradients of the physical and chemical parameters where, within a few tens of centimeters from the vent, the temperature decreases by tens of °C, while pH values increase from 2–3 to 5.6–6.8 [5].

According to measurements on board the *Mir* submersibles, temperature of the biotope water varied from 35°C (over the most thermophilic *Alvinella pompejana* at 9°N EPR) to 8°C (over the settlement of *Bathymodiolus azoricus* at Menez Gwen). The range of pH (measured on board the ship) variation was from 3.8 (over the most thermophilic *Alvinella pompejana* at 9°N EPR) to 7.49 over the clam colonies at the Guaymas vent field. H_2S concentration (measured on board the ship) decreased with pH growth and varied from 0.3 to 9.0 mg l^{-1} [14]. Abundance and biomass of bacteria increases a hundred times as compared to fluids [15, 16].

These factors create a powerful geochemical barrier with huge gradients of temperature, as well as of microbial biomass and concentration of toxic reduced compounds (H_2S, H_2, CH_4) which enter into the cold bottom water.

Some authors [17–19] concluded that mechanisms controlling characteristics of the fluids on the scale of active site are much more complex than a simple dilution of the "end-member" fluid with ocean water that does not allow for extrapolation of end-member composition of the fluid on the characteristics of the habitat of organisms [4]. Along with a simple (conservative) dilution of fluids with sea water, various physical–chemical and biogeochemical processes take place, resulting in a considerable decrease in the metal contents in the water of biotopes relative to fluids.

Strong fluctuations of chemical parameters are generally associated with the temperature changes; therefore, the temperature in the first approximation is considered as a main indicator of the chemical environmental condition [5, 7]. But there is also an inverse relationship: aggregated settlement of hydrothermal fauna, in particular symbiotrophic mussels and shrimps, redistributes chemical components of habitat, consuming from water hydrogen sulfide, sulfide ion, nitrates, and nitrites followed by excreting ammonium ion and dissolved organic carbon into the water of biotope. These observations were made by [4] based on the "Alchemist" flow injection analyzer in situ for measurement of the basic geochemical conditions: T^{o}, $\Sigma(H_2S + HS)$, and $\Sigma(NO_3^- + NO_2^-)$ in the diluted fluid of the diffuse vent and in water over settlements of hydrothermal animals on the Lucky Strike field (MAR). The maximum temperature (27°C), $\Sigma(H_2S + HS)$ (40 μmol), and a minimum of nitrate (15 mmol) were measured in the fluid, while at some distance from the vent where abundant clusters of shrimp were noticed and then in the water over mussel biotope, the temperature was lower by 10°C and 20°C accordingly, whereas $\Sigma(H_2S + HS)$ reduced to 2–5 μmol. On the contrary, the nitrate and nitrite concentrations in water over fauna settlements were higher than in the fluid. Similar distribution suggests a transformative fauna impact on the basic chemical environmental parameters, namely, the mussel community consumes the hydrogen sulfide and sulfide ions from the water and excretes nitrates and nitrites into the surrounding water to a greater extent than that of the shrimps [4]. H_2S and CH_4 fuels bacterial chemosynthetic communities which produce organic carbon for the bottom fauna [20].

At the Rainbow vent field, concentrations of chemical species that fuel bacterial autotrophy (ΣS, CO_2, CH_4, and NO_3) were significantly higher for *Rimicaris* and *Mirocaris* shrimp habitats than for *Bathymodiolus* mussels; the latter were present in very diluted environment with sulfide concentrations ranging from 0.7 to 1 μmol [4]. The abundance of chemolithoautotrophic bacteria and rates of the sulfide oxidation (CO_2 assimilation) and/or CH_4 oxidation commonly differ in various environments and decrease with distance from the hydrothermal vent and are different for various vent fields [15, 16].

To date hydrothermal biological community structure is thought to be shaped not only by temperature but also chemical speciation of particular elements which is modified as a consequence of the organism–habitat interactions [4, 5, 21].

3 Trace Metals in the Biotope Water of Some Deep-Sea Hydrothermal Ecosystems

Until recently, the attention of most researchers has been attracted to the study of hydrothermal vent fluids. It was summarized that the high-temperature hydrothermal vent fluids (calculated per "end-member," i.e., the fluid with zero Mg concentration) are enriched in methane, sulfide, and trace metals with respect to the

Table 1 Physicochemical properties, average concentrations of H_2S (mmol), CH_4, and trace metals (μmol) in the hydrothermal "end-member" fluids* of some the Mid-Atlantic Ridge (MAR), East Pacific Rise (EPR), and Guaymas Basin (Gulf of California) vent fields compared to the ocean water

Parameter	Ocean water [22, 23]	Menez Gwen, MAR [24]	Broken Spur, MAR [3]	Rainbow, MAR [24]	9°50′N, EPR [2]	Guaymas Basin [17]
T°C	2	271	360	365	405	315
pH	7.8	4.4	–	2.8	3.8	5.9
H_2S	0	1.5	9.3	1.6	9.0	5.3
CH_4	0.002	2.0	0.13	2.6	6.0	–
Mn	0.0013	59	254	2,250	321	236
Fe	0.0045	18	1,970	24,000	2,452	180
Cu	0.007	1.9	43	140	11.8	1.0
Zn	0.012	3.9	72	160	30.7	40
Ni	0.009	<2		3.0		
Sb	0.001	0.004		3.1		
Co	0.0002	<2		13		
Cd	0.0007	0.01		0.13		
Ag	0.00002	0.011		0.05	0.009	
Pb	0.0001	0.038		0.148		

*Mg concentration in the hot "end-member" fluids = 0 as it lost by formation of Mg-OH silicates that results in generation of H^+ which accounts for the low pH
Empty spaces indicate no data

background ocean water [22]. It is known that total sulfur (ΣS) in the ocean water is entirely in the form of sulfate-ion SO_4^{2-}, while in the water of hydrothermal biotopes, sulfur occurs mainly by hydrogen sulfide H_2S and HS^- ions, which serve as "fuel" for the processes of bacterial chemosynthesis and methanotrophy because the molecules of H_2S and CH_4 are electron donors during the chemosynthesis [20]. In the biotopes of shrimps and mussels, the concentration of total sulfur is higher than in ocean water that allows to assume the existence along with sulfate, H_2S, and HS^- in these water samples.

From Table 1 one can see the basic geochemical parameters of deep-sea hydrothermal fluids in comparison with the ocean water. Along with considerable enrichment of different types of fluids in trace metals compared to ocean water, the following can be seen. The high-temperature fluids from the black smokers at the hydrothermal vent fields at MAR (Broken Spur, Snake Pit, Rainbow etc.) and EPR (9°50′N and Guaymas) contain 50–1,000 times more Fe, Mn, Zn, Cu, and Sb and 5–20 times more Ni, Co, Cd, Ag, and Pb compared to the low-temperature hydrothermal solutions from the Menez Gwen field (MAR).

Over the recent time, the trace metal composition of diluted fluids, i.e., water above the hydrothermal fauna settlements, has been investigated in the following publications: [3–6, 9–12, 14, 21, 25].

Table 2 Concentrations of magnesium (mmol) and trace metals (μmol) in the water of biotope at the Menez Gwen, Rainbow, and Broken Spur deep-sea hydrothermal vent fields (MAR) compared to the ocean water

Some characteristics of water in different organisms habitats	Mg	Fe	Mn	Zn	Cu	Ni	Cr	Co	Pb	Cd	Ag	As	Sb
Menez Gwen													
pH 6.4, transparent, mussels habitats	46	0.50	0.85	1.21	0.08	0.24	0.02	0.20	0.022	0.004	0.003	0.43	0.02
pH 5.1, transparent, mussels habitats	39	2.78	12.9	29.2	10.8	0.30	0.08	0.23	0.030	0.008	0.025	0.15	0.05
pH 5.36, transparent, mussels habitats	52	6.55	3.79	0.15	4.25	0.19	0.08	0.20	0.028	0.003	0.020	0.12	0.02
Rainbow													
$T > 11$°C, shimmering water, shrimps habitat	56	1,138	2.65	4.59	0.98	0.015	0.01	0.11	0.038	0.010	0.005	0.37	0.46
$T > 11$°C, shimmering water, shrimps habitats	53	33.3	111	39.7	0.16	0.017	0.005	0.28	0.022	0.012	0.007	0.66	0.09
$T > 11$°C, shimmering water, shrimps habitats	54	171	4.15	1.19	2.04	0.014	0.02	0.12	0.016	0.009	0.008	1.32	0.16
Transparent, mussels habitats	71	0.16	5.62	0.55	0.14	0.066	0.05	0.01	0.011	0.002	0.006	0.40	0.71
Transparent, mussels habitats	50	0.54	7.31	2.75	0.35	0.039	0.015	0.05	0.02	0.005	0.007	0.21	0.17
Yellow opalescent, shrimps habitat	75	0.27	2.84	7.64	0.35	0.010	0.01	0.02	0.025	0.005	0.007	0.97	0.23
Black muddy	41	3,466	331	51.38	5.19	0.024	0.03	0.51	0.045	0.028	0.005	0.97	0.82
Transparent, mussels habitats	50	7.58	22.0	4.05	0.08	0.134	0.04	0.32	0.037	0.006	0.005	1.27	0.20
Broken Spur													
Shimmering water, shrimps habitats	66	5.37	1.31	3.59	2.04	0.72	0.01	0.033	0.01	0.134	0.009	0.17	0.08
Transparent, mussels habitats	59	1.29	0.22	0.30	0.33	1.61	0.01	0.003	0.01	0.029	0.002	1.28	0.04
Ocean water [23]	54	0.0045	0.0013	0.012	0.007	0.009	0.0048	0.0002	0.0001	0.0007	0.00002	0.022	0.001

Table 2 lists the measured concentrations of a number of trace metals and magnesium in the collected biotope water samples of dominant fauna at the Menez Gwen, Rainbow, and Broken Spur vent fields compared to the reference ocean water. At the Rainbow vent fields, the pH failed to be measured, but abnormally high temperature (>11°C) was recorded in the so-called shimmering water. The Rainbow and Broken Spur water samples were sorted into two groups as a function of the dominant fauna location. The so-called shimmering water of the Rainbow and Broken Spur vent fields is inhabited by shrimp communities, while the low-temperature diffusers provide habitats for symbiotrophic mussels (see [52]). At the Rainbow vent field, the water samples from areas influenced by high-temperature fluids (black smokers) were saturated with the fine-dispersed sulfides ("black" solutions), where very high concentration of Fe, Zn, and Cu has been registered.

One can see that the Mg concentration is quite close to the average value in the background ocean water that suggests a very high dilution of fluids (note that in the "end-member" fluids, Mg concentration is close to the analytical zero). In some cases the concentration of Mg (71 mmol) is even a little higher than in the ocean water. Approximately the same result, though also without explanation, was obtained for some vents at the Menez Gwen and Lucky Strike vent fields [5].

Data listed in Table 2 show that trace metal concentrations in the water of biotope of the Menez Gwen, Rainbow, and Broken Spur vent fields are much higher as compared with the ocean water. Despite strong dilution of hydrothermal vent fluids, water of biotope is enriched with metals respectively to the ocean water from one (As, Sb) to five (Fe) orders of magnitude. The high concentrations have been detected for Fe, Mn, Zn, Co, and Pb in water samples collected in the area influenced by the high-temperature fluid from Rainbow black smoker. High content of Co was caused by influence of host ultramafic rocks. Cu, Ni, Ag, Cd, As, Sb, Se, and Hg were found in concentrations 2–3 orders of magnitude higher than in reference ocean water, and Cr showed the minimal enrichment (half order of magnitude) with respect to ocean water.

It is known that the low pH, the high temperature, and the Cl^- ion concentration induce Cl complexes dominating fluid speciation, which results in the formation of aqueous metal chloride complexes. However there is no clear evidence that Cd and Sb concentrations increase with increasing aqueous chloride concentrations [24]. Transition and trace metals variability obviously is linked with their great affinity to form sulfide and Fe–Mn hydroxide precipitates, including possible precipitation in the sampler.

The Menez Gwen water of biotope with $pH > 4$ is known to be enriched in gases, mainly in CO_2 (75% of the amount of gas) and to a lesser extent in H_2S (10–20%). On the contrary, the fluids of the Rainbow and Broken Spur vent sites that passed phase separation [26] are enriched in chloride ions and associated heavy metals, most of which show here the maximum concentrations in the tens to hundreds of times greater than those in the background ocean water (Table 2). The Broken Spur vent field is one of the youngest fields at MAR. It is located on basalt basement and consists of massive sulfide edifices, predominantly with focused high-temperature

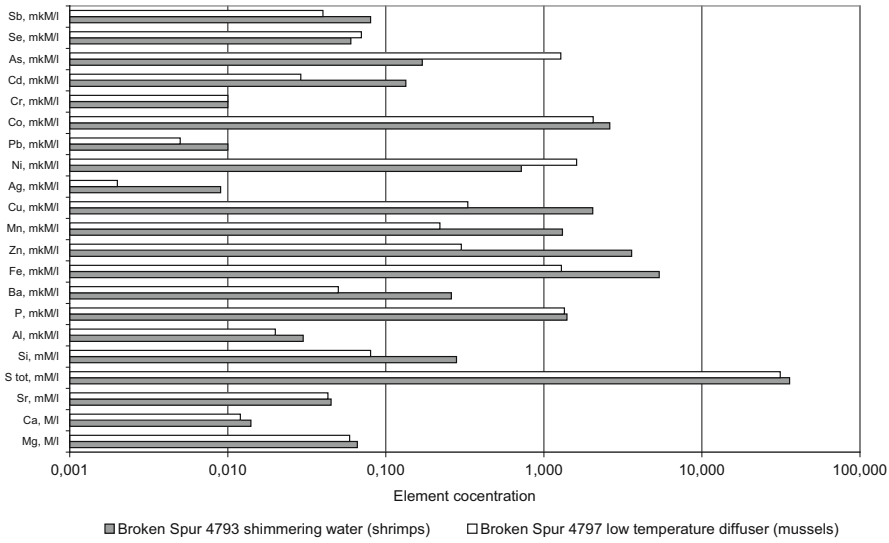

Fig. 1 Chemical element concentrations in shimmering water above shrimp settlements and in low-temperature diffusers above mussel settlements at the Broken Spur vent field (MAR)

vent fluids. The Broken Spur main feature is its extremely high concentration of hydrogen sulfide: to 11 mmol [3].

It should be noticed that our data on trace metal concentrations in the water of biotopes of the Broken Spur are close in order of magnitude to data of [3], obtained for the diluted fluid of this field.

According to [27], mussels at the MAR hydrothermal fields demonstrate the highest concentration of Mn at the Rainbow and Lucky Strike vent fields – 5 and 13 μmol respectively. At the Menez Gwen, Al, Mn, Co, Cd, and Hg showed the reduced concentrations.

It is known that low pH, high temperature, and high concentrations of Cl^- ions cause dominance of Cl complexes among other forms of dilute fluids that promote the formation of dissolved chlorine complexes with trace metals. However, there is no reliable evidence that the concentration of dissolved Cd and Sb depends on the growth of the Cl complex concentration in the water [24]. Most likely, it seems to be an influence of sulfide-forming trace elements which form sulfides upon concentration of the various sulfur forms and particles of the Fe–Mn (oxy)hydroxides concentration in the water of biotope.

Our data on the Broken Spur biotope water show that in the shimmering water (with higher temperature) inhabited by shrimp populations, concentrations of most part of trace metals (with the exception of As and Ni) were higher than that above the mussel biotope (Fig. 1). This confirms that an influence of hot fluids upon the trace element concentrations decreases with a distance from the vent. It is interesting to note that "end-member" fluid concentration of Fe, Mn, Cu, and Zn in the vent fluids of the Rainbow field was much higher compared to those at the Broken Spur

[3, 19, 24]. Despite this, a difference between the concentrations of metals in the water of biotope of these two fields does not exceed one order of magnitude. As a whole, our data on the Pb, Cu, Cd, Mn, Fe, Co, and Zn concentrations in the water of the shrimps and mussel biotopes at the Rainbow vent field are similar to those of [4, 21].

The Lost City vent field is the most low-temperature one: there are numerous white smokers with temperature of fluids from <40 to 90°C. The vents are located on the seafloor mountain Atlantis Massif, where reactions between seawater and upper mantle peridotite produce methane- and hydrogen-rich fluids that are highly alkaline (pH 9–11) [28–30]. At the Lost City hydrothermal field, we examined the chemical composition (Table 3) of warm ($T = 24$–36°C) diluted fluids emitted from the snow-white porous carbonates composed of the authigenic aragonite, calcite, Na–Ca carbonate, and brucite, some of them being covered with bacterial mats. The measured concentration of Mg at two stations was lower than in the ocean water. The highest H_2S concentration (8 mg/l) in the least diluted fluids corresponded to the minimal Mg (21.6 mmol). The presence of sulfate-ion SO_4^{2-} with rather high concentrations (from 11.99 mmol/l in the least diluted samples to 24.84 mmol/l in the most diluted ones) is characteristic for these fluids. The other distinguished feature is the relatively high concentration of As (about 1–2 mmol), which is comparable with that of Cu and Ni. This could be caused by analogy with the low-temperature hydrothermally induced water near back-arc basins and island arcs which are known to be enriched in As compared to deeper-situated Mid-Ocean Ridges likely due to their different environmental conditions.

The trace metals in the Lost City diluted fluids have revealed elevated concentrations (from 1 to 4 orders of magnitude) with respect to ocean water. Fluids having the higher H_2S concentrations contain more Co, Zn, Ni, and Cr than the more diluted ones, while in the case of Fe, Mn, Ag, Pb, Cd, and As, there was no clear difference. The concentrations of trace metals in the low-temperature Lost City diluted fluids were much lower (except As) than in the water samples collected above shrimps and mussels habitats of the high-temperature Broken Spur and Rainbow vents (see above).

The hydrothermal field 9°50′N at the East Pacific Rise (EPR) is located in the axial part of the rift zone of high-spreading ridge with the highest rate of basaltic crust formation (>12 cm/year). The physical–chemical parameters and concentrations of chemical elements measured in the diluted fluids are listed in Table 4.

Data of Table 4 shows that different trace metals enrich water of biotopes in different ways, demonstrating strong fluctuations in the concentrations in different areas within the same hydrothermal field depending on the type of emission and the vent location (mouth, slope, or foot of sulfide edifice), as well as on the degree of fluid's dilution, i.e., the temperature, pH, Eh, and concentration of H_2S. In the least diluted fluids emanating from the black smokers (Stations 4626, 4632, 4668) with lower concentrations of Mg, reduced values of Eh and pH, and increased H_2S concentrations, we have registered elevated concentrations of trace metals. High-temperature ($T > 330$°C) vent fluids supply large masses of metals which when mixed with seawater undergo various physical and chemical changes, as was mentioned above.

Table 3 Average concentrations (± standard deviation) of magnesium, hydrogen sulfide (mg l^{-1}), sulfate-ion (mmol), and trace metals (μmol) in the water of biotope at the Lost City vent field compared to the ocean water

Station	Property of biotope water	Mg	H_2S	SO_4^{2-} mmol	Fe	Zn	Mn	Cu	Ag	Ni	Pb	Co	Cr	Cd	As
Lost City															
4800	Transparent, $T = 24°C$ ($n = 3$)	21.3 (±2.2)	8.0 (±0.5)	11.99 (±5.5)	6.07 (±0.9)	0.66 (±0.08)	0.19 (±0.003)	0.024 (±0.005)	0.008 (±0.003)	0.33 (±0.04)	0.006 (±0.001)	0.32 (±0.02)	0.07 (±0.01)	0.005 (±0.001)	0.94 (±0.01)
4803	Opalescent, $T = 32°$ ($n = 3$)	43.5 (±5.0)	3.1 (±0.2)	20.99 (±1.6)	0.58 (±0.08)	0.25 (±0.03)	0.14 (±0.004)	0.064 (±0.010)	0.009 (±0.003)	0.26 (±0.03)	0.005 (±0.001)	0.21 (±0.02)	0.04 (±0.008)	0.011 (±0.001)	2.11 (±0.31)
4806	Muddy, $T = 32°$ ($n = 2$)	55.0 (±6.0)	0.7 (±0.1)	24.84 (±1.3)	8.51 (±1.0)	0.59 (±0.11)	0.23 (±0.006)	0.043 (±0.008)	0.009 (±0.004)	0.33 (±0.04)	0.006 (±0.002)	0.15 (±0.04)	0.03 (±0.007)	0.014 (±0.002)	1.69 (±0.08)
Ocean water [23]															
		52.2	0.0	28.1	0.0045	0.012	0.0013	0.007	0.00002	0.009	0.0001	0.0002	0.0048	0.0007	0.022

Table 4 Values of pH, concentrations of magnesium (mmol), and trace metals (μm) in the water of biotope at the 9°50′N vent field, East Pacific Rise

Station	pH	Eh, mv	H_2S, mg/l	Sampling location	Mg	Fe	Mn,	Zn	Cu	Ni	As	Cr	Co	Ag	Cd	Pb	Sb
4626	4.9	−243	5.5	Black smoker	44	490	105	8.10	0.85	0.41	0.24	0.01	0.29	0.004	0.001	0.021	0.01
4631	6.1	−174	0.6	Shimmering water	44	4.84	2	1.60	0.47	0.12	0.36	0.26	0.23	0.020	0.003	0.027	0.02
4632	5.16	−185	1.8	Black smoker	36	309	39	2.90	0.27	0.09	0.13	0.08	0.25	0.039	0.003	0.018	0.03
4637	5.68	−180	1.2	Black smoker	71	10.9	5	7.05	3.10	0.41	0.17	0.11	0.16	0.002	0.003	0.017	0.06
4642	5.25	−144	0.3	Black smoker	54	113	40	24.2	185	0.31	0.08	0.31	0.18	0.003	0.002	0.026	0.04
4668	3.8	−147	9.0	Black smoker	37	1607	214	23.2	8.59	2.71	0.22	1.20	0.23	0.007	0.002	0.008	0.05
4671	5.22	−161	1.3	Black smoker	51	355	57	4.75	0.20	0.93	0.08	0.47	0.11	0.016	0.003	0.098	0.02
Ocean water [23]					54	0.0045	0.0013	0.012	0.007	0.009	0.022	0.0048	0.0002	0.00002	0.0007	0.0001	0.001

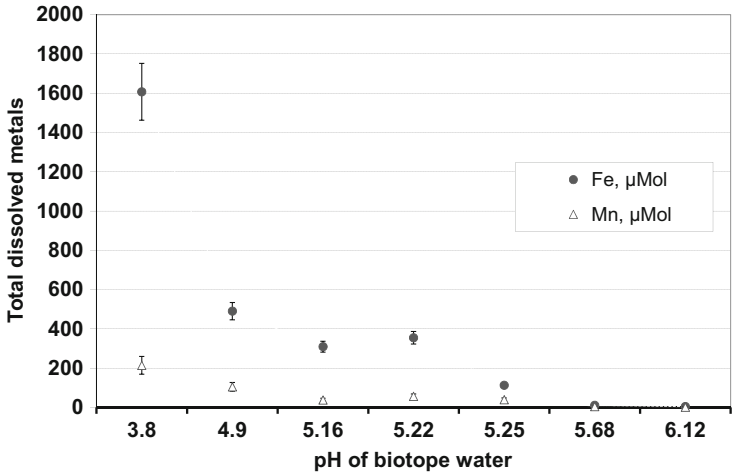

Fig. 2 Concentrations of the total dissolved Fe and Mn (μmol) in dependence on pH in the biotope water at the hydrothermal vent field 9°50′N, the East Pacific Rise

A nonconservative behavior of Fe and Mn in the biotope water at the 9°50′N vent field has been revealed based on a nonlinear depletion of the total dissoluble (TD) Fe and Mn concentrations (Fig. 2). This decrease reached up to 160 and 20 times, respectively, while pH increased from 3.80 to 6.12 as a result of mixing fluids and seawater [14]. This depletion was obviously caused by the formation of their own mineral phases (Fe sulfides and Fe–Mn hydroxides) within mixing zone that has been suggested by X-ray diffraction analysis of suspended particles collected at the same 9°50′N vent site: the ore minerals (pyrite, chalcopyrite, and marcasite) were a predominant minerals of a biogenic portion of the particles >0.45 μm [31]. Recently TDMn has been determined to be a conservative tracer in dispersing hydrothermal plumes [32]. Thus according to this and to our data [14], TDFe and TDMn may serve as tracers of the fluid-bottom seawater mixing zone along with firstly well-documented tracers such as temperature, pH, and H_2S concentration [5]. Concentrations of other trace metals in the water of biotope were essentially (in 3–50 times) lower than that in the initial fluids.

The Guaymas Basin hydrothermal field (Southern Trough) in the Gulf of California is characterized by a number of geological and geochemical characteristics which differ from the other fields, as noted above (see [8]). An exceptional feature of the semi-enclosed Guaymas Basin (Gulf of California) hydrothermal vent field is the thick organic-rich sedimentary cover on the seafloor. This cover is a result of high sedimentation rates due to Colorado River sediment input directly before dam construction or tidal resuspension of previously supplied terrigenous sediments in the Upper Gulf of California [33–35] and biogenic particles from the highly productive euphotic zone [36–38].

The results of element determination for the four water samples are listed in Table 5. Samples collected from shimmering water with abundant Vestimentiferan

Table 5 Values of pH, concentration of Mg (mmol), and trace metals (μmol) in the water of biotope over Vestimentiferans and clams settlement at the Guaymas Basin, Southern Trough (Gulf of California)

Station	pH	Mg	Fe	Mn	Zn	Cu	Ni	As	Cr	Co	Ag	Cd	Pb	Sb
4700	7.49	43	7.47	0.48	18.75	0.29	0.25	0.1	0.47	0.16	0.026	0.004	0.016	0.05
4709	5.4	34	20.62	43.62	0.32	0.66	0.39	0.7	0.76	0.19	0.002	0.002	0.041	0.03
Ocean water [23]	8.2	54	0.0045	0.0013	0.012	0.007	0.009	0.022	0.0048	0.0002	0.00002	0.0007	0.0001	0.001

settlements (St. 4700) had a weakly acidic character (pH 5.4). Water samples collected from a nearby diffuser vent at St. 4709 where clams and mussels inhabit were more alkaline (pH 7.49). In both cases, pH is rather low in comparison to ocean water (usually pH 8.0–8.2; [39]). Water of more acidic character is more deficient in Mg and enriched in Mn compared to more alkaline water. The Mg concentrations of both types of biotope water are somewhat lower than observed in ocean water. In both cases, the trace metal concentrations are much higher in the water of biotopes relative to the reference ocean water. According to our data, water from Vestimentiferan biotope is enriched in As, Cr, Cu, Fe, Mn, and Pb relative to fluids of the second type, but deficient in Ag, Cd, Sb, and Zn (Table 4). The Mn concentration is significantly higher than that of Fe; this differs from water of biotope at the hydrothermal vent fields of the Mid-Atlantic Ridge and 9°50′N of the East Pacific Rise, where Fe is found in higher concentrations than Mn [24, 40]. A reason may be attributed to the following: high-temperature fluids are discharged to the surrounding seawater through the vents and by ascending through the overlying sediments, which are rich in Mn. This leads to the enrichment of fluids for Mn relative to Fe [17], which is a characteristic feature of Guaymas Basin fluids compared to other vent fields.

A currently available data (concentration limits or average) of the total concentration of trace elements (suspension and solution) in the water of biotope at the Mid-Atlantic Ridge, East Pacific Ridge, and Guaymas Basin are listed in Table 6. These data were taken from publications of different authors [4–6, 9–12, 21, 25].

It should be noticed that concentrations of many metals in the water of the hydrothermal biotopes exceed that in the anthropogenically contaminated nearshore water.

The calculated (median) average of each metal concentration allowed us to better understand some features of metal distribution in the water of the animals' habitats at both the slow-spreading (<6 cm/year) Mid-Atlantic Ridge and the fast-spreading (>11 cm/year) East Pacific Rise (Table 7). The averaged data on the MAR low-temperature vents are presented by the Menez Gwen and Lost City fields, while the high-temperature vents of fields studied at the MAR – at the Rainbow and Broken Spur fields, as well as the high-temperature vents of EPR 9°50′N and 13°N. From comparison of Tables 1 and 7, it follows that the concentrations of the typically hydrothermal metals in the end-member fluids such as Fe, Mn, Zn, and Cu decreased sharply (up to four orders of magnitude) in the near-bottom water of the hydrothermal fields. This is obviously caused by the formation of Fe, Mn, Zn, and Cu mineral phases (sulfides, and hydroxides) within the mixing zone. The concentrations of other metals in the biotope water are 3–50 times lower than in the initial fluids.

Analysis of these data has revealed that in water above the fauna settlements at the high-spreading East Pacific Rise fields (with the velocities >11 cm/year), the average concentration of a number of metals (Fe, Mn, Zn, Cr, Pb, and Ag) was several times higher than in the water of biotopes at the low-spreading Mid-Atlantic Ridge (<6 cm/year) with both the high- and low-temperature hydrothermal vents. Among the MAR biotopes, the average concentration of most metals in biotope

Table 6 Concentrations[a] of total (dissolved + particulated) trace metals (μmol) measured in the water of biotope of some deep-sea hydrothermal vent sites at the MAR, EPR, and Guaymas Basin (Gulf of California) by different authors

Vent field	Reference	Fe	Mn	Zn	Cu	As	Cr	Sb	Co	Pb	Cd	Ag	Ni	Hg
Menez Gwen[b]	[21]	0.21	0.04	0.07	0.17				0.02	0.003	<0.0001			$<10^{-6}$
Menez Gwen	[9]	0.5	0.85	1.21	0.08	0.43	0.02	0.02	0.2	0.022	0.004	0.003	0.24	
Menez Gwen	[5]				0.06–0.33					0.004–0.014				
Rainbow	[4]				1.6–3.7					0.05–0.08	0.009–0.03			
Rainbow: mus-shr[c]	[21]	3.8–10.3	0.7–1.4	0.52–0.43	1.99–0.5				0.02	0.01–0.001	<0.0001			$<10^{-6}$–0.002
Rainbow: mus-shr[c]	[9]	0.16–3.27	2.84–7.31	0.55–7.64	0.14–0.35	0.21–0.97	0.02–0.03	0.17–0.72	0.01–0.05	0.01–0.025	0.002–0.005	0.006–0.007	0.01–0.066	
Broken Spur: mus-shr[c]	[10]	1.29–5.37	0.22–1.31	2.05–2.62	0.33–2.04	0.17–1.28	0.01–0.01	0.04–0.08		0.003–0.033	0.01–0.01	0.029–0.134		0.002–0.009
1.61–0.72														0.0002–0.0004
Lost City	[10]	0.72–6.07	0.07–0.19	0.22–0.66	0.02–0.07	0.74–0.94	0.02–0.07		0.15–0.32	0.005–0.006	0.005–0.014	0.008–0.009	0.26–0.33	
9°50′N EPR: mus-alvin[d]	[11]	5–11	1.8–5	1.6–7	0.27–3.1	0.13–0.36	0.01–0.31	0.13–0.57	0.16–0.29	0.017–0.027	0.001–0.003	0.002–0.039	0.09–0.41	
9°50′N EPR	[25]	72–730		2.9–41.3	0.08–2.1					0.02–0.52	0.003–0.035			
13°N EPR	[6]	5.2–62.6		0.30–27.3	0.18–1.6					0.011–0.260	0.002–0.047			
Guaymas Basin	[12]	7.47–20.62	1.48–43.6	0.32–18.75	0.29–0.66	0.10–0.73	0.47–0.76	0.03–0.05	0.16–0.19	0.016–0.041	0.002–0.004	0.002–0.026		

[a]Average or limits
[b]Average for Menez Gwen and Rainbow
[c]Mus-shr–water above mussel and shrimp settlements
[d]Clam-alvin–water above clam, mussel, and alvinellid settlements
Empty spaces indicate no data

Table 7 Total dissoluble metals in the end-member fluids and biotope water above vent fauna settlements at the MAR and EPR field

	Low-T° vent sites at the slow-spreading MAR				High–T° vent sites at the slow-spreading MAR and fast-spreading EPR			
		Biotope water[b]				Biotope water[d]		
Metal	End member fluid[a]	Average (median)	Minimal	Maximal	End member fluid[c]	Average (median)	Minimal	Maximal
Fe (μmol)	1.8–28	0.35	0.21	6.5	17–24,000	11.3	0.16	62.6
Mn (μmol)	59–68	0.44	0.04	0.85	63–2,250	7.15	0.22	43.6
Zn (μmol)	2.4–5.1	0.64	0.07	1.21	5–160	5.66	0.3	27.3
Cu (μmol)	0.6–2.9	0.16	0.06	0.33	1–140	1.24	0.14	3.7
Ni (μmol)	<2	0.24	0.18	0.3	<2–3	0.48	0.01	1.61
Cr (μmol)		0.02	0.01	0.03		0.39	0.01	0.76
Co (μmol)	<2	0.02	0.01	0.03	<2–13	0.11	0.003	0.29
As (μmol)		0.23	0.12	0.43		0.49	0.1	1.28
Pb (μmol)	0.021–0.056	0.01	0.003	0.022	0.033–0.265	0.05	0.001	0.08
Cd (μmol)	0.009–0.012	0.002	0.0001	0.004	0.018–0.44	0.021	0.0001	0.134
Ag (μmol)	0.004–0.02	0.005	0.003	0.02	0.005–0.047	0.012	0.002	0.039
Hg (nmol)		0.5	0.001	0.3		0.5	0.001	2

Trace metal concentrations were taken from papers
[a]Menez Gwen [19, 24]
[b]Menez Gwen [5, 9, 21]
[c]Broken Spur, Rainbow, Snake Pit [24]; 9°N, Guaymas [17]
[d]Broken Spur [10]; Rainbow [4, 9, 21]; 9°50′N [11]; 13°N [6]; Guaymas Basin (Gulf of California) [12]
Averages were calculated by the author
Empty spaces indicate no data

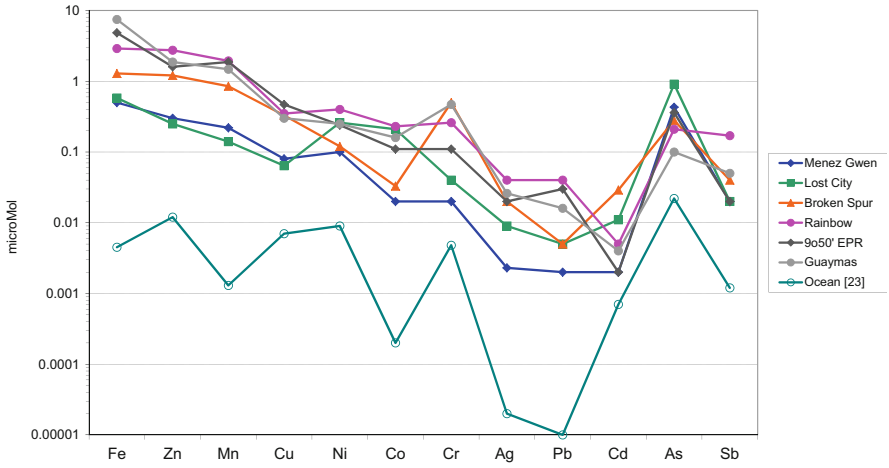

Fig. 3 Comparison of the average concentrations of the total dissolved trace metals (μmol) in the biotope water above the *Bathymodiolus* sp. settlements at some hydrothermal vent fields compared to the ocean water

water of the high-temperature Broken Spur and Rainbow vents was only 2–10 times higher than that in the water of the low-temperature Menez Gwen vents.

Taking into account average values of metal concentrations in water above *Bathymodiolus* sp. mussel settlements at the different hydrothermal vent fields, one can notice the following. The average concentrations of Fe, Mn, Zn, Cu, As, Cd, Cr, Pb, and Ag are only from 2 to 10 times higher in the biotope water of high-temperature vent fields (Rainbow, Broken Spur, 9°50′N, Guaymas) than concentrations of these metals in the low-temperature Menez Gwen vent field (Fig. 3)

Thus we come to conclude that although the metal concentrations differ strongly in end-member fluids of the high- and low-temperature vent fields, differences in metal levels are noticeably diminished down in the biotope water. This is obviously a result of complex physical, chemical, and biogeochemical processes.

4 Trace Metal Speciation in the Biotope Water of Some Deep-Sea Hydrothermal Vent Sites

Trace metal speciation is known to determine their biological availability and thus play an important role in bioaccumulation. In habitual photosynthetic marine environment, there are two basic sources of metals for bottom fauna: food and water, a significant proportion of metal being taken up from the water through the permeable surfaces, i.e., gills. This pathway depends on speciation of dissolved metals, including the hydrophilic and/or hydrophobic properties of metal complexes [41]. The dissolved and suspended forms of metals in the hydrothermal

biotope water are controlled by not only simple dilution of fluids with bottom seawater but more complex biogeochemical processes, namely, by an additional and/or secondary formation of suspended forms of trace metals when fluids are mixed with seawater. At the deep-sea hydrothermal vent fields, the trace metal bioaccumulation is predetermined by specific chemical environment of each hydrothermal field [42].

A nonconservative character of the geochemical behavior of Fe, Zn, Cu, and Pb in the mixing zone of fluids and seawater when temperature of water in biotope decreased from 25 to 2.5°C was revealed at the hydrothermal field 13°N, EPR [6]. The main mass of zinc, iron, and cadmium occurred in suspended particulate matter (>2 μm pore size of filter), while Cu and Pb were almost equally distributed between dissolved and suspended occurrence forms. However, a significant trend (at confidence level of 95%) in the concentration decrease of suspended and dissolved forms of metals was recorded only for Fe.

According to [21], a predominance of the suspended particulate form over soluble Al, Mn, Co, Cu, Mo, Cd, Fe, Zn, Pb, and Hg in the fauna microhabitats was found for both *Bathymodiolus* mussels and *Rimicaris* and *Mirocaris* shrimps at Menez Gwen, Lucky Strike, and Rainbow vent fields, while soluble metals prevailed in non-inhabited areas. This might imply that organisms during their metabolism contribute suspended matter into the surrounding water that could alter bioavailability of metals. Proportion of dissolved and suspended forms varied depending on type of a community. In the water of the Lucky Strike and Rainbow hydrothermal fields, contribution of particulate Zn over settlements of shrimp varied from 70 to 95% of the total Zn content, while above the mussels colonies, it didn't exceed 10%. It could be explained by a predominance of reduced forms of sulfur and thus a greater degree of S complexation in shrimps microbiotopes compared to the mussels ones [21].

Our data suggested that dissolved form (<0.45 μm) was dominated for most trace metals studied in the near-bottom water of the 9°50′ hydrothermal vent field; its contribution was estimated to be from 60% (Fe) to 95% (Cu) from total metal concentration in water. The near-bottom hydrothermal suspended particulate matter (SPM) collected nearby plumes is from 4 to 180 times enriched in metals compared to SPM from the reference deep-water area of the Pacific Ocean (as normalized by Al) as one can see from Fig. 4.

It is of importance to notice that composition of the suspended particles was similar over the shrimps' and mussels' settlements in each of the three fields studied, Menez Gwen, Rainbow, and Lucky Strike, but it varied considerably between fields. So silicates and aluminum silicate dominated in the Menez Gwen particles; barite was the most frequently detected in the Lucky Strike particles while Fe-hydroxides and sulfides in the Rainbow field particles. In all cases sulfides were presented by pyrite and marcasite (Fe), sphalerite (Zn), and chalcopyrite (Cu) [21].

At the fast-spreading ridge axes as EPR, the metal enrichment of the >2 μm fraction of suspended particulate matter results from the settlement and accumulation of particulate matter close to the organisms, acting as a secondary metal source. The enrichment observed in the dissolved fraction can be related to the dissolution

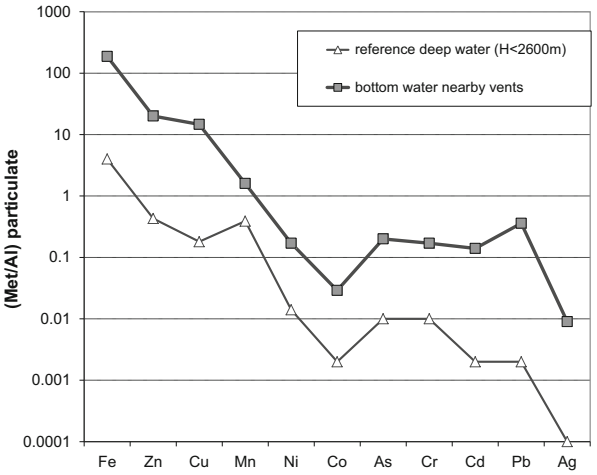

Fig. 4 Ratio metal/Al in the suspended particulate matter from the reference water column (depth < 2,600 m) and from the hydrothermally influenced near-bottom water (depth > 2,600 m) in water at the hydrothermal vent field 9°50′N, the East Pacific Rise b data from [31]

or oxidation of particles (mainly polymetallic sulfide) or to the presence of small particles and large colloids not retained on the 2 μm filter. SEM observations indicate that the bulk particulate observed at the 13°N, EPR, is characteristic of crystalline particles settling rapidly from the high-temperature smoker (sphalerite, wurtzite, and pyrite), amorphous structures, and eroded particles formed in the external zone of the chimney. Precipitation of Zn, Cu, Cd, and Pb with Fe as wurtzite, sphalerite, and pyrite is the main process taking place there [6].

Previously it was assumed that the emitting fluids to form metal sulfides or oxides are deposited relatively quickly, whereby the flow of metal into the ocean is negligibly small [13]. However, from the recent data, it follows that metals in the biotope water were associated with organic compounds which stabilize precipitation of metals, and thereby the flow of metal into the ocean may be increased. So, the dissolved amino acids which are known to be present in significant concentrations in hydrothermally influenced seawater contain functional groups which are capable of chelating metal ions [43]. The data of [44] have demonstrated an interesting features related to the complexation of some metals with dissolved amino acids in the deep-sea hydrothermal habitats. “In situ” measurements by voltammetric method recorded the Cu stable complexes with organic ligands (such as a thiol type) in water within the pH range from 2.1 to 7.8.

Recently an important role of organic complexation in some MAR vent fields has been documented for Fe, Mn, Cr, and Zn; organic complexation contributes to the fact that the flow of dissolved metals in the ocean from the hydrothermal systems increases, averaging 9% for Fe and 14% for Cu in their balance [45].

In the water of mussels *Bathymodiolus azoricus* habitats at the Lucky Strike vent field, MAR data from speciation measurements show that the hydrophobic organic fraction of Cu (C18Cu) was very low (<3%): Cu is found mainly as inorganic and hydrophilic organic complexes (non-C18Cu). This result is especially interesting because this latter fraction is liable to be more bioavailable than the former one.

Oxygen and sulfides data demonstrate that the Cu 5.15 μmol anomaly at pH 6.5 was found in the transition area between suboxic and oxic waters. The increase of dissolved Cu should correspond to the oxidative redissolution of copper sulfide particles formed in the vicinity of the fluid exit [46].

In a recent research of [47] using the latest techniques of the thermal desorption together with the gas and mass spectroscopy, the presence of a large variety of compounds of dissolved organic carbon in a dilute hydrothermal fluids was shown. These authors have identified and quantitatively determined the quasi-volatile fractions of dissolved organic matter (DOM), *n*-alkanes, mono- and polyaromatic hydrocarbons, along with fatty acids, and they established a predominance of non-polar compounds among the DOM.

The research of [48] provided a new data on speciation of sulfide and iron in high-temperature fluids emanating from vents in the East Pacific Rise and the Eastern Lau Spreading Center: pyrite nanoparticles composed of iron and sulfur account for up to 10% of the filterable iron (less than 200 nm in size) in these fluids, and these particles form before the discharge of the vent fluid. These authors estimated that pyrite nanoparticles sink more slowly than larger plume particles and are more resistant to oxidation than dissolved Fe(II) and FeS. From this, these authors suggest that the discharge of iron in the form of pyrite nanoparticles increases the probability that vent-derived iron will be transported over long distances in the deep ocean [48]. On the other hand, the data of [49] clearly shows that at the Central Indian Ridge segment, a large part of the dissolved Fe emitted from the hydrothermal sources was in the dissolved fraction rather than in the colloidal fraction, and the hydrothermal Fe is distributed over 3,000 km distance from the vents at a depth of approximately 3,000 m.

As it was mentioned above (see [50]), at the fast-spreading and high-temperature EPR fields, the most thermophilic fauna was met, and trace metal speciation is of importance in faunal groups distribution around hydrothermal vents.

Research of [51] suggested a relationship between a proportion of the oxygen, iron, and sulfur forms and the distribution pattern of two specific taxa in different microhabitats at the 9°50′N field. Vestimentiferan *Riftia pachyptila* hosts in its trophosome bacterial endosymbionts producing organic carbon in the chemosynthesis reactions, whereas Polychaete *Alvinella pompejana* living on the walls of the active sulfide chimneys does not depend upon reactions involving endosymbionts and directly adsorbs bacterial colonies inside or on the surface of its tubes. In a lower pH (<5) and higher temperature (>30°C), microbiotopes of Polychaete *Alvinella* formation of FeS molecular complexes reduced concentration of free H_2S in the water and thereby induced hydrogen sulfide's detoxification. In the water of Vestimentiferan *Riftia pachyptila* habitat with higher pH (>5.7) and relatively low temperature (<25°C), the concentration of aqueous complex FeS was insignificant due to the high concentration of free H_2S and its water complex (H_2S/HS) which has been utilized by bacterial symbionts for chemosynthesis to transform CO_2 into organic carbon.

5 Conclusions

Deep-sea hydrothermal biotopes are an example of complicated biogeochemical systems due to various processes of trace element supply and removal by the different components of ecosystem. Measurements of trace metal concentrations were performed in the water of biotopes of the Mid-Atlantic Ridge hydrothermal fields (Menez Gwen, Rainbow, Broken Spur, Lost City), as well as of the 9°50′N (East Pacific Rise) and Guaymas Basin (Gulf of California). In the deep-sea hydrothermal vent environment, the trace metal concentrations decrease sharply during fluid dilution with seawater but stay much higher (by factor up to 10^5) in water above the fauna settlements compared to the reference deep ocean water.

Along with a simple (conservative) dilution of fluids with sea water, various physical–chemical and biogeochemical processes take place resulting in a considerable decrease in the metal contents in the water of biotopes as compared to fluids. The analysis of the published data on the water above the colonies of bottom animals at the fields with high- and low-temperature vents at the MAR and EPR [4–6, 9, 11, 12, 21, 32] has revealed the following. The concentrations of the typically hydrothermal metals in the end-member fluids such as Fe, Mn, Zn, and Cu decreased sharply (up to four orders of magnitude) in the near-bottom layer of the hydrothermal field; that is obviously caused by the formation of Fe, Mn, Zn, and Cu mineral phases (sulfides and hydroxides) within the mixing zone. The concentrations of other metals in the biotope water are 3–50 times lower than in the initial fluids.

The significant differences in trace metal levels were found between the low- and high-temperature biotope water. Taking into account average (median) values, one can notice that the concentrations of Fe, Mn, Zn, Cu, As, Cd, Cr, Pb, and Ag are only 2–10 times higher in the biotope water of high-temperature vent fields than concentrations of these metals in the low-temperature Menez Gwen vent field. Although the metal concentrations differ strongly in end-member fluids of the high- and low-temperature vent fields, differences in metal levels are noticeably diminished down in the biotope water.

From our data, the total dissoluble Fe and Mn at the 9°50′N vent field (EPR) may serve as tracers of the fluid-bottom seawater mixing zone, along with earlier well documented tracer of the dissoluble Mn at the Rainbow field, MAR [32]. It may supplement list of the tracers such as temperature, pH, and H_2S concentration established earlier.

The chemical speciation of S and Fe in the water of the Vestimentiferan's and Polychaete's microbiotopes at the 9°50′N field serve as a key to the biological structure and the proportion of taxa [51].

An important role of organic complexation in the water of some MAR vent biotopes has been well documented for Fe, Mn, Cr, Cd, and Zn [43–47]. This may decrease the heavy metal bioavailability and thus diminish a toxic impact to organisms. On the other hand, organic complexation contributes to the fact that the flow of dissolved metals from the hydrothermal systems into the ocean

increases. Besides, hydrothermal discharge of Fe in the form of pyrite nanoparticles [48] as well as in the real soluble fraction rather than the colloidal fraction [49] increases the probability that vent-derived Fe will be transported over long distances in the deep ocean.

Acknowledgments I would like to thank Professor, Academician RAS Alexander Lisitzyn (PP Shirshov Institute of Oceanology) who has initiated Russian hydrothermal investigations about 40 years ago and supported this work. I am grateful to Professor A.Yu. Lein (PP Shirshov Institute of Oceanology) for the collection of water samples and Prof. Nils G. Holm (Stockholm University, Sweden) for the measurement of chemical composition of dissolved fluids from Rainbow and Lost City vent sites by inductively coupled plasma atomic emission spectroscopy (ICP-AES). This research was funded by the Russian Scientific Foundation (Project No 14-50-00095 "World Ocean in XXI century: climate, ecosystems, mineral resources and disasters").

References

1. Corliss JB, Dymond J, Gordon LI, Edmond JM, von Herzen RP, Ballard RP, Green K, Williams D, Bainbridge A, Crane K, Andel TH (1979) Submarine thermal springs on the Galapagos Rift. Science 203:1073–1083
2. Von Damm KL (1990) Seafloor hydrothermal activity: black smoker chemistry and chimneys. Annu Rev Earth Planet Sci 18:173–204
3. James RH, Elderfield H, Palmer MR (1995) The chemistry of hydrothermal fluids from the Broken Spur site, 29°N Mid-Atlantic Ridge. Geochim Cosmochim Acta 59:651–659
4. Desbruyères D, Biscoito M, Caprais JC, Colaço A, Comtet T, Crassous P, Fouquet Y, Khripounoff A, Le Bris N, Olu K, Riso R, Sarradin PM, Segonzac M, Vangriesheim A (2001) Variations in the deep-sea hydrothermal vent communities on the Mid-Atlantic Ridge near the Azores plateau. Deep-Sea Res I 48:1325–1346
5. Sarradin PM, Caprais JC, Riso R, Kerouel R, Aminot A (1999) Chemical environment of the hydrothermal mussel communities in the Lucky Strike and Menez Gwen vent fields, Mid. Atlantic Ridge. Cah Biol Mar 40:93–104
6. Sarradin PM, Lannuzel D, Waeles M, Crassons P, Le Bris N, Caprais JC, Fouquet Y, Fabri MC, Riso R (2008) Dissolved and particulate metals (Fe, Zn, Cu, Cd, Pb) in two habitats from active hydrothermal field on the EPR at 13° N. Sci Total Environ 392:119–129
7. Le Bris N, Gaill F (2006) How does the annelid *Alvinella pompejana* deal with an extreme hydrothermal environment? Rev Environ Sci Biotechnol doi:10.1007./sl 1157-006-9112-1
8. Galkin SV, Demina LL (2016) Geologic-geochemical and ecological characteristics of selected hydrothermal vent areas. Hdb Env Chem.
9. Demina LL, Galkin SV (2008) On the role of abiogenic factors in the heavy metal bioaccumulation by the hydrothermal fauna at the Mid-Atlantic Ridge. Oceanology 48:784–797
10. Demina LL, Holm NG, Galkin SV, Lein AY (2010) Concentration function of the deep-sea vent benthic organisms. Cah Biol Mar 51:369–373
11. Demina LL, Galkin SV, Lein AY, Lisitzin AP (2007) First data on the microelemental composition of benthic organisms from the 9°50′N hydrothermal field, East Pacific Rise. Dokl Earth Sci 415:905–907
12. Demina LL, Galkin SV, Shumilin EN (2009) Bioaccumulation of some trace metals in the biota of hydrothermal fields of the Guaymas basin (Gulf of California). Bul Soc Geol Mexicana 61:31–45

13. Edmond JM, Von Damm KL, McDuff RE et al (1982) Chemistry of hot springs on the East Pacific Rise and their affluent dispersal. Nature 297:187–191
14. Demina LL, Holm NG, Galkin SV, Lein AY (2013) Some features of the trace metal biogeochemistry in the deep-sea hydrothermal vent fields (Menez Gwen, Rainbow, Broken Spur at the MAR and 9o50′N at the EPR): a synthesis. J Mar Syst 126:94–105
15. Jannasch HW, Wirsen GO (1979) Chemosynthetic primary production at east pacific floor spreading centers. Bioscience 79:592–598
16. Gal'chenko VF, Lein AY, Galimov EM (1988) Role of bacteria-endosymbionts in the feeding of invertebrates from the deep-sea active hydrothermal areas. Oceanology 28:1020–1031
17. Von Damm KL, Edmond JM, Measures CI, Grant B (1985) Chemistry of submarine hydrothermal solutions at Guaymas Basin, Gulf of California. Geochim Cosmochim Acta 49:2221–2237
18. Johnson KS, Childress JK, Beehler CL (1988) Short-term temperature variability in the Rose Garden hydrothermal vent field: an unstable deep-sea environment. Deep-Sea Res 38:1711–1721
19. Charlou JL, Donval JP, Douville E, Jean-Baptiste P, Radford-Knoery J, Fouquet Y, Dapoigny A, Stievenard M (2000) Compared geochemical signatures and the evolution of Menez Gwen (37°50′N) and Lucky Strike (37°17′N) hydrothermal fluids, south of the Azores Triple Junction on the Mid-Atlantic Ridge. Chem Geol 171:49–75
20. Desbruyères D, Almeida A, Biscoito M (2000) A review of the distribution of hydrothermal vent communities along the northern Mid-Atlantic Ridge: dispersal vs environmental controls. Hydrobiologia 440:201–216
21. Kádár E, Costa V, Martins I, Santos RS, Powell JJ (2005) Enrichment in trace metals (Al, Mn, Co, Cu, Mo, Cd, Fe, Zn, Pb and Hg) of the macro-invertebrate habitats at hydrothermal vents along the Mid-Atlantic Ridge. Hydrobiologia 548:191–205
22. German CR, Von Damm KL (2004) Hydrothermal processes. In: Holland HD, Turekian KK (eds) Treatise on geochemistry, vol 6, Oceans and marine geochemistry. Elsevier, Pergamon, pp 182–216
23. Bruland KW, Lohan MC (2004) Controls of trace metals in sea water. The oceans and marine geochemistry. In: Holland HD, Turekian KK (eds) Treatise on geochemistry, vol 6. Elsevier, Amsterdam, pp 23–47
24. Douville E, Charlou JL, Oelkers EH, Bienvenu P, Jove Colon CF, Donval JP, Prieur Y, Fouquet Y, Appriou P (2002) The Rainbow vent fluids (36°14'N, MAR): the influence of ultramaphic rocks and phase separation on trace metals content in Mid-Atlantic Ridge hydrothermal fluids. Chem Geol 184:37–48
25. Di Meo-Savoie CA, Luther I, George W, Cary SC (2004) Physicochemical characterization of the microhabitat of the epibionts associated with *Alvinella pompejana*, a hydrothermal vent annelid. Geochim Cosmochim Acta 9:2055–2066
26. Bogdanov JuA (1997) Hydrothermal deposits of the Mid-Atlantic Ridge rifts, Nauchny Mir, Moscow, 166 pp (in Russian)
27. Kádár E, Costa V, Santos RS, Powell JJ (2006) Tissue partitioning of micro-essential metals in the vent bivalve *Bathymodiolus azoricus* and associated organisms (endosymbiont bacteria and a parasite polychaete) from geochemically distinct vents of the Mid-Atlantic Ridge. J Sea Res 56:45–52
28. Kelley DS, Karson JA, Blackman DK, Früh-Green GL, Butterfield DA, Lilley MD, Olson EJ, Schrenk MO, Roe KK, Lebon JT, Rivizzigno R (2001) AT3-60 Shipboard Party, An off-axis hydrothermal vent field near the Mid-Atlantic Ridge at 30°N. Nature 412:145–149
29. Kelley DS, Karson JA, Fruh-Green GL, Yoerger DR, Shank TM, Butterfield DA, Hayes JM, Schrenk MO, Olson EJ, Proskurowski G, Jacuba M, Bradley A, Larsin B, Ludwig K, Glikson D, Buckman K, Bradley AS, Braselton WJ, Roe K, Elend MJ, Delacour A, Bernasconi SM, Lilley MD, Baross JA, Summons RE, Sylva SP (2005) A serpentinite-hosted ecosystem: the Lost City hydrothermal field. Science 307:1428–1434

30. Lein AY, Bogdanov YA, Sagalevich AM (2004) A new type of hydrothermal field at the Mid-Atlantic Ridge: Lost City field, 30°N. Dokl Earth Sci 394:380–383
31. Lukashin VN, Demina LL, Gordeev VV, Gordeev VY (2012) The geochemistry of deep water particulate matter over the hydrothermal field at 9°50′N (the East Pacific Rise). Oceanology 52:271–283
32. German CR, Thurnherr AM, Knoery J, Charlou JL, Jean-Baptiste P, Edmonds HN (2010) Heat, volume and chemical fluxes from submarine venting: a synthesis of results from the Rainbow hydrothermal field, 36°N MAR. Deep-Sea Res I 57:518–527
33. Calvert SE (1966) Accumulation of diatomaceous silica in the silica in the sediments in the sediments of the Gulf of California. Geol Soc Am Bull 77:569–596
34. Carriquiry JD, Sánchez A (1999) Sedimentation in the Colorado River delta and Upper Gulf of California after nearly a century of discharge loss. Mar Geol 158:125–145
35. Carriquiry J, Sánchez A, Camacho-Ibar VF (2001) Sedimentation in the northern Gulf of California after cessation of the Colorado River discharge. Sediment Geol 144:37–62
36. Lonsdale P (1977) Clustering of suspension-feeding macrobenthos near abyssal hydrothermal vents at oceanic spreading centres. Deep-Sea Res 24:857–863
37. De la Lanza-Espino G, Soto LA (1999) Sedimentary geochemistry of hydrothermal vents in Guaymas Basin, Gulf of California. Mexico Appl Geochem 14:499–510
38. Thunell RC (1998) Seasonal and annual variability in particle fluxes in the Gulf of California: a response to climate forcing. Deep-Sea Res I 45:2059–2083
39. Millero F (1996) Chemical oceanography. CRC, Boca Raton, 469 pp
40. Von Damm KL, Lilley MD (2004) Diffusive from hydrothermal fluids from 9°50′N East Pacific Rise: origin, evolution and biogeochemical controls. In: Wilcock WSD, DeLong EF, Kelley DS, Baross JA, Cary SC (eds) The subseafloor biosphere at Mid-Ocean Ridges, Geophysical monograph series 144. American Geophysical Union, Washington, pp 245–269
41. Wang WX (2002) Interactions of trace metals and different marine food chains. Mar Ecol Prog Ser 243:295–309
42. Cosson RP, Thiebaut E, Company R, Castrec-Rouelle M, Colaco A, Martins I, Sarradin PM, Bebianno MJ (2008) Spatial variation of metal bioaccumulation in the hydrothermal vent mussel *Bathymodiolus azoricus*. Mar Envir Res 65:405–415
43. Sumoondur A, Koschinsky A, Osterlag-Henning C et al (2006) Dissolved organic compounds in hydrothermal fluids from the Mid-Atlantic Ridge: implication for the behavior of metals at vent sites. Geophys Res Abstr 8:06642, SRef-ID:1607-7962/gra/EGU06-A-06642
44. Sander SG, Koschinsky A, Massoth G, Scxott M, Hunter KA (2006) Organic complexation of Cu in deep-sea hydrothermal vent systems. Environ Chem 4:81–89
45. Sander SG, Koschinsky A (2011) Metal flux from hydrothermal vents increased by organic complexation. Progress article. Nat Geosci 4:145–150
46. Sarradin PM, Waeles M, Bernagout S, Le Gall C, Sarrazin J, Riso R (2009) Speciation of dissolved copper within an active hydrothermal edifice on the Lucky Strike vent field (MAR, 37°N). Sci Total Environ 407:869–878
47. Konn C, Charlou JL, Donval JP, Holm NG (2012) Characterization of dissolved organic compounds in hydrothermal fluids–gas chromatography–mass spectrometry. Case study: the Rainbow field (36°N, Mid Atlantic Ridge). Geochem Trans 13. http://www.geochemicaltransactions.com/contents/13/1/8
48. Yücel M, Gartman A, Chan CS, Luther GW (2011) Hydrothermal vents as a kinetically stable pyrite (FeS_2) nanoparticle source to the ocean. Nat Geosci 4:367–371
49. Nishioka J, Obata H, Tsumune D (2013) Evidence of an extensive spread of hydrothermal dissolved iron in the Indian Ocean. Earth Planet Sci Lett 361:26–33
50. Galkin SV (2016) Structure of hydrothermal vent communities. Hdb Env Chem.
51. Luther GW, Rozan TF, Tallefert M, Nuzzio DB, Di Meo C, Shank TM, Lutz RA, Cary SC (2001) Chemical speciation drives hydrothermal vent ecology. Nature 410:813–816

Structure of Hydrothermal Vent Communities

S.V. Galkin

Abstract Deep-sea hydrothermal vent communities are characterized by complicated taxonomic, trophic, and spatial structure. Different animals consume chemosynthetic bacterial production to a variable extent and by different ways. Different animal groups demonstrate variable degree of adaptations to the extreme environment of hydrothermal vent systems. According to their ecological requirements, vent animal populations occupy different zones within the vent field. The boundaries of different vent fauna assemblages could be rather sharp or feebly marked appearing to be defined by gradients of water chemistry as well as the hydrodynamic regime within the vent field. To ensure the correct analyses of bioconcentration function (BCF) of vent organisms, such factors as taxonomic position, trophic specialization, patterns of physiology, ontogenetic stages, and spatial disposition of animal population within the vent field should be taken into consideration.

Keywords Community structure, Hydrothermal vents, Microdistribution, Trophic specialization

Contents

S.V. Galkin (✉)
P.P. Shirshov Institute of Oceanology Russian Academy of Sciences (IORAN), Nakhimovsky pr., 36, 117997 Moscow, Russia
e-mail: galkin@ocean.ru

L.L. Demina, S.V. Galkin (eds.), *Trace Metal Biogeochemistry and Ecology of Deep-Sea Hydrothermal Vent Systems*, Hdb Env Chem (2016) 50: 77–96,
DOI 10.1007/698_2015_5018,
Published online: 3 February 2016

1 Introduction

Hydrothermal vent communities were initially discovered at 29 May 1976 in the area of Galapagos Spreading Center (eastern Pacific Ocean). On this day, large white clam shells lying within cracks of basalt lava at the depth about 2,500 m were photographed by the Deep Tow camera system "Angus." The length of shells amounted to 20 cm, and this fact caused a sensation because in those times the bivalves bigger than 3 cm were unknown from the deep sea.

The discovery of hydrothermal vent ecosystems was prepared by foregoing advances in marine geology throughout the twentieth century. As far back as 1912, the idea of the drift of continents was suggested by Alfred Wegener. In the 1950s and in early 1960s, the processes of seafloor spreading were confirmed and have led to general acceptance of global plate tectonic theory. In the middle of 1960s, Elder [1] predicted the existence of thermal springs along mid-ocean ridges. Thus, the presence of hot springs on the seafloor with temperatures as great as 300–400°C was anticipated [2–4]. Although, while the existence of hydrothermal vents itself was predicted by geologists, the biological effect of this phenomenon appeared fully unexpected. First observers in the DSRV "Alvin" dive series were astounded by the richness and biodiversity of vent communities uncommon for deep-sea ecosystems [5–7]. By very conservative estimates, the biomass here amounted to 10 kg/m^2 that is 3–4 orders of magnitude higher than in surrounding background benthic community. Following the first "Alvin" dive series to Galapagos vents, microbiologists postulated that the elevated concentration of hydrogen sulfide in vent fluids were a source of reduced sulfur for free-living chemolithoautotrophic sulfur-oxidizing bacteria.

Thus, the main distinctive feature of hydrothermal vent ecosystems is their orientation on chemosynthetic primary production contrary to most of other ecosystems of our planet driven by photosynthesis. The outstanding discovery was the elucidation that the dominants in these ecosystems harbored chemosynthetic bacteria capable of using hydrogen sulfide emitted from the hydrothermal vent [8–10].

At ridge-axis hydrothermal systems, the low- to moderate-temperature fluids which vent organisms live in are usually simply diluted versions of high-temperature (~350°C) fluids of black smokers, with the diluent being cold seawater. Compared to seawater, black-smoker fluids have a low pH (3–5) and are especially enriched in sulfide (H_2S), hydrogen (H_2), methane (CH_4), manganese (Mn), and other transition metals (iron, zinc, copper, lead, cobalt, aluminum). While some vent organisms are adapted to high temperature, it is the chemistry of hydrothermal fluids that sustains the chemosynthetic basis of life at vent ecosystems. The most important elements providing chemosynthetic bacterial activity are hydrogen sulfide (H_2S) and methane (CH_4). The concentration of these elements in vent fluid amounts 3–12 mM and 25–100 μM per 1 kg, respectively [11]. However, reduced compounds themselves provide no energy. It is oxidation of sulfide and methane that yields energy; both oxidant and reductant are required. The oxidant is primarily molecular oxygen in the surrounding seawater. It should be noted that hydrogen

sulfide is highly susceptible to spontaneous oxidation in seawater. Namely, the mixing zone (restricted area of simultaneous presence of oxygen and reduced compounds) provides the life zone for bacteria and bacteria-linked fauna. For this reason, hydrothermal vent communities are very confined in space compared with the background communities of surrounding deep sea.

Russian investigations of hydrothermal vent ecosystems have been started in 1984 using initially DSRV "Pisces" and (since 1988) DSRV "Mir-1" and "Mir-2" (see Chap. 8, present edition: Sagalevich A.M. "Manned submersibles Mir and the world-wide research of hydrothermal vents"). Thereafter, more than 20 vent areas were explored (some of them many times). All underwater deep-sea images of hydrothermal landscapes used in present paper were taken in situ with submersibles photo and video cameras. Presented images of vent animals before preservation were taken in vivo immediately after collection onboard of RV "Akademik Mstislav Keldysh."

2 Taxonomic Composition

Such features of hydrothermal environment as the high temperature, low oxygen, high acidity, high heavy metal concentration, etc., make this habitat unfavorable for most deep-sea animals. To live here special adaptations are required. The trophic structure of hydrothermal communities is also unusual for the deep-sea ecosystems. Such unusual specialization causes taxonomical originality of deep-sea vent fauna. These factors causes many vent animals to be an endemic ones for these habitat that don't live in any other biotopes.

The list of hydrothermal vent species greatly expanded during the last decades and still evolving every year. The first vent fauna enumeration was made by Hessler and Smithey [12] who preliminary listed 22 taxa. The list of species published by Tunnicliffe [13] numbered 236 species and 135 genera. The later list by Desbruyères and Segonzac [14] recorded ca. 440 species from 285 genera. Wolff [15] referred 712 vent species registered, of which 508 species are vent endemic, 35 also represented at cold seeps, 66 species known also from other (non-vent) environments, and 103 species of doubtful status (referred to genus only and not recorded being new species). The number of taxa used in global biogeographical network analysis attempted by Moalic et al. [16] totals 591 species and 331 genera described from 63 vent fields. New species are described from additional samples in known vent locations and from new locations.

Dominating taxa and most common animals in vent communities are mollusks, arthropods, and polychaetes. By Wolff's [15] estimate, these prevailing groups amount 36.1%, 34.3%, and 18,1% of all vent animals, respectively. These three groups are able to adjust themselves to extreme conditions regarding temperature, salinity, and deficiency of oxygen unlike more stenotopic groups such as sponges, cnidarians, echinoderms, and ascidians. Moreover, mollusks and polychaetes can find protection in shells or tubes against the continuous precipitation of particles from vent environment. The water inside tubes or shells may act as a buffer against

rapid changes in temperature and chemical properties [15]. More than 70% of molluskan species belong to the group Archaeogastropoda, many of which are limpet shaped and of moderate or small sizes (families Provannidae, Peltospiridae, and Lepetodrilidae). Most abundant bivalves are mussels of the genus *Bathymodiolus* (more than 20 species) reported from all major vent sites. Among Arthropods, crustaceans make up more than 90% of vent species (225 species are described from vents). The most diverse group are the copepods (>80 species). No less than two thirds copepod species belong to the family Dirivultidae with the most diverse genus *Stigiopontius* (23 species). Many copepods live associated with other vent organisms: vestimentiferans, bivalves, shrimps, and crabs [15, 17]. Decapods are also rather abundant in vent communities (about 70 species). Among them, the shrimps belonging to the families Alvinocarididae and Mirocarididae (ca. 18 species) were recorded from the most known vent sites (some species also in seeps) [18]. Exosymbiotrophic shrimps *Rimicaris exoculata* forming dense swarms in the nearest vicinity of hot vents are known as iconic species of most Atlantic vent sites. Around 20 crab species are known from vents, most of them belong to the superfamily Bythograeoidea. No less than 10 species of galatheid squat lobsters are recorded from different vent sites, most of which are referred to the genus *Munidopsis*. Remarkable group are hydrothermal Cirripedia with 14 species belonging to 6 vent endemic genera. About 130 polychaete species are referred from vents. Scale worms Polynoidae are the most diverse polychaete family (more than 45 species). Vestimentiferan tube worms (now referred to Polychaeta, order Siboglinida, family Siboglinidae [19]) number 16 species. Polychaetes of the vent endemic family Alvinellidae (13 species) are common at most Eastern Pacific vent fields.

Besides these dominating groups, representatives of some taxa are relatively rare or absent at vents. Thus, sea anemones are rather numerous at the periphery of vent fields, whereas other cnidarians are rare or absent in hydrothermal environment. Hexactinellid sponges were often observed at far field of vents; however, dense aggregations of hexactinellids in the zone of strong hydrothermal conditions are unknown. At the same time, we have observed crowded settlements of Demospongiae near the base of active sulfide edifices in Guaymas Basin. Representatives of such groups as Sipunculoidea, Phoronida, and Brachiopoda were not reported from vents. Relative scanty are echinoderms which dominate elsewhere in the deep sea; however, vent-endemic holothurians *Chiridota hydrothermica* form sometimes dense aggregations at Western Pacific vents [20]. Such crustacean taxa as tanaids and isopods which are otherwise abundant in background deep-sea sediments are few in numbers in vent deposits. Nemertines, Turbellaria, Echiura, and leeches are represented in vent environments by single species.

3 Trophic Structure of Vent Communities: Feeding Specialization of Dominant Animals and Food Web

The most remarkable representatives of vent fauna were of course vestimentiferan tube worms. Adult vestimentiferans are fully lacking of digestive tract. Vestimentiferans live in obligate symbioses with sulfide-oxidizing bacteria. Great numbers of bacteria live within the cells of special organ – so-called trophosome, which occupies the major portion of body of the worm (3.7 billions of bacterial cells per 1 g of trophosome tissue). The worm itself lives in a tube, exposing only bright red tentacles outside (Fig. 1). This forepart named obturaculum is used for the uptake of the oxygen, hydrogen sulfide, and carbon dioxide from the seawater. These compounds are transported through the well-developed blood system to the bacteria inhabiting trophosome (Fig. 2.). On the contrary, the organic matter produced by bacteria goes to the worm. Such mode of nutrition is called **symbiotrophy**. Up to now 16 vestimentiferan species were described from different depths and different oceans.

Besides of Vestimentifera, large hydrothermal bivalves of the families Vesicomyidae (Fig. 3) and Mytilidae (Fig. 4) are also characterized by symbiotrophic mode of nutrition. Although, unlike vestimentiferans, they preserve normal digestive system, symbiotic bacteria are enclosed in hypertrophied gills. It is interesting to notice that bathymodiolin mussels host not only sulfide-oxidizing but also methanotrophic bacteria.

The two main groups of symbiotrophic animals use hydrothermal environment in some different ways. Bivalves use their long foot to uptake hydrothermal fluid from relative deep cracks or fissures in basalt lava. Vestimentiferans use only compounds dissolved in surrounding water. Therefore, tube worms are more strictly associated with high active hot vents, while bivalves could settle in sites with relative weak diffuse flow (see below). Along with bacterial symbionts, mussels and clams may derive some portion of their nutrition from suspension feeding.

Another group of symbiotrophic animals are gastropods of the family Provannidae. Two species *Alviniconcha hessler*i and *Ifremeria nautilei* dominate vent communities of Western Pacific. *Alviniconcha* hosts only sulfide oxidizing and *Ifremeria* – both sulfide-oxidizing and methanotrophic symbionts.

The Atlantic vent communities distinctly differ from the Pacific ones. At the Atlantic vents, the predominant taxa are not vestimentiferans but shrimps. The shrimps *Rimicaris exoculata* form dense swarms close to hot vents (Fig. 5). The feeding type of hydrothermal shrimps is unusual. They eat filamentous symbiotic bacteria growing on mouthparts and inner surface of shrimp carapax.

Many hydrothermal animals use free-living bacteria encrusting different surfaces. The most numerous are lepetodrillid mussels, so-called limpets. They are small but often form very dense populations, e.g., at Axial Seamount on the Juan de Fuca Ridge.

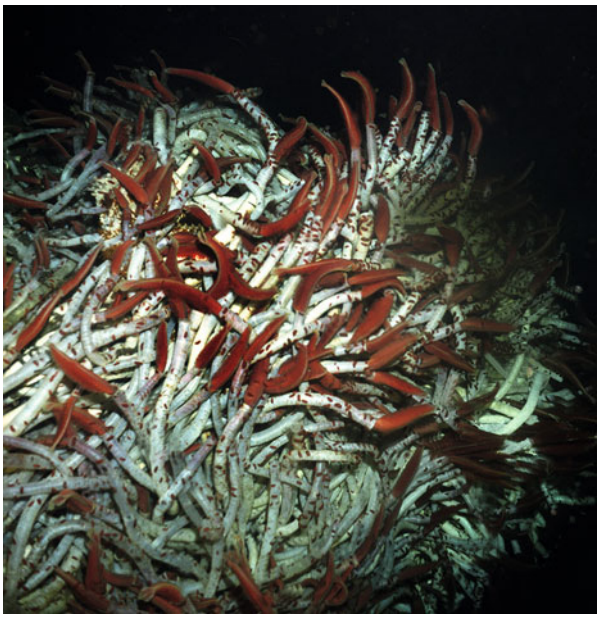

Fig. 1 Giant vestimentiferans *Riftia pachyptila* in Guaymas Basin, Gulf of California; depth ca. 2,000 m. The tubes of vestimentiferans are colonized by numerous Polynoid polychaetes grazing bacterial overgrow from tubes surface

Fig. 2 *Riftia pachyptila* collected at 9°N EPR (extracted from the tube). Long dark gray department of the body (so-called trunk) includes trophosome – habit area of sulfide-oxidizing bacteria

The same mode of nutrition is characteristic to others polychaetes – polynoids, which form rather dense populations on the tubes of giant vestimentiferans (Fig. 1). The most thermophilic metazoan animal is the so-called Pompeii worm *Alvinella pompejana* (Fig. 6). These animals live on the walls of black smokers and can sustain the temperature of more than 40°. *Alvinella* also feed on bacterial mat thriving in this biotope. It's worth to mention that many hydrothermal organisms do not exist in the temperature condition higher than 15–20°.

Fig. 3 Vesicomyid clams *Calyptogena magnifica* from 21°N EPR immediately after the collection

Fig. 4 The mussels *Bathymodiolus thermophilus* collected at 9°N EPR

High production of hydrothermal communities attracts many carnivores and scavengers. Among them different crustaceans are especially numerous. Bythograeid crabs are characteristic for the most vent fields worldwide. Turrid gastropods are common at many vent sites. Numerous sea anemones and Chaetopterid polychaetes often form dense populations at the periphery of Atlantic vent fields.

Also galatheid squat lobsters are common near the vents. Most of them represent ordinary background species, but often form aggregations at the periphery of vents. Good visible, these animals could serve as an indicator of the vent for deep-sea submersibles pilots and observers. Also cephalopod mollusks are common carnivores in eastern Pacific communities.

Fig. 5 Dense swarms of shrimps *Rimicaris exoculata* close to hot vents at TAG hydrothermal area (Mid-Atlantic Ridge, depth 3,600 m)

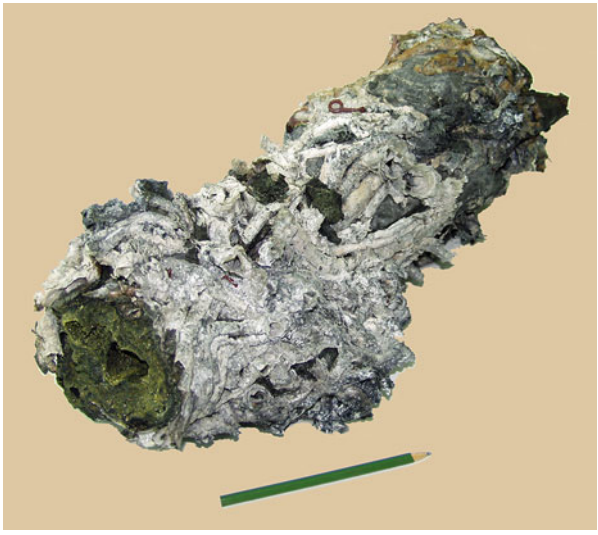

Fig. 6 Sampled fragment of high-temperature black smoker overgrown by alvinellid tubes (from 9°N EPR, depth 2,514 m)

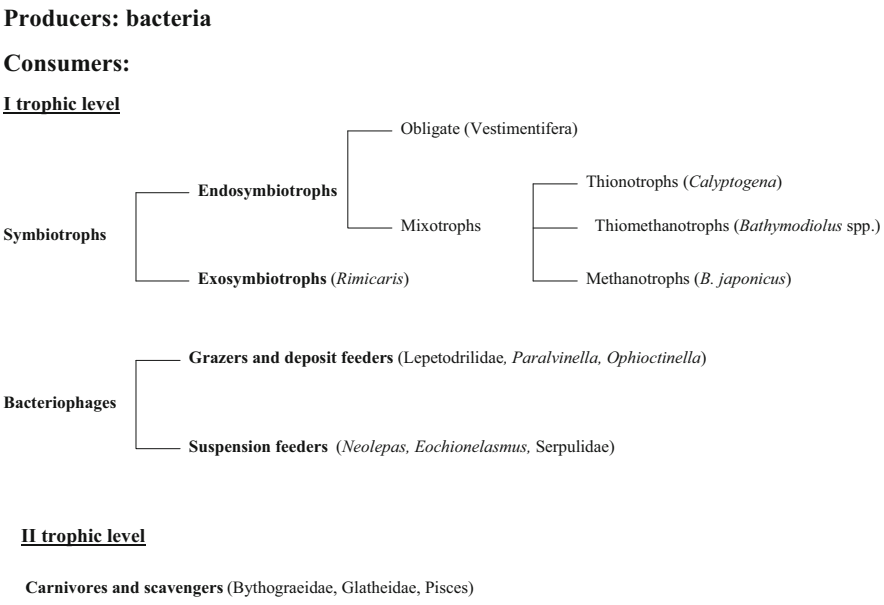

Fig. 7 Principal trophic groups of hydrothermal fauna (in *brackets*: typical representatives)

One more important trophic group of vent communities is various filter feeders. They utilize suspended bacteria from the water column. Among them there are both specialized vent endemic species (e.g., balanomorph barnacles) and nonspecialized background forms attracted by high productivity: various corals, brisingid starfishes, sponges, etc. These animals mostly use photosynthetic-derived organic particulates that are concentrated by bottom-water currents (convection cells) induced by hydrothermal activity.

Thus, in spite of high taxonomic diversity, the general trophic structure of vent communities is still constant (Figs. 7 and 8). Chemosynthetic and methanotrophic bacteria represent the main primary producers in hydrothermal vent ecosystems. Bacteria are present in vent communities in three main forms: (1) suspended bacterial aggregations in water column, (2) microbial mats or overgrow on hard animate (e.g., tubes, shells) and inanimate (sulfide, basalts) surfaces, and (3) symbiotic bacteria in animal's tissues. Each of these sources is consumed by certain groups of animals. The first level of consumers comprises metazoan animals directly linked to bacteria. There are host invertebrates (symbiotrophs, e.g., vestimentiferans), mixotrophs (e.g., mussels and snails), and specialized suspension feeders and grazers feeding on microorganisms that colonize substrates. Organic matter produced by these organisms is consumed by different carnivores, scavengers, and omnivores and thus involved in biogeochemical cycle.

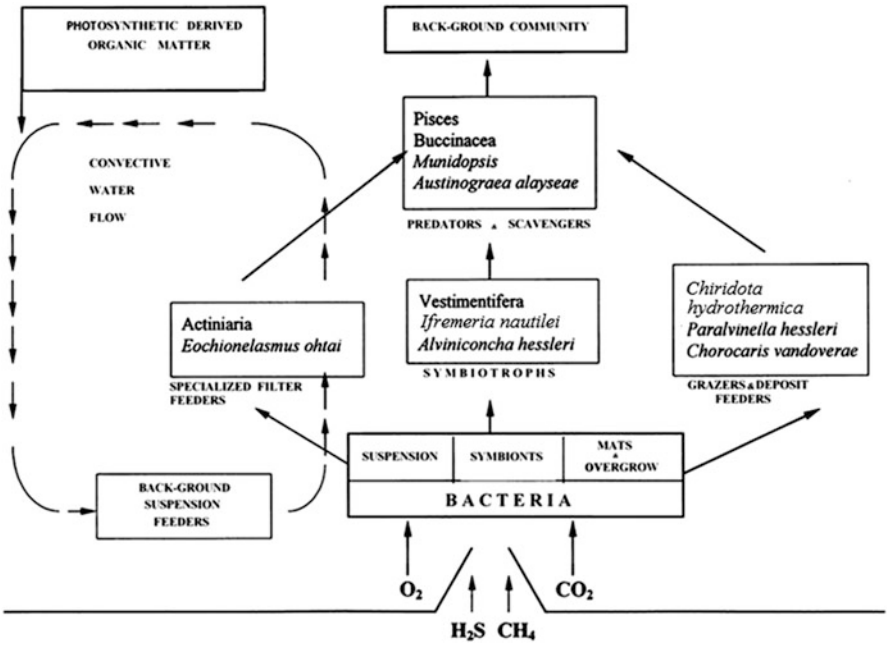

Fig. 8 The food web of hydrothermal vent community (by the example of the Manus Basin hydrothermal vent). Vertical height reflects trophic layer. Adapted from: [21]

4 Distribution of Organisms Within a Vent Field and Microscale Faunal Zonation

A vent field is characterized by a virtual absence of "normal" deep-sea animals, abundance of vent animals around fluid flows, and dispersed fauna between vents. An active field provides a varied set of microhabitats for colonization. Temperature, toxicity of fluid, proportion of dissolved gases (especially H_2S, CH_4, CO_2), age, and mineralogy of substratum are patterns reflected in the surface fauna. In addition, local hydrodynamic regimes vary with the micro-topography at each vent site. As a result, a faunal zonation is often obscure and difficult to recognize.

Microdistribution of vent fauna within the field is addressed in numerous regional studies. Several schemes of habitat zonation have been proposed for different vent areas [12, 22–24]. In our work, we use a generalized scheme of vent field zonation based on microdistribution patterns of vent organisms in different regions proposed by Galkin [25, 26] (Fig. 9).

A "typical" hydrothermal field provides several main microhabitats each of which has its own suite of potentially dominant megafaunal types. This "landscape-determining" species usually dominate corresponding assemblages and could be used as indicator taxa. The forms of venting within the field vary from very hot black smokers and moderate temperature, diffuse flow through basalt and sulfide

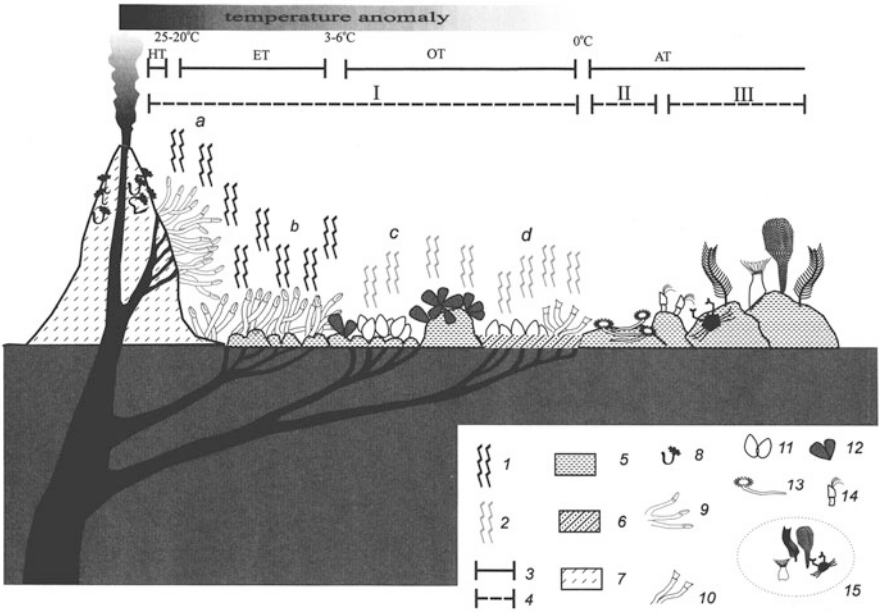

Fig. 9 Generalized scheme of vent field zonation (e.g., eastern Pacific communities). (*a–d*) Dominant forms of venting: (*a*) warm fluid diffuse flow through sulfide edifices; (*b*) the same – through basalt; (*c*) low-temperature diffuse flow through basalt; (*d*) the same through soft sediment. (*1*) Warm fluid diffuse flow (often obvious, characterized by "shimmering"). (*2*) Low-temperature diffuse flow (usually marked with bacterial mats and overgrowth on adjacent substratum). (*3*) Temperature zones: *HT* high-temperature zone (hot vent zone); *ET* euthermal zone ("shimmering" water zone, warm venting zone); (*O*) oligothermal zone (low-temperature zone, cool venting zone); *AT* ambient deep-sea water temperature. (*4*) Hydrothermal field zonation: (*I*) vent zone (means a space of direct mixing of hydrothermal fluid with seawater); (*II*) periphery of vent zone (near field); (*III*) periphery of vent field (far field). (*5–7*) Dominant substratum: (*5*) basalt lava, (*6*) soft sediment, (*7*) sulfide edifices. (*8–15*) Dominant macrofauna (indicator groups): (*8*) Polychaeta (Alvinellidae); (*9*) Vestimentifera (Tevniida) (*Riftia*, *Ridgeia*); (*10*) Vestimentifera (*Lamellibrachia* and *Escarpia*); (*11*) Bivalvia (Vesicomyidae); (*12*) Bivalvia (Mytilidae); (*13*) Polychaeta (Serpulidae); (*14*) Cirripedia (Neolepadinae); (*15*) background (nonspecialized) suspension feeders and scavengers. Adapted from: [25]

cracks to slow low-temperature seeps through basalt talus and soft sediments. Obviously, temperature is likely to change, but variation in water chemistry, particularly in the concentration of sulfides and other substrates for bacterial growth, are important and are surely taking place. The oxygen in the cooler ground water that dilutes the rising sulfide-rich fluid will reduce the sulfide concentration by oxidation. Varying sulfide concentrations will influence animal distribution in much the same way as does flow rate. Subterranean dilution of vent water will simultaneously cool it, decrease the flow rate by reducing the density differential, and diminish the sulfide concentration.

Among a variety of factors determining animal distribution, the temperature and substratum characteristics are the most easy to estimate during bottom

observations. Because of its conservative property, temperature is used as a general index of water quality. Precise data is lacking in many cases, but the temperature for certain habitats can be approximated using visual characters. It is known that black smokers have a temperature of 275–400°C, and "white smokers" temperatures of 100–250°C [27]. Warm water diffuse flow is often obvious, characterized by "shimmering" which is well pronounced when the temperature differential between emitting fluid and ambient sea water exceeds 3–5°C (e.g., [28]). Sites of low-temperature diffuse flow are usually marked with bacterial mats and overgrowth on adjacent substratum.

The dominant forms of venting are warm, diffuse flow, and black smokers. Generally speaking, the "vent zone" means a space of direct mixing of hydrothermal fluid with seawater. High concentrations of reduced compounds accompanied with the substantial presence of oxygen provide circumstances for the growth of bacteria (both free living and symbionts). Common features of the vent zone are bacterial mats and overgrowth. High temperature and toxicity prevent the penetration of nonspecialized animals into the vent zone. The vent zone is the most chemically and spatially heterogeneous environment of the hydrothermal field. In the eastern Pacific and several areas in the western Pacific, alvinellid and some polynoid polychaetes dominate the hottest extremes culminating, in most cases, with alvinellid polychaetes at the high temperature extremes of around 40°C. Beyond this extreme habitat (called the high-temperature zone or hot vent zone), the zone of warm and low-temperature diffuse flow (through sulfide edifices, basalts, or talus, rarer through sediment) is typically dominated by dense clusters of megafaunal species that rely to a large extent on chemoautotrophic bacteria in their nutrition. These assemblages are usually constrained within sharp boundaries defined by water chemistry and flow patterns of the venting water. A hot extreme to most inhabitants of vent zones seems to be about 25–30°C. Competition for space is another important factor defining the distribution of potentially dominant animals near the vents. For the most part, the investigated deep-sea communities have a more or less pronounced faunistic boundary which can be established within the vent zone. This boundary approximately corresponds to the limits of the "shimmering water zone" where the fluid's flow rate, temperature, and presumably sulfide concentration is still relatively high. The most specialized vent organisms are associated with the "shimmering water" habitats (euthermal or warm venting zone), such as tevniid vestimentiferans in eastern Pacific, the provannid gastropods *Alviniconcha* and *Ifremeria* in the western Pacific, and bresiloid shrimps *Rimicaris* in the Atlantic. The biotopes of diffuse venting with inconspicuous temperature anomalies (oligothermal or cool venting zone) are usually dominated by symbiotrophic/mixotrophic bivalves which rely on a relatively low flow and/or are adapted to utilize subterranean fluid sources. In most Pacific and Atlantic communities, the low-temperature zone with diffuse venting is dominated by vesicomyid clams and mytilids. Because the clams appears to use their foot to take up sulfide from vent waters and their gills to take oxygen and organic carbon from sea water [29], they are commonly found wedged foot downward into cracks (*Calyptogena magnifica*) or into soft sediment (other vesicomyid species).

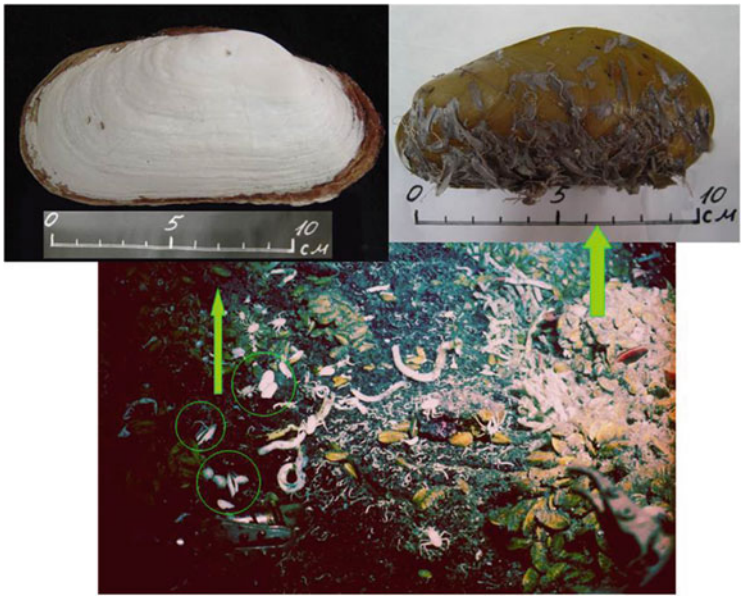

Fig. 10 Distribution of bivalve populations *Calyptogena magnifica* (*left*) and *Bathymodiolus thermophilus* (*right*) at hydrothermal site "Mussel Bed" (9°N EPR, depth 2,523 m). In *center*: dead tubes of *Riftia pachyptila*, galatheid crabs, and serpulid polychaetes on bare basalts

Temperature measurements by Fustec et al. [24] and Hessler et al. [30] support this contention; therefore, the animal requires a specific gradient of water conditions. The vent mussel *Bathymodiolus* is found under a wider range of conditions than the clam. Its siphons project into sea water while it attaches via byssal threads. Besides symbiotrophy, mytilids are capable of filter feeding on suspended particles of both vent-grown bacteria and general deep-sea particulate organics [31]. As a result, they are found under an unusually broad range of conditions. Mussels occur in the throat of vents in dense *Riftia* thickets, as well as on rocks that are near, but not directly bathed by vent fluid (Fig. 10). Hessler et al. [30] point to the ability of *Bathymodiolus* to survive where the flow is lower than will sustain *Calyptogena*. Within the vent field, mytilids may constitute a substantial fraction of biomass at any level of vent flow but will dominate where it is lowest. In addition to vesicomyids, lamellibrachiid vestimentiferans can be found in the sedimented areas of diffuse venting lacking temperature anomalies. The conditions in this habitat correspond, as a matter of fact, to cold seep habitats, but may be observed in peripheral zones of some vent sites, e.g., in Guaymas Basin and Middle Valley of the Juan de Fuca Ridge.

Beyond the central region, called the vent zone, there are the "near-field" (or "periphery of vent zone") populations of specialized suspension feeding and grazing megafaunal species that are presumable dependent on primary chemosynthetic production by free-living microorganisms, either directly or through the short

planktonic, benthic, and detrital food webs. Boundaries of these populations are also sharp and again appear to be defined by gradients of water chemistry as well as the hydrodynamic regime within the vent field. Anemones, serpulid worms, and enteropneusts characterize these zones in the eastern Pacific. In the western Pacific communities in the "near-field" area are marked by dense settlings of balanomorph barnacles. Similar niches in some Atlantic communities, in the Marianas Trough, and in the Indian Ocean are occupied by actinostolid sea anemones. Some obligate deposit feeders (gastropods, ophiuroids, holothurians) may occur in this area. Vent fields are often surrounded by numerous non-vent suspension feeders. Gorgonians, brisingids, sea anemones, and sponges may occur in greater abundance than elsewhere in the deep sea. A possible food source for these inhabitants could be bacterial aggregates which might rain fall-out in the peripheral areas which nourish these filter feeders. Another source might be advection of "normal" food materials from surrounding deep-sea regions. Some carnivorous species (galatheids, shrimps, crabs) also may concentrate in this named "periphery of vent field" or "far-field" zone. Some vagrant species from this group (e.g., the deep-sea crab *Macrooregonia macrochira* on the Juan de Fuca Ridge) make a good long-range indicator of vent proximity [32].

Thus, in "classical" deep-sea hydrothermal communities, five more or less prominent zones can be identified, each of which is dominated by certain mega-faunal groups: (1) high-temperature zone (hot vent zone): water temperature extreme up to 40°C, dominant substratum (solid sulfide edifices), indicator fauna (alvinellids and some polynoid polychaetes). (2) Euthermal zone (shimmering water zone, warm venting zone): temperature anomalies range from a few to 25–30°C, dominant substratum (solid sulfide edifices, pillow and sheet lava, basalt and sulfide talus), indicator fauna (tevniid vestimentiferans, provannid gastropods, bresiloid shrimps, and sometimes mytilids). (3) Oligothermal zone (low-temperature zone, cool venting zone): low-temperature anomalies, dominant substratum (pillow and sheet lava, non-active sulfide edifices, basalt and sulfide talus, soft sediments), indicator fauna (vesicomyids, mytilids). (4) Periphery of vent zone (near field): temperature anomalies (inconspicuous or absent), dominant substratum (same as (3)), indicator fauna (specialized suspension feeders feeding on bacteria). (5) Periphery of the vent field (far field): temperature anomalies (absent), dominant substratum (same as (4)), indicator fauna (non-vent suspension feeders). Zones (1–3) compose the "vent zone" (Fig. 9).

In disjunct biogeographical regions, established zones are marked by vicariating taxa and assemblages (Table 1).

This idealistic scheme is complicated by the influence of various local factors. Complexity is also added by many mobile animals not restricted to certain assemblages, and "background" deep-sea fauna, which may enter the hydrothermal community to feed. But as a whole, the three habitats within a vent zone and two outside them are more or less distinguishable (see also [21, 33, 34]). The influence of different factors determining the spatial structure of vent communities (water chemistry, substratum characteristics, tropical specialization, and behavior of animals) is discussed.

Table 1 Microscale faunal zonation and vent fauna vicariation (adapted from: [26])

	Temperature anomaly gradient			No temperature anomalies	
	~40°C	25°C	3–5°C	0°C	
Temperature zones	High-temperature zone (h)	Euthermal zone (shimmering water zone) (e)	Oligothermal zone (low-temperature zone) (o)	Background zone	
Zones of hydrothermal field	Vent zone			Periphery of vent zone (near-field zone)	Periphery of vent field (far-field zone)
Bacterial mats	Pronounced			Absent	
Dominant substratum	Solid sulfide edifices	Solid sulfide edifices, basalts	Non-active sulfide edifices, basalts, soft sediment	Basalts, soft sediment	Basalts, soft sediment
Dominant trophic groups	D, ESB	SB, ESB, D	MX, D	F, C	F, C
Maximal level of vent endemism	Family	Order	Family	Family	–
Vent regions	*Faunal assemblages*				
Northeast Pacific	*Paralvinella sulfincola*	*Ridgeia piscesae*	*Calyptogena n.*sp. cf. *pacifica*	Not pronounced	Majidae
		Paralvinella palmiformis			Hexactinellida
		Lepetodrilus fucensis			
East Pacific	*Alvinella pompejana*	*Riftia pachyptila*	*Calyptogena magnifica*	Serpulidae	Actiniaria
	Alvinella caudata	*Oasisia alvinae*		*Thermopalia taraxaca*	Gastropoda
		Tevnia jerichonana	*Bathymodiolus thermophilus*	*Saxipendium coronatum*	Octocorallia
		Bythograea thermidron		*Neolepas zevinae*	Hexactinellida
Gulf of California	*Paralvinella grasslei*	*Riftia pachyptila*	*Arcovesica* n. spp.	Not pronounced	Octocorallia
		Bythograea thermydron			Lithodidae
		Paralvinella bactericola			

(continued)

Table 1 (continued)

	Temperature anomaly gradient			No temperature anomalies	
Southwest Pacific	*Paralvinella fijiensis* *Paralvinella unidentata*	*Alviniconcha hessleri*	*Bathymodiolus brevior*	*Eochinelasmus ohtai*	Octocorallia
		Ifremeria nautilei	*Arstinograea alayseae*	*Phymorhynchus* sp.	Actiniaria
				Chiridota sp.	Hexactinellida
					Brisingidae
Atlantic	*Rimicaris exoculata*	*Rimicaris exoculata*	*Chorocaris chacei*	*Chaetopteridae*	Actiniaria
			Bathymodiolus spp.	*Phymorhynchus* sp.	
			Calyptogena sp.	*Ophioctinella acies*	

Designations: *D* bacterial deposit feeders, *ESB* exosymbiotrophs, *SB* endosymbiotrophs, *MX* mixotrophs, *F* filter feeders, *C* carnivores

The influence of depth on the spatial structure of vent communities is a major biological problem. We can only suggest that the vent communities in deeper water generally become spatially more complicated. In particular, the above-described characteristic zonation is well pronounced only in vent areas below 1,500 m. In shallow-water communities lacking specific hydrothermal organisms, only one background assemblage might exist (e.g., Steinahol, Kolbensey, Piyp Volcano). On the Loihi Volcano (980 m), only the population of obligate shrimps *Opaepele loihi* is present. In Okinawa and Ogasawara areas (600–800 m), only two zones (euthermal and oligothermal) marked by mytilids and vesicimyids, respectively, could be established, and to distinguish the boundary between these habitats here was somewhat difficult. High-temperature zones marked by alvinellids were observed at vents only deeper than 1,500 m.

Another poorly investigated factor defining spatial structure is temporal variation in the communities. Usually, young virgin vent fields are populated by only one or two distinct assemblages. Mature communities are characterized by higher spatial heterogeneity resulting in a mosaic distribution of various assemblages. Senescence of the field, a decrease of activity, and clogging of local vents result in simplification of spatial structure.

5 Concluding Remarks

Deep-sea hydrothermal vent communities are characterized by complicated taxonomic, trophic, and spatial structure. Different animals consume chemosynthetic bacterial production to a variable extent and by different ways. Different animal groups demonstrate variable degree of adaptations to the extreme environment of hydrothermal vent systems. According to their ecological requirements, vent animal populations occupy different zones within the vent field. For example, the distribution of riftiid vestimentiferans and shrimps is mainly restricted by warm vent zone. Alvinellid and some polynoid polychaetes dominate the hottest extremes culminating, in most cases, with alvinellid polychaetes at the high temperature extremes of around 40°C. On the contrary, vesicomyid clams prefer the zone almost lacking temperature anomalies. The vent mussels may occur in the throat of vents in dense *Riftia* thickets, as well as on rocks that are near, but not directly bathed by vent fluid. The boundaries of different vent fauna assemblages could be rather sharp or feebly marked appearing to be defined by gradients of water chemistry as well as the hydrodynamic regime within the vent field. The idealistic scheme is complicated by the influence of various local factors. Complexity is also added by many mobile animals not restricted to certain assemblages and "background" deep-sea fauna which may enter the hydrothermal community to feed. As a whole, the different habitats within a vent zone are more or less distinguishable.

The influence of different factors determining the spatial structure of vent communities (water chemistry, substratum characteristics, trophic specialization, and behavior of animals) remains not clear. Although we suggest to ensure the

correct analyses of bioconcentration function of vent organisms, the following factors should be taken into considerations: (1) taxonomic position of animals, (2) trophic specialization, (3) patterns of nutrition physiology, (4) the stages of ontogenesis (bioconcentration function could differ in juvenile and adult organisms), and (5) spatial disposition of animal populations relative to local vents.

Acknowledgments We thank the captain of the R/V *Akademik Mstislav Keldysh* and his crew, the pilots, and crew of the submersibles MIR for their essential collaboration during the cruises. Many thanks to scientist who helped us with sorting sample collection and taxonomic identifications. We also acknowledge Drs. L.Moskalev, A. Mironov, A. Gebruk, and M. Turkay for productive discussions. This work was partially funded by the Russian Science Foundation (Grant No. 14-50-00095) (analyses and generalization of the material).

References

1. Elder JW (1965) Physical processes in geothermal areas. AGU Monogr 8:211–239
2. Talwani M, Windish CC, Langseth ML (1971) Reykjanes ridge crest: a detailed geographical study. J Geophys Res 76:473–517
3. Lister CRB (1972) On the thermal balance of a mid-oceanic ridge. Geophys J Roy Astron Soc 26:515–535
4. Wolery TJ, Sleep NH (1976) Hydrothermal circulation and geothermal flux at mid-ocean ridges. J Geol 84:249–275
5. Lonsdale P (1977) Clustering of suspension-feeding macrobenthos near abyssal hydrothermal vents at oceanic spreading centres. Deep-Sea Res 24:857–863
6. Corliss JB, Ballard RD (1977) Oases of life in the cold abyss. National Geographic 152:440–453
7. Enright JT, Newman WA, Hessler RR, McGowan JA (1981) Deep-ocean hydrothermal vent communities. Nature 289:219–221
8. Cavanaugh CM, Gardiner SL, Jones ML, Jannasch HW, Waterbury JB (1981) Prokaryotic cells in the hydrothermal vent tube worm. Science 213:340–342
9. Felbeck H (1981) Chemoautotrophic potential of the hydrothermal vent tube worm, Riftia pachyptila Jones (Vestimentifera). Science 213:336–338
10. Rau GH (1981) Hydrothermal vent clam and tube worm $^{13}C/^{12}C$: further evidence of non-photosynthetic food source. Science 213:338–340
11. Elderfield H, Schulz A (1996) Mid-ocean ridge hydrothermal fluxes and the chemical composition of the ocean. Annu Rev Earth Planet Sci 24:191–224
12. Hessler RR, Smithey WM Jr (1983) The distribution and community structure of megafauna at the Galapagos Rift hydrothermal vents. In: Rona PA, Boström K, Lanbier L, Smith KL Jr (eds) Hydrothermal processes at seafloor spreading centers, NATO Conference, Marine Sciences 12 (IV), pp 735–770
13. Tunnicliffe V (1991) The biology of hydrothermal vents: ecology and evolution. Mar Biol Oceanogr – Annu Rev 29:319–407
14. Desbruyeres D, Segonzac M (1997) Handbook of deep-sea hydrothermal vent fauna. IFREMER, Brest, 279 p
15. Wolff T (2005) Composition and endemism of the deep-sea hydrothermal vent fauna. Cah Biol Mar 46:97–104
16. Moalic Y, Desbruères D, Duarte CM, Rosenfeld AF, Bachraty C, Arnaud-Haond S (2012) Biogeography revisited with network theory: retracing the history of hydrothermal vent communities. Syst Biol 61(1):127–137

17. Humes AG, Segonzac M (1998) Copepoda from deep hydrothermal sites and cold seeps: description of a new species of *Aphotopontius* from the East Pacific rise and general distribution. Cah Biol Mar 39:51–62
18. Komai T, Segonzac M (2005) A revision of the genus *Alvinocaris* Williams and Chace (Crustacea: Decapoda: Caridae: Alvinocarididae), with description of a new genus and new species of Alvinocaris. J Nat Hist 39:1111–1175
19. Rouse GW, Fauchald K (1997) Cladistics and polychaetes. Zool Scr 26:139–204
20. Smirnov AV, Gebruk AV, Galkin SV, Shank T (2000) New species of holothurian (Echinodermata: Holothurioidea) from hydrothermal vent habitats. J Mar Biol Assoc UK 80:321–328
21. Galkin S (1997) Megafauna associated with hydrothermal vents in the Manus Back-Arc Basin (Bismark Sea). Mar Geol 142:197–206
22. Desbruyères D, Crassous P, Grassle J, Khripounoff A, Reyss D, Rio M, Van Praet M (1982) Donnees ecologiques sur un nouveau site d'hydrothermalisme actif de la ride du Pacifique oriental. C R Acad Sci Paris 295(III):489–494
23. Laubier L, Desbruyères D (1985) Oases at the bottom of the ocean. Endeavour 9(2):67–76
24. Fustec A, Desbruyères D, Juniper SK (1987) Deep-sea hydrothermal vent communities at 13^0 N on the East Pacific Rise: microdistribution and temporal variations. Biol Oceanogr 4 (2):121–164
25. Galkin SV (2002) Hydrothermal vent communities of the World Ocean. Structure, typology, biogeography. GEOS, Moscow, 99 p (in Russian)
26. Galkin SV (2010) Structure and biogeography of hydrothermal vent communities of the World Ocean. Zh Obshch Biol 71(3):205–218, in Russian
27. BRIDGE (1994) Workshop Report No. 4. Diversity of vent ecosystems (DOVE), Marine Biological Association, Plymouth
28. Desbruyères D, Alayse-Danet AM, Ohta S, Antoine E, Barbier G, Briand P, Godfroy A, Crassous P, Jollivet D, Kerdoncuff J, Khripounoff A, Laubier L, Marchand M, Perron R, Derelle E, Dinet A, Fialamedioni A, Hashimoto J, Nojiri Y, Prieur D, Ruellan E, Soakai S (1994) Deep-Sea hydrothermal communities in Southwestern Pacific Back-Arc Basins (the North Fiji and Lau Basins): composition, microdistribution and food-Web. Mar Geol 116 (1–2):227–242
29. Arp AJ, Childress J, Fisher CR (1984) Metabolic and blood gas transport characteristics of the hydrothermal vent bivalve, *Calyptogena magnifica*. Physiol Zool 57:648–662
30. Hessler RR, Smithey WM Jr, Keller CM (1985) Spatial and temporal variation of giant clams, tube worms and mussels at deep-sea hydrothermal vents. Bull Biol Soc Wash 6:411–428
31. Le Pennec M, Lucas A, Petit H (1983) Etudes preliminaires sur un Mytilidae des sources hydrother-males du Pacifique. Haliotis 13:69–82
32. Tunnicliffe V, Jensen RG (1987) Distribution and behavior of the spider crab *Macroregonia macrochira* Sakai (Brachiura) around the hydrothermal vents of the Northeast Pacific. Can J Zool 65:2443–2449
33. Hessler RR, Smithey WM, Boudrias MA, Keller CH, Lutz RA, Childress JJ (1988) Temporal change in megafauna at the rose garden hydrothermal vent (Galapagos Rift; eastern tropical Pacific). Deep-Sea Res 35:1681–1709
34. Van Dover CL, Hessler RR (1990) Spatial variation in faunal composition of hydrothermal vent communities on the East Pacific Rise and Galapagos spreading center. In: McMurray GR (ed) Gorda Ridge: a seafloor spreading center in the United States' exclusive economic zone. Springer, New York, pp 253–264

Sources and Forms of Trace Metals Taken Up by Hydrothermal Vent Mussels, and Possible Adaption and Mitigation Strategies

Andrea Koschinsky

Abstract Vent mussels are ubiquitous in most hydrothermal fields, despite the metal-rich environment they live in, with dissolved metal ions, colloidal and particulate metal forms in concentrations orders of magnitude higher than in ambient seawater. Different studies at various hydrothermally active sites on the Mid-Atlantic Ridge and East Pacific Rise have shown that metal concentrations in the tissues of the mussel generally reflect metal loads of their environments, displaying spatial gradients, with bioconcentration factors up to 10^5. Gills and digestive glands accumulate the highest amounts of metals, which is related to their direct role in food uptake, while mantle and foot show moderate metal enrichments. Metal uptake in the form of mineral particles has been identified as an important source of metals in the mussel tissues. While closer to the active vent sites metal sulfides forming during mixing of hot hydrothermal fluid and seawater are more dominant, with increasing distance iron oxides with metals adsorbed from seawater play a more important role for metal accumulation by the vent mussels. Although the shells of hydrothermal mussels have low metal concentrations compared to the soft tissues, they are a record of the chemical composition of the seawater – hydrothermal fluid mixture. Different species of *Bathymodiolus* mussels from the Pacific and Atlantic display similar metal accumulations and adaptation strategies, while vent clams show some similarities, but also some differences compared to *Bathymodiolus*.

Some of the metals (e.g., alkali and earth alkaline elements, Zn and Mn) taken up by the mussels appear to be bioregulated. They are essential elements and their concentration ranges in the mussel tissues are usually less variable than other heavy metals, although their variability in the fluids is comparably high. Strategies of the

A. Koschinsky (✉)
Department of Physics and Earth Sciences, Jacobs University Bremen, Campus Ring 1, 28759 Bremen, Germany
e-mail: a.koschinsky@jacobs-university.de

L.L. Demina, S.V. Galkin (eds.), *Trace Metal Biogeochemistry and Ecology of Deep-Sea Hydrothermal Vent Systems*, Hdb Env Chem (2016) 50: 97–122,
DOI 10.1007/698_2016_2,
Published online: 11 May 2016

vent mussels to cope with high concentrations of potentially toxic metals such as Cu, Cd, and Hg include binding to metallothioneins, which are strongly metal-binding proteins, and possibly immobilization of the metals in the form of granules stored in the tissue. These ways of mitigating heavy metal toxicity have also been found for other organisms including non-vent bivalves. Another yet to be proven possibility is the excretion of organic ligands into the water which binds to the metals and makes them less bioavailable.

Due to the challenges of sampling hydrothermal vent mussels and their environmental compartments, many questions remain open or hypotheses still need to be tested; studies often differ in their approach and a comparison of results is not straightforward. Hence, more systematic studies focusing on specific metal groups, experiments under defined conditions and a comparison of different species of vent mussels are desirable. Apart from the many open questions that refer directly to the understanding of metal accumulation and adaptation of hydrothermal vent mussels to their challenging environment, a better knowledge in this field may also help to support other fields of research. These include estimation of hydrothermal metal fluxes into the ocean and elucidation of survival strategies of organisms in other metal-rich environments.

Keywords Adaptation, *Bathymodiolus*, Digestive gland, Gills, Hydrothermal vent mussel, Metal accumulation

Contents

1 Introduction

Hydrothermal vent sites provide habitats for a rich fauna including mussels that thrive in an environment rich in both nutrients and potentially toxic components [1]. Compared to littoral mussels, hydrothermal vent mussels are exposed to very specific conditions in their habitats, which are characterized by more extreme and dynamic features than the habitats of most other marine bivalves. Hydrothermal vent mussels usually thrive in the mixing zone between hot hydrothermal vent fluids of low pH, high content of reduced gases, and metal concentrations

significantly above seawater, and the ambient cold oxic seawater of pH around 8. Hydrothermal vent mussels are mixotrophs, i.e. they can take up food by different routes: (1) Filtration of water through their gills [2]. The hydrothermal environment usually also provides particulate matter rich in organic carbon and other nutrients, including bacterial flocs and degrading organic matter, which mussels can take up by filtration, similar to their littoral relatives such as *Mytilus edulis*. (2) Symbiosis with endosymbionts that reside in their gills [3]. Those symbiotic bacteria use the oxidation of reduced gases, such as methane, hydrogen sulfide, and hydrogen, as energy source and gain carbon from carbon dioxide provided by the fluids or the seawater. (3) Direct absorption of dissolved amino acids and possibly other dissolved components [4]. Hence, the availability of hydrothermal fluid components is required for survival of hydrothermal mussels, but at the same time also poses a significant challenge to the organisms since the dissolved and particulate metal concentrations in their habitats mostly exceed concentrations that are usually toxic to bivalves and other marine organisms. Investigation of the uptake, accumulation and adaptation or mitigation of metals by hydrothermal mussels is not an easy task because of the intense dynamics and variability of environmental conditions that the mussels are exposed to over their lifetimes. Hydrothermal fluid emissions vary on short to medium time scales and bottom currents also change the ratio of hydrothermal fluid to seawater on short time scales, which leads to distinct variations in environmental conditions in the fluid-seawater mixing zone where hydrothermal microbes, mussels, and other organisms thrive [5, 6]. Mussels experience semidiurnal transitions in temperature, oxygen, pH, and intermittent sulfide as was shown in several studies [7, 8]. These studies emphasize the need for integration of multiple observational scales in environmental studies.

Furthermore, dissolved and particulate metal forms and concentrations change with distance from the hydrothermal fluid discharge site, due to mixing with ambient seawater (Fig. 1). Since the behavior of most metals along the mixing transect between hydrothermal fluid and seawater is not just characterized by dilution of metal-rich fluid with metal-poor seawater, but also by precipitation of metals as sulfide, sulfate and oxide minerals, or by sorption on particulate matter formed in the mixing zone, the depletion of metal concentrations away from the fluid source is not linear with mixing. Dissolved concentrations of metals tend to decrease rather quickly during mixing with seawater, while at the same time the contribution of colloidal or particulate metal loads increase relative to the dissolved concentrations. While close to the vent, particulate matter is mostly comprised of sulfide minerals precipitating directly from the metal- and sulfide-rich fluid, with increasing mixing with oxic seawater further away from the discharge site divalent Fe oxidizes and forms Fe oxide precipitates [9]. Colloids, being the interim form between truly dissolved ions and particulate forms, behave physically like dissolved components, i.e. they do not sink in the water column, but physico-chemically they have features of particles, such as charged surfaces, on which other ions including truly dissolved trace metal ions can adsorb and bind [10]. Such uptake of colloids and mineral particles may be one of the exposure and uptake routes of trace metals

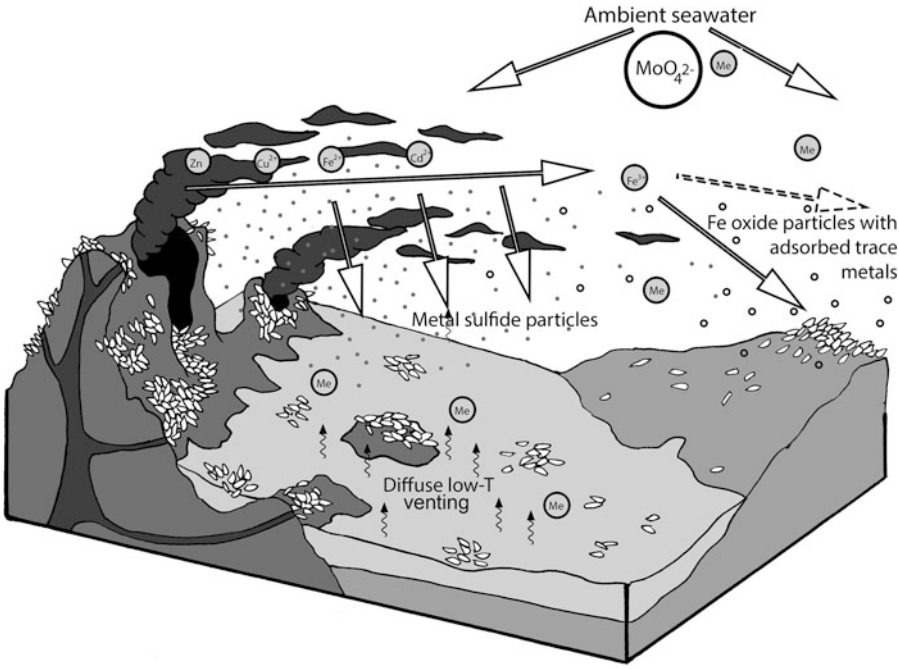

Fig. 1 Simplified sketch of a hydrothermal mussel habitat, demonstrating sources of dissolved and particulate metals for the uptake in hydrothermal vent organisms; the further away the mussels live from the discrete emanation site, the more does the impact of metal sulfide particles and high dissolved hydrothermal metal concentrations decrease, and the nature of the particulate matter changes to Fe hydroxide minerals while for the dissolved components seawater input plays a larger role

by the mussels. Hence, a good understanding of the uptake of different physical forms of metals (dissolved – colloidal – particulate) is of utmost importance to investigate the adaptation and mitigation strategies of the mussels to cope with high potentially toxic metal loads.

Apart from the physical form of the metal, also its chemical form, i.e. its chemical speciation, plays a dominant role in the uptake routes and bioconcentration in tissues. While free metal ions such as Cu^{2+} are often considered to be the most bioavailable and toxic form, metals often occur in chemically complex forms in natural aqueous systems rather than as free ions [11]. This includes inorganic complexes, such as $CuCl^+$ or $Cu(HS)^+$, or organic complexes in which the central ion is chemically bound to an organic molecule such as an amino acid that has one or more functional groups providing free electron pairs for the bond formation with the metals. These complexes are known to be often very stable and to be the dominant chemical form for many metals, especially for Cu, but also for Fe, Zn, Co, Ni, and many other metals. Solution complexation also competes with mineral precipitation and sorption and can hence significantly increase metal solubility in an aqueous system. Analyses of the dissolved Cu

speciation in an active hydrothermal edifice of the Lucky Strike vent field revealed that most dissolved Cu was present as inorganic and hydrophilic organic complexes [12]. An increase in Cu with pH until about 6.5 was interpreted to be related to the oxidative redissolution of Cu sulfide particles in the transition zone between anoxic and oxic waters, representing a secondary dissolved Cu source that may become available for the uptake by vent mussels thriving in this anoxic-oxic transition zone.

While some metal complexes appear to be less bioavailable and less toxic than the free metal ions, for some complexes it is vice versa, e.g. Hg methyl mercury components are more toxic to most organisms than Hg^{2+}. In addition, the stability and chemical reactivity of most chemical compounds is dependent on pH (especially if complex formation involves protons or hydroxyls) and temperature, which can be highly variable between sites and fluctuate on different time scales during the lifetime of the mussel [13]. This clearly demonstrates that a profound physico-chemical characterization of the habitat environment is necessary to interpret the metal tissue concentrations and uptake, possible toxicity and mitigation strategies of the hydrothermal vent mussels. In a study on metal toxicity for hydrothermal vent Archea [14] it was found that sulfide ameliorates Zn, Co, and Cu toxicity by formation of dissolved metal sulfide complexes and sulfide precipitates. Thus it might also be possible that chemical speciation of metals with sulfide or other strongly complexing ligands allows hydrothermal mussels to tolerate otherwise toxic metal concentrations. Also possible synergistic effects and interactions of different metals should be taken into account. As an example, Se (in the form of selenite) known for its role in antioxidant defense was shown to protect against negative effects of Cu exposure in *Mytilis edulis* by induction of antioxidant defenses such as glutathione and Se-dependent glutathione peroxidase [15]; similar mechanisms of this or other element couples could also play a role in mediating toxic metal effects in hydrothermal mussel habitats. For example, dissolved Hg uptake appears to be reduced following exposure to other metals such as Ag, Cd, Cu, and Zn [16].

The goal of this paper is to summarize the state of the art in research of metal accumulation by hydrothermal mussels, to discuss the data in the context of environmental sources and forms of the metals, and to point out possible adaption and mitigation strategies that hydrothermal vent mussels appear to use to cope with the high metal content of their food sources and living environment. This paper also includes brief comparisons with other hydrothermal organisms and with non-hydrothermal mussels.

2 Metal Sources and Concentrations in Tissues of Vent Mussels

2.1 General Patterns and Spatial Variability of Metal Accumulation

Trace metal uptake and accumulations in marine invertebrates including mussels vary strongly; this variability is related to species, age, size, sex, physiological state, and environmental conditions including temperature and salinity [17]. Furthermore, the metal exposure history may have an effect on the uptake and storage of further metal loads, since metal exposure may induce physiological and biochemical changes in the cell that may impact the uptake of more metal loads [16]. Since hydrothermal mussels such as *Bathymodiolus* mussels are mixotrophs, the distribution of trace metals between different food sources will play an important role for the uptake and accumulation in the body tissues as well. Uptake of metals, together with the food, can be directly via the fluid and its dissolved components, or via the particles that remain in the gills during filtering or are ingested directly. Indirect uptake can occur via the symbiotic bacteria living in the gills of the mussels. These bacteria provide nutrients to their host and during this uptake pathway also a transfer of metals may be possible. Hydrothermal fluid flow and the physicochemical composition of the hydrothermal fluids in the mussel habitats may also fluctuate on small to medium time scales over the life times of the mussels, as well as the way of nutrition, i.e. the ratio of food uptake by filtration and by symbiosis with the bacteria [18]. The uptake pathway will also determine how the metal taken up will be transformed and in which organ it will accumulate, or if and how it can be excreted. To shed more light onto these complex processes, thorough and systematic studies of different sources of metals in the habitats of the vent mussels, the concentrations and binding forms of metals of the food sources, and metal concentrations and binding forms in the tissues, such as gills, digestive gland, and muscle tissue (foot) are required.

Despite a significant number of individual studies in this field (Table 1), there are still many open questions and the picture of results is highly diverse. This is largely due to the fact that most studies differ strongly from each other in their setup, focus, mussel species, and chemical elements analyzed. However, some general trends can nevertheless be deducted from a review of these studies. Bioconcentration factors of the trace metals Fe, Mn, Zn, Cu, Ni, Cr, Co, As, Pb, Cd, Ag, and Hg in *Bathymodiolus* mussels collected at three vent fields from the MAR and one vent field from the East Pacific Rise (EPR) were found to be in the range of 10^2–10^5 which is largely similar to that of littoral mussels [19]. However, the total concentrations of many metals are significantly higher in the tissues of hydrothermal vent mussels than of their littoral relatives such as *Mytilus edulis*, which reflects the higher load of trace metals in the hydrothermal environment. The metal accumulation in the soft tissues of the mussels is largely a reflection of their metal-rich vent habitat [20, 21], with Fe often being in the range of >1,000 mg/kg dry weight,

Table 1 Comparison of average metal concentrations (in mg/kg dry weight) in (a) soft tissues and (b) shells of hydrothermal *Bathymodiolus* mussels and other hydrothermal mussel and clam species; average values are given, if not stated otherwise

Hydrothermal site	Species	Tissue	As	Cd	Cr	Cu	Fe	Hg	Mn	Mo	Pb	Zn	References
(a) *Soft tissues*													
Logatchev, Irina II	*B. puteoserpentis*	Gills		2.8	0.77	187	757		4.8	1.0	6.8	187	[20]
Logatchev, Irina II	*B. puteoserpentis*	Digestive gland		11.1	1.52	23	1495		4.3	1.4	1.2	75	[20]
Logatchev, Irina II	*B. puteoserpentis*	Foot		8.77	1.42	15.3	128		5.8	0.38	0.38	46.4	[20]
Logatchev, Quest	*B. puteoserpentis*	Gills		6.5	1.13	148	361		6.7	4.2	29.7	118	[20]
Logatchev, Quest	*B. puteoserpentis*	Digestive gland		1.4	1.11	30	403		6.7	1.2	6.6	80	[20]
Logatchev, Quest	*B. puteoserpentis*	Foot		0.11	0.78	6	89		5.4	0.52	3.76	39.1	[20]
5°S, Golden Valley	*B. puteoserpentis*	Gills		9.7	1.46	352	352		15.2	36.7	10.9	169	[20]
5°S, Golden Valley	*B. puteoserpentis*	Digestive gland		1.3	0.96	53	196		3.8	7.1	1.4	104	[20]
5°S, Golden Valley	*B. puteoserpentis*	Foot		0.2	0.60	45.5	129		7.1			76	[20]
Lilliput	*B.* spp.	Gills		2.3	2.37	290	280		3.2	72.0	1.6	126	[20]
Lilliput	*B.* spp.	Digestive gland		7.7	3.97	91	830		4.5	86.6	10.3	65	[20]
Lilliput	*B.* spp.	Foot		0.16	0.68	10.6	78		4.3	5.29	0.11	42.5	[20]
Broken Spur	*B. puteoserpentis*	Foot	6.26	0.04	0.87	6.4	171	0.244	7.6		0.05	7.5	[19]
Broken Spur	*B. puteoserpentis*	Other organs	2.43	0.27	2.88	85.1	1495	0.221	8.0		0.05	93.6	[19]

(continued)

Table 1 (continued)

Hydrothermal site	Species	Tissue	As	Cd	Cr	Cu	Fe	Hg	Mn	Mo	Pb	Zn	References
Broken Spur	*B. puteoserpentis*	Gills	29.4	2.62	4.09	380	6541	2.07	5.6		7.95	258	[19]
Snake Pit[a]	*B. puteosetpentis*	Gills	145.8	63.9	2.35	975	37495	0.185	102.5		408	57090	[25]
Snake Pit[a]	*B. puteosementis*	Other organs	9.82	9.0	0.26	135	5871	0.032	10.1		10.8	1781	[25]
Snake Pit[a]	*B. puteosementis*	Foot	0.94	0.51	0.46	7.9	295	0.022	6.85		15.2	99.5	[25]
Snake Pit	*B. puteosetpentis*	Gills	71.0										[56]
Menez Gwen	*B. azoricus*	Gills	6.56	1.24	1.05	124	233	0.99	5.1		16.3	162	[25]
Menez Gwen	*B. azoricus*	Other organs	1.07	2.3	0.34	24	124	0.15	2.7		17.0	77	[25]
Menez Gwen	*B. azoricus*	Foot	1.24	0.5	2.85	9.4	51.2	0.12	2.8		15.3	42.1	[25]
Menez Gwen	*B. azoricus*	Digestive tract	0.49	7.81	0.37	29.5	107	0.47	1.9		7.0	62.3	[25]
Menez Gwen[b]	*B. azoricus*	Gills		3.2/ 7.4		57/130	183/ 206		6.3/4.8			168/ 197	[21]
Menez Gwen[b]	*B. azoricus*	Digestive gland		4.0/ 2.3		30/172	198/ 200		3.8/2.1			82/ 111	[21]
Menez Gwen	*B. azoricus*	Gills				47		4.4				111	[29]
Menez Gwen	*B. azoricus*	Digestive gland				22		4.6				40	[29]
Menez Gwen	*B. azoricus*	Gills		4.44				2.42	4.0				[38]
Menez Gwen	*B. azoricus*	Digestive gland		28.9				2.85	5.94				[38]
Menez Gwen	*B. azoricus*	Whole tissue				41	120					180	[30]
Menez Gwen	*B. azoricus*	Whole tissue						3.76					[22]

Rainbow	*B. azoricus*	Whole tissue	10.0										[32]
Rainbow	*B. azoricus*	Gills	50.0	1.37	6.70	423	4240	0.61	25.1		21.0	229	[25]
Rainbow	*B. azoricus*	Other organs	12.5	1.3	2.56	20	1231	0.33	16.5		5.9	94	[25]
Rainbow	*B. azoricus*	Foot	13.5	0.85	1.16	9.7	734	0.034	5.3		1.4	53	[25]
Rainbow	*B. azoricus*	Gills		1.8		52	2066		9.1			106	[21]
Rainbow	*B. azoricus*	Digestive gland		1.5		11	1854		8.1			45	[21]
Rainbow	*B. azoricus*	Gills				67		1,0				106	[29]
Rainbow	*B. azoricus*	Digestive gland				18		1.3				80	[29]
Rainbow	*B. azoricus*	Gills					4000						[39]
Rainbow	*B. azoricus*	Whole tissue				70	2700					140	[30]
Rainbow	*B. azoricus*	Gills		2.25				8.23	24.6				[38]
Rainbow	*B. azoricus*	Digestive gland		13.31				12.5	17.7				[38]
Rainbow	*B. azoricus*	Whole tissue						0.34					[22]
Lucky Strike	*B. azoricus*	Whole tissue	12.0										[32]
Lucky Strike[a]	*B. azoricus*	Gills		47.2/ 17.6		80/109	361/ 488		9.5/7.2			1977/ 768	[21]
Lucky Strike	*B. azoricus*	Gills				70		4.1				555	[29]
Lucky Strike	*B. azoricus*	Digestive gland				52		2.4				201	[29]
Lucky Strike	*B. azoricus*	Gills				250						500	[39]
Lucky Strike	*B. azoricus*	Gills		28.55				5.84	7.87				[38]

(continued)

Table 1 (continued)

Hydrothermal site	Species	Tissue	As	Cd	Cr	Cu	Fe	Hg	Mn	Mo	Pb	Zn	References
Lucky Strike	*B. azoricus*	Digestive gland		15.89				2.16	8.63				[38]
Lucky Strike	*B. azoricus*	Whole tissue				226	609					400	[30]
East Pacific Rise	C. *magnifica*	Whole tissue	24.8	9.8	16.6	148	760	0.41	5.0	49.2	6.0	2152	[35]
East Pacific Rise	C. *magnifica*	Gills	33.2	46.0	55.5	219	1931	<6	<7	77.6	23.2	1560	[35]
Galapagos Rift	*B. thermophilus*	Gills	37.0		41.0		310		111	131		217	[23]
Galapagos Rift	*B. thermophilus*	Digestive gland	23.0		30.0		948		26	159		61	[23]
Galapagos Rift	*B. thermophilus*	Foot	8.0		2.00		91		23	11		78	[23]
Guyamas Basin	*A. gigas*	Foot	3.57	3.62	5.57	9.2	125	0.98	10.8		1.84	120	[57]
Guyamas Basin	*A. gigas*	Gills	1.0	1.12	21.4	42.5	284	0.17	8.6		1.42	3110	[57]
Guyamas Basin	*V. gigas*	Gills		115		8,0	403	5.0	18.0		3.0	845	[37]
North Fiji Basin	*B. brevior*	Gills		4.3	0.65	329	417		42.5	173	7.4	235	Koschinsky (unpublished)
North Fiji Basin	*B. brevior*	Digestive gland		2.3	0.18	53	228		32.0	24.2	1.6	202	Koschinsky (unpublished)
North Fiji Basin	*B. brevior*	Foot		1.0	0.24	38	100		24.3	19.4	1.9	116	Koschinsky (unpublished)

Tonga[c]	*B. manusensis*	Gills						16-66					[31]
Tonga[c]	*B. manusensis*	Digestive gland						30-37					[31]
Tonga[c]	*B. manusensis*	Other organs						7-17					[31]
Tonga[c]	*B. brevior*	Gills						38-67					[31]
Tonga[c]	*B. brevior*	Digestive gland						2-42					[31]
Tonga[c]	*B. brevior*	Other organs						1-17					[31]
(b) *Shells*													
Logatchev, Irina II	*B.* spp.	Shell				1.0	44					1.0	[58]
Broken Spur	*B. puteoserpentis*	Shell	0.86	0.03	2.4	2.3	30	0.046	13.5		0.05	11.2	[19]
Snake Pit[a]	*B. puteoserpentis*	Shell	0.47	0.21	1.6	54	720	0.023	1.0		3.00	52	[25]
Menez Gwen	*B. azoricus*	Shell	0.23	0.1	1.72	2.0	77	0.17	0.5		1.00	5	[25]
Menez Gwen	*B. azoricus*	Shell		1.0		1.0	21		4.0			9	[59]
Menez Gwen	*B. azoricus*	Shell				1.0	21		4.0			9	[60]
Menez Gwen	*B. azoricus*	Shell				20	5					31	[41]
Lucky Strike	*B. azoricus*	Shell		1.0		2.0	55		9.0			11	[59]
Lucky Strike	*B. azoricus*	Shell				80	280					40	[41]
Rainbow	*B. azoricus*	Shell		1.0		1.0	51		20.0			11	[59]
Rainbow	*B. azoricus*	Shell	1.9	0.24	1,0	6.8	673	0.037	92.0		2.7	16.4	[25]
East Pacific Rise	C. *magnifica*	Shell	<2	6.9	0.04	5.9	17	<6	<3	<2	<3	3.4	[35]
Guyamas Basin	*A. gigas*	Shell	1.0	3.64	0.61	8.5	191	0.08	56.8		2.72	20	[57]

[a]Data for Snake Pit come from only one sample
[b]Mean levels for two different sites within the hydrothermal field
[c]Data for mussels from the Tonga site are presented in a range because individual values were not given. Three to five samples for each soft tissue was used

followed by Zn and Cu that are often in the range of several 100 mg/kg (Table 1). For metals such as Ba, Pb, Cd, Cr, U and Mo concentrations between a few mg/kg and several tens of mg/kg have been reported. Surprisingly, Mn values are often below 10 mg/kg, although Mn mostly displays the second highest metal concentrations in the fluids, after Fe. Mercury was found to be mostly below 10 mg/kg in mussels from the MAR [22], with a few exceptions (Table 1).

The majority of studies have focused on *Bathymodiolus* mussels, which are widespread on the Mid-Atlantic Ridge. Here, *B. azoricus*, *B. puteoserpentis*, and *B. spec*. have been investigated, while in studies in the Pacific *B. thermophilus* was abundant. Since it is not clear whether despite the close relationship between the different species of *Bathymodiolus* metal uptake and accumulation follow the same rules, they will be considered separately in the following.

One of the earliest studies on *B. thermophilus* was done by [23] who analyzed a large number of elements in tissues and whole bodies of samples from the Galápagos Rift. One of their major findings was that some elements such as Ag, As, Fe, Mn, Mo, Se, and Zn in *Bathymodiolus thermophilus* specimens were enriched in a similar range as in coastal mussels such as *Mytilus edulis* or higher, corresponding to the high concentrations of these elements in the vent environment, with the strongest enrichments in gills and digestive glands. Fe:Mn ratios in these tissues were similar to the respective ratios in the sediment of the habitat, leading to the conclusion that these and possibly other elements were largely derived from filtered particulate matter which had been adsorbed onto the mucous membranes of the gills. In the North Fiji Basin, *Bathymodiolus brevior* mussels [24] were sampled and analyzed for trace metals in different tissues. While only a few individuals were analyzed, the average concentrations of Fe, Mn, V, Mo, Cr, Co, Ni, Cd, and Pb were found to be in same range as for other mussel species from the other hydrothermal sites (Table 1, Fig. 2).

Studies from the Mid-Atlantic Ridge (MAR) covered many different vent fields, which differ in their habitat conditions including substrates, fluid composition, and temperature of the fluids. Hence, the relatively large spread of data reported was to be expected. According to a study by [25] on the role of abiogenic factors in the bioaccumulation of heavy metals, concentrations of metals in tissues from different hydrothermal sites at the MAR correlate directly with their concentrations in the released fluids, with some exceptions. This, however, does not apply to all metals and all observations made in different studies. The positive correlation of alkaline-earth metals in the mussel tissues observed in a study on *Bathymodiolus* mussels from the MAR [20] is consistent with relationships in freshwater mussel species, in which a comparative accumulation of alkaline-earth metals was observed and Ca concentration was shown to be a highly significant predictor for the concentrations of Mg, Sr, and Ba [26]. The similar trends of this element group (together with K) in the hydrothermal mussels can only partly be explained by their coherent geochemical behavior. Probably this element group is largely regulated by biological functions, as Ca and Mg are involved in numerous metabolic processes on both cellular and inter-cellular level and they are also known to interact and control each other in living beings [27]. While Ba is mostly enriched in hydrothermal fluids, K,

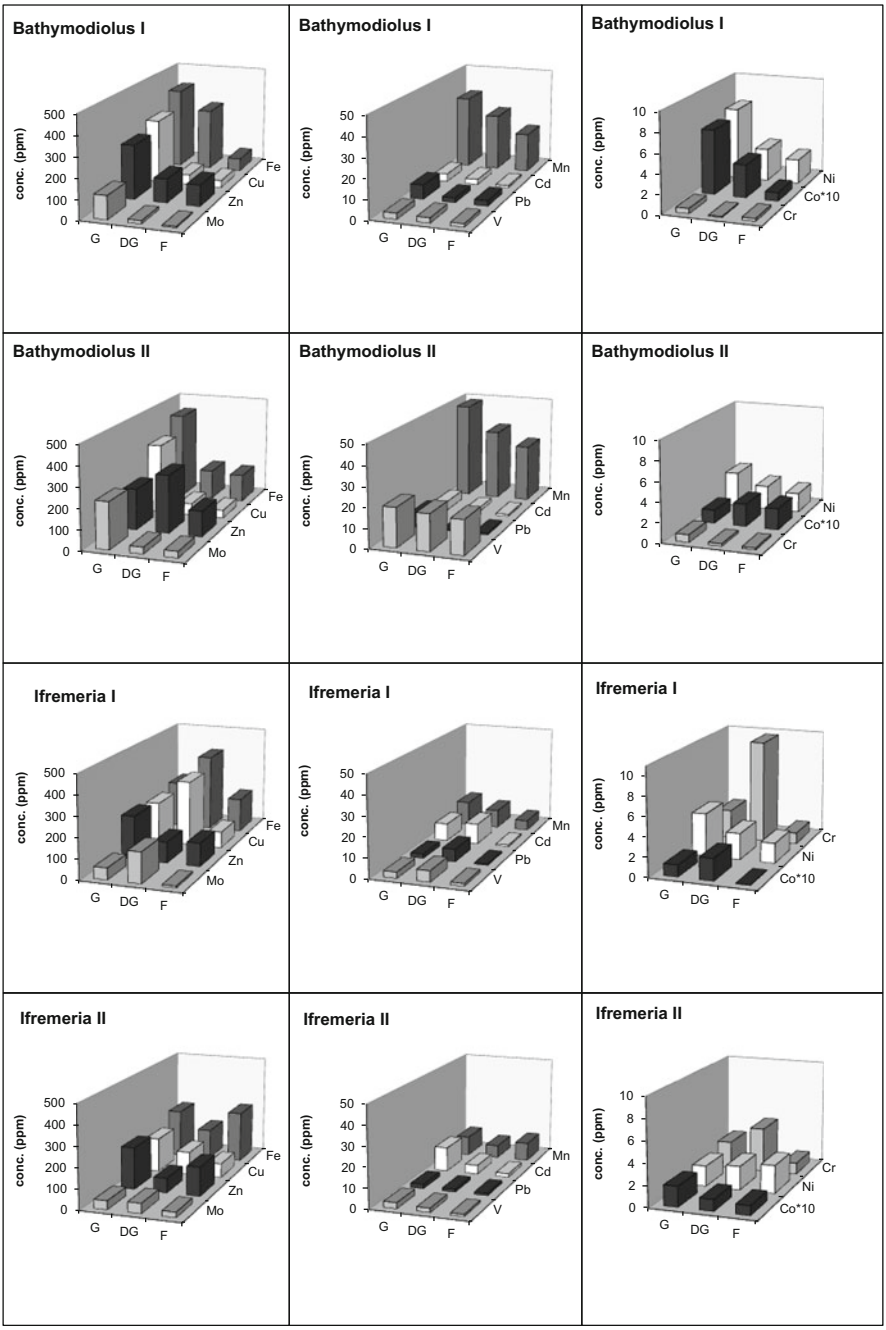

Fig. 2 Metal concentrations in the tissues (G=gills, DG=digestive gland, F=Foot) of two individual mussels of the species *Bathymodiolus brevior* collected in the North Fiji Basin, in comparison with tissue concentrations in two individuals of the snail *Ifremeria nautilei*; all animals were collected from the same site venting diffuse low-temperature fluid. The graph

Ca, and Sr can be enriched or depleted compared to ambient seawater. In contrast, Mg is always depleted and often even zero in hot endmember fluids, due to the quantitative removal as Mg hydroxide [28]. Precipitation of minerals from fluid components, such as anhydrite ($CaSO_4$, controlling Ca and partly Sr concentrations by Sr substituting Ca in the crystal lattice) and barite ($BaSO_4$, strongly limiting Ba solubility) must be considered.

Chromium, which is typically not strongly enriched in hydrothermal fluids, does not show strong accumulation in mussel tissue (Table 1), probably reflecting a rather low content of Cr in the environment. As U and Mo are mostly even depleted in hydrothermal fluids compared to ambient seawater their partial enrichment in the gills and digestive gland can only be attributed either to inclusion of particulate sulfides (especially for Mo) or to uptake from ambient seawater, as these two elements have rather high concentrations in seawater (in the range of a few µg/kg) compared to other elements. The latter could take place either in the form of dissolved anions (molybdate and uranyl carbonate complex, the dominant forms in seawater) or adsorbed onto Fe oxyhydroxide particles taken up by the mussel. This could also explain the high concentrations of Fe, Cr, Mo, and U concentrations in the gills and digestive glands of *Bathymodiolus* mussels in the Lilliput hydrothermal field at the MAR, which live in the Fe oxyhydroxide-rich sediment in a low-temperature vent field [20].

The highest Hg concentrations in organisms from the MAR were found in the shallow hydrothermal vent field Menez Gwen, while those from Lucky Strike and Rainbow were richer in Cu and Zn [29]. These results agree with a previous report [22] on the highest Hg concentrations in *B. azoricus* at Menez Gwen compared to the other two sites and were referred to chemical differences in the fluid geochemistry and differences in nutritional contributions of methanotrophic and thiotrophic symbionts within the mussels. Higher Hg in smaller mussels was attributed to the higher metabolic rate or greater surface/volume ratio of smaller individuals. This is, however, in contrast to results of [30] who report higher Hg concentrations for Rainbow compared to the other fields, indicating that results do not always agree between individual studies. Hydrothermal mussels from the Tonga arc showed Hg concentrations 10–100 times higher than in other hydrothermal fields, which indicates that the hydrothermal fluids and possibly sediment and ore particles very rich in Hg are the source of this extreme Hg accumulation [31]. Enrichments were highest in gills and digestive glands compared to mantle and residues. Monomethyl mercury concentrations, however, were orders of magnitude lower in both the mussel tissues and sediments.

Arsenic concentration and speciation in hydrothermal fauna from the MAR differs between species, suggesting different sources of As uptake. In the mussel *B. azoricus* arsenosugars were more abundant than arsenobetaine, dimethylarsinate,

Fig. 2 (continued) demonstrates the variability of metal accumulations between individuals of the same species, while at the same time certain metal distribution patterns are obvious that distinguish the different species of hydrothermal organisms from each other

and inorganic As [32]. It is suggested that these organic As components were formed as part of the chemolithoautotrophic food production.

Differences in metal accumulations in mussel tissues were not only observed between different vent sites. Other studies comparing metal accumulations in different individual mussels from the same vent site revealed significant differences, which probably reflect small-scale spatial differences of fluid compositions and the short- to medium-term variability of the physico-chemical environment in the mussel habitats, as discussed earlier. For example, a comparison of six distinct locations of Eiffel Tower in the Lucky Strike vent field indicated that the metal accumulations in *B. azoricus* are related to their spatial distribution and reflect the fine-scale environmental gradients that influence the physiological status of the animals [6]. In the Logatchev hydrothermal field at 15°45′N on the MAR, at site Irina II Fe concentrations in the gills and digestive gland, Zn in the gills, and Cd in the gland and foot were much higher than in all other tissues of all other sites, pointing to the influence of sulfide minerals from the sulfide mound structures from which the mussel samples were retrieved [20]. Mussels from the site Quest in the Logatchev field had by far the highest Pb and Ba contents compared to the mussels from the other active sites in that field, which was linked to the high content of these elements in the sediment from where the mussels were sampled [20]. Similarly, [21] described major differences in metal bioaccumulation between five vent sites within three main vent fields, where these differences were obvious between the main field (Menez Gwen, Lucky Strike, and Rainbow on the MAR), but also between individual sites within one main field. Mussels from Rainbow bioaccumulated more Fe and Mn but less Ag, Cd, Cu, and Zn than mussels from Menez Gwen and Lucky Strike (Table 1). However, in all these sites the levels of these metals in the tissues of *B. azoricus* were higher than in the respective tissues of coastal mussels. This is in accordance with other studies [33, 34].

On top of the small-scale geochemical differences in the habitats, the stage of ontogenesis of the individuals may play a role, since it had been observed that *B. azoricus* depends more strongly on filter-feeding at a young age compared to a larger energy gain by the metabolic activity of the chemosynthetic endosymbionts for larger mussels [18]. This argument has also been used to explain why the very small *Bathymodiolus* mussels found in the young low-temperature vent field Lilliput at 9°S on the MAR showed strong signatures of metals from the thick iron oxyhydroxide coatings on which the mussels were living, such as high Fe, Cr, and Cd contents in the digestive gland and high Cu and Mo in the gills and gland, although the dissolved concentrations of these metals were rather low [20] (Table 1).

While the majority of studies on trace metal accumulation by hydrothermal bivalves have been carried out on the genus *Bathymodiolus*, a few other publications present data for the hydrothermal vent clams *Calyptogena magnifica* from the East Pacific Rise [35, 36] and for *Vesicomya gigas* from the Guaymas Basin in the Gulf of California [37]. Like for *Bathymodiolus*, metal accumulation in the soft tissues was found, and also the dominance of Fe and Zn as enriched metals was consistent with the studies on mussels, followed by Cu, Cd, and Pb, while Mn was

again low compared to the high Mn concentrations in the surrounding fluids (Table 1). These studies also point out the probable importance of particulate matter (organic or mineral particles) as a source of metals for uptake.

Since mineral precipitation starts right after the hot hydrothermal fluid of low pH cools and mixes with ambient seawater, mussels living close to the active venting can be assumed to be exposed to a high load of sulfide particles, specifically of Fe, Zn, and Cu (Fig. 1). Indeed, X-ray diffraction analyses of gills from *Bathymodiolus* showed the presence of pyrite (Fe sulfide) and wurtzite (Zn sulfide), indicating that suspended mineral particles were actively filtered from the water through the gills of the mollusks [25]. Colaço et al. [29] also found such hydrothermal mineral fragments in the stomachs of *B. azoricus* and other vent organisms. The characterization of dissolved and particulate (>2 μm) metals in active vent habitats at the EPR [12] had confirmed that particulate matter that vent fauna is mostly exposed to consists of crystalline sulfide particles such as sphalerite, pyrite and wurtzite and eroded particles from the smokers settling rapidly in the vicinity of high-temperature smokers; these particles act as a secondary source of metals for the organisms.

In addition to the amount of metals taken up from the fluid and inorganic or particulate matter in the environment, the symbiotic bacteria in the gills may influence metal accumulation by the mussel. In endosymbionts and lysosomes of *B. azoricus* high concentrations of several metals were found, e.g. all Al in the gill of mussels appears to be associated with bacterial cells [38] and high amounts of Hg in the endosymbionts [30] were reported as well.

2.2 Metal Partitioning Between Tissue Types

The partitioning behavior of chalcophile (Cu, Cd, Zn, Pb, and Fe) elements in the *Bathymodiolus* mussels shows largely consistent results among different studies. Generally, the gills in *Bathymodiolus* mussels, which are the organs functioning with dependence on chemosynthetic bacteria, show the highest degree of bioaccumulation of heavy metals. However, the digestive glands are also significantly enriched in metals [25]. While the general enrichment of chalcophile elements and some other trace metals in the gills and digestive gland is well established (Fig. 3), there seem to be local differences in the partitioning between these two tissues, as shown in Table 1. Comparison of element ratios in the different tissues revealed that high Fe/Cu ratios and Fe/Zn ratios were mostly associated with digestive gland samples, while those with low Fe/Cu and Fe/Zn ratios were largely gill samples [20], which points to a preferential enrichment of Fe in the digestive glands and of Zn, Cu (and also Pb) in the gills. For other elements including Cd, Cr, Mn, and Mo, the respective roles of gills or digestive gland for preferential uptake are less clear, but generally, the foot which is not directly involved in food uptake and exchange with the environment, and the mantle which controls secretion of the shell has the lowest concentrations of all elements [38, 39]. In a study of ^{210}Po and

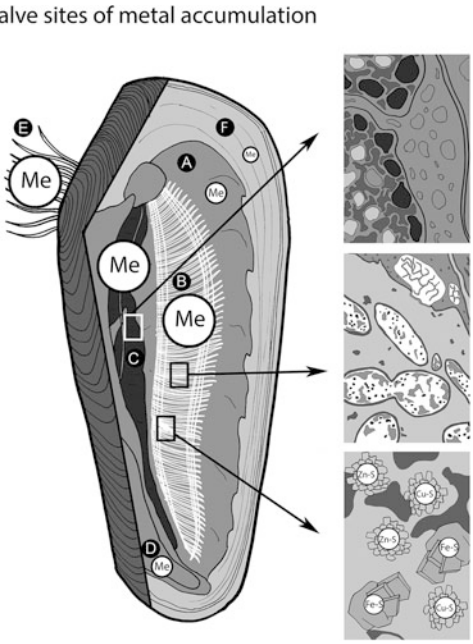

Fig. 3 Sketch of a cross section through a hydrothermal mussel, showing the major organs and tissues in which trace metals can accumulate: *A* mantle, *B* gills, *C* digestive gland, *D* foot, *E* byssus thread, *F* shell. Sites, relative magnitudes and types of metal accumulation are shown for the different tissues (metal-rich granules in the digestive gland, symbiotic bacteria and metal-bearing mineral particles in the gills)

^{210}Pb (two natural radionuclides within the ^{238}U decay chain) in mussels from the Menez Gwen field (MAR), again high levels of both isotopes were found in the gills, but Po was also comparably enriched in other tissues including the digestive gland [40]. The only tissue that shows even an order of magnitude higher metal concentrations than gills and digestive glands is the byssus thread and these concentrations were proportional to the levels in the water [38, 39].

Even within single vent sites, for individual mussels living close to each other in a basically similar environment, the distribution of trace metals between the different tissues can vary. This is demonstrated in Fig. 2; here, the trace metal distributions between gills, digestive gland, and foot are compared for two randomly selected individuals of the species *Bathymodiolus brevior* collected within a single low-temperature diffuse vent site in the North Fiji Basin [24]. Not only do the absolute concentrations vary between the two mussels, such as much higher V concentrations in one mussel (which may be related to higher Mn in this sample), but sometimes even the order of enrichment is different, e.g. for Zn which is higher in the gills of one mussel and higher in the digestive gland of the other mussel. However, general trends that are characteristic of the species are also clearly visible; this becomes obvious when the data are compared with the data of two individuals of the snail *Ifremeria nautilei* that were collected at the same site as the

Bathymodiolus mussels. While for the mussels Cu and Mo are largely accumulated in the gills, it is about equally distributed in the gills and glands by the snail. Manganese is generally much higher in the mussels, even in the foot, than in all tissue samples of the snails. In contrast, Cr shows a much stronger accumulation especially in the digestive gland by the snail, and also Cd is higher in the tissues of the snail. Although it is difficult to deduce general trends from just a few individuals per species, general metal accumulation patterns in tissue types of species, with a range of variations between individuals, have also been confirmed in other studies listed in Table 1.

Comparing metal partitioning of *Bathymodiolus* mussels with the vent clams from the Pacific [35–37] one obvious difference was the dominant role of the gills for Cd enrichment in the clams, while in *Bathymodiolus* mussels both gills and digestive gland showed similar Cd concentration ranges. This may have to do with the differences in the digestion system of the mussels and the clams and the reduced digestive system of the clams. The difference for Cd accumulation in clams and mussels agrees with results reported by [16] that uptake rates, body burden and subcellular distribution of Cd differ between clams and mussels. The gills of the hydrothermal clams showed high concentrations of many other metals such as Zn, Fe, and Hg as well while the kidneys of the clams were found to be enriched in Cu, As, Se, Mo, and Ag. However, since different organs (gills, mantle, and/or gonads, kidneys, and pericardium in the clams) and partly different metals were analyzed, a direct comparison of the two types of bivalves is hampered.

While the order of metal accumulation in the soft tissues in hydrothermal mussels was found to be byssus thread $>$ gills $\geq$ digestive gland $>>$ mantle $\approx$ foot in most studies, the shells of these mussels, being composed of the Ca carbonate minerals calcite and/or aragonite, show lowest trace metal concentrations (Fig. 3). These concentrations, however, are mostly higher than in shells of comparable species from metal-contaminated sites [41]. The shells of the hydrothermal mussels were found to carry the signatures of the fluids [41], as has also been shown in a study on rare earth element (REE) distributions in *Bathymodiolus* shells from the Mid-Atlantic Ridge [42]. The REE patterns of these shells, e.g., showed positive Eu anomalies, which are a typical feature of hot hydrothermal fluids. In contrast the littoral *M. edulis* shells studied for comparison do not show Eu anomalies, consistent with the lack of any high-temperature hydrothermal activity in their coastal environments. Similarly, REE + Y patterns in *M. edulis* mussel shells from the North Sea reflected the pattern of the seawater such as a negative Ce anomaly and small positive Y and Gd anomalies [43], indicating that in general mussel shells may be good proxies for environmental conditions in their habitat. These studies also indicate that although the Ca carbonate of a mussel shell is precipitated from the extrapallial fluid of the mussel and not directly from seawater, the environmental conditions prevailing during vital processes and biomineralization are still largely reflected in the trace metal signatures of the shells.

The metals with the reported highest concentrations in shells of hydrothermal bivalves are Fe and Mn (up to 673 mg/kg Fe and 92 mg/kg Mn for *B. azoricus* in the very metal-rich Rainbow field, Table 1); while this is consistent with highest

concentrations for Fe in soft tissues, it contrasts with the low accumulation of Mn in soft tissues compared to the high concentrations in the fluids. This may be related to the different uptake and storage mechanisms; in the shells, Ca^{2+} can be replaced by other cations in the carbonate structure, and Mn^{2+} as a divalent cation appears to fit well into the lattice. Copper and Zn are the metals with the next highest accumulations in the shells, with up to 20 mg/kg. All other metals are in the range of a few mg/kg or even less (Table 1).

3 Bioregulation Strategies of Hydrothermal Vent Mussels for Metal Uptake and Mitigation

Hydrothermal organisms have been shown to survive and thrive in metal-rich environments without visible damage, at metal concentrations that would be toxic for many other marine organisms. For those metals that have bioessential functions, including some alkali and earth alkaline elements, and some trace metals such as Fe and Zn, a selective uptake and accumulation in the range of positive effects can be assumed. As hydrothermal habitats are rich in many metals such as Hg, Pb, Cu, and As, that have no bioessential functions or exert toxic effects above certain element-specific threshold levels, hydrothermal organisms can be expected to possess special mechanisms of adaptation to these extreme conditions, or possibly even mediation strategies to influence their environment in a way that it becomes less harmful.

As reported above, the consistent accumulation patterns of alkaline and earth alkaline metals in tissues of vent mussels point to such a bioregulation of these largely essential elements. A clue to a bioregulation of metal uptake also comes from the fact that although Zn concentrations in hydrothermal fluids and precipitates are as strongly variable as, e.g., Cu and Fe concentrations, Zn concentrations in the mussel tissues vary over a smaller range than the other chalcophile elements including Cu and Fe. Furthermore, Zn mostly shows a stronger relationship to K, Mg, and Sr, in mussel tissues than to Cu, Cd, and Fe [20]. Similarly, Mn concentrations vary in a range of orders of magnitude in hydrothermal fluids but do not show significant differences between tissue types and locations of vent mussels. This may hint to a similar regulation mechanism for the micronutrient Mn as for Zn. In studies on littoral mussels, a lack of correlation between Zn in habitat water and in body tissues was also observed. Klerks and Fraleigh [44] (and references therein) point to a regulation of internal Zn levels by the mussels to explain these results. Experiments with the mussel *Perna perna* gave similar Zn and Mn concentrations in the soft tissues of experimentally contaminated mussels as of the reference mussels from their natural unpolluted habitat [45]. Although the environment of the littoral mussels is quite different from a hydrothermal vent habitat, including levels of trace metals, the average Zn and Mn concentrations in littoral mussels are in a similar range as in hydrothermal mussels (around 100 mg/kg Zn

and 10 mg/kg Mn). Correspondingly, regulation mechanisms postulated for littoral mussels may partly or largely also apply to hydrothermal mussels and may explain, among other effects, the relatively limited concentration ranges of Zn and Mn concentrations in hydrothermal mussels.

Several mechanisms of adaption or bioregulation in metal-rich environments have been discussed [46]. Organisms exhibit selectivity with regard to the uptake of essential and non-essential metals. Uptake will depend on the permeable surfaces of the organisms through which the metals can be taken up, the properties of barriers hindering uptake, and the tendency for the metal taken up to leave the animal again through the permeable surfaces. These processes can generally be described by the Fick's Law of diffusion. While organisms need to reach certain concentration ranges of essential elements to meet the requirements of their metabolism, they need to limit non-essential metal accumulation or bioavailability to a limit below the toxicity threshold. Once a trace metal has entered the body of the organism, it will be accumulated or excreted. Certain tissues such as the digestive gland may also act as temporary or permanent storage sites for detoxified metals. Metals that are potentially toxic must be removed by excretion from the specific tissues and can then be eliminated from the animal or biotransformed prior to storage in inert, non-toxic form.

Trace metal exposure may induce production of specific metal-binding ligands; here, sulfur-containing ligands including metallothionein-like proteins appear to play an important role in mediating metal uptake and accumulation [16]. Metallothioneins (MT) are heat-stable, soluble, sulfur-bearing proteins that are involved in intracellular metal regulation and are known to have strong metal-binding properties in the order Hg > Cu > Cd > Zn. They have been found in the tissues of all invertebrates investigated so far. *Bathymodiolus* mussels were shown to possess such MT [34] and these MT are very similar to those from coastal mussels such as *Mytilus* [47]. In experiments *Bathymodiolus azoricus* mussels were exposed to sub-lethal (50 µg/L) concentrations of Cd and a linear accumulation during the 24 days of experiment without significant elimination during 6 days of depuration occurred [48]. At the same time, MT levels increased in the gills during the first 18 days while some other stress related biomarkers including antioxidant enzymes remained unchanged. The results indicated that the MT defense system plays an important role to protect hydrothermal mussels from metal-toxic effects and were able to detoxify the effects of Cd exposure in this experiment. While not much can be said at this point about potential differences of the role of MT between different mussel species, a study comparing adaptation to metal toxicity of two hydrothermal shrimp species (*Mirocaris fortunata* and *Rimicaris exoculata*) from the Rainbow vent field and two coastal shrimps showed significant differences in MT levels and antioxidant enzymatic activities between all four species [49].

Apart from metal binding to a ligand such as MT within the body, it is also conceivable that an organism excretes a ligand into the fluid in order to modify the bioavailability and toxicity of trace metals. This has been observed in experiments with hydrothermal microbes that were exposed to increasing Cu concentrations [50]. Specific Cu-binding ligands were analyzed in the culture solutions of these

experiments and it was shown that the concentrations of the Cu-binding ligands would increase with increasing Cu concentrations, with a very strong increase at a certain level, which may be a kind of threshold concentration of Cu toxicity for those microbes. Apparently, the microbes had produced these ligands in order to mediate Cu bioavailability or toxicity. While so far no evidence exists that hydrothermal mussels possess similar mechanisms to excrete metal-binding ligands into solution in order to mediate their uptake, it might be worthwhile to investigate this possibility in future studies.

Some organisms have been found to accumulate and store metals in various types of metal-rich granules in their tissue, which probably contain the metal in an insoluble and non-bioavailable form. Different forms of granules with different anions such as phosphate or carbonate have been observed [51], but the high concentrations of sulfide in hydrothermal environments would also speak for the existence of sulfide precipitates forming insoluble metal granules in hydrothermal animal tissues. Although according to [16] such metal-rich granules have little if any effect in modifying trace metal uptake, they could still be an important storage place for detoxified metals. Electron spectroscopic imaging and electron energy loss spectroscopy on selected tissues of several species of hydrothermal animals from the North Fiji Basin [52], e.g. on the digestive gland of the gastropod *Ifremeria nautilei*, had shown such precipitates which were enriched in both sulfur and Cd. This agrees with high Cd concentrations of up to 10 ppm that were measured in the digestive glands of *Ifremeria* (Fig. 2). Other metals could not be detected in these precipitates, which however may be due to the methodological constraints. While such metal-rich clusters were not observed in tissue of the digestive gland of *Bathymodiolus brevior* in that study, it cannot be ruled out that they still exist but were not detected. Metal-rich granules were also found in the kidneys of the vent clam *Calyptogena magnifica*, where they were associated with the hemocytes and interstitial cells and the cells of the kidney tubules [36].

In summary, hydrothermal mussels can survive in metal-rich environments by either excreting non-essential or toxic amounts of metals they have taken up, or they can actively reduce the uptake by barriers or possibly by modifying the medium in which the metals are present (e.g., the hydrothermal fluid – seawater mixture). Further strategies include detoxification by transformation of the metal form and storage of the metals (Fig. 3). Bryan [53] reviewed the metal handling strategies of certain invertebrates and found that the polychaete *Nereis diversicolor* kept Zn levels in its body constant by excretion of excess metal, and uptake is apparently not controlled. In contrast, excess copper taken up by this polychaete is detoxified and stored in membrane bound vesicles, but is not excreted. Although according to [53], for mussels the metal concentrations in the body largely reflect the environmental concentrations, the observation that, e.g., Zn in hydrothermal mussels is much less variable than Cu, despite the similar high variability of the two metals in the fluids and precipitates of the habitat, would argue for a similar different handling mechanism for Zn and Cu by the mussels.

4 Concluding Remarks

While for coastal mussels and other coastal organisms a rather large number of data sets and publications exist for metal concentrations in tissues and their relationship to the geochemical environment, the number of comparable studies for hydrothermal vent organisms is much lower. This is rooted in the limited opportunities and the difficulties to sample hydrothermal vent organisms from up to about 4,000 m water depth, where hydrothermal vent sites occur, and to take environmental samples at the same time, which however only represent a snapshot of the moment of sampling and can vary with time. Nevertheless, the available information published so far allows to draw a number of conclusions and to define open questions that might stimulate future research in this field.

Bioaccumulation of trace metals by hydrothermal mussels is defined by the sum of a number of abiotic and biological parameters of the environment, which may interact and influence each other [25]. Concentrations of some metals in the tissues correlate directly with the metal load in the environment and reflect the high variability of metal concentrations in the fluids and particles they are exposed to. Some other metals such as the essential earth alkaline metals, Zn, and possibly Mn, seem to be biologically regulated by the organism and mostly vary in a smaller range in the tissues, although their concentrations are also strongly variable in the hydrothermal fluids. It has been shown by several studies that direct uptake of metals can be in dissolved form from the fluid or seawater, or from mineral particles precipitating in the fluid-seawater mixing zone. However, the respective role of fluids and particles in metal uptake by mussels and for the site of storage is not yet well resolved. No information exists so far about the potential role of metal-bearing colloids, which are a transient form between dissolved ions and particles; since they can be assumed to be present in large quantities in the vent environments [54], their role in metal uptake and accumulation calls for future research in this field.

Some general patterns such as highest accumulations of Fe and chalcophile metals (Cu, Zn, Cd, Pb) in gills and digestive tract are found in most hydrothermal animals and general trends differentiate different genii from each other. However, it is not yet clarified whether different species of the same genus, such as *Bathymodiolus azoricus* and *Bathymodiolus puteoserpentis* from the Mid-Atlantic Ridge, differ in their metal accumulation and adaptation strategies, or whether concentrations and processes related to metal uptake agree within the large natural range of variations. Systematic field studies or possibly cultivation experiments with different species under identical conditions might help to solve this question. Also the role of different symbiotic bacteria for the transfer of metals to the host organism needs to be studied in more detail.

Apart from the connection of metal accumulation in mussel tissues to the environmental conditions and available sources of these metals, possible chemical transformation and detoxification of metals taken up by the mussels are assumed to control metal accumulation and toxicity of the metals. Here, metallothioneins which are strongly metal-binding proteins with functional groups containing sulfur, appear to play an important role for regulating chalcophilic metals such as Cd and

Cu. Metal storage in immobile granules in different organs has been found in a number of hydrothermal vent organisms, but whether this is a general important metal regulation strategy of hydrothermal vent mussels still needs to be investigated. Bio-mediation of metal speciation in solution in order to ameliorate metal toxicity may be another possible, but yet to be proven pathway of survival strategies of vent mussels in metal-rich environments. Since change of the metal speciation, e.g. into strongly soluble organic complexes, would also have a significant impact on the further fate of hydrothermal metals and their fluxes into the ocean [55], this could be of relevance for the ocean beyond the direct hydrothermal vent sites.

A systematic study of the metal loads in hydrothermal mussels may also be a potential tool to integrate metal fluxes in highly dynamic hydrothermal mixing zones over the lifetime of the mussels, provided that the accumulation pathways are understood [20]. This would help to determine hydrothermal metal fluxes into the ocean, especially from diffuse vent sites, which are often very dynamic in their fluid discharge and have generally much lower metal concentrations than hot focused vent fluids. However, due to their much larger spatial extension and biological control of metal fluxes, their quantitative role in controlling hydrothermal metal fluxes may still be significant. Demina et al. [19] suggest that due to the high bioconcentration factors of metals in the tissues of hydrothermal vent mussels and the high biomass, the hydrothermal fauna may even be considered as a biological filter of metals in the oceans, of which mussels, because of their abundance in most vent fields, might play a major role.

Apart from the relevance for the hydrothermal research community, the understanding of bio-geo interactions in metal-rich hydrothermal environments can also be of interest for a larger community, including researchers interested in understanding the possible evolution of life on early Earth, which may have taken place in an environment very similar to today's submarine hydrothermal systems. Today we do not only find natural metal-rich environments, but societies also have to cope with anthropogenic pollution of aquatic systems with metals; here, native organisms may be much less adapted to the increased metal load, and potential mitigation strategies or biotechnological processes might benefit from the knowledge of metal mitigation and adaptation of organisms in naturally metal-rich environments such as hydrothermal vent sites.

Acknowledgements Discussions with Christian Borowski (MPI for Marine Microbiology, Bremen) on biological topics of hydrothermal fauna were very helpful for writing this chapter. Autun Purser (Alfred Wegener Institute for Polar and Marine Research, Bremerhaven) is acknowledged for the drawings in this chapter. A special thanks goes to Adilah Ponnurangam (Jacobs University Bremen) for her general support at various stages of this chapter.

References

1. Tunnicliff V (1991) The biology of hydrothermal vents: ecology and evolution. Oceanogr Mar Biol Annu Rev 29:319–407
2. Page HM, Fiala-Medioni A, Fisher CR, Childress JJ (1991) Experimental evidence for filter-feeding by the hydrothermal vent mussel, *Bathymodiolus thermophilus*. Deep Sea Res A Oceanogr Res Pap 38:1455–1461. doi:10.1016/0198-0149(91)90084-S

3. Fiala-Médioni A, McKiness Z, Dando P, Boulegue J, Mariotti A, Alayse-Danet A, Robinson J, Cavanaugh C (2002) Ultrastructural, biochemical, and immunological characterization of two populations of the mytilid mussel *Bathymodiolus azoricus* from the Mid-Atlantic Ridge: evidence for a dual symbiosis. Mar Biol 141:1035–1043
4. Fiala-Médioni A, Michalski JC, Jollès J, Alonso C, Montreuil J (1994) Lysosomic and lysozyme activities in the gill of bivalves from deep hydrothermal vents. C R Acad Sci III Sci Vie 317:239–244
5. Perner M, Bach W, Hentscher M, Koschinsky A, Garbe-Schönberg D, Streit WR, Strauss H (2009) Short-term microbial and physico-chemical variability in low-temperature hydrothermal fluids near 5°S on the Mid-Atlantic Ridge. Environ Microbiol 11:2526–2541
6. Martins I, Cosson RP, Riou V, Sarradin P, Sarrazin J, Santos RS, Colaço A (2011) Relationship between metal levels in the vent mussel *Bathymodiolus azoricus* and local microhabitat chemical characteristics of Eiffel Tower (Lucky Strike). Deep Sea Res I Oceanogr Res Pap 58:306–315
7. Johnson KS, Childress JJ, Beehler CL, Sakamoto CM (1994) Biogeochemistry of hydrothermal vent mussel communities: the deep-sea analogue to the intertidal zone. Deep Sea Res I Oceanogr Res Pap 41:993–1011. doi:10.1016/0967-0637(94)90015-9
8. Nedoncelle K, Lartaud F, Contreira Pereira L, Yücel M, Thurnherr AM, Mullineaux L, Le Bris N (2015) Bathymodiolus growth dynamics in relation to environmental fluctuations in vent habitats. Deep Sea Res I Oceanogr Res Pap 106:183–193
9. Mottl MJ, McConachy TF (1990) Chemical processes in buoyant hydrothermal plumes on the East Pacific Rise near 21°N. Geochim Cosmochim Acta 54:1911–1927
10. James R, Parks G (1982) Characterization of aqueous colloids by their electrical double-layer and intrinsic surface chemical properties. In: Matijević E (ed) Surface and colloid science. Springer, New York, pp 119–216
11. Sunda WG, Ferguson RL (1983) Sensitivity of natural bacterial communities to additions of copper and to cupric ion activity: a bioassay of copper complexation in seawater. In: Trace metals in seawater, vol 9. Plenum Press, New York, pp 871–891
12. Sarradin P, Waeles M, Bernagout S, Le Gall C, Sarrazin J, Riso R (2009) Speciation of dissolved copper within an active hydrothermal edifice on the Lucky Strike vent field (MAR, 37°N). Sci Total Environ 407:869–878
13. Johnson KS, Childress JJ, Beehler CL (1988) Short-term temperature variability in the Rose Garden hydrothermal vent field: an unstable deep-sea environment. Deep Sea Res A Oceanogr Res Pap 35:1711–1721
14. Edgcomb VP, Molyneaux SJ, Saito MA, Lloyd K, Böer S, Wirsen CO, Atkins MS, Teske A (2004) Sulfide ameliorates metal toxicity for deep-sea hydrothermal vent archaea. Appl Environ Microbiol 70:2551–2555
15. Trevisan R, Ferraz Mello D, Fisher AS, Schuwerack P, Dafre AL, Moody AJ (2011) Selenium in water enhances antioxidant defenses and protects against copper-induced DNA damage in the blue mussel *Mytilus edulis*. Aquat Toxicol 101:64–71
16. Wang W, Rainbow PS (2005) Influence of metal exposure history on trace metal uptake and accumulation by marine invertebrates. Ecotoxicol Environ Saf 61:145–159
17. Eisler R (1981) Trace metal concentrations in marine organisms. Pergamon Press, Oxford, p 685
18. Martins I, Colaço A, Dando PR, Martins I, Desbruyères D, Sarradin P, Marques JC, Serrão-Santos R (2008) Size-dependent variations on the nutritional pathway of *Bathymodiolus azoricus* demonstrated by a C-flux model. Ecol Model 217:59–71
19. Demina LL, Holm NG, Galkin SV, Lein AY (2013) Some features of the trace metal biogeochemistry in the deep-sea hydrothermal vent fields (Menez Gwen, Rainbow, Broken Spur at the MAR and 9°50′N at the EPR): a synthesis. J Mar Syst 126:94–105
20. Koschinsky A, Kausch M, Borowski C (2014) Metal concentrations in the tissues of the hydrothermal vent mussel *Bathymodiolus*: reflection of different metal sources. Mar Environ Res 95:62–73
21. Cosson RP, Thiébaut É, Company R, Castrec-Rouelle M, Colaço A, Martins I, Sarradin P, Bebianno MJ (2008) Spatial variation of metal bioaccumulation in the hydrothermal vent mussel *Bathymodiolus azoricus*. Mar Environ Res 65:405–415

22. Martins I, Costa V, Porteiro F, Cravo A, Santos RS (2001) Mercury concentrations in invertebrates from Mid-Atlantic Ridge hydrothermal vent fields. J Mar Biol Assoc U K 81:913–915
23. Smith DR, Flegal AR (1989) Elemental concentrations of hydrothermal vent organisms from the Galápagos Rift. Mar Biol 102:127–133
24. Dubilier N, Windoffer R, Giere O (1998) Ultrastructure and stable carbon isotope composition of the hydrothermal vent mussels' *Bathymodiolus brevior* and B. sp. *affinis brevior* from the North Fiji Basin, western Pacific. Mar Ecol Prog Ser 165:187–193
25. Demina LL, Galkin SV (2008) On the role of abiogenic factors in the bioaccumulation of heavy metals by the hydrothermal fauna of the Mid-Atlantic Ridge. Oceanology 48:784–797
26. Jeffree RA, Markich SJ, Brown PL (1993) Comparative accumulation of alkaline-earth metals by two freshwater mussel species from the Nepean River, Australia: consistences and a resolved paradox. Mar Freshw Res 44:609–634
27. Bara M, Guiet-Bara A, Durlach J (1993) Regulation of sodium and potassium pathways by magnesium in cell membranes. Magnes Res 6:167–177
28. Von Damm KL (1995) Controls on the chemistry and temporal variability of seafloor hydrothermal fluids. In: Humphris SE, Zierenberg RA, Mullineaux LS, Thomson RE (eds) Seafloor hydrothermal systems: physical, chemical, biological, and geological interactions. American Geophysical Union, Washington, DC, pp 222–247
29. Colaço A, Bustamante P, Fouquet Y, Sarradin PM, Serrão-Santos R (2006) Bioaccumulation of Hg, Cu, and Zn in the Azores triple junction hydrothermal vent fields food web. Chemosphere 65:2260–2267
30. Kádár E, Costa V, Segonzac M (2007) Trophic influences of metal accumulation in natural pollution laboratories at deep-sea hydrothermal vents of the Mid-Atlantic Ridge. Sci Total Environ 373:464–472
31. Lee S, Kim S, Ju S, Pak S, Son S, Yang J, Han S (2015) Mercury accumulation in hydrothermal vent mollusks from the southern Tonga Arc, southwestern Pacific Ocean. Chemosphere 127:246–253
32. Taylor VF, Jackson BP, Siegfried M, Navratilova J, Francesconi KA, Kirshtein J, Voytek M (2012) Arsenic speciation in food chains from Mid-Atlantic hydrothermal vents. Environ Chem 9:130–138
33. Rousse N, Boulegue J, Cosson RP, Fiala-Medioni A (1998) Bioaccumulation des métaux chez le mytilidae hydrothermal *Bathymodiolus* sp. de la ride médio-atlantique. Oceanol Acta 21:597–607
34. Geret F, Rousse N, Riso R, Sarradin P, Coson RP (1998) Metal compartmentalization and metallothionein isoforms in mussels form the Mid-Atlantic Ridge; preliminary approach to the fluid–organism relationship. Cah Biol Mar 39:291–293
35. Roesijadi G, Crecelius EA (1984) Elemental composition of the hydrothermal vent clam *Calyptogena magnifica* from the East Pacific Rise. Mar Biol 83:155–161
36. Roesijadi G, Young JS, Crecelius EA, Thomas LE (1985) Distribution of trace metals in the hydrothermal vent clam, *Calyptogena magnifica*. Bull Biol Soc Wash 6:311–324
37. Ruelas-Inzunza J, Soto LA, Páez-Osuna F (2003) Heavy-metal accumulation in the hydrothermal vent clam *Vesicomya gigas* from Guaymas basin, Gulf of California. Deep Sea Res I Oceanogr Res Pap 50:757–761
38. Kádár E, Santos RS, Powell JJ (2006) Biological factors influencing tissue compartmentalization of trace metals in the deep-sea hydrothermal vent bivalve *Bathymodiolus azoricus* at geochemically distinct vent sites of the Mid-Atlantic Ridge. Environ Res 101:221–229
39. Kádár E, Costa V, Santos RS, Powell JJ (2006) Tissue partitioning of micro-essential metals in the vent bivalve *Bathymodiolus azoricus* and associated organisms (endosymbiont bacteria and a parasite polychaete) from geochemically distinct vents of the Mid-Atlantic Ridge. J Sea Res 56:45–52
40. Charmasson S, Le Faouder A, Loyen J, Cosson RP, Sarradin P (2011) 210Po and 210Pb in the tissues of the deep-sea hydrothermal vent mussel *Bathymodiolus azoricus* from the Menez Gwen field (Mid-Atlantic Ridge). Sci Total Environ 409:771–777
41. Kádár E, Costa V (2006) First report on the micro-essential metal concentrations in bivalve shells from deep-sea hydrothermal vents. J Sea Res 56:37–44

42. Bau M, Balan S, Schmidt K, Koschinsky A (2010) Rare earth elements in mussel shells of the Mytilidae family as tracers for hidden and fossil high-temperature hydrothermal systems. Earth Planet Sci Lett 299:310–316
43. Ponnurangam A, Bau M, Brenner M, Koschinsky A (2016) Mussel shells of *Mytilus edulis* as bioarchives of the distribution of rare earth elements and yttrium in seawater and the potential impact of pH and temperature on their partitioning behavior. Biogeosciences 13:751–760
44. Klerks PL, Fraleigh PC (1997) Uptake of nickel and zinc by the zebra mussel *Dreissena polymorpha*. Arch Environ Contam Toxicol 32:191–197
45. Bellotto VR, Miekeley N (2007) Trace metals in mussel shells and corresponding soft tissue samples: a validation experiment for the use of *Perna perna* shells in pollution monitoring. Anal Bioanal Chem 389:769–776
46. Deplede MH, Rainbow PS (1990) Models of regulation and accumulation of trace metals in marine invertebrates. Comp Biochem Physiol 97C:1–7
47. Hardivillier Y, Leignel V, Denis F, Uguen G, Cosson R, Laulier M (2004) Do organisms living around hydrothermal vent sites contain specific metallothioneins? The case of the genus *Bathymodiolus* (Bivalvia, Mytilidae). Comp Biochem Physiol C Toxicol Pharmacol 139:111–118
48. Company R, Serafim A, Cosson RP, Fiala-Médioni A, Camus L, Serrão-Santos R, João Bebianno M (2010) Sub-lethal effects of cadmium on the antioxidant defence system of the hydrothermal vent mussel *Bathymodiolus azoricus*. Ecotoxicol Environ Saf 73:788–795
49. Gonzales-Rey M, Serafim A, Company R, Gomes T, Bebianno MM (2008) Detoxification mechanisms in shrimp: comparative approach between hydrothermal vent fields and estuarine environments. Mar Environ Res 66:35–37
50. Klevenz V, Sander SG, Perner M, Koschinsky A (2012) Amelioration of free copper by hydrothermal vent microbes as a response to high copper concentrations. Chem Ecol 28:405–420
51. Marigomez I, Soto M, Cajaraville MP, Angulo E, Giamberini L (2002) Cellular and subcellular distribution of metals in molluscs. Microsc Res Tech 56:358–392
52. Giere O, Borowski C (2001) Chapter 7: Bakterien-Tier-Symbiosen als Charakteristika hydrothermaler Ökosysteme. In: Hydrothermale Fluidentwicklung, Stoffbilanzierung und spezielle biologische Aktivität im Nord-Fidschi-Becken - HYFIFLUX II - SO 134" - In German unpublished. Abschlussbericht (Final report BMBF project Project) No. 03 G 0134:154
53. Bryan GW (1984) Pollution due to heavy metals and their compounds. In: Kinne O (ed) Marine ecology, 5th edn. Wiley, London, pp 1289–1431
54. Yücel M, Gartman A, Chan CS, Luther GW III (2011) Hydrothermal vents as a kinetically stable source of iron-sulphide-bearing nanoparticles to the ocean. Nat Geosci 4:367–371
55. Sander SG, Koschinsky A (2011) Metal flux from hydrothermal vents increased by organic complexation. Nat Geosci 4:145–150
56. Larsen EH, Quétel CR, Munoz R, Fiala-Medioni A, Donard OFX (1997) Arsenic speciation in shrimp and mussel from the Mid-Atlantic hydrothermal vents. Mar Chem 57:341–346
57. Demina LL, Galkin SV, Shumilin E (2009) Bioaccumulation of some trace elements in the biota of the hydrothermal fields of the Guaymas Basin (Gulf of California). Bol Soc Geol Mex 61:31
58. Balan AS (2010) Trace metals in the nacreous layer of Mytilidae mussel shells from the North Sea and the Mid Atlantic Ridge as proxies for environmental conditions
59. Cravo A, Foster P, Almeida C, Bebianno MJ, Company R (2008) Metal concentrations in the shell of *Bathymodiolus azoricus* from contrasting hydrothermal vent fields on the mid-Atlantic ridge. Mar Environ Res 65:338–348
60. Cravo A, Foster P, Almeida C, Company R, Cosson RP, Bebianno MJ (2007) Metals in the shell of *Bathymodiolus azoricus* from a hydrothermal vent site on the Mid-Atlantic Ridge. Environ Int 33:609–615

Factors Controlling the Trace Metal Distribution in Hydrothermal Vent Organisms

Liudmila L. Demina and Sergey V. Galkin

Abstract Despite the numerous published data, the evaluation of the various conditions, influencing the trace metal distribution and accumulation in the different hydrothermal organisms, is not completed up till now. In this chapter we aimed to clear out the influence of the main factors, affecting the trace metal bioaccumulation in the deep-sea hydrothermal vent biota: environmental factors, acting outside the organisms, and biological ones, acting inside the organisms and within the biological communities. Among the environmental conditions there are such site-specific differences as depth, temperature, and fluid chemical composition that control trace metal concentrations in water of the biotope, as well as mineralogical features of substratum. Meanwhile the biogenic factors include stage of ontogenesis, species differences, trophic level and feeding type, and etc. For this purpose we consider data on the Fe, Mn, Zn, Cu, Cd, Pb, Ag, Ni, Co, Cr, As, Se, Sb, and Hg concentrations in the benthic organisms inhabiting the following hydrothermal vent fields at the Mid-Atlantic Ridge (MAR): Menez Gwen, Rainbow, Lost City, Broken Spur, as well at the 9°50′N at the East Pacific Rise (EPR), and the Guaymas Basin (Gulf of California). To clarify some of the influencing factors, we have aimed to summarize the available data on factors that control the trace metal distribution in hydrothermal vent organisms, including not only *Bathymodiolus* mussels, but also other dominant organisms, such as *Rimicaris* shrimps, vestimentiferan tube worms *Riftia pachyptila*, whose feeding strategy relies on microbial symbiotrophy. Distribution patterns of some trace metals studied in different taxa gave an evidence of the influence of environmental and biological parameters on their bioaccumulation in the hydrothermal vent organisms.

L.L. Demina (✉) and S.V. Galkin
P.P.Shirshov Institute of Oceanology Russian Academy of Sciences (IO RAS),
Nakhimovsky pr., 36, 117997 Moscow, Russia
e-mail: l_demina@nai.ru; galkin@ocean.ru

L.L. Demina, S.V. Galkin (eds.), *Trace Metal Biogeochemistry and Ecology of Deep-Sea Hydrothermal Vent Systems*, Hdb Env Chem (2016) 50: 123–142,
DOI 10.1007/698_2016_5, © Springer International Publishing Switzerland 2016,
Published online: 27 April 2016

Keywords Bioaccumulation, Deep-sea hydrothermal vent biocommunities, Environmental and biological factors, Trace metals

Contents

1 Introduction

The bottom fauna of the deep-sea hydrothermal vent fields function in an environment inaccessible for photosynthesis, which is saturated by the heavy metals and reduced compounds (H_2S, H_2, and CH_4) serving as an energy source for bacterial chemosynthesis. The levels of heavy metals in the hydrothermal areas and in the regions subject to anthropogenic loads are close in order of magnitude. This makes the studies of the concentration function of the hydrothermal fauna interesting both for practical assessment of the limits of tolerance of living organisms in conditions of extreme metal contents and from the point of view of the fundamental problem of geochemical migration of chemical elements in the ocean. Deep-sea hydrothermal biological communities demonstrate a strong concentration function that is reflected in the high values of the bioconcentration factor (BCF). According to data of [1–3], the BCF of trace metals estimated for *Bathymodiolus* mussels, collected from the four Mid-Atlantic Ridge (MAR) hydrothermal fields, varies within the limits of $n10^2$–$n10^5$ and they are similar to that of the littoral mussels.

The trace metals are known to be accumulated in different organs of marine organisms coming from the water in the course of metabolic processes and at feeding and respiration. Amongst the heavy metals, the highest content in the organisms' tissues (up to $n \times 10^5$ mg/kg dry weight) is characteristic of Fe and Zn. These metals dominate in the fluids and are crucially important for the living organisms.

At the hydrothermal vent fields the most abundant and dominant communities involve those organisms, whose feeding strategy relies on bacterial symbiotrophy, which functionally depends on reduced compounds of the fluids. Amongst them at the Mid-Atlantic Ridge there are *Bathymodiolus* spp. mussels, *Rimicaris exoculata*

shrimps. Fauna assemblages within the vent fields at the East Pacific Rise (EPR) and Guaymas Basin dominated in the alvinellid polychaetes *Alvinella pompejana*, the vestimentiferan tube worms *Riftia pachyptila*.

In the *Bathymodiolus* mussel's gills, hosting intracellular endosymbiotic bacteria, the contents of all the trace metals were permanently higher (by a factor of 2–10) as compared to the other tissues, which are an organ free of endosymbionts [4–8]. In the *Rimicaris* shrimps the main target organ of Fe, Zn, Mn, Co, Ni, Cu, Pb, Ag, As, and Hg accumulation were maxillipeds (mouth appendages), associated with chemoautotrophic bacteria, where metal contents exceeded one order of magnitude than in other tissues. The peak concentrations of metals were the following (mg/kg dry weight): 55,400 Fe; 5,830 Zn; 4,082 Cu; 250 Ni; 151 Mn; 12.6 Ag; and 62.4 As [3]. The elevated contents of metals were also characteristic for the trophosome of vestimentiferan tube worms *Riftia pachyptila*, whose feeding depends on the bacterial symbionts [9]. Besides, the high contents of selected metals were also observed in the mantle (Co, Mn, and Cr) and digestive glands (Cd) of the mollusk *Bathymodiolus*, as well as in chitin and gonads of the carnivorous crab *Segonzacia* [7]. Despite originating from trace metal-rich environments, mean concentrations of Fe, Mn, Zn, Cu, and Cd were the lowest ones in the mussel carbonate shells [7, 10–12]. In shells contents of heavy metals, as a rule, were 1–2 orders of magnitude as low as in the soft tissues.

The spatial distribution of the bottom fauna at the MAR vent fields showed a similarity. The highly specialized ectosymbiont-harboring *Rimicaris exoculata* shrimps are commonly present in the active zones (black smoke and shimmering water) close to vents, where nutrients (H_2S and CH_4) determine the most favorable habitat conditions; while the symbiotrophic *Bathymodiolus* mussels colonize the foot of chimneys, where the low temperature outflows are located [13, 14].

Thus, organs of different taxa demonstrated various capacities for accumulating metals which are obviously associated with the biochemical function of different organs, as well as with the environmental conditions.

In the hydrothermal ecosystems there was found a relationship between environmental parameters and distribution patterns of biological communities [13–16]. The distribution type, density, and biomass of organisms are of fundamental importance for the understanding of the community ecology and biological productivity at deep-sea hydrothermal vents. At the MAR vent fields biomass of the only soft tissues of the most abundant *Bathymodiolus* mussels reaches up to 19 kg/m^2 [17], while combined with shells – up to 60 kg/m^2 [18]. In previous chapters it was demonstrated that the deep-sea hydrothermal vent ecosystems are rather complicated, and our knowledge about biogeochemical processes still remain limited. *Bathymodiolus* mussels are known to be the dominant fauna occupying hydrothermal vent ecosystems throughout the World Ocean. Some specific factors influencing the trace metal bioaccumulation in the *Bathymodiolus* mussels have been evidenced in Koschinsky [19].

In this chapter we aimed to better understand the two types of factors affecting trace metal accumulation in the vent living organisms: environmental factors and biological factors acting within the organisms. The trace metals Fe, Mn, Zn, Cu, Co,

Ni, Cr, As, Cd, Pb, Se, Sb, and Hg were studied in different groups of the dominant vent organisms.

Bottom fauna under consideration were sampled from different vent fields (Menez Gwen, Rainbow, Broken Spur, and Snake Pit) at the slow-spreading Mid-Atlantic Ridge (MAR), as well as from 9°50′N at the fast-spreading East Pacific Rise (EPR) and Guaymas Basin (Gulf of California). These fields differ in such basic environmental parameters as temperature and composition of emitting fluids, host rocks (basalt or ultramafic), and substratum type. Trace metal distribution in water of biotope of these vent fields was summarized in Demina [20].

2 Sampling and Analytical Methods

Specimens of the invertebrates were collected during the 49th and 50th cruises of the Russian research vessel "Akademik Mstislav Keldysh" (June–October, 2003 and July–August, 2005, respectively) in the deep-sea hydrothermal vent fields using the "Mir-1" and "Mir-2" manned submersibles. Bottom fauna samples were collected using the "slurp-gun" and sieve nets operated by the submersibles. Individuals were measured and dissected into the main organs, which are for mussels: shell, gills, mantle, foot, muscle, and remaining tissues; small individuals were used as a whole body. We collected live mussels with undamaged shells. Soft tissues were removed from shells using plastic knife, rinsed with deionized water followed by cleaning with a toothbrush in order to remove particles stuck to shells. Shrimp organs included carapax, muscle, maxillipeds, and total body in some cases, and those from crabs were chitin, muscle, gonads, and gills. Vestimentiferans' organs were the following: trophosome, vestimentum, obturaculae, tube, and opistosome. Specimens of alvinellid polychaetes *Alvinella pompejana* were analyzed as a whole.

The dried (60°C) samples of total animals and their tissues were stored in insulated plastic bags until analysis. Powdered samples (from 20 to 50 mg weight) were digested with 2 ml of mixture (1:1) of the concentrated HNO_3 (69% v/v) and 30% H_2O_2 in teflon vessels in an MWS-2 microwave system (Berghof, Germany). After cooling solutions were diluted 1:10 with the deionized water. The analysis accuracy was controlled by use of the International reference materials – NIST SRM 2976 (mussel tissue), IAEA MA-A-2/T fish flesh, and GSD-7. A comparison of metal contents in certified standard reference materials with the measured values has revealed that percentage recovery was 90–95% for Fe, Zn, Mn, and Cu, 85–90% for Pb, Ag, Co, Cd, and Cr, and 82–85% for Se, Sb, and Hg.

3 Environmental Factors that Influence on Trace Metal Bioaccumulation

The faunal distribution in hydrothermal environment has been shown to depend on the fluid dilution processes, concentration and speciation of sulfide [13, 14, 21, 22] and flow intensity or substratum type [23]. It is known that the hot hydrothermal fluids, emitting from the vent edifices, determine most of ecological and biogeochemical features of the vent ecosystem. Some differences in mean concentrations of big group of trace metals (Fe, Mn, Zn, Cu, Ni, Cr, Co, As, Pb, Cd, Ag, and Hg) between the biotope water of the low- and high-temperature hydrothermal vent fields at the MAR and EPR were shown in Demina [20].

Metal enrichments in mussel tissues vary between different vent sites, reflecting differently the fluid and particle compositions that can serve as metal source [3, 6–8]. The comparison of trace metal bioaccumulation in the dominating taxa dwelling within the different vent fields allows us to reveal the influence of the environmental conditions on the trace metal bioaccumulation.

3.1 Inter-Sites and Specific Variation

The trace metal composition of the hydrothermal biotope water is the basic environmental parameter while studying the biogeochemical features. To clear out a relationship between the trace metal concentrations in the biotope water and in tissues of organisms sites, we should compare taxon at the level of genus inhabiting vent sites with different trace metal's loads.

The dominating taxon at the Mid-Atlantic Ridge is *Bathymodiolus* spp., which inhabits a highly variable environment with exceptionally high concentrations of reduced sulfur species and heavy metals at both the low-temperature vent fields (Menez Gwen) and the high-temperature ones (Rainbow, Broken Spur, and Snake Pit). For comparison we have chosen the two most contrasting of them: the basalt-hosted shallow-water Menez Gwen and the ultramafic-hosted deep-water Rainbow. In the latter, biotope water is enriched in some metals, primarily in Fe and Mn, up to two orders of magnitude relatively the Menez Gwen ones [7]. In the mussel's gills, hosting the intracellular endosymbiotic chemosynthetic bacteria, that functionally depend on reduced compounds of the fluids, the contents of all the metals studied were permanently higher (by a factor of 2–10) as compared to the other tissues free of endosymbionts [6–8].

Average bioconcentration factor (BCF) of trace metals in the whole mussels ($C_{\text{whole organism}}/C_{\text{water}}$) at the Broken Spur and Rainbow hydrothermal vent fields decreased in the following order: ($n{\cdot}10^5$) Hg, Fe, Cu > ($n{\cdot}10^4$) Co, Pb > ($n{\cdot}10^3$) Cd, Zn, Ni, Ag > ($n{\cdot}10^2$) Mn, As, Sb. It should be noticed that the toxic metal Hg was characterized by the highest BCF, along with micronutrients Fe and Cu. Apparently

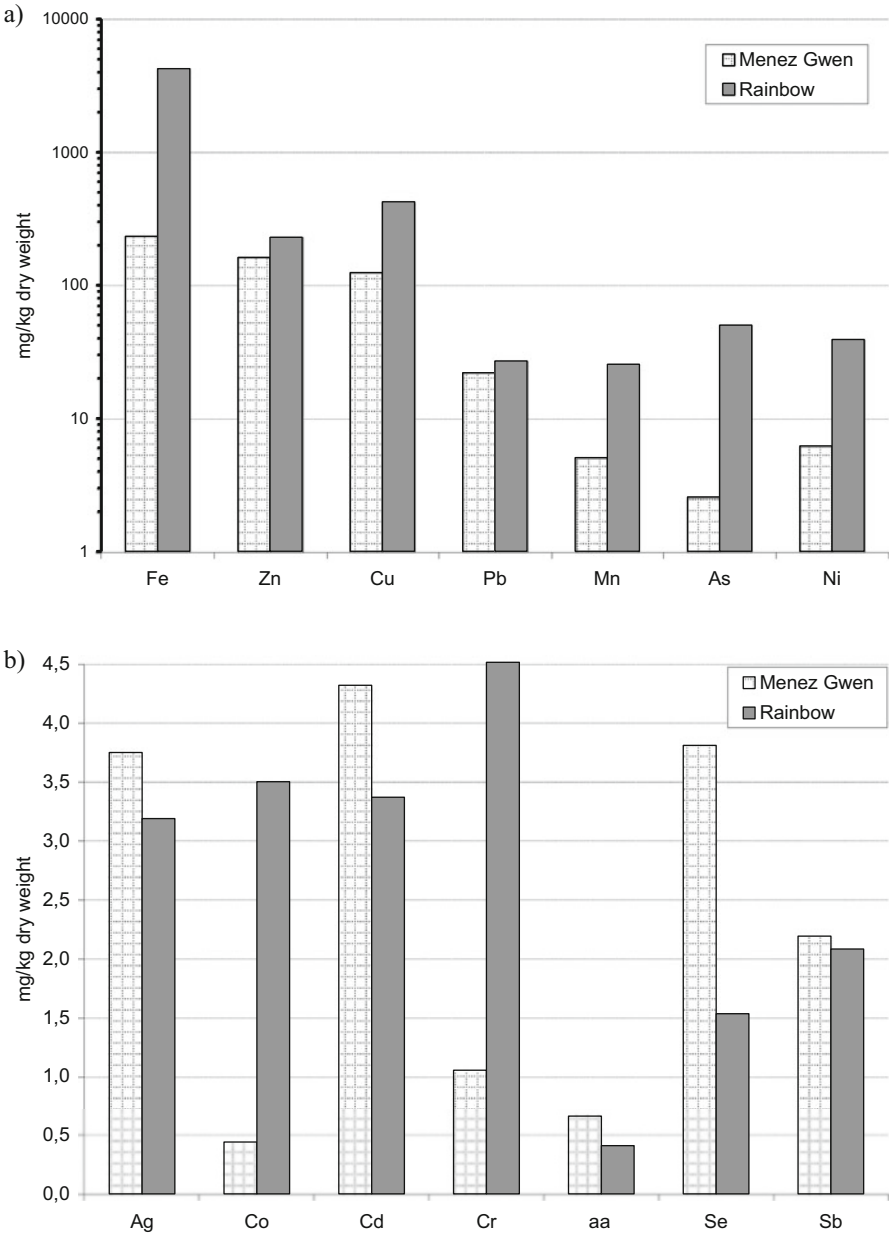

Fig. 1 Comparison of average concentrations of trace metals (mg/kg dry weight) in gills of *Bathymodiolus azoricus* mussels sampled from the Menez Gwen and Rainbow hydrothermal vent fields at the Mid-Atlantic Ridge. (**a**) Fe, Zn, Cu, Pb, Mn, As, and Ni; (**b**) Ag, Co, Cd, Cr, Hg, Se, and Sb

it means that BCF is not linked with biological need of metals and probably depends on the metal bioavailability [2].

From our data, the contents of Fe, Mn, Zn, Co, Ni, Cu, As, Se, and Sb in gills of *Bathymodiolus* mussels at the high-temperature Rainbow vent site are much greater than that at the low-temperature Menez Gwen site (Fig. 1). This fact corresponds to the elevated trace metal concentrations of these metals in the biotope water at the Rainbow compared to that at the Menez Gwen. The Student *t*-test resulted in significant difference ($p < 0.05$) in case of Fe, Mn, Cu, As, Ni, Cr, and Co. The lowest differences were characteristic of Zn, Pb, and Sb; while Hg, Ag, Cd, and Se showed even a little higher content in mussel gills from the Menez Gwen against the Rainbow vent field (Fig. 1b). The effect of fluids' character became apparent in the increased accumulation of Hg in the soft tissues of the *Bathymodiolus azoricus* in the Menez Gwen [24, 25]. This was attributed to phase separation of the fluids in which Hg to the greatest degree is associated with a light gas phase, which is characteristic of sources of the field Menez Gwen, rather than in heavy saline solutions of the Rainbow field.

On the other hand, at the Rainbow vent field, mussel's abundance is lower than in the Menez Gwen field [15]. In opinion of D. Desbruyères, the elevated suspended particulate matter's concentrations and high particle fluxes in the Rainbow field biotope may negatively affect the filtering activity of mussels. This could result in lower accumulation of some metals in the Rainbow specimens.

Mussel shells, in spite of the low trace metal content, might serve as a great reservoir of majority of heavy metals in the hydrothermal areas, reflecting the exposure to varying trace metal concentrations in the biotope water. From Fig. 2 one can see that variability in trace metal contents in the *Bathymodiolus* shells, collected from 5 different vent fields, is very similar to that in gills as a whole. Mussel shells from the high-temperature vent sites (Broken Spur, Snake Pit, Rainbow, 9°50′N) contain noticeably more metals than shells from the low-temperature Menez Gwen field, where the biotope water is depleted in metals. The most pronounced difference was detected for Fe, Mn, Zn, Ni, As, Co, Pb, and Se. The Fe and Mn enrichment (to 10–20-fold) in shells of the high-temperature vents corresponds to their higher concentrations in the biotope water relative to the rest of the metals. Shells from the Rainbow vent site are particularly enriched (up to 10 times) in Ni and Co relatively other metals (Fig. 2a, b); this is evidently caused by the elevated Ni and Co concentration in the initial Rainbow fluids as a result of serpentinization of the ultramafic-hosted Rainbow field during hydrothermal circulation [26]. Less pronounced differences were detected between the Zn, Cu, Ag, Cd, Cr, Hg, and Sb contents in shells from different sites.

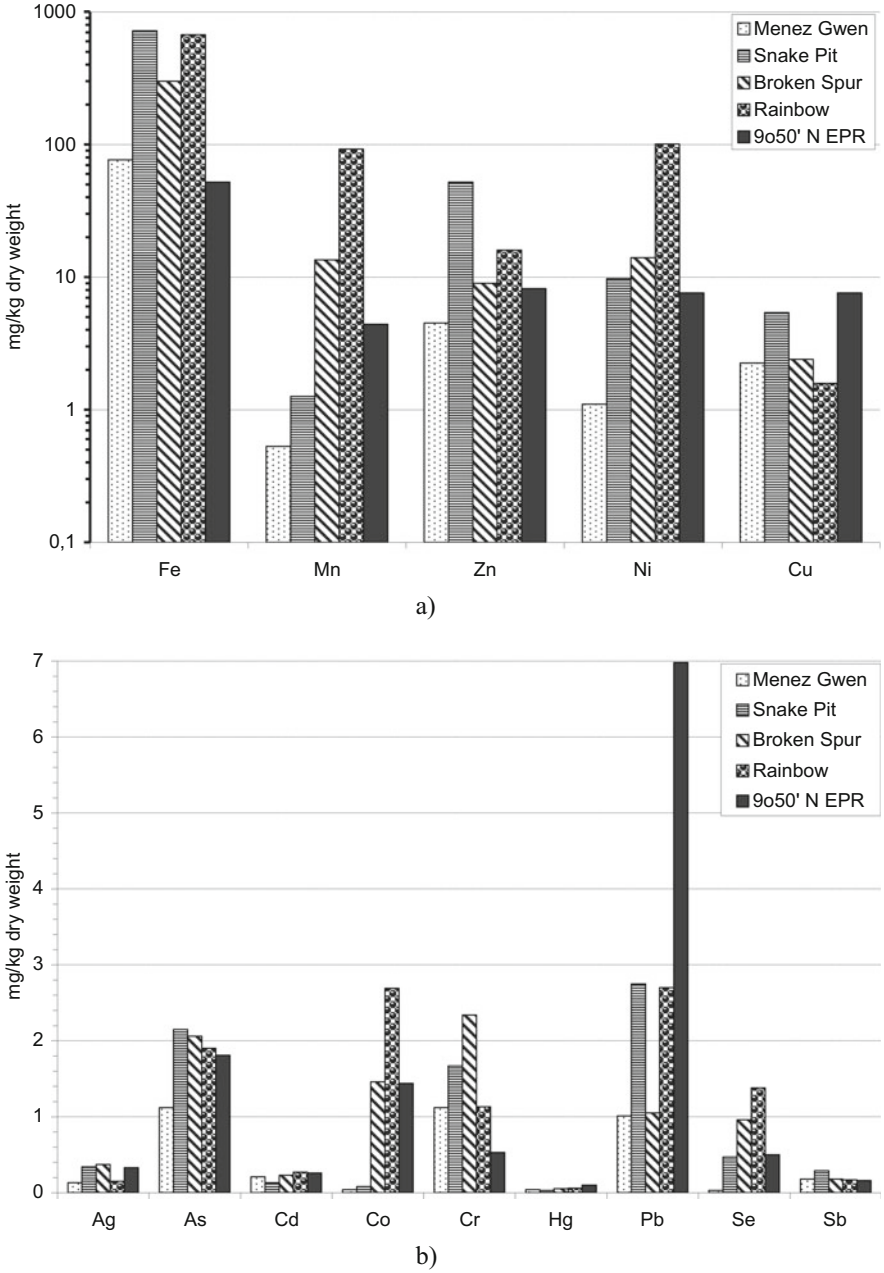

Fig. 2 Comparison of average concentrations of trace metals (mg/kg dry weight) in shells of mussels *Bathymodiolus* spp. from the five different hydrothermal vent fields of the MAR and EPR. (**a**) Fe, Mn, Zn, Ni, and Cu; (**b**) Ag, As, Cd, Co, Cr, Hg, Pb, Se, and Sb

3.2 *Influence of the Mineral Composition of Suspended Particulate Matter in the Biotope Water and Substratum*

Differences in bioaccumulation, that depends on the composition of water habitats, may be increased due to the influence of mineral composition of substratum, on which the fauna lives, and of suspended particulate matter as well. This can be seen by comparing the distribution of trace elements in the gills of the same genus *Bathymodiolus* inhabiting two fields: Menez Gwen (sulfate substratum – barite and anhydrite) and the Snake Pit (sulfide substratum). As it is known, the *Bathymodiolus* mussels in the trophic strategy rely not only on the symbiotrophy but on the filter-feeding also. In other words, the trace metals are accumulated from the suspended particulate matter as well. In the *Bathymodiolus* gills from Snake Pit the content of trace elements, especially chalcophile metals Fe, Zn, Cu, As, Ag, and Pb, is 1–2 orders of magnitude higher than that Menez Gwen, except Hg (see above).

Kádár et al. (2005) have revealed that in water column above the colonies of the *Bathymodiolus* mussels the particulate forms of Fe, Mn, Cu, and Cd were dominating, which have been formed at mixing of fluids with biotope water; while above the sites devoid of fauna, the dissolved metals prevailed over the particulate ones. The suspended particles were mainly represented by aluminosilicates, barite, iron hydroxides at the Menez Gwen vent field, while at the Rainbow – exclusively by sulfides (pyrite, chalcopyrite, and sphalerite) [27]. As it was known, the *Bathymodiolus* mussels in the trophic strategy rely not only on the symbiotrophy but on the filter-feeding also. In other words, the trace metals are accumulated from the suspended particulate matter as well. Gills of the *Bathymodiolus* mussels, collected from the wall of sulfide chimney at the Snake Pit vent field, demonstrated the abnormally high concentrations of chalcophile metals: Fe 3.75, Zn 5.71%; Cu 975, Pb 407, As 145, Cd 63.9, Ag 54.4, Sb 37.3, and Au 1.25 mg/kg. Moreover, an analysis of this specimen using the X-ray diffraction technique with a DRON-2 device (analyst Dr. O.M. Dara) showed the presence of sulfide particles of Fe (pyrite) and Zn (wurtzite) [7]. This evidently confirms the active filtration by the mussels of the biotope water, enriched in suspended sulfides. Earlier, the hydrothermal sulfide minerals were detected in digestive glands tracts of *Bathymodiolus* mussels and *Rimicaris* shrimps, sampled at the Rainbow field [24].

The mineral composition of substratum apparently influences the concentration levels of some trace metals in not only the mussels, but also in the other sedentary bottom organisms. For example, polychaetes *Paralvinella* inhabiting the sulfide edifice (composed mostly from sphalerite ZnS) of the Axial Seamount hydrothermal field (Juan de Fuca Ridge, East Pacific Rise) contain Zn and Cu 10 times more, Cd and Pb 3 times more, than analogous taxa, inhabiting basalt substratum [28].

4 Biological Influence

The deep-sea hydrothermal organisms have to survive in the extremal habitat conditions of high temperature (up 80°C) and pressure (360 bar), devoid (or depleted) of oxygen, but rich in reduced compounds (H_2S, CH_4, and H_2) and heavy metals, toxic to organisms. Adaptation strategy of the hydrothermal organisms evolved over a long geological time: the age of the hydrothermal bottom communities is estimated at 430 million years: they were identified in the Silurian deposits [29]. Age of thermophilic archae bacteria was determined as about 3.5 billion years, it means that they exist approximately from the middle Archean, and they are much older than their hosting symbiotrophic organisms [30]. The most important mechanisms of adaption or bioregulation in metal-rich environments have been discussed in Koschinsky [19]. Here we consider some other biological factors influencing the trace metal bioaccumulation.

4.1 Ontogeny Stage

To understand are there any relationships between the trace metal contents and age of the organisms, we have analyzed body size (length) series of the two different groups of the dominating organisms: the *Bathymodiolus azoricus* mussels from the Rainbow vent field (MAR), as well as vestimentiferan tube worm *Riftia pachyptila* from the 9°50′N (EPR).

We examined trace metal contents in 41 specimens of mussels *Bathymodiolus azoricus*, with the shells' length varying from 24 to 116 mm, which were divided into six groups. It is important to notice that mussels were sampled at one and the same mussel bed (or mussel cluster); it means that they grew in the same proximity of methane and hydrogen sulfide sources, i.e., under the equal environmental conditions. From Fig. 3 it follows that contents of essential metals such as Fe, Mn, Ni, and Cu in shells were noticeably higher (3–50-fold) in younger mussels having smaller sizes. For the rest of metals an appropriate variation in their contents was not recorded in such a way [31]. Reduction of trace metal bioaccumulation in dependence on the mussel age can be attributed (under equal environmental conditions) by reduction in metabolism, and, consequently, intensity of accumulation of metals by organisms at later stages of ontogeny.

In the mussel gills the differences in metal contents were detected for Zn, Ni, Co, Se, and Sb: a 2–5-fold decrease with a growth of the mussel size. It should be noted that a pronounced tendency of the enhanced accumulation with increase in the shell length was revealed only with respect to Hg [7]. Unlike this, in *Bathymodiolus* mussels, taken from the Menez Gwen, Rainbow, and Lucky Strike vent fields (MAR) a clear inverse relationship between shell length and the mercury content was registered only for gills: small mussels had higher Hg concentrations in their gills than larger mussels, unlike in their digestive glands [32]. The apparent

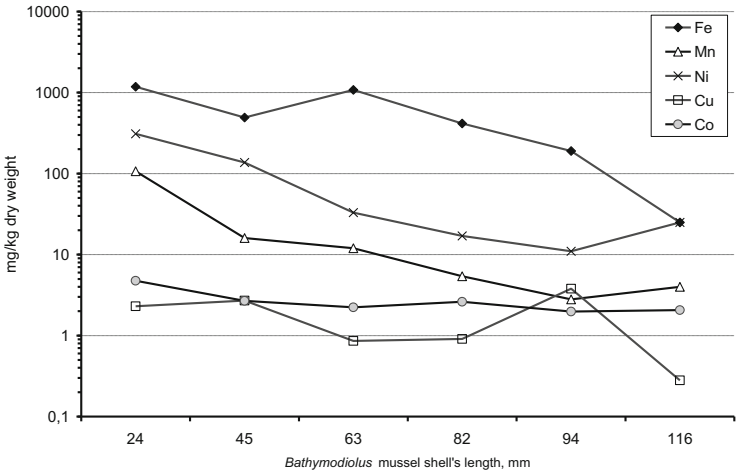

Fig. 3 Variations in concentrations of Fe, Mn, Ni, Cu, and Co in shells of *Bathymodiolus azoricus* mussels versus length of shells, the Rainbow hydrothermal vent field (MAR)

contradiction between the trends in the accumulation of Hg with mussels growth according to our data and data of Kádár et al. (2006) can be easily attributed by the fact that these authors have studied mussels with length from 3 to 12 cm, whereas we examined mussels with the shell length from 24 to 116 mm, i.e., in the other range of the age.

In the soft tissues of the *Archivesica gigas* clams from the Guaymas Basin area [33] and *Calyptogena magnifica* clams from the 21°N (EPR) [10] there were not detected any age-related patterns in the bioaccumulation of Zn, Fe, Cu, Mn, and Cd.

In samples of vestimentiferan tube worm *Riftia pachyptila* ($n = 31$), having different tube length, a distribution of metal contents in different organs was studied. The elevated concentrations of many metals were recorded in trophosome (bacterial endosymbionts hosted), as well as in vestimentum and obturaculum [34]. As one can see from Fig. 4, younger individuals (tube length from 10 to 21.5 cm, on average 14 cm) accumulate less Fe and Zn compared to older (tube length 128 cm on average) specimens; these two metals are physiologically important, as they are involved in the synthesis of hemoglobin and can be transported to the trophosome from the plume [35]. The rest of metals did not show a defined pattern of metal accumulation versus age. Ruelas-Inzunza et al. (2005) observed that for *Riftia pachyptila* from the Guaymas Basin, content of Cd and Fe in vestimentum increased accordingly with the size of specimens [9].

From these summarized data, one can outline only trends in some trace metal accumulation depending on the stage of ontogeny.

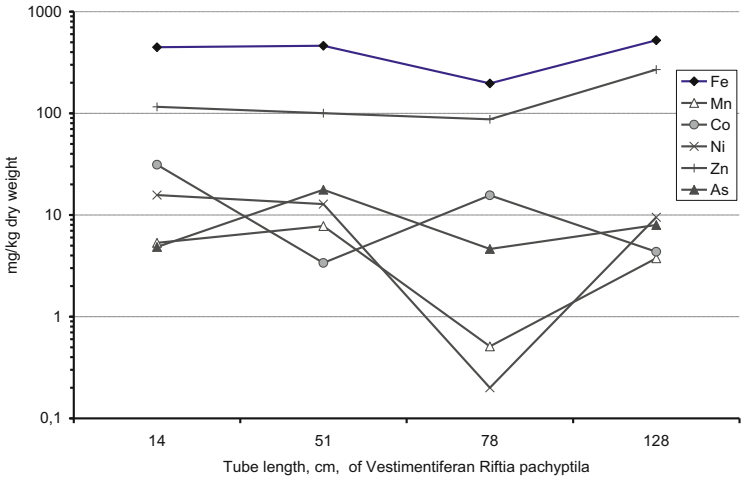

Fig. 4 Variations in concentrations of Fe, Mn, Ni, Cu, Co, Zn, and As in the trophosome of vestimentiferan *Riftia pachyptila* versus tube length, the Guaymas Basin (Gulf of California)

4.2 Trophic Specialization and Food Web

Isotopic data testify that chemosynthetic primary production, which feed hydrothermal organisms, was created by chemolithoautotrophic bacteria; in the course of metabolic processes while transferring to higher trophic level, fractionation of stable isotopes of C and N led to the weighting $\delta^{13}C$ and $\delta^{15}N$ [36].

At various hydrothermal fields of the MAR and EPR, the consumers of the first trophic level involve organisms, that depend on chemosynthesis, but in a different way utilizing its products. (1) Endosymbiotrophers – Vestimentiferans and Bivalve molluscs (mussels and clams), in the gills and trophosome of which intracellular bacteria function. (2) Ectosymbiotrophers – shrimps, using bacterial organic matter by use of external organs – maxillipeds. (3) Bacteriophages – grazers (polychaetes Alvinellidae) and the filter-feeders (polychaetes Serpulidae), feeding on bacterial mats and filtering bacteria from the water column [14].

Consumers of the second trophic level are carnivores – predators and scavengers: mainly crustaceans and some species of gastropods.

The organisms that belong to the same first trophic level, but differ in the manner of utilizing of chemosynthetic products, interact differently with the chemical components of the environment. The close functional relationship between invertebrates and bacterial symbionts induces the mass transfer of chemical elements between them.

For instance, on the Snake Pit and Rainbow vent fields (MAR), symbiotrophic mussels *Bathymodiolus* consume the hydrogen sulfide and sulfide ions from the water, ensuring their bacterial symbionts by "fuel" for chemosynthesis to a much greater extent than ectosymbiotic shrimps [13]. According to our data, the gills of

the *Bathymodiolus* mussels are on average by 1–2 orders of magnitude enriched in Fe, Mn, Zn, Cu, Pb, Ba, Ag, Sb as compared to maxillipeds of shrimp *Rimicaris*.

Similarly, content of Fe, Zn, and Cu in the *Bathymodiolus* gills, hosting chemosynthetic bacteria, is 2–5 times more than in bacteria themselves, who are the primary producers [1].

Bioaccumulation of some metals is characterized by variation within the food chain of the hydrothermal field Menez Gwen (MAR), namely the enrichment in Fe, Zn, and Cu of the secondary consumers (predators) compared with primary consumers (mixotrophic mussels), as well as with the primary producers – bacterial endosymbionts [1]. Thus, these authors have revealed trophic level-specific variations in essential metal accumulation in the Menez Gwen hydrothermal community of the Mid-Atlantic Ridge. They have demonstrated a general trend of biomagnification of Cu, Fe, and Zn from primary producers (endosymbiont bacteria) to primary (symbiont reliant species and filter-feeders) and secondary consumers (predators and scavengers).

In chitin and soft tissues (mainly gills) of another predator – the galatheid crab *Munidopsis*, the high concentrations of many metals (especially Mn, Cu, and Cd) were detected, significantly greater than those in the soft and hard tissues of the mussels, which this crab feeds by. This is, apparently, due to the peculiarities of the metabolism of this crab as predator, leading to the above-mentioned increase of bioaccumulation of metals up the food chain.

The potential transfer of Cu, Zn, and Hg through two trophic links at the Azores triple junction (Menez Gwen, Lucky Strike, and Rainbow fields) was evaluated: (1) the *Bathymodiolus azoricus* mussel and the *Branchipolynoe seepensis* commensal worm and (2) three different species of shrimps and the crab *Segonzacia mesatlantica*. A distinct increase in Hg accumulation from mussel foot (prey) to a commensal worm (predator), and from shrimps species to the crab was revealed; however, the differences were not statistically significant. Cu and Zn concentrations in the different species presented the same pattern of increase from prey to consumer, i.e., from mussel mantle to commensal worm [5].

In our opinion, the high levels of some essential metals (Cu and Mn) in the soft tissues of the crab *Munidopsis alvisca*, inhabiting the Guaymas Basin vent field (Gulf of California), seem to be caused by metabolic peculiarities. Furthermore, type of feeding is of importance, namely, preying on other organisms such as the symbiotrophic *Riftia pachyptila* and the clams *Archivesica gigas* and *Nuculana grasslei*. The sea anemones *Phelliactis pabista* are typical predators, they can scavenge both fragments of bacterial mats, and organic matter, enriched in metals, and thus might enhance their metal bioaccumulation [34].

Thus, it is possible to identify only some trends in the transfer of metals in food chains of benthic communities in hydrothermal vent fields.

5 Effect of Faunistic Zonality

Within hydrothermal fields the bottom organisms are distributed according to the thermal zonality reflecting impact of fluids [13, 14]. At the 9°50′N vent area, EPR, four groups of dominant organisms (about 50 samples) were examined for metal content in soft tissues. The first group consisted of the most thermophilic fauna of the episymbiont-bearing polychaetes *Alvinella pompejana*, which inhabit the walls of the active vent chimneys, where the temperature varies within the range 10–81°C, and the H_2S concentration reaches up to millimolar level, toxic for common organisms [37]. An exclusive feature of *Alvinella pompejana* is that the level of thermal stability of *Alvinella pompejana* cuticular interstitial collagen (of the most well-known extracellular proteins of the animal kingdom and a relevant marker of thermal adaptation) is significantly higher (up to 46°C) than that of other vent annelids [38]. The second group inhabited cooler (6–25°C) seeps (shimmering water) and involved the vestimentiferan tube worms *Riftia pachyptila* that have a trophosome – the organ, which hosts bacteria and is the location of sulfide oxidation and carbon fixation. The third group was marked by bivalve endosymbiotrophic *Bathymodiolus thermophilus* mussels and *Calyptogena magnifica* clams that commonly reside on basalts in a zone insignificantly affected by fluid (2–6°C), where shimmering water is not observed. In the fourth group of fauna, prevailing in the peripheric zone of the vent field, carnivorous crabs *Munidopsis* and *Bythograea*, as well as suspension feeding polychaetes *Laminatubus* (Serpulidae) were examined.

Among the animals, polychaete *Alvinella pompejana* was an animal with the peak trace metal content [18, 39]. In its tubes, covered with filamentous bacterial mats, the metal content reached the following values: Fe 16.1, Zn 3.73, Cu 1.08 (% dry weight); Ni 700; Co, Pb, Mn, As 400; Cr 50; Cd 20; Sb 10; Hg 6 mg/kg dry weight. Much lower average metal contents were found in the soft tissues of Vestimentiferan *Riftia*, mussels *Bathymodiolus*, and clams *Calyptogena* (Fig. 5). So one can notice an abrupt change in trace metal content while more thermophilic organisms are substituted for less thermophilic ones.

The average heavy metal contents in soft tissues of organisms decreased differently for specific groups of elements. Fe, Zn, and Cu, which are distinguished by much higher average contents, than that of other elements, have the most significant enrichment in the *Alvinella pompejana* tissues relatively to other animal groups (Fig. 5a). Mn, As, Pb, and Ni, which have a much lower levels of content in biota (2–120 mg/kg dry w.), decreased from *Alvinella* to *Riftia*. Concentrations of Co and Cr, as well as Se, Sb, Hg, and Cd (commonly <10 mg/kg dry w.) were the highest in *Alvinella* tissues also, but between the rest of animals the metal contents differ insignificantly (Fig. 5a, b). Some increase in the content of most metals was defined in the carnivorous crabs *Bythograea* dwelling in the peripheral zone with the background temperatures. This increase was possibly caused by the trophic specialization: crabs are predators, consuming specialized organisms – symbiotrophs of the lower trophic level that are enriched in many trace metals [3].

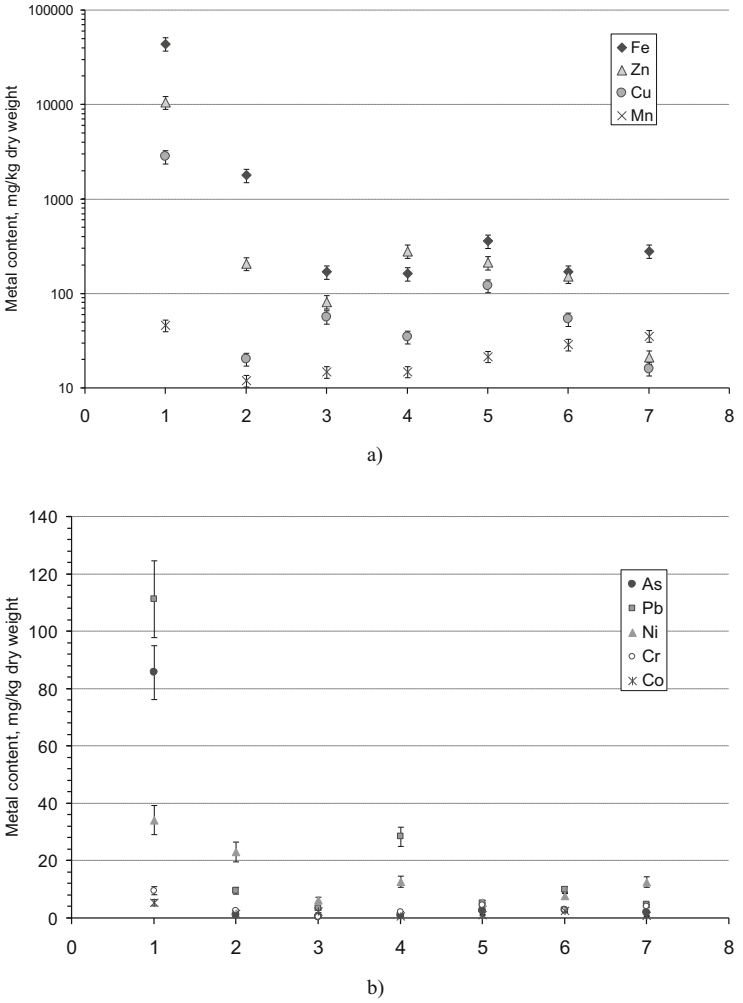

Fig. 5 Variations in average concentrations of the trace metal (mg/kg dry weight) in soft tissues of different groups of organisms inhabiting zones with different water temperature at 9°50′N vent field, EPR. (**a**) Fe, Mn, Zn, and Mn; (**b**) As, Pb, Ni, Cr, and Co. Animals' groups (number of samples): 1 – polychaetes *Alvinella pompejana* (4), 2 – vestimentiferan *Riftia pachyptila* (15), 3 – mussels *Bathymodiolus thermophilus* (17), 4 – clams *Calyptogena magnifica* (12), 5 – crabs *Bythograea* (6), 6 – crabs *Munidopsis* (5), and 7 – polychaetes *Laminatubus (Serpulidae)*

6 Conclusions

Available data on the trace metals under consideration (Fe, Mn, Zn, Cu, Co, Ni, Cr, Pb, Cd, Ag, As, Sb, Se, and Hg) allowed us to conclude that peculiarities of their accumulation are different in the different organs and organisms, and depend on the two main factors: (1) the environmental conditions and (2) biological factors. The first factor includes the trace metal concentration in fluids and biotope water, as

well as pattern of distribution around vent source, while amongst the second ones there are ontogeny and trophic level.

Comparison between the dominating taxa dwelling within the different fields of the MAR allowed us to reveal the influence of the environmental conditions on the bioaccumulation of metals. Inter-site comparison of the trace metal partitioning in gills of the *Bathymodiolus* mussels, that host bacterial endosymbionts, resulted in a significant difference only between the high-temperature vent areas (Rainbow, Broken Spur), on the one hand, and low-temperature Menez Gwen, on the other hand.

Research results may suggest the relationship between the metal levels in the biotope water and the tissues of organisms. Concentration level of Fe, Mn, and Zn (principle metals in fluids) is reflected in the shells of *Bathymodiolus* mussels. Enrichment of the Rainbow fluids in Ni and Co resulted in their elevated contents (up to 10 times relatively other metals) in *Bathymodiolus* shells.

Among the animals, polychaete *Alvinella pompejana*, inhabiting the hottest places of the vent chimneys at the 9°50′N field (EPR) with the highest concentrations of many metals, demonstrated the highest concentrations of the trace metals in their tissues. Along with this, the abnormal enrichment in chalcophile metals (Fe, Zn, Cu, Pb, As, Cd, Ag, Sb, and Au) of the *Bathymodiolus* mussels' gills, collected from the wall of sulfide chimney at the Snake Pit vent field, confirmed by finding there of the sulfide particles of Fe (pyrite) and Zn (wurtzite) gave an evidence of the direct influence of mineral composition of suspended particles in the biotope water upon some metals accumulation in bodies of the dominant vent animals.

Stage of ontogeny, being one of the important biological factors, has a noticeable effect on distribution pattern of such micronutrients as Fe, Mn, Ni, and Cu in *Bathymodiolus* shells: 3–50-fold higher in younger mussels relatively older ones. In the mussel gills the significant differences in metal contents were detected also for essential metals Zn, Ni, Co, Se, and Sb: a 2–5-fold decrease with a growth of the mussel length. Unlike this, in the trophosome of younger tube worm *Riftia pachyptila* individuals (average tube length 14 cm), accumulation of Fe and Zn decreases with age. These micronutrients participate in the hemoglobin synthesis and, according to [35], can be transported to trophosome from the plumes. The rest of metals did not show a defined pattern of metal accumulation versus age.

Some trends of certain micronutrients trophic level-specific variations in benthic communities at the hydrothermal vent fields were identified in [1, 3, 5, 39]. At the Azores triple junction (MAR) and the 9°50′N (EPR) vent fields there was demonstrated a general trend of increased accumulation of Cu, Fe, and Zn from primary producers (endosymbiont bacteria) to primary consumers (symbiont reliant species and filter-feeders) and to secondary consumers (predators and scavengers). Besides, an increase in toxic metal Hg accumulation from prey to predator through trophic links was also revealed [5]. So, based on this, one can outline only tendency towards higher concentration of some metals in predators relatively prey.

Acknowledgements We would like to thank the Russian Scientific Foundation (Project No 14-50-00095 "World Ocean in XXI century: climate, ecosystems, mineral resources and disasters") for financial support of this research over the period of preparation of this chapter.

References

1. Kádár E, Costa V, Segonzac M (2007) Trophic influences of metal accumulation in natural pollution laboratories at deep-sea hydrothermal vents of the Mid-Atlantic Ridge. Sci Total Environ 373:464–472
2. Demina LL, Holm NG, Galkin SV, Lein AY (2010) Concentration function of the deep-sea vent benthic organisms. Cah Biol Mar 51:369–373
3. Demina LL, Holm NG, Galkin SV, Lein AY (2013) Some features of the trace metal biogeochemistry in the deep-sea hydrothermal vent fields (Menez Gwen, Rainbow, Broken Spur at the MAR and 9°50′N at the EPR): a synthesis. J Mar Syst 126:94–105
4. Rousse N, Boulegue J, Cosson R, Fiala-Médioni A (1998) Bioaccumulation des métaux chez le mytilidae hydrothermal *Bathymodiolus* sp. de la ride médio-atlantique. Oceanol Acta 21 (4):597–607
5. Colaço A, Bustamante P, Fouquet Y, Sarradin PM, Serrão-Santos R (2006) Bioaccumulation of Hg, Cu, and Zn in the Azores triple junction hydrothermal vent fields food web. Chemosphere 65:2260–2267
6. Cosson RP, Thiebaut E, Company R, Castrec-Rouelle M, Colaco A, Martins I, Sarradin P-M, Bebianno MJ (2008) Spatial variation of metal bioaccumulation in the hydrothermal vent mussel *Bathymodiolus azoricus*. Mar Environ Res 65:405–415
7. Demina LL, Galkin SV (2008) On the role of abiogenic factors in the bioaccumulation of heavy metals by the hydrothermal fauna of the Mid-Atlantic Ridge. Oceanology 48:784–797
8. Koschinsky A, Kausch M, Borowski C (2014) Metal concentrations in the tissues of the hydrothermal vent mussel Bathymodiolus: reflection of different metal sources. Mar Environ Res 95:62–73
9. Ruelas-Inzunza J, Páez-Osuna F, Soto LA (2005) Bioaccumulation of Cd, Co, Cr, Cu, Fe, Hg, Mn, Ni, Pb and Zn in trophosome and vestimentum of the tube worm *Riftia pachyptila* from Guaymas basin, Gulf of California. Deep-Sea Res I 52:1319–1323
10. Roesijadi G, Crecelius EA (1984) Elemental composition of the hydrothermal vent clam *Calyptogena magnifica* from the East Pacific Rise. Mar Biol 83:155–161
11. Kádár E, Costa V (2006) First report on the micro-essential metal concentrations in bivalve shells from deep-sea hydrothermal vents. J Sea Res 56:37–44
12. Cravo A, Foster P, Almedia C, Company R, Cosson R, Bebianno MJ (2007) Metals in the shell of *Bathymodiolus azoricus* from a hydrothermal vent site on the mid-Atlantic ridge. Environ Int 33:609–615
13. Desbruyères D, Biscoito M, Caprais J-C, Colaço A, Comtet T, Crassous P, Fouquet Y, Khripounoff A, Le Bris N, Olu K, Riso R, Sarradin P-M, Segonzac M, Vangriesheim A (2001) Variations in the deep-sea hydrothermal vent communities on the Mid-Atlantic Ridge near the Azores plateau. Deep-Sea Res I 48:1325–1346
14. Galkin SV (2002) Hydrothermal vent communities of the World Ocean. Structure, typology, biogeography. GEOS, Moscow, 199 pp (in Russian)
15. Desbruyères D, Almeida A, Biscoito M (2000) A review of the distribution of hydrothermal vent communities along the northern Mid-Atlantic Ridge: dispersal vs. environmental controls. Hydrobiologia 440:201–216
16. Van Dover CL (2007) The ecology of deep-sea hydrothermal vents. Princeton University Press, 417 pp

17. Gebruk AV, Chevaldonné P, Shank T, Lutz RA, Vrienhoek RC (2000) Deep-sea hydrothermal vent communities of the Logatchev area (14°45′N, Mid-Atlantic Ridge): diverse biotope and high biomass. J Mar Biol Assoc 80:383–394
18. Demina LL, Galkin SV (2010) Polychaetes Alvinella pompejana is an extrathermophile and metal "champion". Priroda 8:14–21 (in Russian)
19. Koschinsky A (2016) Sources and forms of trace metals taken up by hydrothermal vent mussels, and possible adaption and mitigation strategies. Handb Environ Chem. doi:10.1007/698_2016_2
20. Demina LL (2016) Trace metals in water of the hydrothermal biotopes. Handb Environ Chem. doi:10.1007/698_2016_1
21. Luther GW, Rozan TF, Tallefert M, Nuzzio DB, Di Meo C, Shank TM, Lutz RA, Cary SC (2001) Chemical speciation drives hydrothermal vent ecology. Nature 410:813–816
22. Le Bris N, Sarradin PM, Caprais JC (2003) Contrasted sulphide chemistries in the environment of 13°N EPR vent fauna. Deep Sea Res I 6:737–747
23. Sarrazin J, Juniper SK (1999) Biological characteristics of a hydrothermal edifice mosaic community. Mar Ecol Progr Ser 185:1–19
24. Colaso P, Bustamante Y, Fouquet J, Sarradin PM, Serro-Santos R (2006) Bioaccumulation of Hg, Cu, and Zn in the Azores Triple Junction hydrothermal vent fields food web. Chemosphere 65(11):2260–2267
25. Martins I, Costa V, Porteiro F, Cravo A, Santos RS (2001) Mercury concentrations in invertebrates from Mid-Atlantic Ridge hydrothermal vent fields. J Mar Biol Assoc UK 81 (6):913–915
26. Douville E, Charlou JL, Oelkers EH, Bienvenu P, Jove Colon CF, Donval JP, Fouquet Y, Prieur Y, Appriou P (2002) The Rainbow vent fluids (36°14′N, MAR): the influence of ultramafic rocks and phase separation on trace metals content in Mid-Atlantic Ridge hydrothermal fluids. Chem Geol 184:37–48
27. Kádár E, Costa V, Martins I, Santos RS, Powell JJ (2005) Enrichment in trace metals (Al, Mn, Co, Cu, Mo, Cd, Fe, Zn, Pb and Hg) of the macro-invertebrate habitats at hydrothermal vents along the Mid-Atlantic Ridge. Hydrobiologia 548:191–205
28. Lukashin VN, Galkin SV, Lein AY (1990) Features of chemical composition of animals from deep-sea hydrothermal areas. Geochem Intern 2:279–285
29. Kuznetsov AP, Maslennikov VV (2000) History of the ocean hydrothermal fauna. VNIRO Publishing House, Moscow, 118 pp (in Russian)
30. Bonch-Osmolovskaya EA (2002) Thermophilic microorganisms in the marine hydrothermal systems. In: Gebruk AV (ed) Biology of hydrothermal systems. KMK Scientific Press Ltd, Moscow, pp 131–140 (in Russian)
31. Demina LL, Galkin SV, Dara OM (2012) Trace metal bioaccumulation in the shells of mussels and clams at deep-sea hydrothermal vent fields. Geochem Int 50(2):133–147
32. Kádár E, Santos RS, Powell JJ (2006) Biological factors influencing tissue compartmentalization of trace metals in the deep-sea hydrothermal vent bivalve Bathymodiolus azoricus at geochemically distinct vent sites of the Mid-Atlantic Ridge. Environ Res 101:221–229
33. Ruelas-Inzunza J, Soto LA, Páez-Osuna F (2003) Heavy-metal accumulation in the hydrothermal vent clam *Vesicomya gigas* from Guaymas basin, Gulf of California. Deep Sea Res I 50:757–761
34. Demina LL, Galkin SV, Shumilin EN (2009) Bioaccumulation of some trace metals in the biota of hydrothermal fields of the Guaymas basin (Gulf of California). Bul Soc Geol Mexicana 61:31–45
35. Cosson-Manevy MA, Cosson RP, Gaill RP (1988) Transfert, accumulation et régulation des éléments minéraux chez organismes des sources hydrothermales. Oceanol Acta 8:219–225
36. Galkin SV, Gebruk AV, Krylova EM, Len AY, Vinogradov GM, Vereshchaka AL (2006) Trophic structure of the North Atlantic hydrothermal biocommunities: data on isotopic analysis. In: Vinogradov ME, Vereshchaka OL (eds) Ecosystems of the Atlantic hydrothermal vents. Nauka, Moscow, pp 95–118 (in Russian)

37. Le Bris N, Gaill F (2006) How does the annelid *Alvinella pompejana* deal with an extreme hydrothermal environment? Rev Environ Sci Biotechnol. doi:10.1007/sl1157-006-9112-1
38. Gaill F, Hunt S (1991) The biology of annelid worms from high temperature hydrothermal vent regions. Rev Aquat Sci 4:107–137
39. Demina LL, Galkin SV, Lein AY, Lisitzin AP (2007) First data on the microelemental composition of benthic organisms from the 9°50′N hydrothermal field, East Pacific Rise. Doklady Earth Sci 415(6):905–907

The Deep Biosphere of the Subseafloor Igneous Crust

Magnus Ivarsson, N.G. Holm, and A. Neubeck

Abstract The igneous portion of the subseafloor crust is considered to be the largest potential microbial habitat on Earth; thus, it is somewhat of a paradox that our knowledge regarding its abundance, diversity and ecology is sparse, close to non-existent. This is mainly due to issues involved in sampling live species, and therefore much of our present knowledge of the deep biosphere is based on a fossil record. However, drilling and sampling techniques are constantly being developed to facilitate sampling of live microorganisms, and recent molecular studies show a positive progress towards better recovery and less contamination. Here we discuss the subseafloor igneous crust as a microbial habitat, its physical and geochemical prerequisites to support life and what type of life that could sustain in such an extreme environment. We also discuss what the fossil record, and the few successful molecular studies, tells us regarding what type of microorganisms exist in the deep subseafloor settings. It appears as if the igneous crust is more diverse than previously expected consisting of both prokaryotes and eukaryotes in close interplay with each other and their physical environment. As our knowledge increases so does the questions, and hopefully future technique development can provide us with an increased understanding of this deep, hidden world.

Keywords Basalts, Endoliths, Microbial habitats, Oceanic igneous crust, The deep biosphere

M. Ivarsson (✉)
Department of Palaeobiology, Nordic Center for Earth Evolution (NordCEE), Swedish Museum of Natural History, Svante Arrhenius väg 9, Box 50007, 104 05 Stockholm, Sweden
e-mail: magnus.ivarsson@nrm.se

N.G. Holm and A. Neubeck
Department of Geological Sciences, Stockholm University, Svante Arrhenius väg 8, 106 91 Stockholm, Sweden
e-mail: nils.holm@geo.su.se

L.L. Demina and S.V. Galkin (eds.), *Trace Metal Biogeochemistry and Ecology of Deep-Sea Hydrothermal Vent Systems*, Hdb Env Chem (2016) 50: 143–166,
DOI 10.1007/698_2015_5014,
Published online: 4 December 2015

Contents

1 Introduction

Until quite recently the crystalline part of the oceanic crust was considered "barren", and life associated with the deep biosphere appeared to be confined to hydrothermal vents. The last two decades have involved a change in view of the ocean crust and its potential to harbour life, and today the subseafloor biosphere is considered to be widespread at both ocean ridges as well as off-axis [1–3]. The concept of a deep biosphere in subseafloor basalts is based on a combination of several lines of direct or circumstantial evidence. Initially, the idea of microorganisms dwelling in the ocean crust was based on observations of microorganisms in association with hydrothermal active areas on the ocean floor and in vent fluids originating from deep beneath the crust. Hydrothermal vents were considered as windows into a potential but not yet confirmed subseafloor biosphere [4]. An increasing awareness and knowledge of a subsurface biosphere in the terrestrial basement further strengthened the concept of an oceanic counterpart [5, 6]. In the 1990s marine sediments were shown to contain significant portions of microorganisms, and it would thus be logical to assume a similar microbial colonization of the igneous part of the crust [7]. The discovery of granular and tubular etch marks in volcanic glass and a possible microbial involvement in their formation sparked the exploration of the subseafloor biosphere in the 1990s [8–13]. Since then the abundance, diversity and origin of these ichnofossils have been discussed, but still today their biological origin is questioned [14], especially the ancient ones found in ophiolites as old as 3.5 Ga [15, 16].

During the last decade fossilized microorganisms have been observed in drilled cores and dredged samples from the ocean floor and in ophiolites [17–22]. The microorganisms are being found fossilized in carbonate- and zeolite-filled veins and vesicles in the basalts or open pore spaces and represent microbial communities that once lived in these fractures. Surprisingly, a majority of these findings represent fungi. But also consortia of fungi and prokaryotes have been reported [23].

Due to issues involved in sampling live species in subseafloor igneous rocks, only a handful of molecular studies have been carried out successfully on dredged [24–26] and drilled samples [27–29]. A wide variety of bacteria, archaea and fungi [30] have been found during deep subsurface sampling, but the risks of seawater contamination have been hard to overcome. However, new techniques that enable sampling and long-term monitoring of drill holes hopefully will result in more accurate sampling of live species.

Still, our knowledge of the deep biosphere of the subseafloor crust is limited with respect to abundance, diversity and ecology and is a research frontier in geological, biological and oceanological sciences. This review aims to cover our gained knowledge so far and discuss future prospects in the search for life in the deep ocean floors.

2 Basalts as Microbial Habitats

The total rock volume of the oceanic crust is estimated to 2.3×10^{18} m^3, which is 6–10 times that of the total marine sediments. The upper part of the ocean crust consists of a 500–1,000 m section of permeable basalts (pillow lavas), a middle layer down to ~1.5 km of sheeted dikes and a deeper layer to about 4 km depth of gabbroic rock (Fig. 1). The upper layer is characterized by extensive fracturing, about 10% porosity and permeabilities of about 10^{-12} to 10^{-15} m^2 [3, 31]. These values decrease slightly with depth and age of the crust as fractures are filled by compression and precipitation of secondary minerals. Roughly 60% of the oceanic crust is hydrologically active, and the total fluid volume of the igneous crust corresponds to 2% of the total ocean [3]. Thus, the entire water volume of the ocean circulates through the ocean crust every 10^5 to 10^7 years, which means that the oceanic crust is the largest aquifer system on Earth [3, 32]. Indirectly this means that the ocean crust is the largest potential microbial habitat on Earth. Microorganisms are passively transported or actively migrating through this system wherever pore space and fluid flow permit. Fractures occur with varying size and frequency depending on where in the volcanic pile they occur (Fig. 2a, b). Pillow lavas, for instance, have a highly fractured glassy rim due to quick cooling at contact with cold seawater. The interiors, on the other hand, are massive with lower fracturing.

In addition to fractures created by tension release or quick cooling, parts of the subseafloor basalts are highly vesicular as a result of pressure release during magma extrusion (Fig. 2c, d). As the pressure decreases, dissolved magmatic gases come out of solution as gas bubbles in the magma. When the magma is extruded as lava at the surface, the lava solidifies around the gas bubbles forming vesicles. Basalt can contain coherent systems of vesicles interconnected with each other or through microcracks.

The microorganisms of the subseafloor basalts take advantage of the open pore space in the rocks for migration and colonization and are categorized depending on where in the rock they live and their behaviour in relation to the substrate they

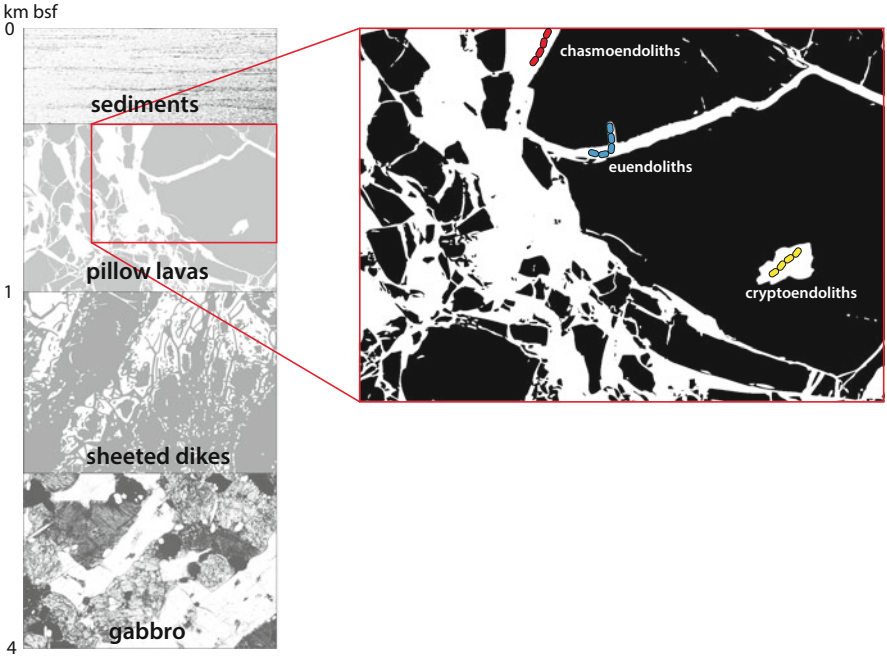

Fig. 1 Sketch showing the partition of the subseafloor igneous crust into three different parts: the upper pillow lavas, the middle sheeted dikes and the lower gabbros. In the *right panel* the division of microorganisms with respect to occurrence in the pore space is visualized. Microorganisms that actively penetrate into rock interiors and create habitable cavities are called euendoliths. Microorganisms that invade pre-existent fissures and cracks are called chasmoendoliths, and microorganisms that invade pre-existent structural cavities are called cryptoendoliths

inhabit. All rock-dwelling microorganisms are termed endoliths. Microorganisms that actively penetrate into rock interiors and create habitable cavities are called euendoliths. Microorganisms that invade pre-existent fissures and cracks are called chasmoendoliths, and microorganisms that invade pre-existent structural cavities are called cryptoendoliths (Fig. 1) [33].

2.1 Metabolic Pathways

Little is known of metabolic reactions in the subseafloor crust due to restricted accessibility of live microbial communities. In the dark, subsurface environment, in the absence of sunlight, microorganisms gain energy from coupling of reducing and oxidizing (redox) reactions that are thermodynamically favourable. The base of the deep subseafloor biosphere is thought to consist of chemoautotrophs, organisms that obtain energy by the oxidation of electron-donating molecules in their environment in contrast to photoautotrophs that utilize solar energy. Organisms that use

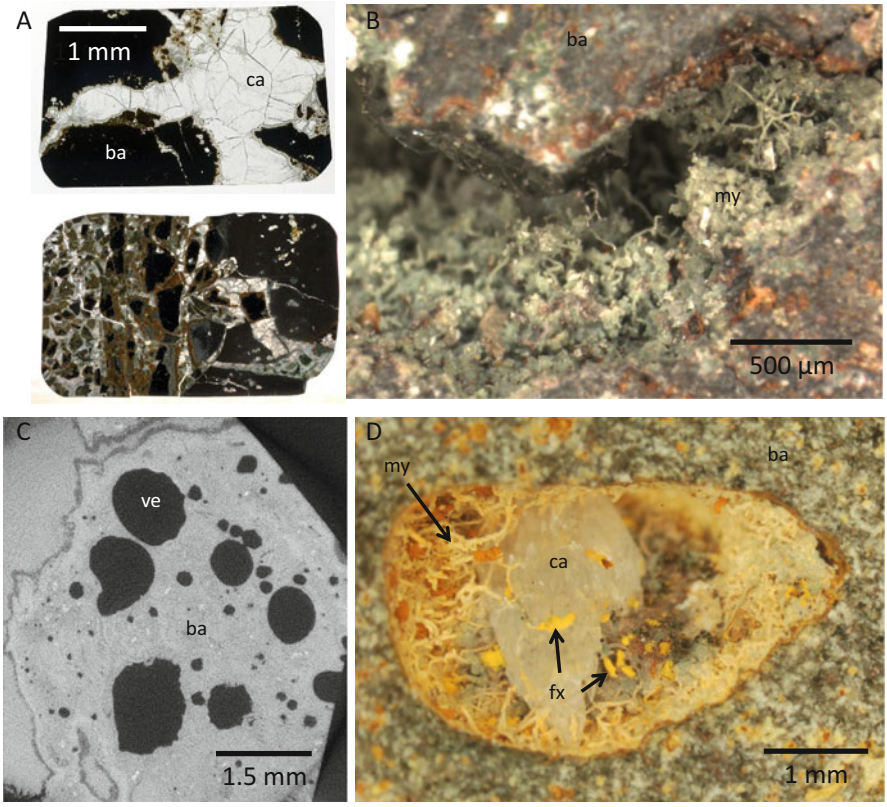

Fig. 2 Microphotographs showing veins and vesicles in basalt with associated microbial communities. Samples from ODP Leg 197, drilled at the Emperor Seamounts in the Pacific Ocean. (**a**) Two scanned thin sections with calcite filling the voids. The topmost thin section shows distinct fracturing of basalt with calcite veins representing the interior of pillow lava and the lower panel a brecciated sample representing the rim. The latter one contains glass fragments (*black*) and *brown-yellowish fragments* palagonite (altered glass). (**b**) An open fracture in basalt where the walls are lined by a fungal community fossilized by a greyish clay (montmorillonite). Filamentous hyphae are seen protruding from the fracture walls forming a mycelium in the open space. (**c**) A SRXTM slice of a highly vesicular basalt with open vesicles (in *black*) distributed throughout the sample. (**d**) An open vesicle in basalt with euhedral calcite crystals and a fungal mycelium associated with bacterial microstromatolites (in *yellow*) called *Frutexites*. *ba* basalt, *ca* calcite, *my* mycelium, *ve* vesicle, *fx* Frutexites

inorganic substrates like CO_2 and minerals to obtain energy are called lithoautotrophs.

The available information on possible metabolic reactions in the deep subsurface is based on analysed chemical components from rocks and fluids within the crust and vent fluids (Fig. 3). The most accessible electron donors in subseafloor settings are H_2, CH_4, H_2S, S^0, $S_2O_3^{2-}$, Fe^{2+}, Mn^{2+}, NH_4^+, NO_2^- and organic matter. Possible electron acceptors are CO_2, SO_4^{2-} or O_2. Possible metabolic pathways

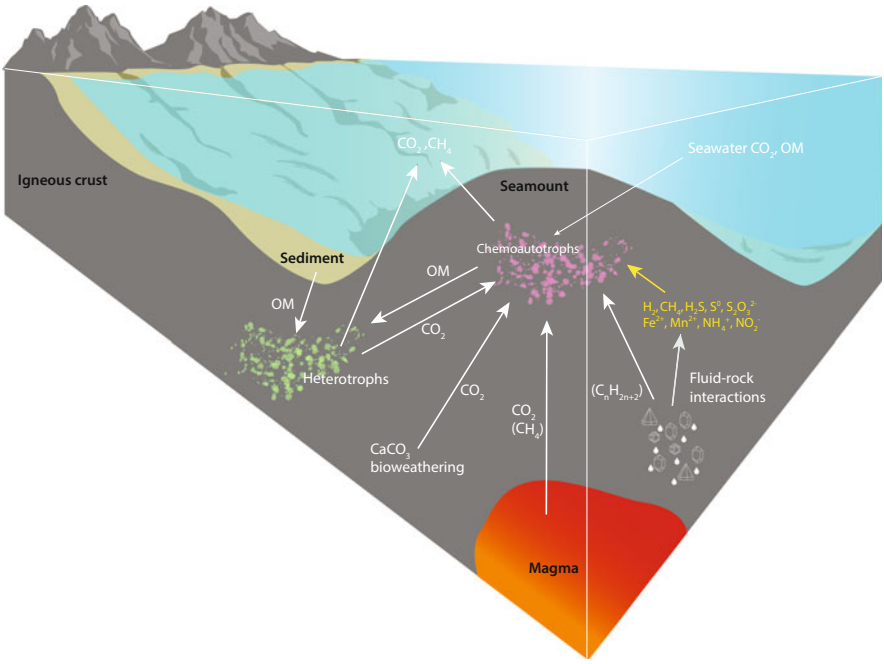

Fig. 3 Schematic of possible carbon sources in the igneous crust. Chemoautotrophs use mainly CO_2 from the magma or the seawater. Possible energy sources for chemoautotrophy are also included (*yellow arrows*). Heterotrophs use organic matter (OM) introduced to the system either from the overlying sediments or by seawater. Another possible OM source is the chemoautotrophic communities. Thus, the chemoautotrophs fix dissolved CO_2 from the fluids and build biomass that the heterotrophs scavenge. In the process of degrading carbohydrates, the heterotrophs produce CO_2 that could trigger further chemoautotrophic growth. Fluid-rock interactions also produce hydrocarbons but the significance in a microbial context is unknown

differ depending on what type of host rock the microorganisms exist in. Basalt is comprised of roughly 9% FeO and 0.1% each of MnO and S. Whereas alteration of ultramafic rocks (serpentinization) produces high pH fluids poor in Fe and S but highly enriched in H_2, CH_4 and simple hydrocarbons, alteration of basalt results in acidic fluids enriched in reduced Fe and S compounds and to a smaller extent in H_2 and CH_4 [31]. Reduced Fe, Mn and S components are, thus, the most likely energy sources for microorganisms in basalt systems. This is supported by molecular analyses and cultivation approaches on seafloor-exposed basalt. Microorganisms involved in Fe-cycling (oxidation and reduction) are still not entirely determined but have been found within *Zetaproteobacteria*, *Alphaproteobacteria* (including *Hyphomonas* species) and *Gammaproteobacteria* (including *Marinobacter* species) [26, 34]. Fe-reducing microorganisms including *Shewanella* species have also been cultivated from seafloor basalt samples [25–35]. Activities and rates of Fe redox reactions are relatively slow at low temperatures, but the microorganisms can catalyse the reactions and gain metabolic energy in the process. Cold-adapted

Fe-oxidizing bacteria have, thus, a competitive advantage at low temperatures [36]. Mn^{2+}-oxidizing microorganisms have also been recovered from basalts [37] including the *Bacillus* genus within the *Firmicutes*, *Marinobacter* and *Pseudoalteromonas* within *Gammaproteobacteria* and *Sulfitobacter* within *Alphaproteobacteria* [38, 39]. However, Mn^{2+} oxidation is not known among autotrophy yet. The presence of microbial S-cycling in subseafloor basalts has been suggested [31]. Genes required in sulphate reduction have been detected [39] as well as distant relatives to known sulphate-reducing *Deltaproteobacteria* [26, 39]. Lever et al. [29] showed the presence S-cycling microbes from deep drilled basalts at the Juan de Fuca Ridge, but still the knowledge of S-cycling microorganisms is scarce from subseafloor basalts.

A way to understand the metabolism of the deep subseafloor biosphere is to compare it with the better-known terrestrial counterpart. The simplest ecosystem that we can imagine in the terrestrial subsurface biosphere is based on reduced gases like molecular H_2 and CH_4 as sources of energy [40]. The C source would be CO_2 or HCO^{3-}. Hydrogen can be provided in several ways: by degassing from the mantle, by radiolysis of water and by oxidation of Fe^{2+} and simultaneous reduction of water during serpentinization of olivine and pyroxene [41]. Methane may be produced from H_2 and CO/CO_2 by abiotic Fischer-Tropsch-type reactions and, of course, biologically from the same constituents by hydrogenotrophic methanogens, methanogens that only can use CO_2 as a C source and H_2 as an energy source compared to other methanogens that can also use C compounds as acetate and methanol as a C source. Metabolic activity in the subsurface will be limited by kinetics and the supply of energy. In the terrestrial deep biosphere, the energy may be supplied by components dissolved in a slow flow of groundwater. If we think of the subseafloor basement as an environment with no or very little fluid flow, the supply of energy would be a very slow, diffusion-limited process. However, circulation of seawater into basement is a continuous process and is driven by thermal advection with diffuse recharge and focused discharge through basement high to the seafloor [32, 42–44]. Such fluid flow may be active tens of millions of years after the formation of the basement rocks [41, 45–47].

2.2 Cycling of Carbon

Both chemoautotrophic and heterotrophic growths are dependent on available C to build biomass. Knowledge of C abundance and possible C sources in the subseafloor igneous crust is even more obscure than the understanding of metabolic pathways (Fig. 3). Chemoautotrophs mainly use CO_2 as C source and to minor extent carbon monoxide, acetate, formate, methanol, methanethiol, methylamine and methane. The main sources for CO_2 in the subseafloor crust are either the magma or the seawater. Fluids and gases ascending from underlying magma can contain substantial amounts of dissolved CO_2. Magmatic CO_2 is perhaps

most common in volcanic active areas and not in off-axis areas with no nearby magma chamber. The other main source for CO_2 would be seawater. Downward penetration of seawater occurs in recharge areas, such as mid-ocean ridges, subduction zones and seamounts, where the crust is exposed and not covered by sediments. Marine sediments work as a block for downward migration of seawater. Recharge areas are usually volcanic and hydrothermally active and coincide with the areas where magmatic CO_2 is transported upwards to the subseafloor crust. Thus, the main input of CO_2 occurs at recharge zones, and in off-axis areas, the ingress of CO_2 to the system is limited. However, C isotope signatures of vent fluids show that fluids from the igneous crust are scavenged for C by chemosynthetic microorganisms; thus, fluids throughout the igneous crust hold enough dissolved C to sustain an indigenous chemoautotrophic biosphere [48].

Another source of hydrocarbons accessible for microorganisms is compounds produced by fluid-rock interactions like the Fischer-Tropsch-type reaction. Simpler hydrocarbons like CH_4 to more complex molecules like fatty acids can be produced in such reactions; however, the extent of such processes is not known and difficult to estimate, and it is questionable if enough compounds are produced to support a deep biosphere.

Seawater and downward migration of fluids from overlying sediments can probably introduce organic matter, more complex than simple hydrocarbons, into the igneous crust. The amounts of such downward transport are also difficult to estimate but could perhaps support heterotrophs in the upper parts of the crust. In deeper settings heterotrophs probably are dependent on chemoautotrophic communities as carbon source. A symbiotic relationship between chemoautotrophs and heterotrophs at depth would be the ideal model of an indigenous biosphere and was suggested by Bengtson et al. [23]. In such a relationship the chemoautotrophs fix dissolved C from the fluids by oxidation of reduced elements like Fe^{2+} or Mn^{2+}, and the heterotrophs feed on their biomass. The heterotrophic growth releases CO_2 that theoretically could support chemoautotrophic growth and, thus, an indigenous biosphere independent from the surface input of C. However, there are many question marks in such a model. For instance, is the subseafloor basalts limited in CO_2 to such an extent that CO_2 produced by heterotrophy would be crucial for chemoautotrophic growth?

2.3 Microorganisms in the Subseafloor Igneous Crust

Considering the abundant microbial presence in hydrothermal fluids escaping from vents on the ocean floors and that deep sea sediments are estimated to contain the Earth's largest proportion of microorganisms [7, 49], it would be probable to assume that a significant biosphere would be hosted in deep crustal environments as well. Basalts exposed at the seafloor and, thus, more accessible compared to deeper basalts are commonly coated with biofilms [34, 50, 51]. Seafloor-exposed basalt appears to be dominated by bacteria according to quantitative molecular

studies like PCR or FISH. Phylogenetically, the microbial communities are dominated by *Proteobacteria*, *Actinobacteria*, *Bacteroidetes*, *Chloroflexi*, *Firmicutes* and *Planctomycetes* phyla [26, 39, 52–54]. The function of the observed species is poorly understood, but within the *Gammaproteobacteria* some species group closely with known methane- and sulphide-oxidizing groups [26], and within the *Alphaproteobacteria* some species group with chemoorganotrophic groups [54]. The archaea are much less known but tend to be dominated by members of the *Crenarchaeota* [24, 25, 52, 55]. Knowledge of viral and eukaryotic communities is absent with the exception of one study that found several fungal species on basalts from Vailulu'u Seamount [30]. The density of microbial communities on seafloor-exposed rocks is not very well known but seems to be heterogeneously distributed and influenced by venting and topography of the basalts, as microbial communities are preferentially concentrated to pits and grooves on the mineral surfaces [34]. The few estimates that have been performed indicate communities with densities of 6×10^5 to 1×10^9 cells g^{-1} [26, 39, 53].

Molecular studies of microbial communities from subseafloor basalts are rare even though the first visualization of DNA-stained material in volcanic glass is 20 years old [12]. The presence of *Gamma-*, *Beta-* and *Alphaproteobacteria* lineages in gabbroic layers [27] has been reported as well as anaerobic archaea such as *Archaeoglobus* and *Methanosarcina* [28, 56]. However, none of the studies were able to fully exclude possible microbial contamination from seawater during sampling. The function of the subseafloor lineages was also unknown even though the *Proteobacteria* seemed to be involved in hydrocarbon degradation. Lever et al. [29] were able to exclude seawater contamination and indicated the presence of *Methanosarcinales*, anaerobic methane-oxidizing archaea (ANME-1) and a cluster of microbes that fall within uncultured sulphate reducers. They were able to combine functional genes indicative of methane-cycling and sulphate reduction with $\delta^{13}C$- and $\delta^{34}S$-isotopic values to show clear signs of microbial activity. Furthermore, studies of crustal fluids collected on ocean ridge flanks have indicated the presence of *Firmicutes* [56, 57], bacteria that do not group closely with cultivated microorganisms and whose function is unclear, although they have been connected to N- or S-cycling. Carbon isotope signatures of vent fluids further show that fluid circulation may support an indigenous chemosynthetic deep biosphere [48]. Besides this rather fragmentary and circumstantial evidence, our understanding of the biosphere of the subseafloor crust is based on the fossil record.

3 Microbial Fossils in Subseafloor Basalts

3.1 Ichnofossils

Microbially produced etch marks in volcanic glass are a widespread phenomenon in the ocean crust and produce conspicuous granular and tubular cavities [11, 58–60]

(Fig. 4). These etch marks are trace fossils in the sense that they are not body fossils but traces of microbial euendolithic activity, and the correct terminology is thus ichnofossils [61, 62]. The ichnofossils run perpendicular to a glass surface and inwards into the glass. The granular type consists of micron-sized, near-spherical voids carved into the fresh glass and subsequently filled with authigenic minerals like clays and Fe oxides/hydroxides. These globular voids commonly occur in clusters along surfaces of volcanic glass and are irregularly distributed on both sides of a fracture. The tubular type consists of straight or smoothly curved tubes with sometimes segmented, branched or spiralling textures. The diameter of the tubes is on the order of one to a few microns and between ten to hundreds of microns in length. The tubular type usually occurs in assemblages that form a band, 50–100 μm in width, perpendicular to the glass surface. They are irregularly distributed with respect to the opposing side of any cracks and commonly associated with the granular type. To characterize the ichnofossils even further, McLoughlin et al. [61] erected two novel ichnogenera: *Granulohyalichnus* igen. nov. and *Tubulohyalichnus* igen. nov., which correspond to the granular and tubular

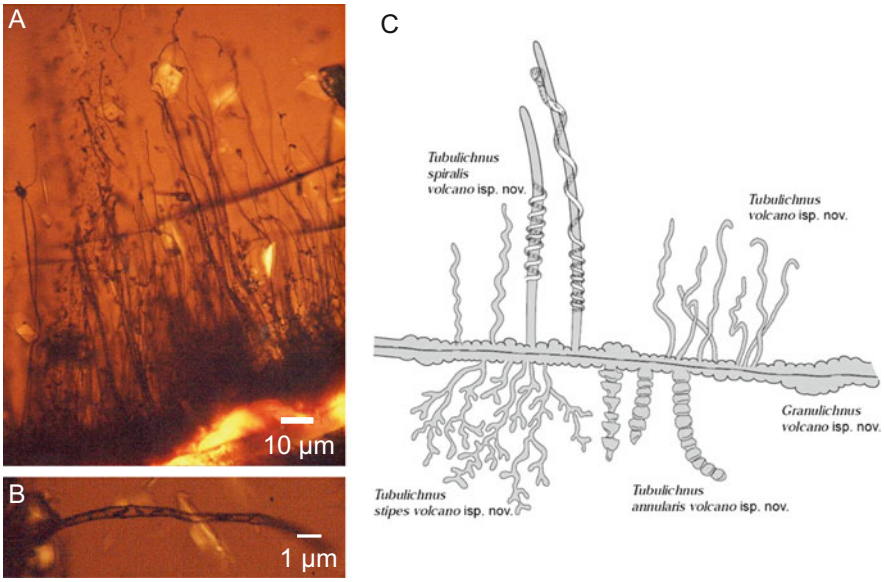

Fig. 4 Ichnofossils in volcanic glass. (**a**) Microphotograph of tubular ichnofossils extending perpendicular into the glass from a vein filled with clay minerals. (**b**) Close-up of a tubular ichnofossil with a fine ornament on the tube wall. Samples from ODP Leg 197, site 1203 (sample 1203A-30R1-1, 63) drilled at the Detroit Seamounts of the Emperor Seamounts in the Pacific Ocean. (**c**) Line drawing showing the various ichnotaxa radiating from a central fracture. From *left to right*: helical shaped or coiled *Tubulohyalichnus spiralis* isp. nov.; simple unornamented and unbranched *Tubulohyalichnus simplus* isp. nov.; on the *lower side* of the fracture, branched *Tubulohyalichnus stipes* isp. nov.; annulated *Tubulohyalichnus annularis* isp. nov.; on *both sides* of the fracture, *Granulohyalichnus vulgaris* isp. nov. (*Note*: this is a schematic juxtaposition of the ichnotaxa; all five have not been observed alongside one another in natural samples; approximate relative scales are illustrated.) Modified from McLoughlin et al. [61]

bioeroded textures (Fig. 4c). These ichnogenera are further subdivided into five ichnospecies on the basis of morphological variations (see ref 62 for a more detailed description). Fisk and McLoughlin [63] further produced a comprehensive photographic atlas of the ichnofossils.

Ichnofossils in volcanic glass were first recognized by Ross and Fisher [64] who reported etched grooves in glass shards from a Miocene tephra. They compared the etch marks with fungal borings in carbonate grains and suggested that fungi were responsible for the production of the ichnofossils. In the early and mid-1990s, several observations were made of granular and tubular microstructures in volcanic glass of drilled and dredged samples from the ocean floor [8–13]. The biogenic origin of these ichnofossils was argued based on (1) elevated values of C, N and P in association with the etch marks, (2) C-isotope values that indicated biologic activity [65], (3) observations of partially fossilized and encrusted microbial cells in the etch marks with forms and sizes that match the form and sizes of the etch marks and (4) nucleic acids and DNA that were detected in and in close association with the etch marks by biological stains. DNA of both bacteria and archaea has been detected in rocks that contain bioeroded etch marks [12, 24].

Thorseth et al. [8] proposed a mechanism for the microbial dissolution of volcanic glass. Controlled laboratory experiments in seawater showed how microorganisms cultivated on volcanic glass produced etch pits and alteration rinds on glass fragments [9]. Thorseth et al. [8] suggested that bacteria are able to create microenvironments with local variations in pH. Depending on which bacterium is present, the pH can be either high or low. At high pH the glass Si–Al network would suffer strong dissolution. At low pH elements like Fe, Ti and Al would be kept in dissolution and be removed from the local area. The laboratory experiments showed how microorganisms produced etch pits resembling the granular bioalteration textures, but tunnel structures exceeding 10 μm failed to be produced in the volcanic glass. However, a conceptual model of how granular and tubular microstructures can be produced microbially in volcanic glass has been developed by a series of authors [8, 9, 11, 60, 66, 67]. In this model microorganisms are introduced to pore spaces and rims of glass shards by circulating fluids. The microorganisms attach to the surfaces of fresh glass and initiate etching of the glass and with time granular and tubular cavities are created.

There is a distinct difference between biotic alteration textures and abiotic alteration textures [11, 59, 60]. Abiotic alteration of volcanic glass affects the whole surface of a glass shard uniformly and produces unembayed, smooth alteration fronts parallel to the surface of the glass shard. In contrast, microbial alteration textures consist of irregularly distributed local cavities [11, 59].

Even though the mechanism of biological dissolution and production of ichnofossils has been extensively described in various reports [8, 60, 61, 68, 69], still today the microorganisms responsible for the production of these structures have not yet been identified, and the biological origin of the structures has been questioned [15], and alternative abiotic formation processes have been suggested [14]. Especially, ichnofossils in ancient ophiolites and greenstone belts [60, 70] have been questioned [16]. Abiotic formation of ichnofossils has been suggested as

the remains of fluid inclusion trails and radiation damage trails, but the most common type is ambient inclusion trails (AITs) [69]. AITs are usually described as the result of mineral grains that have been propelled through a relative soft substrate leaving a tubular microcavity behind. AITs are characteristic in appearance with longitudinal striae, polygonal in cross section, and sometimes with a terminal grain, thus relatively easy to distinguish from tubular ichnofossils formed by microbial activity [69].

Establishing biogenic origin of ichnofossils in volcanic glass is of highest priority since they constitute such an extensive feature in subseafloor volcanic glass and may be an important tool to estimate the total biomass of the seafloor [71] but also since they are common throughout the geologic record in ophiolites and greenstone belts and represent some of the oldest traces of life on Earth [11, 70].

3.2 Fossilized Microorganisms

Encrusted or completely fossilized coccoidal microorganisms have been found in subseafloor cherts [72], on dredged basalt samples [73] and in drilled basalt samples [18, 19]. Filamentous fossilized microorganisms have been found in veins and vesicles in ocean floor basalts [17–20, 74, 75] and in ophiolites [21, 22] of Devonian age. The filamentous microfossils occur in abundance and form complex networks that can fill the entire pore space of a vein system (Fig. 5). The diameters range from 2 to ~30 μm and the length can vary from 10 μm to <1 mm. Their morphology is highly varied, and they occur as curvilinear segmented, branched or amorphous filaments. The segmented filaments can vary in appearance from thicker filaments with septa-like segmentation to thinner and simpler morphologies that resemble trichomes [76]. Central swellings and a turgid appearance can also be observed as well as bean-shaped structures.

The fossilized microorganisms are represented by crypto-, chasmo- and euendoliths and consist of two main types: (1) microorganisms embedded and preserved in vein-filling minerals like carbonates or zeolites (Fig. 5a) or (2) as microbial communities preserved and mineralized in open pore spaces (Fig. 5c). In the first type live microorganisms have been entombed in vein-filling phases and subsequently preserved and fossilized. They usually consist of poorly crystalline clay phases and iron oxides but with a high organic content characterized by high carbon content, phosphates, hydrocarbons, lipids and chitin [18–20]. The second type rarely contains organics probably due to the fossilization and mineralization in open systems where organic matter can be oxidized, scavenged by other microorganisms or transported by fluids. However, they are usually preserved by a clay phase, just as the first type, and iron oxides.

The overall concept is that microorganisms colonized open pore space in basalts, while fluid flow was active, and that fossilization occurred due to mineral in-filling or mineral replacement of the microorganisms. The microbial colonization occurs

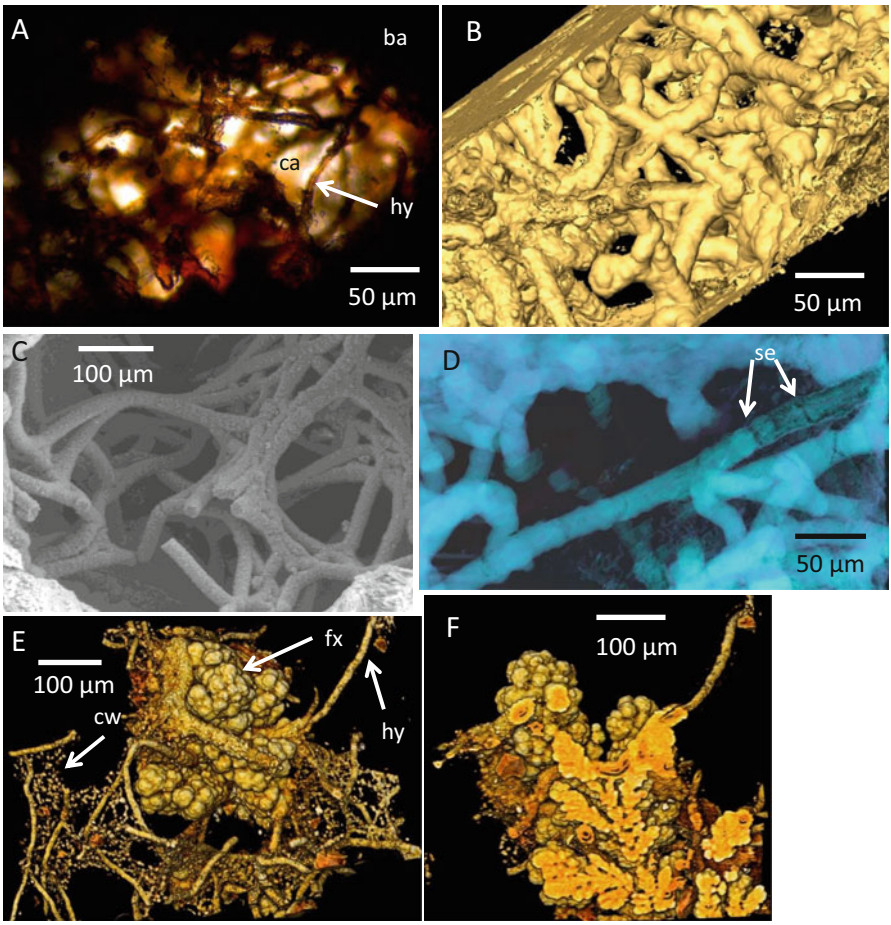

Fig. 5 Fossilized microorganisms in veins and vesicles. (**a**) Microphotograph of a calcite-filled vein in basalt with an entrapped and fossilized mycelium of fungal hyphae. (**b**) SRXTM isosurface rendering of a thin section in profile. The same mycelium as in **a**. Note the higher quality in detailed information between the microphotograph and the tomogram. (**c**) ESEM micrograph of a fungal mycelium fossilized as montmorillonite in an open vesicle. (**d**) Tomographic reconstruction (voltex) of a fungal mycelium embedded in calcite. Repetitive septa are visible along the hyphae. (**e**, **f**) SRXTM volume rendering of a microbial consortium including three types of organisms: one hyphae and two types of prokaryotes (*Frutexites* and "cobwebs" of cells). The prokaryotes use the mycelium as a framework for their growth. The *Frutexites* form a cauliflower-like structure with a distinct direction of growth (shown in the cross section in **f**). Minute cells are suspended in between the hyphae forming an organized "cobweb"-like ultrastructure. *ba* basalt, *ca* calcite, *hy* hyphae, *se* septum, *cw* "cobwebs", *fx Frutexites*

relatively early after the cooling of the host rock and prior to substantial formation of secondary minerals. The initial stage of the microbial colonization is onset by the formation of a biofilm that lines the interiors of the pore space. This is today seen as

a fossilized crust consisting of various hematite, hematite-carbon and clay layers [23, 77]. This fossilized biofilm can be smooth to botryoidal in appearance due to various assimilated spherical and cell-like aggregates. From the basal film filamentous structures protrude, either solely or more commonly in great abundance, and form complex, mycelium-like networks in the open pore space. Thus, the filamentous microorganisms are always rooted at the vein or vesicle wall, firmly anchored to a crust or secondary mineralizations.

Most filamentous, mycelial-like communities have been recognized as remains of fungal mycelium consisting of both fungal hyphae and yeast-like growth states and with sporophores, fruiting bodies and resting structures like sclerotia. They have characteristic fungal morphologies like repetitive septa, anastomoses between branches, a central pore and chitin in the cell walls [20, 77, 78]. Bengtson et al. [23] further showed that these complex fungal mycelia have functioned as a framework on which prokaryotic communities have existed (Fig. 5e, f). Minute cells suspended on strings in between the hyphae with a cobweb-like appearance were interpreted as possible iron oxidizers with an ultrastructure similar to *Pyrodictium* or *Euryarchaeon* SM1. Microstromatolites (*Frutexites*), remains of iron-oxidizing prokaryotic communities, were also observed in close association with fungal hyphae. Thus, fungi and chemoautotrophic prokaryotes exist in symbiotic-like relationships, which probably is a prerequisite for eukaryotic colonization of and persistence in the subseafloor crust. Bengtson et al. [23] further showed that both fungi and *Frutexites* actively bored in secondary calcite with the result of tunnel-like structures produced by hyphae and granular cavities by the *Frutexites*.

The chemical composition of the filamentous microorganisms is usually dominated by a mix of Si, Fe, Al, Mg and C with minor amounts of Na, K, Ti and Ca. The mineralization is usually poor but corresponds to smectite- or montmorillonite-like clays. Peckmann et al. [21] reported that filamentous microorganisms consisted of the clay minerals chamosite and illite. They suggested that the clays were a result of microbial clay authigenesis which in turn was favourable for the preservation of the filamentous microfossils. The interiors of the filaments and hyphae are dominated by iron oxides/oxyhydroxides [18, 19, 23, 77, 79]. Filamentous microfossils have been shown to have, at least partially, a high organic content varying between ~10 and 50 wt% C. The C content varies greatly both between closely associated filaments and within the same filament. Filamentous microfossils have also been shown to contain phosphates, hydrocarbons and lipids, which have been used as evidence for their biogenic origin [19]. Propidium iodide (PI), a dye that binds to cells with damaged cell membranes and traces of DNA, has been used to stain fossils successfully [18].

The enrichment of C and the high degree of organic remains are probably a result of irregular distribution and local enhancements of organic material during the fossilization process. Silicification is known to preserve cells and morphology of microbes to some extent [80]; however, metal cations are known to inhibit the autolysis (self-destruction of cells) and thus preserve dead bacterial cells [81, 82]. Ferris et al. [83] suggested that ferric ions inhibit autolysis of bacterial cells and result in intact preservation of the cells. Iron is also known to form

complex and stabilize organic compounds for long periods of time [84]. It is probable that the high iron content of the fossilized microorganisms is responsible for the high grade of preservation considering the high amounts of C and the occurrence of organic remains like lipids and chitin.

3.3 Extracting and Interpreting Palaeobiological Information

Microorganisms interact with their environment during their entire life cycle, which is recorded on a cellular level and preserved as their life cycles end. In fact, fossilized microorganisms can be compared to snapshots of the geochemical and ecological conditions that prevailed at the time of entrapment. By extracting and analysing the palaeobiological information that has been recorded in the microfossils, it is possible to reconstruct the ecology and palaeoenvironment of the microorganisms. The type of data that is possible to collect is microbial morphology, element and mineral composition, oxidation states, isotopes, speciation of carbon (inorganic or organic) and characterization of organic compounds. Such data enable interpretations of metabolic pathways, nutrient supply, redox conditions and type of microbial communities.

However, interpretations of such delicate matters call on cautiousness. Diagenetic processes often lead to degradation of organic matter and recrystallization that erase and replace the primary composition and make advanced interpretations frail. When establishing biogenicity and subsequent interpretations regarding the type of microorganism, metabolic pathways and ecology, a wide range of aspects including morphology, chemical content, biomarkers, geological context and indigenousness with the host rock need to be considered prior to a valid conclusion that can be reached [77, 85].

Interpretations based on chemical composition and geological context have been done. Filamentous and coccoidal microfossils from subseafloor environments are usually encrusted by iron oxides and oxide hydroxides [18, 19, 24, 73, 79]. Iron-oxidizing microorganisms are known to accumulate oxidized iron in their cells, cell walls or as deposits on their surfaces [86]. Iron encrustations found on microfossils could thus be the results of microbial involvement in iron-oxidizing reactions. Ferrous iron is the most accessible element with a redox potential of use for autotrophic microorganisms in hydrothermal basaltic environments, and filamentous iron oxides collected from vent waters at submarine seamounts show remarkable similarities with filamentous iron-oxidizing microorganisms living on the seafloor that have been identified as *Gallionella* spp., *Leptothrix ochracea* or *Mariprofundus ferrooxydans* [34, 87, 88]. This suggests that iron plays an important role for microorganisms of the subseafloor biosphere.

Some microfossils found in subseafloor settings also have encrustations of manganese. Manganese is, just like iron, abundant in basaltic environments and

with a redox potential accessible for microorganisms. It has even been proposed that microbially mediated manganese oxidation occurs in subseafloor settings [73]; however, from laboratory experiments and cultivation of manganese oxidizing microorganisms, manganese oxidation has not yet been proven in autotrophy [86]. Ivarsson et al. [76] described a system in which chromite in basalt had been oxidized by manganese oxides and that microbes were involved in the chromite oxidation to gain energy from the reaction. Despite being somehow hypothetical, the study shows alternative energy sources and metabolic pathways for chemoautotrophic microorganisms and that geochemical fluctuations at a micro level can influence microbial metabolism in this type of environments. Ivarsson et al. [89] further showed that Mn oxides identified as todorokite associated with microbial consortia are biogenic in origin by using electron paramagnetic resonance spectroscopy (EPR). However, if the fungal or prokaryotic part of the microbial consortia or perhaps both were responsible for the oxidation of Mn^{2+} to Mn^{4+}, oxide mineral was not determined.

Ivarsson et al. [90] introduced the study of fluid inclusions in combination with the study of fossilized microorganisms as a tool to constrain the temperatures, fluid composition and depth at the time of fossil preservation. Even fossilized microorganisms preserved as fluid inclusions in a palaeo-hydrothermal system from the Milos Island, Greece, were studied [91]. The fluid inclusions were aqueous (liquid ± vapour) and/or hydrocarbon phases. Oil and solid hydrocarbons were interpreted as decomposed biological matter. Microthermometry showed that the microorganisms were trapped and preserved at ~100°C in boiling water.

The advantage with palaeontological material over molecular methods is the obtained spatial apprehension that facilitates in-detailed studies of morphology, community structure and the interaction between the microorganisms and their physical environment. But advanced interpretation relies on the instrumentation. There have been advancements in development of techniques suitable for microfossil studies. Benzerara et al. [92, 93] have used a combination of focused ion beam milling (FIB), transmission electron microscopy (TEM) and synchrotron-based scanning transmission X-ray microscopy (STXM) to study microfossils. Schopf and Kudryavtsev [94] have used Raman tomography to produce three-dimensional visualizations of microfossils and detection of carbonaceous material. ToF-SIMS has been used to detect in situ biomarkers in filamentous fossils from subseafloor basalts [19]. The development of synchrotron-based methods with the capability of higher resolution (down to nm scale) compared to ordinary instruments or multitask functions may open up for new possibilities in analysing microfossils. STXM is an example of a new method to study element and organic composition of a microfossil on nm scale, and synchrotron-radiation X-ray tomographic microscopy (SRXTM) is an example of a method to produce three-dimensional visualizations on μm scale of microfossils [20, 23, 95].

Ultimately, the ambition is to refine the data detection limit as well as the collection and interpretation of information with the aim to develop protocols to use fossilized microorganisms as indicators of palaeo-conditions. This is a long-term goal that demands a profound understanding of preservation mechanisms and

diagenetic processes; thus, before fossilized microorganisms can be used as tools to restrain palaeo-conditions of a system, intense research is needed.

4 Sampling the Subseafloor Biosphere

In order to advance from studying fossilized microorganisms to actually sample live species, phylogenetic studies need to be performed coupled with cultivation of sampled microorganisms. The last decades have involved a rapid development of methods and instruments for analysing molecular phylogenetics among microorganisms, mostly based on the small subunit rRNA (16S rRNA). These techniques are efficient tools and have revolutionized the understanding of prokaryotes, not least in association with hydrothermal vents [96]. The main advantage is that they are cultivation independent. Since only about 1% of all prokaryotes can be cultivated, these techniques provide an alternative to more traditional methods based on culturing. Thus, methods for analysing microorganisms are developed and accessible; the only obstacle is sampling of the deep biosphere without the risk of contamination.

At the moment, the subseafloor biosphere is accessible through ocean drilling only, which poses two major obstacles, incomplete drill cores and contamination during the drilling. The average rock recovery is usually between 10% and 30%. This is due to difficulties in drilling fragmented formations that consist of poorly cemented basalt and lava sections. Drilling such rocks tends to fragment the formations further and results in even lower recovery.

Drilling in ocean basement also introduces seawater into the ocean crust for cooling the drill bit and removal of drilling debris. In a microbial context introduction of seawater will lead to contamination of core and fluid samples. Thus, any microbes found in ocean drill cores or in water samples from the drill hole may come from the introduced seawater. Tests have been performed to evaluate possible contamination from the drilling [97]. In one test perfluorocarbon tracers were injected with the drill fluids, and in another test fluorescent microbeads were introduced to the core as it enters the core liner. Both tests showed that contamination in ocean drilling cannot be controlled at this stage due to the exposure of core surfaces and subsequent transfer of contamination from these surfaces into the sample during processing such as trimming, thin section preparation, etc.

Core interiors, on the other hand, would be less affected by the contamination of drill fluids compared to core surfaces. Mason et al. [27] crushed core samples to isolate core interiors. They used fluorescent microspheres that were deployed in a plastic bag wedged into the core catcher that ruptured as the first cored material entered the core barrel. The cores were rinsed and assessed by microscopy to ensure that the microspheres were dispersed. Microspheres were only observed on the exterior of the cores and not the interiors which would indicate that the samples were not contaminated by the drilling fluids. However, molecular analysis showed that one rock sample from a core contained microorganisms closely related

to microorganisms from the seawater which may indicate contamination; thus, the method with microspheres may not be completely trustworthy.

Future IODP (International Ocean Discovery Program) missions with the aim to explore the deep biosphere focus instead on good recovery and continuous sequences of basement rock. Their drilling strategy is to use a seabed rock drill equipped with a wireline coring system. This technique differs from the drilling equipment of a JOIDES Resolution-type vessel and will result in shallower drill depths but will instead secure a high recovery. This will enable to identify targets for future investigations.

CORKs (Circulation Obviation Retrofit Kits) are underwater borehole laboratories for multidisciplinary in situ measurements including temperature, pressure, chemical monitoring, fluid sampling and also microbiological monitoring and sampling. They are designed to stop bottom water influx, which means that the conditions in a borehole can stabilize after a while and return to conditions prior to drilling. Repetitive return with ROVs and sampling of the CORKs enable long-term monitoring of a borehole and in the best case the natural conditions of the subseafloor crust. More than 30 CORKs have been installed throughout the world's ocean floor, and the coupled techniques used are continuously developed to meet the scientific demands. For instance, the Flow-through Osmo Colonization Systems (FLOCS) consists of a series of cassettes containing various minerals and osmotic pumps to stimulate in situ colonization and growth of subsurface microorganisms.

5 Concluding Remarks

The exploration of the deep biosphere of the subseafloor crust has only recently begun, and we are still, literally, groping in the dark. Considering that the ocean crust covers more than 2/3 of the Earth surface and that the subseafloor biosphere extends down to depths of at least one thousand metres in the basaltic crust, we are facing a huge challenge. Subseafloor basalts also play an important role as habitats for life throughout Earth's geological history. A continuous record of ichnofossils from greenstone belts and ophiolites shows that oceanic basement has harboured microbial life from ~3.5 Ga up until today, representing most of the history of life [11]. Tubular ichnofossils have been found in Archean volcanic rocks from both the ~3.5 Ga Barberton greenstone belt of South Africa and pillow lavas from the ~3.4 Ga Pilbara Supergroup of Western Australia [11, 70, 98, 99].

At the moment we are limited by issues involved in sampling, and there is an urgent need for development of new drilling methods and sampling techniques. With, hopefully, emergent techniques in the future that allow contaminant-free studies of the subseafloor biosphere, fundamental questions await to be answered:

- How deep is the subseafloor biosphere? And does it vary with depth?
- How diversified and abundant is the deep subseafloor biosphere?
- What is its ecological role?

- What are the accessible energy sources and the metabolic pathways of the microorganisms?
- How important is the subseafloor biosphere for the chemical flux between the ocean crust and the seawater?
- How temperature, pressure and pH dependent/resistant are the microorganisms of the subseafloor biosphere?
- How far back in deep time can we track the deep biosphere by investigating ophiolites?

Acknowledgements We would like to thank Marianne Ahlbom at the Department of Geological Sciences, Stockholm University, for the assistance with ESEM analysis, Stefan Bengtson and Veneta Belivanova (Swedish Museum of Natural History) and Federica Marone (Swiss Light Source, Paul Scherrer Institute) for producing SRXTM images. Nicola McLoughlin at the University of Bergen is acknowledged for the permission to use Fig. 4c. This work was funded by the Swedish Research Council (Contract No. 2012-4364) and the Danish National Research Foundation (DNRF53).

References

1. Edwards KJ, Bach W, McCollom T (2005) Geomicrobiology in oceanography: microbe-mineral interactions at and below the seafloor. Trends Microbiol 13:449–456
2. Schrenk MO, Huber JA, Edwards KJ (2009) Microbial provinces in the subseafloor. Ann Rev Mar Sci 2:279–304
3. Orcutt BN, Sylvan JB, Knab NJ, Edwards KJ (2011) Microbial ecology of the dark ocean above, at, and below the seafloor. Microbiol Mol Biol Rev 75:361–422
4. Deming JW, Baross JA (1993) Deep-sea smokers – windows to a subsurface biosphere. Geochim Cosmochim Acta 57:3219–3230
5. Pedersen K, Ekendahl S (1990) Distribution and activity of bacteria in deep granitic groundwaters of southeastern Sweden. Microb Ecol 20:37–52
6. Pedersen K (1993) The deep subterranean biosphere. Earth Sci Rev 34:243–260
7. Parkes RJ, Cragg BA, Bale SJ, Getliff JM, Goodman K, Rochelle PA, Fry JC, Weightman AJ, Harvey SM (1994) Deep bacterial biosphere in Pacific Ocean sediments. Nature 371:410–413
8. Thorseth IH, Furnes H, Heldal M (1992) The importance of microbiological activity in the alteration of natural basaltic glass. Geochim Cosmochim Acta 56:845–850
9. Thorseth IH, Torsvik T, Furnes H, Muehlenbachs K (1995) Microbes play an important role in the alteration of oceanic crust. Chem Geol 126:137–146
10. Furnes H, Staudigel H (1999) Biological mediation in ocean crust alteration: how deep is the deep biosphere? Earth Planet Sci Lett 166:97–103
11. Furnes H, McLoughlin N, Muehlenbachs K, Banerjee N, Staudigel H, Dilek Y, de Wit M, Van Kranendonk M, Schiffman P (2008) Oceanic pillow lavas and hyaloclastites as habitats for microbial life through time – a review. In: Dilek Y, Furnes H, Muehlenbachs K (eds) Links between geological processes, microbial activities and evolution of life. Springer, Berlin, pp 1–68
12. Giovannoni SJ, Fisk MR, Mullins TD, Furnes H (1996) Genetic evidence for endolithic microbial life colonizing basaltic glass-seawater interfaces. Proc Ocean Drill Prog Sci Res 148: 207–214
13. Fisk MR, Giovannoni SJ, Thorseth IH (1998) Alteration of oceanic volcanic glass: textural evidence of microbial activity. Science 281:978–980

14. Lepot K, Philippot P, Benzerara K, Wang G-Y (2009) Garnet-filled trails associated with carbonaceous matter mimicking microbial filaments in Archean basalt. Geobiology 7:393–402
15. Schopf JW (2006) Fossil evidence of Archaean life. Philos Trans R Soc B 361:869–885
16. Grosch EG, McLoughlin N (2014) Reassessing the biogenicity of Earth's oldest trace fossil with implications for biosignatures in the search for early life. Proc Natl Acad Sci U S A 111: 8380–8385
17. Schumann G, Manz W, Reitner J, Lustrino M (2004) Ancient fungal life in North Pacific Eocene oceanic crust. Geomicrobiol J 21:241–246
18. Ivarsson M, Lindblom S, Broman C, Holm NG (2008) Fossilized microorganisms associated with zeolite-carbonate interfaces in sub-seafloor hydrothermal environments. Geobiology 6: 155–170
19. Ivarsson M, Lausmaa J, Lindblom S, Broman C, Holm NG (2008) Fossilized microorganisms from the Emperor Seamounts: implications for the search for a subsurface fossil record on Earth and Mars. Astrobiology 8:1139–1157
20. Ivarsson M, Bengtson S, Belivanova V, Stampanoni M, Marone F, Tehler A (2012) Fossilized fungi in subseafloor Eocene basalts. Geology 40:163–166
21. Peckmann J, Bach W, Behrens K, Reitner J (2008) Putative cryptoendolithic life in Devonian pillow basalt, Rheinisches Schiefergebirge, Germany. Geobiology 6:125–135
22. Eickmann B, Bach W, Kiel S, Reitner J, Peckmann J (2009) Evidence for cryptoendolithic life in Devonian pillow basalts of Variscan orogens, Germany. Palaeogeogr Palaeoclimatol Palaeoecol 283:120–125
23. Bengtson S, Ivarsson M, Astolfo A, Belivanova V, Broman C, Marone F et al (2014) Deep-biosphere consortium of fungi and prokaryotes in Eocene sub-seafloor basalts. Geobiology 12: 489–496
24. Thorseth IH, Torsvik T, Torsvik V, Daae FL, Pedersen RB, Keldysh-98 Scientific Party (2001) Diversity of life in ocean floor basalt. Earth Planet Sci Lett 194:31–37
25. Lysnes K, Thorseth IH, Steinsbau BO, Øvreås L, Torsvik T, Pedersen RB (2004) Microbial community diversity in seafloor basalt from the Arctic spreading ridges. FEMS Microbiol Ecol 50:213–230
26. Santelli CM, Orcutt BN, Banning E, Bach W, Moyer CL, Sogin ML, Staudigel H, Edwards KJ (2008) Abundance and diversity of microbial life in ocean crust. Nature 453:653–657
27. Mason OU, Nakagawa T, Rosner M, Van Nostrand JD, Zhou J, Maruyama A, Fisk MR, Giovannoni SJ (2010) First investigation of microbiology of the deepest layer of ocean crust. PLoS One 5(11), e15399
28. Orcutt BN, Bach W, Becker K, Fisher AT, Hentscher M, Toner BM et al (2010) Colonization of subsurface microbial observatories deployed in young ocean crust. ISME J 5:692–703
29. Lever MA, Rouxel A, Alt JC, Shimizu N, Ono S, Coggon RM et al (2013) Evidence for microbial carbon and sulphur cycling in deeply buried ridge flank basalt. Science 339: 1305–1308
30. Connell L, Barrett A, Templeton A, Staudigel H (2009) Fungal diversity associated with an active deep sea volcano: Vailulu'u Seamount, Samoa. Geomicrobiol J 26:597–605
31. Bach W, Edwards KJ (2003) Iron and sulphide oxidation within the basaltic ocean crust: implications for chemolithoautotrophic microbial biomass production. Geochim Cosmochim Acta 67: 3871–3887
32. Fisher AT, Becker K (2000) Channelized fluid flow in oceanic crust reconciles heat-flow and permeability data. Nature 403:71–74
33. Golubic S, Friedmann I, Schneider J (1981) The lithobiontic ecological niche, with special reference to microorganisms. J Sediment Res 51:475–478
34. Edwards KJ, Bach W, Rogers DR (2003) Geomicrobiology of the ocean crust: a role for chemoautotrophic Fe-bacteria. Biol Bull 204:180–185
35. Gao H, Obraztova A, Stewart N, Popa R, Fredrickson JK, Tiedje JM, Nealson KH, Zhou J (2006) *Shewanella loihica* sp. nov., isolated from iron-rich microbial mats in the Pacific Ocean. Int J Syst Evol Microbiol 56:1911–1916

36. Edwards KJ, Bach W, McCollom TM, Rogers DR (2004) Neutrophilic iron-oxidizing bacteria in the ocean: their habitats, diversity, and roles in mineral deposition, rock alteration, and biomass production in the deep-sea. Geomicrobiol J 21:393–404
37. Templeton AS, Staudigel H, Tebo BM (2005) Diverse Mn(II)-oxidizing bacteria isolated from submarine basalts at Loihi Seamount. Geomicrobiol J 22:127–139
38. Dick GJ, Lee JY, Tebo BM (2006) Manganese(II)-oxidizing *Bacillus* spores in Guaymas Basin hydrothermal sediments and plumes. Appl Environ Microbiol 72:3184–3190
39. Mason OU, Di Meo-Savoie CA, Van Nostrand JD, Zhou J, Fisk MR, Giovannoni SJ (2008) Prokaryotic diversity, distribution, and insights into their role in biogeochemical cycling in marine basalts. ISME J 3:231–242
40. Pedersen K (2000) Exploration of the deep intraterrestrial microbial life: current perspectives. FEMS Microbiol Lett 185:9–16
41. Holm NG, Neubeck A (2009) Reduction of nitrogen compounds in oceanic basement and its implications for HCN formation and abiotic organic synthesis. Geochem Trans 10:9
42. Stein C, Stein S (1994) Constraints on hydrothermal heat flux through the oceanic lithosphere from global heat flow. J Geophys Res 99:3081–3099
43. Fisher AT, Davis EE, Hutnak M, Spiess V, Zühlsdorff L, Cherkaoui A, Christiansen L, Edwards K, Macdonald R, Villinger H, Mottl MJ, Wheat CG, Becker K (2003) Hydrothermal recharge and discharge across 50 km guided by seamounts on a young ridge flank. Nature 421: 618–621
44. Bekins BA, Spivack AJ, Davis EE, Mayer LA (2007) Dissolution of biogenic ooze over basement edifices in the equatorial Pacific with implications for hydrothermal ventilation of oceanic crust. Geology 35:679–682
45. Fehn U, Cathles LM (1986) The influence of plate movement on the evolution of hydrothermal convection cells in the oceanic crust. Tectonophysics 125:289–312
46. Fisher AT, Von Herzen RP (2005) Models of hydrothermal circulation within 106 Ma seafloor: constraints on the vigor of fluid circulation and crustal properties, below the Madeira Abyssal Plain. Geochem Geophys Geosyst 6
47. Hutnak M, Fisher AT, Harris R, Stein C, Wang K, Spinelli G, Schindler M, Villinger H, Silver E (2003) Large heat and fluid fluxes driven through mid-plate outcrops on ocean crust. Nat Geosci 1:611–614
48. McCarthy MD, Beaupré SR, Walker BD, Voparil I, Guilderson TP, Druffel ERM (2011) Chemosynthetic origin of ^{14}C-depleted dissolved organic matter in a ridge-flank hydrothermal system. Nat Geosci 4:32–36
49. Whitman WB, Coleman DC, Wiebe WJ (1998) Prokaryotes: the unseen majority. Proc Natl Acad Sci U S A 95:6578–6583
50. Sudek LA, Templeton AS, Tebo BM, Staudigel H (2010) Microbial ecology of Fe(hydr)oxide mats and basalts rock from Vailulu'u Seamount, American Samoa. Geomicrobiol J 26: 581–596
51. Templeton AS, Knowles EJ, Eldridge KL, Arey BW, Dohnalkova AC, Webb SM, Bailey BE, Tebo BM, Staudigel H (2009) A seafloor microbial biome hosted within incipient ferromanganese crusts. Nat Geosci 2:872–876
52. Mason OU, Stingl U, Wilhelm LJ, Moeseneder MM, Di Meo-Savoie CA, Fisk MR, Giovannoni SJ (2007) The phylogeny of endolithic microbes associated with marine basalts. Environ Microbiol 9:2539–2550
53. Einen J, Thorseth IH, Øvreås L (2008) Enumeration of *Archaea* and *Bacteria* in seafloor basalt using real-time quantitative PCR and fluorescence microscopy. FEMS Microbiol Lett 282: 182–187
54. Santelli CM, Edgcomb VP, Bach W, Edwards KJ (2009) The diversity and abundance of bacteria inhabiting seafloor lavas positively correlate with rock alteration. Environ Microbiol 11:86–98

55. Fisk MR, Storrie-Lombardi MC, Douglas S, Popa R, McDonald G, Di Meo-Savoie C (2003) Evidence of biological activity in Hawaiian subsurface basalts. Geochem Geophys Geosyst 4: 1103
56. Cowen JP, Giovannoni SJ, Kenig F, Johnson HP, Butterfield D, Rappé MS, Hutnak M, Lam P (2003) Fluids from aging ocean crust that support microbial life. Science 299:120–123
57. Nakagawa S, Inagaki F, Suzuki Y, Steinsbu BO, Lever MA, Takai K, Engelen B, Sako Y, Wheat CG, Horikoshi K, Integrated Ocean Drilling Program Expedition 301 Scientists (2006) Microbial community in black rust exposed to hot ridge flank crustal fluids. Appl Environ Microbiol 72:6789–6799
58. Furnes H, Staudigel H, Thorseth IH, Torsvik T, Muehlenbach K, Tumyr O (2001) Bioalteration of basaltic glass in the oceanic crust. Geochem Geophys Geosyst 2(8)
59. Staudigel H, Furnes H, Banerjee NR, Dilek Y, Muehlenbachs K (2006) Microbes and volcanoes: a tale from the oceans, ophiolites, and greenstone belts. GSA Today 16:4–10
60. Staudigel H, Furnes H, McLoughlin N, Banerjee NR, Connell LB, Templeton A (2008) 3.5 billion years of glass bioalteration: volcanic rocks as a basis for microbial life? Earth Sci Rev 89:156–176
61. McLoughlin N, Furnes H, Banerjee NR, Muehlenbachs K, Staudigel H (2009) Ichnotaxonomy of microbial trace fossils in volcanic glass. J Geol Soc Lond 166:159–169
62. McLoughlin N, Brasier MD, Wacey D, Green OR, Perry RS (2007) On biogenicity criteria for endolithic microborings on early Earth and beyond. Astrobiology 7:10–26
63. Fisk M, McLoughlin N (2013) Atlas of alteration textures in volcanic glass from the ocean basins. Geosphere 9:317–341
64. Ross KA, Fisher RV (1986) Biogenic grooving on glass shards. Geology 14:571–573
65. Furnes H, Muehlenbachs K, Tumyr O, Torsvik T, Xenophontos C (2001) Biogenic alteration of volcanic glass from the Troodos ophiolite, Cyprus. J Geol Soc Lond 158:75–84
66. Staudigel H, Chastain RA, Yayanos A, Bourcier W (1995) Biologically mediated dissolution of glass. Chem Geol 126:147–154
67. Staudigel H, Yayanos A, Chastain R, Davies G, Verdurmen EAT, Sciffman P, Bourcier R, De Baar H (1998) Biologically mediated dissolution of volcanic glass in seawater. Earth Planet Sci Lett 164:233–244
68. Thorseth IH, Furnes H, Tumyr O (1995) Textural and chemical effects of bacterial activity on basaltic glass: an experimental approach. Chem Geol 119:139–160
69. Mcloughlin N, Staudigel H, Furnes H, Eichmann B, Ivarsson M (2010) Mechanisms of microtunneling in rock substrates – distinguishing endolithic biosignatures from abiotic microtunnels. Geobiology 8:245–255
70. Furnes H, Banerjee NR, Muehlenbachs K, Staudigel H, de Wit M (2004) Early life recorded in Archean pillow lavas. Science 304:578–581
71. Staudigel H, Tebo B, Yayanos A, Furnes H, Kelley K, Plank T, Muehlenbachs K (2004) The oceanic crust as a bioreactor. In: Wilcock WSD, DeLong EF, Kelley DS, Baross JA, Cary SC (eds) The subseafloor biosphere at mid-ocean ridges, Geophysical monograph series 144. American Geophysical Union, Washington, pp 325–341
72. Al-Hanbali HS, Sowerby SJ, Holm NG (2001) Biogenicity of silicified microbes from a hydrothermal system: relevance to the search for evidence of life on earth and other planets. Earth Planet Sci Lett 191:213–218
73. Thorseth IH, Pedersen RB, Christie DM (2003) Microbial alteration of 0–30-Ma seafloor basaltic glasses from the Australian Antarctic Discordance. Earth Planet Sci Lett 215:237–247
74. Ivarsson M, Holm NG (2008) Microbial colonization of various habitable niches during alteration of oceanic crust. In: Dilek Y, Furnes H, Muehlenbachs K (eds) Links between geological processes. Springer, Microbial Activities and Evolution of Life, pp 69–111
75. Cavalazzi B, Westall F, Cady SL, Barbieri R, Foucher F (2011) Potential fossil endoliths in vesicular pillow basalt, Coral Patch Seamount, eastern north Atlantic Ocean. Astrobiology 11: 619–632

76. Ivarsson M, Broman C, Holm NG (2011) Chromite oxidation by manganese oxides in subseafloor basalts and the presence of putative fossilized microorganisms. Geochem Trans 12:5
77. Ivarsson M, Bengtson S, Skogby H, Belivanova V, Marone F (2013) Fungal colonies in open fractures of subseafloor basalt. Geo-Mar Lett 33:233–243
78. Ivarsson M (2012) The subseafloor basalts as fungal habitats. Biogeosciences 9:3625–3635
79. Ivarsson M, Gehör S, Holm NG (2008) Micro-scale variations of iron isotopes in fossilized microorganisms. Int J Astrobiol 7:93–106
80. Toporski JKW, Steele A, Westall F, Thomas-Keprta KL, McKay DS (2002) The simulated silicification of bacteria – new clues to the modes and timing of bacterial preservation and implications for the search for extraterrestrial microfossils. Astrobiology 2:1–26
81. Herbold DR, Glaser L (1975) *Bacillus subtilis* N-acetylmuramic acid L-alanine amidase. J Biol Chem 250:1676–1682
82. Leduc M, Kasra R, Van Neijenoort J (1982) Induction and control of the autolytic system of *Escherichia coli*. J Bacteriol 152:26–34
83. Ferris FG, Fyfe WS, Beveridge TJ (1988) Metallic ion binding by *Bacillus subtilis*: implications for the fossilization of microorganisms. Geology 16:153–157
84. Lalonde K, Mucci A, Ouellet A, Gélinas Y (2012) Preservation of organic matter in sediments promoted by iron. Nature 483:198–200
85. Ivarsson M (2006) Advantages of doubly polished thin sections for the study of microfossils in volcanic rock. Geochem Trans 7:5
86. Ehrlich HL (1996) Geomicrobiology, third edition, revised and expanded. Dekker, New York
87. Emerson D, Moyer CL (2002) Neutrophilic Fe-oxidizing bacteria are abundant at the Loihi Seamount hydrothermal vents and play a major role in Fe oxide deposition. Appl Environ Microbiol 68:3085–3093
88. Boyd TD, Scott SD (2001) Microbial and hydrothermal aspects of ferric oxyhydroxides and ferrosic hydroxides: the example of Franklin Seamount, Western Woodlark Basin, Papua New Guinea. Geochem Trans 7
89. Ivarsson M, Broman C, Gustafsson H, Holm NG (2015) Biogenic Mn-oxides in subseafloor basalts. PLoS One 10(6):e0128863
90. Ivarsson M, Broman C, Lindblom S, Holm NG (2009) Fluid inclusions as a tool to constrain the preservation conditions of sub-seafloor cryptoendoliths. Planet Space Sci 57:477–490
91. Ivarsson M, Kilias SP, Broman C, Naden J, Detsi K (2010) Fossilized microorganisms preserved as fluid inclusions in epithermal veins, Vani Mn-Ba deposit, Milos Island, Greece. Proc XIX CBGA Cong 100:297–307
92. Benzerara K, Yoon T-H, Tyliszczak T, Constantz B, Spormann AM, Brown GE Jr (2004) Scanning Transmission X-ray Microscopy study of microbial calcification. Geobiology 2: 249–259
93. Benzerara K, Menguy N, Banerjee NR, Tyliszczak T, Guyot F, Brown GE Jr (2007) Alteration of submarine basaltic glass from the Ontong Java Plateau: a STXM and TEM study. Earth Planet Sci Lett 260:187–200
94. Schopf JW, Kudryavtsev AB (2005) Three-dimensional Raman imagery of precambrian microscopic organisms. Geobiology 3:1–12
95. Donoghue PCJ, Bengtson S, Dong X-P, Gostling NJ, Huldtgren T, Cunningham JA, Yin C, Yue Z, Peng F, Stampanoni M (2006) Synchrotron X-ray tomographic microscopy of fossil embryos. Nature 442:680–683
96. Cary SC, Campbell BJ, DeLong EF (2004) Studying the deep subsurface biosphere: emerging technologies and applications. In: Wilcock WSD, DeLong EF, Kelley DS, Baross JA, Cary SC (eds) The subseafloor biosphere at mid-ocean ridges, Geophysical monograph series 144. American Geophysical Union, Washington, pp 383–399
97. Smith DC, Spivack AJ, Fisk MR, Haveman SA, Staudigel H (2000) Tracer-based estimates of drilling-induced microbial contamination of deep sea crust. Geomicrobiol J 17:207–219

98. Banerjee NR, Furnes H, Muehlenbachs K, Staudigel H, de Wit MJ (2006) Preservation of microbial biosignatures in 3.5 Ga pillow lavas from the Barberton Green stone Belt, South Africa. Earth Planet Sci Lett 241:707–722
99. Banerjee NR, Simonetti A, Furnes H, Staudigel H, Muehlenbachs K, Heaman L, Van Krankendonk MJ (2007) Direct dating of Archean microbial ichnofossils. Geology 35: 487–490

Manned Submersibles *Mir* and the Worldwide Research of Hydrothermal Vents

Anatoly M. Sagalevich

Abstract The role of deep manned submersibles (DMSs) in scientific research of the ocean is considered. The history of development of DMS is introduced, drawing attention on the steps, generated by submarine accident ("Thresher") and scientific research jumps (hydrothermal vent discovery). Development of the building of DMS in Russia and particularly in P. P. Shirshov Institute of Oceanology, RAS, is considered, concentrating on worldwide research with "Pisces VII" and "Pisces XI" submersibles in 1970–1980s of the twentieth century.

Short description of Mir-1 and Mir-2 design is introduced, as the best 6,000 m DMS in the world.

The introduction of scientific research of hydrothermal fields on ocean bottom, using the Mir submersibles, is done. The methodology of hydrothermal field study, using the Mir submersibles, is described.

Keywords Deep-sea manned submersibles, DMS *Mir*, Hydrothermal vents

Contents

A.M. Sagalevich (✉)
Anatoly Sagalevich, P. P. Shirshov Institute of Oceanology, Russian Academy of Sciences (IO RAS), Nakhimovsky Prospect, 36, 117997 Moscow, Russia
e-mail: sagalev1@yandex.ru

L.L. Demina and S.V. Galkin (eds.), *Trace Metal Biogeochemistry and Ecology of Deep-Sea Hydrothermal Vent Systems*, Hdb Env Chem (2016) 50: 167–194,
DOI 10.1007/698_2015_5019,
Published online: 3 February 2016

> Underwater human observations are the last and most significant link in a long chain of shipboard instrumental researches.
>
> A. Sagalevich

Our understanding of mother Earth goes hand by hand with development of ocean instrumental researches. They radically changed in 1950s of twentieth century, when the large amount of science data about ocean bottom structure was accumulated. These data were obtained by means of echo sounding and with seismic methods. That made it possible for American scientists M. Dietz and H. Menard in 1952–1953 to describe transform faults in the Pacific Ocean for the first time. Continuous seismic profiling systems and magnetic and gravity measurements made it possible for M. Ewing and B. Heezen to make a conclusion about the existence of mid-ocean ridges and to describe ocean rift zones, the length of which is about 60,000 km. On the basis of these data, a fundamentally new theory of Earth constitution was developed based on existence of tectonic plates in constant motion. Implementation of this theory was named Wegener Revolution after great German scientist Alfred Wegener, who had predicted continental drift theory as early as in 1914.

It is also possible to mark several stages in development of biological studies technique and methods, when knowledge about ocean biological resources rose to a totally new level.

At the first stage, ocean biology was studied with the help of shipboard fishing gear, and as a result of multiyear investigations, it was identified that life exists at all depths of ocean. Later combination of traditional biological gear methods with sonar methods and underwater photography allowed gathering totally new information about ocean productivity, biodiversity, and biocommunity distribution. Finally, implementation of satellite remote sensing study made it possible to obtain global maps of bioproductivity distribution over the entire area of the World Ocean.

In line with the development of instruments and methods for collection of information about ocean resources, analytical base was improved, data processing and geological and biological sampling point accurate navigation, and hydrophysical and hydro-chemical measurement systems were created. Evidently information reliability and possibility of its effective use largely depend on study navigational accuracy. Creation and use of navigational satellite systems made it possible to reach ship location accuracy of several tens of meters, and use of hydroacoustic navigation long baseline systems improved navigational accuracy to the first meters with ocean depths of several kilometers.

Improvement and creation of new measuring systems and instruments defined development of system of oceanological information, herewith implementation of microprocessors was very significant, and they allowed development of miniature data-collecting systems with low energy consumption. Implementation of these measuring systems made it possible to make measurements during sampling identifying interrelation of animal existence in natural environment with geological conditions and hydrophysical and hydro-chemical parameter distribution.

In recent decades, there discerned a trend to detailed studies in certain regions of ocean, which are of principal interest from scientific and practical point of view. With currently available amount of data about ocean biology, only detailed scientific studies in local areas can provide totally new information entirely revealing essence of suboceanic phenomena. Identification of biological resource partitioning behavior and the task of planned use thereof defined implementation of new instrumental methods, which make it possible for a researcher to observe the habits of animals directly in natural environment. Such unique possibility was provided to science by deep manned submersibles (DMSs). Man-operated and freely moving DMSs in water column and near bottom equipped with modern instruments evolve into a perfect research tool opening totally new ways during study of ocean depths [1].

Effectiveness of DMS use for resolving scientific problems is defined by their technical specifications like hull hydrodynamic performance; maneuvering ability; view-port observation; scientific, navigational, and special equipping, etc. DMSs are rather restricted in underwater motion, which is defined by their small energy margin and low rate of sailing. Therefore, DMS operation effectiveness to a large extent depends on correct combination of their use with other scientific methods and instrumental studies making it possible to perform reconnaissance operations and obtain information for selection of narrow-local areas, in which detailed studies with the help of DMS offer the greatest promise.

The highest effectiveness was reached by combination of deep manned submersible with deep towed vehicle equipped with side sonars, acoustical profilers, measuring sensors, and photo and television systems. Operation with help of deep tows makes it possible to cover large areas of ocean bottom with studies and identify anomalous regions to be studied with DMS. Just such combination of towed and manned vehicles allowed to provide during latest forty years the most outstanding discoveries in the sphere of study of hydrothermal fields on ocean bottom, beginning with the discovery at Galapagos Rift in 1977 and to date [2].

Recently scientists started to use remotely operated vehicles for the study at great depth. However, practice showed that effectiveness thereof is much lower as compared to manned vehicles due to much longer time needed for various operations near bottom as well as presence of a cable connecting the vehicle with the ship and generating many problems under unfavorable weather conditions. In addition, operation of remotely operated vehicles assumes the use of dynamic positioning system on support ship, which results in long-time operation of propulsion system and consequently high fuel consumption in the case of deep-water operations. Tables 1 and 2 specify statistic data obtained on the basis of several remotely operated and Mir manned vehicle operation analyses. These data demonstrate quite a number of advantages of manned vehicles as per time and energy consumption during research studies as compared to remotely operated vehicles. Besides one of the main advantages of DMS is direct participation of a scientist in scientific observations being under water and controlling study process. Herewith one cannot also exclude emotional component which is constantly present during direct visual observations and often is the determining factor in making discoveries.

Table 1 Effectiveness of the use of the manned submersibles and ROV

Vehicle type	Searching of object after the bottoming	Sampling		High-quality video	Measurements (physical, chemical)	Visual observation
		Simple (rock, single animal)	Complicated (fluid from smoker, slurp-gun probe, etc.)			
DMS (HOV)	<30 min	5–10 min	<30 min	100% continuous based on direct observation	100% trustworthy	100% direct
ROV	60–90 min	40–60 min	No experience: too complicated	20% - fragmentary videorecords, selected through monitor	Measurements are incorrect during working thrusters (too noisy)	30–40% on TV screen

Table 2 The support vessel's fuel consumption during underwater operation

Vessel	Vehicle type	Vessel mode	Fuel consumption (daily)
RV "Akademik Mstislav Keldysh"	DMS "Mir"	Free drift, episodic movements at the speed of 3–4 knots	3–4 t
AOS (1,500 t)	ROV	Dynamic positioning – constantly working engines	8–10 t

Total: ROV – 20% efficiency of bottom time relatively DMS (HOV)

Creation of DMS and use thereof for scientific purposes have rather a long history of almost 70 years. During that period, DMS went a long way of technical improvements from the first cumbersome bathyscaphs to modern compact, light, and maneuverable vehicles, which can operate using as support vessel common scientific research ships equipped with special launch-and-recovery systems.

1 Development of Human-Occupied Submersibles and Expansion of Scientific Researches with Their Use

Bathyspheres were prototype of modern manned vehicles; they were lowered from shipboard on wire. American researcher William Beebe was the first to directly study deep water from a bathysphere in 1930s [3]. He performed biological observations in water column and near bottom up to 1,000 m depth and deeper. In 1934 Beebe together with O. Barton reached the record depth of 923 m. W. Beebe expressed his impression about animal visual observations in water column by the concise phrase: "As I peered down I realized I was looking toward a world of life almost as unknown as that of Mars" (Fig. 1). The deepest submergence in a bathysphere was made by O. Barton in September 1948 – to 1,496 m. On 26 October 1948 in Eastern Atlantic near Cape Verde Islands, outstanding Swiss scientist and bathyscaph designer A. Piccard and French biologist T. Monod made the first ever deep submergence in the full-authority vehicle – FNRS-2 bathyscaph to 1,515 m depth. This date is accounting as the beginning of era of human-occupied submersibles in ocean study [4].

Bathyscaph era extends back over more than 30 years. Bathyscaphs played a significant role in the development of ocean research, especially biological studies. A robust steel sphere is the main composite member of the bathyscaph; it is mounted to a cumbersome metal float filled with petro. With dipping light liquid (petrol) partially is replaced with water, due to that bathyscaph buoyancy reserve decreased and it submerged. The vehicle came up due to jettisoning the hard ballast – metal beads. Bathyscaph horizontal motion was provided by two reversible motors located at the sides of the petrol float. Ballast and propulsion systems were controlled from inside of a steel sphere. Bathyscaph was equipped with external lighting and underwater communications system.

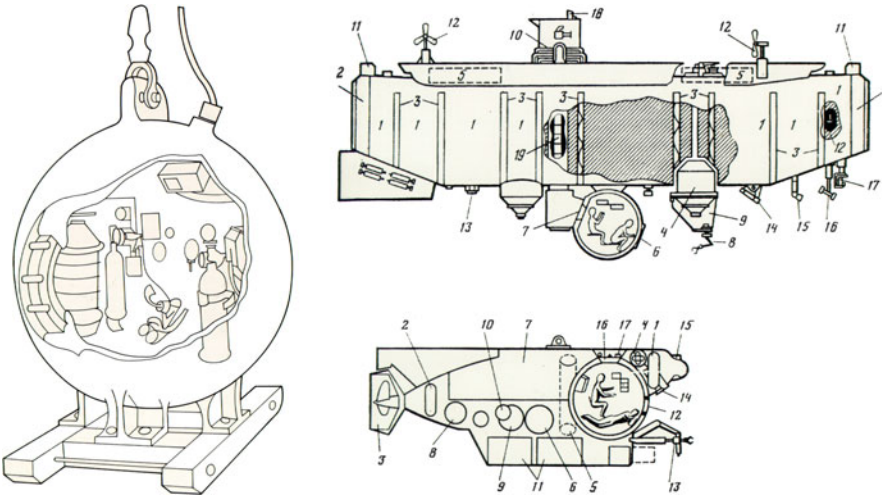

Fig. 1 Three generations of deep manned vehicles: (**a**) bathysphere of W. Beebe, (**b**) bathyscaph, (**c**) contemporary submersible

As compared to modern DMS, bathyscaphs suffer from a number of essential faults; big dimensions and weight (up to 300 t) were such faults, and they made it difficult to use the vehicles from shipboard and caused need to deliver the vehicles to submergence site mostly by towing operation. Besides, bathyscaph operation needed availability of several hundred tons of petrol on board a ship for ballast system operation. First, petrol on board needs strict safety measures; second, its use doesn't contribute to ocean cleanness. Poor maneuvering ability of bathyscaphs related to big dimensions and absence of variable ballast system, which could allow prompt and accurate control of vehicle buoyancy, is another fault of bathyscaphs.

However, during long time, bathyscaphs remained the sole technical means capable to submerge to maximum depth in the ocean. With help thereof in succession, submerge depth records were made, in the progress of which scientific observations were performed. On 23 January 1960, the bathyscaph "Trieste" made the sole-ever submergence of a manned vehicle to Mariana Trench to 10,916 m depth [5] (Fig. 2). The submergence was supported by the Swiss scientist J. Piccard (A. Piccard's son) and American naval officer D. Walsh. Upon that historical submergence, bathyscaph era lasted for more than 20 years more in spite of introduction of new-generation vehicles. Farewell ceremony for the last vehicle of bathyscaph first generation – Trieste II bathyscaph – took place in 1984 in San Diego, and then the bathyscaph was handed over to NAVY Museum in Washington D.C. Another well-known bathyscaph contributed much to science; French Archimede finished to submerge in 1974 upon completion of FAMOUS expedition and studied rift zone of the Mid-Atlantic Ridge in the region of Azores islands [6]. Currently "Archimede" is in the Maritime Museum in the French Cherbourg city.

Fig. 2 Bathyscaph *Trieste*

In 1963 American nuclear-powered submarine (NPS) "Thresher" met an accident and went down at 2,800 m depth. Trieste bathyscaph was the only underwater vehicle capable to find wreckage of the NPS. Preparation and delivery of Trieste to the accident site took two months. The search was complicated also by necessity of Trieste repair after several fruitless submergences. The bathyscaph was towed to the USA coastal base as its sizes and weight didn't allow hoisting it for on-site repair. Besides Trieste in actual fact had no equipment for search, nor there was such search and navigational instruments at that time. Thus, vehicle bottom orientation was made with flags of various colors placed by bathyscaph pilots during submergences [7].

Encountered problems stimulated US leading companies related to underwater technology to develop new manned vehicles and equipment thereof. Herewith initially the task of miniature underwater vehicle development was made so that such vehicles could be transported both on board a ship and by air.

In 1962 syntactic – hard buoyant deep-water – material was invented, which is a composite of glass microballoons and epoxy resin. Implementation of this material made it possible during a number of years to develop a series of miniature underwater vehicles. In 1964–1970 in the USA, there were constructed DMSs "Aluminout" (4,500 m), "Alvin," "Sea Cliff," and "Turtle" (2,000 m), Star vehicle series (up to 1,300 m), and others. In Canada, construction of Pisces DMS series

(up to 2,000 m) started. French diving saucer Denise (450 m) was operated in the ocean. During 1960–1970 in the world, there were constructed several tens of underwater vehicles designed mainly for shallow and mean depths [4].This owes to the fact that technical capacity of the time was more appropriate for construction of such types of vehicles. Firstly, construction of the hulls therefore was easier and cheaper as compared to the hulls of vehicles designed for maximum depths of the ocean. Secondly, then existing deep-water hard buoyancy materials ensured submergence to 4,000 m only. Thirdly, those vehicles were relatively cheap and fully met demands of the time.

Specialists came to the conclusions that maximum submergence depth in the ocean was reached and the work objective was not record breaking, but provision of detailed studies in ocean. Later construction of new-generation manned underwater vehicles came to the front. This owes to doubtless advantages of such type of vehicles over bathyscaphs. Firstly, the vehicles without big floats are much lighter, of smaller sizes, and consequently more mobile and maneuverable. Secondly, their operation is easier. For example, if bathyscaph preparation for the next submergence needs 2–3 days even with good technical condition of all systems, a common vehicle needs only 8–10 h for battery charging. Besides underwater vehicles of 10–15 t weight can be delivered to work site within several hours by air.

Simultaneously with vehicle design, improvements of new equipment therefore were developed: outside-mounted photo cameras in pressure-proof casings, all-around scanning sonar making it possible to detect targets of bottom, multidegree-of-freedom manipulators, etc. In 1964 there appeared the first version of hydroacoustic navigation long baseline system, which made real revolution in DMS underwater orientation, thus making it possible to provide continuously accurate positioning of the vehicle under water. In the early 1970s, there were introduced the first underwater television cameras, initially monochrome ones, and in the mid-1970s colored ones. Various sampling devices were developed, and they were installed on underwater vehicles. DMS transformed to a sort of underwater laboratories providing a researcher with possibility of not only visual observation but also complete environmental study at various depths.

In 1970s the trend to vehicle further miniaturization and their operating depth increase was observed. In 1971 in France, construction of Cyana vehicle (3,000 m, 8.5 t) was completed, which contributed much to science in 1970–1980. In 1973 DMS Alvin is coming again into operation upon modernization. Replacement of the steel sphere with the titanium one and upgrade of the majority of the elements and units increased Alvin operating depth to 4,000 m. Modernization of Alvin was made after its accidental unmanned flooding in 1969 at the depth of 800 m and its recovery in 8 months [4]. Upon its second birth, Alvin made the most significant contribution to science of all other DMSs in the world. With its help, the most outstanding discoveries were made in the sphere of study of hydrothermal fields on ocean bottom.

Creation of DMS of new types – miniature, light, and maneuverable – stimulated numbers of new scientific discoveries in deep ocean; the 1970s was remarked by a number of uncommon experiments with the use of DMS for geological-geophysical

and biological studies of mid-ocean ridges. The providing of such expeditions was encouraged by development of lithosphere plate tectonics, which made real revolution in modern geology. The expeditions to mid-ocean ridges located on plate interfaces were to provide confirmation of main conceptions of this theory. Manned vehicles' visual observations through the view ports were the most important part of used method complex. Already mentioned FAMOUS project organized by US and French scientists on 14°N region of mid-ocean ridge [6] was the first expedition of such type. In the progress of that expedition, emergences of Cyana, Alvin, and Archimede for the first time became the part of an extensive set of studies including both traditional geophysical and geological methods of ocean bottom mapping and deep towed vehicle operation. FAMOUS expedition, which managed to execute complete geological and biological studies and obtain unique results, clearly demonstrated capability of manned submersibles.

In 1976 in the region of Galapagos Rift, accumulation of unusual animals (large bivalve mollusks) was photographed. The next year, Alvin DMS was involved in research, and in the same region at the depth of 2,500 m, phenomenal observations were made, which identified existence of hydrothermal vents and quite unusual fauna around them [2]. Discovery of hydrothermal field laid the foundation of a number of remarkable studies in various regions of the World Ocean – the most outstanding discoveries in oceanology in twentieth century.

In 1979 at 21°N of East Pacific Rise for the first time, black and white smokers with fluid outlet temperature to 355°C, very high content of hydrogen sulfide, plenty of new species of hydrothermal fauna, and improbably high biomass were observed [2]. This discovery was second in significance after discovery of the first hydrothermal vents at Galapagos Rift.

In the 1970s construction of DMSs continued; they were designed for shallow and mean depths. Perry Submarine (USA) and Bruker Physik (Germany) manufactured series of underwater vehicles of lockout type with diving compartment. These vehicles were designed for operation at shallow depths (to 350 m) and provided divers with way out.

Series of eleven Pisces vehicles designed for depths of 1,000–2,000 m was manufactured by Canadian International Hydrodynamics Company. Two of them – Pisces VII and Pisces XI, both with operating depth of 2,000 m – were constructed under the order of the Academy of Sciences of the USSR, and for many years, they were operated by Shirshov Institute of Oceanology, RAS, for scientific research and underwater technical operations in various regions of the World Ocean [1] (Fig. 3).

Construction of manned vehicles in the USSR started in 1960s. The first deep manned submersible Sever 2 (length of 13 m, weight of about 24 t) was constructed in 1969 under the order of the Ministry of Fisheries of the USSR; it operated mainly for the exploratory fishing purpose. For the same purpose were used TINRO-2 (operating depth of 400 m) and BENTOS-300, which can be rather classified as underwater floating laboratory due to its large sizes and tonnage (600 t). All three mentioned vehicles were duplicated and operated during many years for exploratory fishing purpose. They were occasionally used also for biological and geological studies.

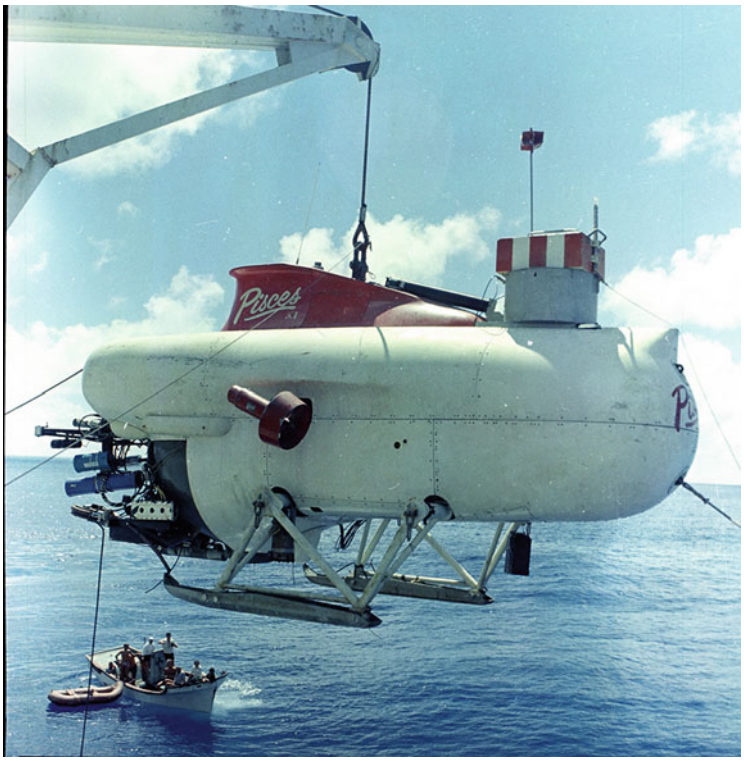

Fig. 3 Pisces XI submersible launching to the water

In 1978 construction of DMS Argus designed in experimental design office of oceanological engineering of the Institute of Oceanology, Academy of Sciences, USSR, was completed. Maximum depth of the vehicle was 600 m, weight of 9 t. It was designed under technical specification, in fact completely identical to the specification of Pisces IV, Pisces VII, and Pisces XI corrected to operating depth of 600 m and designed for use of only domestic components. The vehicle was equipped with hydroacoustic navigational system, outside-mounted photo camera, and television system and six degree-of-freedom manipulator. The vehicle made it possible to perform special hydrophysical measurements.

Up to 1981, Argus was used for oceanological research on the Black Sea and based in the southern department of the Institute of Oceanology, Academy of Sciences, USSR, in Blue Bay (Gelendzhik). Since 1981, when the Institute's new ships *Vityaz* and *Rift* equipped with launch-and-recovery system for DMS were put into operation, Argus operated in various regions of ocean mainly from board those ships. Argus was used for scientific research till the mid-1990s and made 768 dives.

However, domestic research with DMS involvement came to the real international level with purchase of Pisces VII and Pisces XI. These vehicles were installed on big research vessels (RV) equipped with special launch-and-recovery

systems – initially on RV *Akademik Kurchatov* (Pisces XI) and RV *Dmitry Mendeleev* (Pisces VII) – and since 1982 both vehicles based on RV "Akademik Mstislav Keldysh." With the putting of Pisces vehicles into operation, polygon methods of studies started to be used. It made possible to study in details certain regions of the ocean. The study of the Baikal Lake intercontinental rift zone, as well as rift zones of the Red Sea, Reykjanes Ridge, and Gulf of Aden, made it possible to identify them as low-velocity spreading ocean rift zone development. The study of underwater mounts of Indian and Pacific oceans showed that many of them are coated with ore cover enriched with various metals. Hydrophysical and hydroacoustic studies as well as biological observations were the purpose of several expeditions. These expeditions accumulated a large number of photos, video records, geological and biological samples, measurement materials, etc. [8].

With the use of Pisces vehicles, the first domestic studies of hydrothermal fields were performed. In 1986 Pisces VII DMS was involved in methane sipping study on the bottom of the Sea of Okhotsk, and Pisces XI participated in the study of black smokers on Juan de Fuca Ridge at the northeast of the Pacific Ocean and in Guaymas Basin in Gulf of California.

Multiyear operation in ocean with the use of Pisces VII and Pisces XI vehicles made it possible to develop a big complex of new methods providing effective operation of DMS for scientific research of various brands of oceanology. In 1982 for the first time ever on Reykjanes Ridge, underwater studies were executed with two Pisces DMSs simultaneously. These operations demonstrated high effectiveness of such methods, which later was used during many years in the course of research and underwater technical works with Pisces vehicle involvement and later with Mir-1 and Mir-2 involvement. These methods developed by Russian scientists were later implemented by foreign researchers also.

Discovery and first studies of hydrothermal fields challenged development of new manned vehicles designed for deep water. Indeed in the late 1970s, only Alvin could reach the depth of 4,000 m. Only Trieste remained of all bathyscaphs; its operation was related with a mass of technical and financial problems. It was clear that new vehicles are needed, which could submerge to the depths of ocean rift zones, subduction zones, and other sites, depth of which was unreachable for then existed DMS.

In early 1980s, leading oceanological countries started creation of new-generation vehicles with operating depth of 6,000 m. During a decade, five modern 6,000 m vehicles were manufactured: Nautile in France (1985), Sea Cliff in the USA (1986), Mir-1 and Mir-2 in USSR (1987), and Shinkai 6500 in Japan (1989). These vehicles contributed much to the development of deep-water studies of ocean, especially of hydrothermal field study. Table 3 specifies main technical characteristics of 6,000 m vehicles produced in the 1980s of the twentieth century.

Table data demonstrate a number of essential advantages of Mir over foreign vehicles: battery large energy capacity is the most important advantage, which makes it possible for Mir to spend under water twice as much time as compared to other vehicles and to significantly improve study effectiveness.

Table 3 Technical data of the modern submersibles with an operating depth of 6,000 m, built in the 1980s

Vehicle basic data	Nautile	Sea Cliff	Mir-1, Mir-2	Shinkai 6500
Dry weight (tons)	18.5	29.0	18.6	25.2
Length (m)	8.0	8.6	7.8	8.2
Width (m) (with the lateral motors)	2.7	3.6	3.8	3.6
Height (m without cabin)	3.45	3.4	3.0	3.2
With cabin	–	–	3.45	–
Energy reserves (kWt/h)	50	60	100	55
Life support (man/hours)	390	300	246	380
Maximum speed (knots)	2.5	2.0	5.0	2.5
Buoyancy reserve (from the surface) (KGs)	200	250	290	200
Crew	3	3	3	3
Diameter of the main sphere (m)	2.1	2.1	2.1	2.0
Pressure sphere material	Titanium alloy	Titanium alloy	Nickel steel	Titanium alloy
Battery type	Lead-acid		Ni-Cd	Silver-zinc
Year of construction	1985	1986	1987	1989

Sea Cliff was decommissioned in 1998, and only four of the abovementioned 6,000 m vehicles currently operate. Just these vehicles and Alvin during the second half of the 1980s and in the 1990s contributed much to the study of hydrothermal fields on ocean bottom.

Development of modern deep manned submersibles is technically a complicated and very expensive process. Mentioned above 6,000 m vehicles were produced for scientific research in deep ocean, and one of the main tasks to be resolved with the help of these vehicles was the study of hydrothermal fields. Currently it is also under consideration in leading oceanological countries as the task of high state significance. Therefore, in the 1980s, France, the USA, Japan, and USSR allocated funds from state budgets for the development of deep manned submersibles capable to submerge at 98% of World Ocean area.

With the help of Mir-1 and Mir-2 Russian vehicles, multiple studies, mostly international ones, were carried out, during which leading oceanologists-scientists and submarine experts of the world leading countries submerged. With their assistance, a large scope of scientific studies in the World Ocean was performed including hydrothermal field research [9]. In 1994 these vehicles were acknowledged by the US Technology Development Center as the best ever developed deep manned submersibles in the world.

Mir-1 and Mir-2 were put into operation in early 1988 (Fig. 4). At that time, the first major expedition to TAG hydrothermal field (26°N Mid-Atlantic Ridge), which will be mentioned below, was carried out.

After creation of five abovementioned 6000 m vehicles in the 80-s of XX century the next deep manned submersibles were put in the operations only in 25 years.

Fig. 4 Mir-1 and Mir-2 submersibles aboard of RV *Akademik Mstislav Keldysh*

In 2012 Deepsea Challenger single-seat vehicle was created under the supervision of James Cameron, who submerged to Mariana Trench in this vehicle to the depth of 10,989 m. That was the only solo submergence to ocean maximum depth, upon which the vehicle was handed over to Woods Hole Oceanographic Institute and wasn't used any more. Also in 2012 Chinese scientists tested manned vehicle Jaolong with an operating depth of 7,000 m. Currently this vehicle provided research in the Pacific Ocean.

However, the Mir-1 and Mir-2 remain the best manned vehicles of that class, with their help such wide spectrum of deep-water studies and special underwater technical operations performed as with no other DMSs in the world.

2 Development of Mir-1 and Mir-2 Deep Manned Submersibles

In May 1985, a contract on creation of a deep manned submersible with operating depth of 6,000 m was signed between Rauma-Repola Finnish company and P. P. Shirshov Institute of Oceanology of Academy of Sciences of USSR. Contract sign-off was preceded by multiyear work on search for a foreign partner capable to create a modern DMS. This work started in 1976 upon completion of construction and acceptance by the Institute of Oceanology of Pisces VII and Pisces XI built in Canada. The search for a partner was carried out by Professor I. E. Mikhaltsev who

later headed the team on Mir-1 and Mir-2 development. Initially, in 1979, the contract on development of 6,000 m vehicle was signed with Canadian underwater vehicle company headed by the Pisces designer Mack Thompson. However, that contract was not completed, and then a partner was searched in other countries. In 1979–1982, negotiations were held about the development of a 6,000 m vehicle with representatives of France, Sweden, and Switzerland, but due to various reasons, final agreement was not reached. In 1982 negotiations with representatives of Rauma-Repola Finnish company started; they showed high interest in the building of the vehicle with 6,000 m operating depth. During 3 years, Finnish engineers studied world experience of manned vehicle development, studied documentation of Pisces vehicles available in the Institute of Oceanology, and carried out technical examination. During that period, the specialist of the Finnish company discussed with employees of the Institute of Oceanology technical solutions possible for realization during vehicle construction and held negotiations with foreign companies about purchase of structural materials and special equipment. At the same time, Rauma-Repola company carried out research work on development of nickel-rich high-strength steel for the production of vehicle's pressure hulls. In spring of 1985, the Finnish company was ready for the signing of the contract, which included delivery of one DMS with operating depth of 6,000 m and rescue vehicle on the basis of underwater remotely operated vehicle in case of underwater accident. However, after special studies, Finnish engineers came to the conclusion that they are not able to develop a rescue underwater remotely operated vehicle with operating depth of 6,000 m. The partners came to the agreement to replace the rescue vehicle with the second manned vehicle, identical with the main one both as per technical arrangement and hardware equipment. Thus, the contract included Mir-1 and Mir-2, two deep manned submersibles.

Mir vehicle designing started immediately upon contract signing in May 1985. Semispheres for pressure hull of high-strength nickel steel were casted in Rauma-Repola company. At the same time, the development project for Mir vehicles was in progress. The project head was Professor I. E. Mikhaltsev, and his deputy was Doctor A. M. Sagalevich. Project engineering group from the Finnish side was headed by S. Ruohonen. Main conceptions of the "Mir" vehicle technical arrangement were introduced during development period, they were improved in the progress of construction, and some of them were changed in principle. Besides, the Finnish party in accordance with the contract specification and agreement with the customer placed orders for scientific, navigational, and special equipment for Mir at various companies of Europe and the USA. This process was rather complicated at that time. There was valid embargo for high technology supply to the Soviet Union, and not all companies could supply hardware for the soviet deep-water vehicle. In addition test complex was developed for Mir DMS pressure hull and all component and equipment high-pressure testing. The complex included two test high-pressure chambers: the bigger one of 2.5 m diameter designed for operating pressure of 750 atmospheres and the chamber of smaller diameter with operating pressure of 1,100 atmospheres, also instruments for tested items strength characteristics analysis.

In May 1986, the development project for Mir DMS was completed. By that time high-strength nickel steel development was finished, and two first semispheres were casted. Later casting and semisphere machining technology was improved.

In September 1987, construction of Mir-1 and Mir-2 was close to completion. RV *Akademik Mstislav Keldysh* arrived to Mantyluoto port for modernization needed for support of Mir DMS operation in ocean. Installation of launch-and-recovery system for Mir vehicle, location thereof on the ship, and installation of equipment needed for Mir operation provision were also the part of the vehicle supply contract.

In late October, ship modernization was completed, and Mir vehicles were tested in a pool specially constructed in one building of the company. On 10–-11 November, first trials were conducted in the Baltic Sea at the depth of 70 m. All Mir-1 and Mir-2 vehicle sea trials were supported by the same crew: P. Laakso Finnish delivery pilot, A.M. Sagalevich acceptance pilot, and I. E. Mikhaltsev head of the project. The first sea tests were successful, vehicles demonstrated good operational performance, and the ship started for deep-water tests (Fig. 5). The following stage – submergence to 1,100 m – was also successful, although a number of technical deficiencies were detected, which nevertheless didn't impact submergence safety. The submergences were carried out in the Eastern Central Atlantic. Later deep-water submergence to operating depth of 6,000 m lied ahead. These submergences completed the cycle of Mir vehicle sea trials. Test region was selected in accordance with weather conditions and on the basis of tight time considerations: 1987, contract last year, was close to end. The first dive of Mir-1 in coordinates 17°32′N, 30°02′W took place on 11–12 December. It lasted for 14 h

Fig. 5 RV *Akademik Mstislav Keldysh* with two Mirs aboard

and was carried out very slowly, with all safety measures compliance. Mir-1 vehicle reached the depth of 6,170 m. Mir-2, the second vehicle, was tested in 12 h upon Mir-1 had been taken aboard. Submergence also lasted for 14 h in accordance with the already developed and tested scenario; Mir-2 reached the depth of 6,120 m. In the course of testing, a number of major deficiencies were detected: failure of high-pressure pumps; pumping water ballast, at depths over 5,000 m; inoperable condition of echo sounder and hydroacoustic navigational system; and many others. Vehicles were accepted by the customer under provision that all deficiencies would be fixed within the period of warranty repair which was supposed on autumn of 1988. First expeditions were carried out with all detected faults. Herewith vehicle submergence maximum depth was restricted to 4,000 m.

In autumn of 1988, RV *Academic Mstislav Keldysh* with Mir-1 and Mir-2 vehicles on board arrived to Finland again. Rauma-Repola fixed almost all deficiencies on DMS and introduced significant changes to that part of the ship where underwater vehicles were located. Upon warranty repair, Mir vehicles were completely ready for deep-water operation in expeditions [9].

3 Mir-1 and Mir-2 Deep Manned Submersibles: Arrangement and Technical Specifications

The problem of development of modern DMS – miniature, light, maneuverable, having sufficient energy capacity – was resolved by means of calculation, selection of appropriate structural materials, and arrangement of units and elements into an integral structure complying with technical requirement data. A number of structural materials and technical solutions were implemented for the first time in the world practice of deep-water engineering development [10]. Mir vehicle manned sphere was made of nickel high-strength steel with proof stress about 1,700 N/mm^2. Wall thickness is 40 mm. There are three view ports in the sphere: the central one with inner diameter of 200 mm and two side ones, each of 120 mm diameter.

Mir vehicles are the only ones of 6,000 m vehicles with a big central view port. This makes significant advantages with vehicle piloting (good view), scientific studying, and underwater cinema and video shooting by cameras from inside sphere and a number of special underwater operations.

Descent-accent system is one of the main DMS systems. In Mir hardware, it is separated into two complicating systems: main ballast system and vehicle accurate ballasting or variable ballast system. The main ballast system consists of two plastic tanks with total capacity of 1.5 m^3 which are filled with water on the surface while submerging and are aired with breaking the surface (on surface also). This system when not filled provides the vehicle with buoyancy over 1.5 t. When the system is filled with water, the vehicle buoyancy is close to zero. Gentle control of vehicle's buoyancy is controlled by variable ballast system.

Vehicle variable ballast system includes three ballast spheres: two fore ones and aft one. This system controls vehicle's buoyancy in the range ±300 kg. With help thereof, it is possible to control descending and ascending speed within the range 0–30 m/min^{-1} and ensure DMS keeping at any level in water column. Total amount of water ballast pumped into the ballast spheres is 1 t. Water ballast is pumped out of the spheres by high-pressure hydraulic pump. The pump provides water ballast pump-out capacity of 8 L/min at the depth of 6,000 m.

The vehicles are equipped with another, reserve high-pressure pump activated in case of the main one failure. Both pumps are driven by different hydraulic systems. Vehicle ballast trimming is made with the trimming pump pumping water from the aft sphere to the fore ones and back. It is necessary to remark that Mirs are the only deep submersibles in which seawater is used as ballast for descending and ascending. The ballast system of other vehicles is made in accordance with bathyscaph principle: descending due to water inlet to the ballast sphere or for the account of advanced negative buoyancy and ascending due to jettison of hard ballast.

Manned and ballast spheres are linked into integral structure by a frame of high-strength aluminum alloy. The frame is supported by ski made in accordance with special technology with use of syntactic foam, covered by several layers of fiberglass.

Frame load-bearing elements are insulated from main and ballast spheres by special plastic protectors of high-strength insulation material preventing electrolytic corrosion in seawater. Vehicle power supply is made on the basis of nickel-cadmium batteries with capacity of 700 Ah. Two sets of the batteries are installed on the vehicle. One of them with voltage of 120 V with energy margin of 84 kW/h is intended for vehicle operating systems, and another one with voltage of 24 V with energy margin of 17 kW/h is for communication, navigation, and scientific equipment supply as well as for hydraulic and ballast system valves.

Vehicle propulsion system and ballast pump are hydraulically driven. Three hydraulic systems of the vehicle are equipped with independent power units driven by electric motors. The first system supplies propulsion system and the main ballast pump. Ballast system valves, reserve ballast pump, trim pump, manipulators and all hydraulic drives of external moving mechanism are the consumers of the second hydraulic system. The third emergency hydraulic system is intended for jettison of some submersible's parts in case of accident. If the electric motors of the first two hydraulic systems are supplied by the main battery of 120 V voltage, electric motor of the third system of 0.5 kW power can be supplied from both the main battery of 24 V voltage and the emergency one of 24 V voltage installed inside manned sphere.

Vehicle propulsion system includes three hydraulic motors with propellers and nozzles. Main thruster with electric motor of 12 kW power is located in stern part of the vehicle and has a nozzle turning in the range ±60° in horizontal plane. It can accelerate the vehicle to the speed up to 5 knots. Two side thrusters, of 3.6 kW power each, can synchronically turn in the range of ±90° from its horizontal position.

By combining all three thrusters' speed and turns, the pilot can rather flexibly control the vehicle in motion near ground or bottom objects of complex

configuration. All three thrusters are controlled by one joystick. Such propulsion system allows rather easy maneuvering of the vehicle, which is especially important in case of operation in complex relief conditions.

Good hydrodynamic performance of the vehicle is provided by bulb streamlined fairing. The hull is made of a special multilayer syntactic-based material plastered on both sides by several layers of Kevlar epoxy. Due to the use of this light but high-strength buoyant material, the vehicle has additional positive buoyancy of about 100 kg.

The system of emergency ballast is made in the form of two fiberglass containers, filled with magnetic shots. It is held in the lower open part of containers with the help of electromagnets powered by the battery of 24 V and – in case of its disconnection – by emergency battery. Total mass of emergency ballast is 300 kg.

In case of emergency, the vehicle can jettison the main and side thrusters, manipulator wrists, wing, and lower battery box of 1.1 t mass. The vehicle is equipped with emergency buoy. It has detaching hydraulic drive and breaks surface carrying wire line of 8,000 m length.

Life support system is constructed in accordance with scheme conventional for underwater manned vehicles: oxygen is delivered to the cabin from high-pressure metal balloons, and carbon dioxide is absorbed by an absorbent – lithium or sodium hydroxide. Besides, cabin atmosphere is dried with the use of silica gel.

Mir vehicles are equipped with modern navigation and communication systems and big complex of scientific research instruments including shipboard and underwater communication system, hydroacoustic navigation long baseline system, short-range all-around scanning sonar of high resolution, echo sounder which can operate as long-range sonar, hydrophysical and chemical sensors, three-component magnetometer, radiometer, and other instruments. Navigation and measuring complex is made as an integral system of data collection with integral system of registration.

It is necessary to specially mention sampling system, the basis of which is two identical seven degree-of-freedom manipulators and adjustable grip force of fractional weights to 80 kg. Manipulator hands can take geological tubes of 40 cm length, special dip nets for biological sampling, self-shutting sediment, bacterial mat sampler, etc. Suction device can perform biological sampling without damages to five tanks, of 2 L capacity each.

Modern color television cameras with high resolution allow video shooting on professional level. Vehicles are equipped with high-resolution digital photo cameras.

Mir vehicles are equipped with powerful underwater lighting including the lights of various powers. Tables 4 and 5 specify technical specifications of hardware and equipment installed on Mir-1 and Mir-2 vehicles.

Mir vehicle capability – their endurance, maneuvering ability, scientific and navigation equipment – makes it possible to resolve wide range of tasks during deep-water study in ocean. This is confirmed by multiyear operation of vehicles which resulted in a large amount of scientific data, which made invaluable contribution to Russian and world science [9].

Table 4 Technical specification of scientific measuring equipment

NN	Measuring parameter	Range	Accuracy	Manufacturing data
1.	Neil Brown's probe			
	N 01-1126			1986
	N 01-1127			1986
1.1.	Temperature	−3°–32.77°C	±0.002°C	
1.2.	Conductivity	0.00–65.535 mmho/cm	±0.002 mmho/cm	
1.3.	Pressure	0.00–6,553.5 dBar	±0.3 dBar	
		0.0–6,431 m	±3 m	
1.4.	pH	0–10 pH	±0.002 pH	
1.5.	Oxygen	0–20 mL/L	±0.015 mL/L	
2.	Speed of sound	1,400–1,600 m/s	0.2 m/s	1986
3.	High-temperature sensor (Mir-1)	0–500°C	1°C	1994
4.	Autonomous high-temperature sensor	15–304°C	0.3°C	1995
	The number of counts 1,800			
	Intervals 0.5 s–4.8 h			
5.	Autonomous high-temperature sensor	152–416°C	0.3°C	1995
	The number of counts 1,800			
	Intervals 0.5 s–4.8 h			
6.	Light scattering detector (Mir-2)	0–100 mg/L	0.01%–~3 mg/L	1996
		0–33 mg/L		
7.	Three-component velocity meter (Mir-1)	0–2 m/s	1.5%	1997
		0–3 m/s	2%	

4 Study of Hydrothermal Fields with the Mir Deep Manned Submersibles

Currently about 200 regions with bottom hydrothermal fields are known in the World Ocean. Majority of them are in the Pacific Ocean. Active hydrothermal vents were found in 12 regions of the Atlantic Ocean. Before 1986, there was an opinion that active hydrothermal vents could exist only in the regions with high spreading lithosphere plate movement, mainly in the Pacific Ocean, but discovery of TAG hydrothermal field made by American scientist P. Rona on Alvin DMS in 1986 overcame this opinion. Currently American, French, English, and domestic scientists actively work on Atlantic hydrothermal fields.

Studies with Mir vehicles were conducted on the next hydrothermal fields of the Atlantic: TAG (four expeditions); Broken Spur (two); Logachev field, 14°45′N MAR (two); Rainbow field (four); Lost City (two); Menez Gwen (one); and Snake Pit (two) [11]. P. Rona participated in the expedition to TAG in 1991; he made two

Table 5 TV, photo, sampling, and navigation equipment of the "Mir-1" and "Mir-2"

NN	Name	Sub	Technical data
1.	TV camera	Mir-1	Resolution – 720 lines
	OE-1930 (PAL)		
2.	TV camera 3500Z (PAL)	Mir-2	Resolution – 400 lines
3.	TV camera SONY-999 (NTSC)	Mir-1	Resolution – 400 lines
		Mir-2	
4.	Digital camera	Mir-2	14 Mpx
5.	Digital camera	Mir-1	14 Mpx
6.	Manipulators (right, left)	Mir-1	Seven degrees of freedom
		Mir-2	$P = 0$–80 kg
7.	Slurp gun	Mir-2	5 glass × 2 L
8.	Bathometer	Mir-1	20 L
		Mir-2	
9.	Bathometer	Mir-1	Sealed, titanium
		Mir-2	2 × 0.7 L
10.	Geological tube	Mir-1	400 mm × Ø 80 mm
		Mir-2	(Up to 4 pcs for each "Mir")
11.	Biological nets	Mir-1	2–3/dive
		Mir-2	
12.	Traps	Mir-1	
		Mir-2	
13.	Cubic frame for plankton accounting (0.5 × 0.5 × 0.5 m)	Mir-1	Visual accounting of the animals
		Mir-2	
Navigation equipment			
14.	Hydroacoustic long baseline navigation system "Hollming Electronics"	Mir-1	Numbers of transponders up to 16
		Mir-2	Accuracy – <2–3 m
			Operating frequency – 8–14 kHz
			Range response – <5 miles
15.	Gyro-Compass Sperry C-11	Mir-1	Accuracy <0.50–0.1°
		Mir-2	
16.	The fiber-optic gyro PHINS iXSea	Mir-1	0.01 s latitude
		Mir-2	
17.	Echo sounder FURUNO	Mir-1	There is a mode of long-range sonar antenna at the turn of the horizon
	Maximum depth of 2,000 m readings	Mir-2	
18.	Short-range sonar Samsung	Mir-1	Distance 300 m
		Mir-2	Resolution <10 cm
19.	Hydroacoustic ultrashort baseline navigation system	Mir-1	Angle accuracy – 1°
		Mir-2	Distance accuracy – 1.5%

dives on Mir vehicles and highly appreciated their capability. During one of the submerges of Mir-2, in which Professor Y. A. Bogdanov and P. Rona participated, the largest currently known relict hydrothermal mount was discovered. The deposit of this mount is estimated as 10 million tons. This mount is named Mir Mount after vehicles. Under governance of academician A. P. Lisitsyn, a chain of hydrothermal hills with no active thermal vents was discovered, from where the samples with

high content of copper, zinc, ferrum, manganese, nickel, cobalt, gold, argentum, and other metals were lifted [12]. These large deposits of sulfide polymetallic ores discovered by scientists of the Institute of Oceanology, RAS, are very interesting as per possibility of commercial development thereof.

In January 1994, scientists of VNII Oceangeologia from St. Petersburg during expedition on RV *Professor Logachev* discovered a new hydrothermal field at 14°45′N of Mid-Atlantic Ridge. The discovery was made with instruments lowered from shipboard. The region was named Logachev hydrothermal field. In February 1995, Mir-1 and Mir-2 vehicles became the first manned vehicles, on which scientists of the Institute of Oceanology, RAS, and Sevmorgeology submerged to Logachev hydrothermal field. During two dives of Mir vehicles, visual observations were carried out; geological, biological, and water samples and plume suspensions were taken; video records and underwater photos were made; and hydrophysical measurements were provided. During these dives for the first time, crater-type smokers were found, which have no classical pipe – black fluid-smoke ejects directly from the hall on the bottom well and doesn't rise up like in other regions, but rambles along with bottom current. Sample taken directly from plume demonstrated high density thereof. This fact as well as detection of ultrabasic rocks in this hydrothermal field made it possible to make a conclusion that plume is generated in oceanic crust deep layers at the boundary with the upper mantle (Fig. 6).

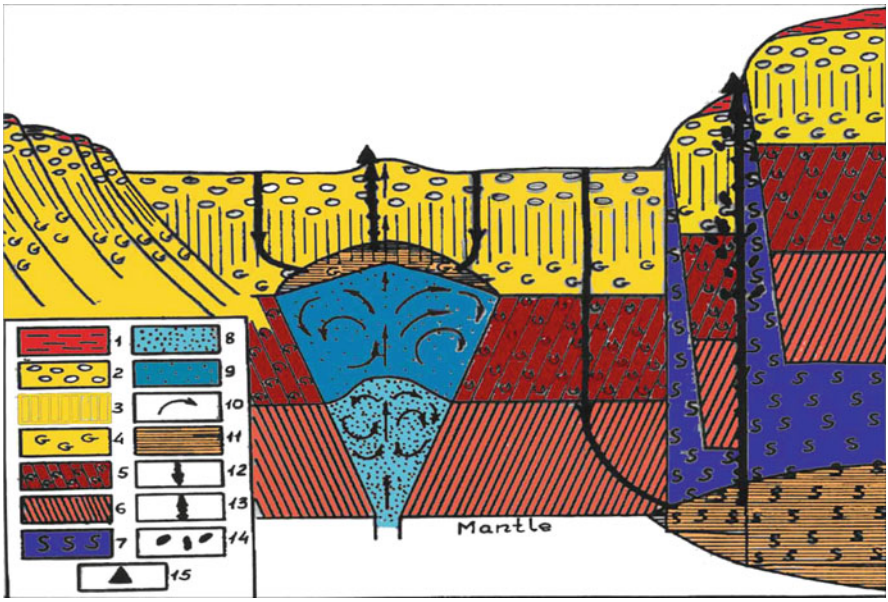

Fig. 6 The scheme of deep ocean circulation (drown by Yu. Bogdanov [14]). Two types of model circulation hydrothermal systems in slow-spreading rifting zones (with an example of MAR): (*1*) sediments, (*2*) pillow lavas, (*3*) dike complex, (*4*) isotropic gabbro, (*5*) layered gabbro, (*6*) cumulative series, (*7*) serpentinites, (*8*) picrites, (*9*) olivine tholeiites, (*10*) convection in magmatic chamber, (*11*) reaction zone, (*12*) seawater, (*13*) ore-bearing hydrothermal field, (*14*) disseminated and stockwork mineralization, (*15*) surface hydrothermal edifice

Hydrothermal field of such type was found for the first time. Analysis of recovered samples revealed apparent copper specialization thereof. Copper content in some of them reached 35%. Hydrothermal fauna here is represented by the shrimps, mussels, eels, actiniae, and other animals specific for hydrothermal outflows of the Atlantic. The majority of animal species were collected by Mir vehicle with suction sampler and nets [14].

In 1996 and 1997 in that region, more detailed study was performed by French scientists with Nautile DMS and by American scientists with Alvin vehicle. But for the first time, Logachev hydrothermal field became available for the human eye from the Mirs. Russian scientists were the first to describe landscape, types of hydrothermal outflows, and main inhabiting species. Foreign colleagues name this region as Russian point [11].

In 1998 one more expedition was carried out to that region with Mir DMS, during which four dives were made and hydrothermal fauna representative collection was combined. She included over 40 benthic species. During one of the dives, *Calyptogena* bivalve mollusks were recovered for the first time. They were found there by American scientist R. Lutz on Alvin DMS.

One should be noted that mechanism of deep hydrothermal circulation, essence of which is here stated in respect of Logachev field, was later studied by French and American scientists in accordance with results of expedition to Rainbow field with Alvin and Nautile vehicles. In October 1998, in the 41st cruise of RV Akademik Mstislav Keldysh, Mir DMS performed six dives to Rainbow hydrothermal field. Those dives confirmed the same scheme of deep hydrothermal circulation in the region as earlier on Logachev field [11].

During the 21st and 22nd cruises of RV *Akademik Mstislav Keldysh*, Mir vehicles visited nine hydrothermal regions in the Pacific Ocean. Study detail degree in various regions depended mainly on operation period in the region. One of the main priorities for Mir vehicle operation in the Pacific Ocean was hydrothermal outflow on Piip Volcano discovered by the scientists of the Institute of Volcanology, RAS, in 1989. Mir vehicle dives were done in July 1990. The scientists of the Institutes of Oceanology and Volcanology saw through Mir vehicle view port hydrothermal outflows, different from previously observed in the Atlantic and Pacific Oceans. Instead of powerful dark pipes, from which black smoke ejected, on Piip Volcano there were found small white pipes with height up to 1.5 m, from which exited high-pressured white substance (Fig. 7). This resembles much gas burner used for welding. Across diameter of several meters around such “white smoker” bottom surface was covered by white substance crust, no fauna was at that area of bottom. Recovered sample analysis showed sodium and barium sulfate predominance [9].

Analyses of gas sample taken from the pipe showed high content of methane (up to 81%). Methane presence in this region explains calyptrogen colony – the northernmost one of the currently discovered [9]. In addition extensive areas of the bottom covered with bacterial mats (in spots over 100 m^2) were found in that region. This means high hydrothermal activity of Piip Volcano, which evidently is on the initial stage of its development and needs more detailed study.

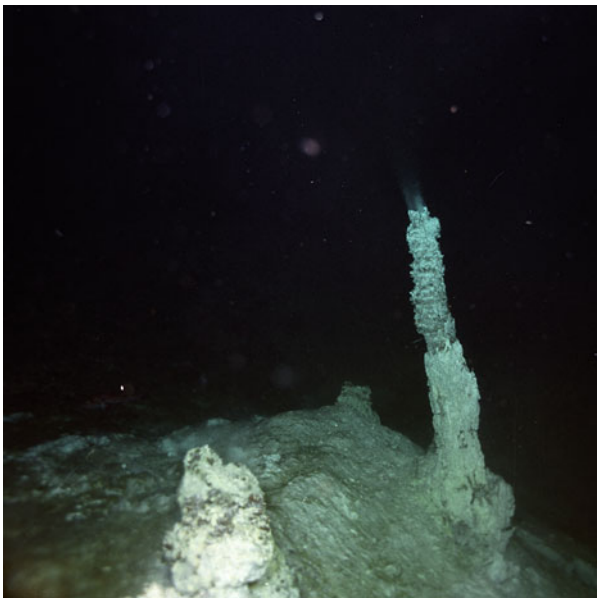

Fig. 7 White smoker at Piip Volcano, 340 m

The deepest hydrothermal field of now known ones was observed from Mir-1 vehicle near Loihi Volcano, south of Hawaiian Islands. During that dive, the crew including A.M. Sagalevich (pilot), T. Kerby, and A. Malakhov from the University of Hawaii observed at depth of 5,000 m mass of small sulfide pipes with 15–30 cm height with yellow substance on the top (evidently bacterial mats). Surface around the pipes was covered with black deposition as if it were carbonized. Unfortunately tight time didn't allow finding active hydrothermal vent. That hydrothermal field will evidently be studied in the nearest future, but the first visual observations were made there from Mir vehicles.

In 1998 the international expedition was made on RV *Akademik Mstislav Keldysh* to the Norwegian Sea with participation of Russian, American, German, and Norwegian scientists. The expedition aimed at the study of hydrothermal activity in a number of regions of the Norwegian Sea. The Håkon Mosby Mud Volcano discovered by American scientists in 1995 was the main study object. During expedition on RV Professor Logachev in 1996, this region was studied with deep towed vehicle and samplers lowered from shipboard. The expedition obtained video records and pictures of bottom surface covered with thick layer of a white substance, which was taken to be gas hydrates. However, already with the first dive of DMS Mir-1 in 1998, this supposition was overthrown. The observers saw vast areas of the bottom covered with bacterial mats. The bacterial mats, pogonophorans, and other animals were sampled. Very high concentrations of methane – up to 6 mL/L^{-1} – were measured. Earlier suggested hypothesis was confirmed that

Håkon Mosby was the powerful methane spring where methane seeps through sediment thickness in the area of 1 km in diameter. During that expedition in the Greenland Sea – the northernmost known region with methane seeping on the bottom – Vestneza Ridge was discovered. From Mir vehicle, the scientists observed bacterial mats covering the bottom in the form of rather large spots – up to 5 m diameter. Similar to Håkon Mosby here, pogonophoran colonies and other symbiotrophic animals were found [15].

In 2002–2003, an extensive complex of hydrothermal field studies was carried out in the Atlantic and Pacific Oceans. During that period, works on seven hydrothermal fields of the Atlantic Ocean and on three fields of the Pacific Ocean were performed. In these expeditions, James Cameron was shooting "Aliens of the Deep" film about hydrothermal fields on ocean bottom. These works made it possible for Russian scientists within a short period to carry out scientific observations on ten hydrothermal fields; a large amount of unique scientific data was obtained. Hydrothermal regions, in which studies with Mir DMS were performed, are specified in Table 6. The map of hydrothermal regions studied with the use of Pisces VII, Pisces XI, and Mir-1 and Mir-2 is shown in Fig. 8 [9].

Extensive biological collections compiled by the Mirs in hydrothermal regions allowed the start of comprehensive study of deep-water biocommunities occupying small areas of bottom, but characterizing very high biomasses. Primary production

Table 6 Hydrothermal regions, studied with the "Mirs"

NN	Research	Year
1.	TAG hydrothermal field	1988, 1991, 1994, 2002
2.	Snake Pit	1988, 2002
3.	Woodlark Basin	1990
4.	Lau Basin	1990
5.	Manus Basin	1990
6.	Piip Volcano	1990
7.	Loihi Volcano	1990
8.	Monterey Canyon	1990
9.	Guaymas Basin	1990, 2003
10.	Hydrothermal field 21°N East Pacific Rise	1990, 2003
11.	Broken Spur hydrothermal field	1994, 1996, 2002, 2003
12.	Logachev hydrothermal field (14°45′MAR)	1995, 1998
13.	Håkon Mosby Mud Volcano (Norwegian Sea)	1998
14.	Rainbow hydrothermal field (29°N MAR)	1998, 2005
15.	Hydrothermal field 9°N East Pacific Rise	2003
16.	Lost City hydrothermal field	2002, 2003
17.	Menez Gwen hydrothermal field	2003
18.	Juan de Fuca Ridge (DMS *Pisces*)	1986
19.	Paramushir Island (DMS *Pisces*)	1986
20.	Vestneza Ridge (79°N Norwegian Sea)	1998

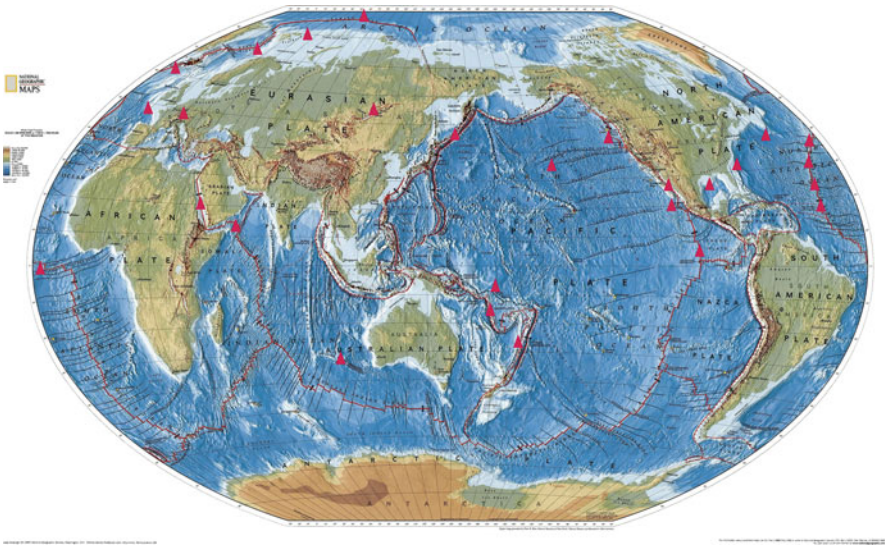

Fig. 8 The map of hydrothermal fields studied with the Mirs

consumed by them is based not on sun energy but on energy of reduced sulfur and carbon oxidation (hydrogen sulfide, methane, hydrocarbons) [13].

These studies resulted in description of new science family, genus, and species taxons. Shrimps make one of the landscape-determining forms in six hydrothermal regions of the Northern Atlantic. There inhabit nine species of shrimps assigned to five genera and two families, of which one family (Mirocarididae), two genera, and two species were described by A. L. Vereshchaka, the employee of the Institute of Oceanology, RAS, who immortalized in Latin names of shrimps the names of the Institute (IO RAN), Mir vehicle, and *Akademik Mstislav Keldysh* mother ship. S. V. Galkin together with E. Southworth (UK) described *Arcovestia ivanovi* – a new species – genus, and family (Arcovestiidae) of vestimentiferan in hydrothermal vents of Manus Basin in the Western Pacific. E. M. Krylova and L. I. Moskalev described a new species of *Ectenagena extenta* vesicomyid clam procured at the depth over 3,000 m in a small field of cold sulfurous seeping in Monterey Bay [14].

One could introduce many such examples. They mean that deep manned submersibles made it possible to make a giant step in biological study of the ocean. They maximally approximated a scientist to study a subject and allowed direct observations of animals in natural environment at great depth near bottom and in water column and compilation of unique collections of geological and biological samples, underwater pictures, and video records, which became a part of gold pool of Russian oceanology.

5 Methods of Hydrothermal Field Study with Mir DMS

As a basic method of hydrothermal field study with Mir DMS was taken polygon method, which was developed as early as the use of Pisces vehicles in the 1970s. As a rule, hydrothermal field occupies a small area of ocean – of 2–5 square miles. To provide study navigational accuracy as a rule, a hydroacoustic polygon is set up: several transponders (hydroacoustic responder beacons) are installed on the bottom – usually of 3–5 pieces; they ensure accurate sensing of vehicle motion over the entire area of the polygon. As a rule, each Mir vehicle during one submergence studies its preset part of the hydrothermal field. When the vehicle moves over the ground (usually at the distance of 2–3 m), video recording is made continuously. The motion is very slow – about 0.5 knots. Such speed of the vehicle makes it possible for the observer to examine small details of the bottom relief and the inhabitants. For detailed study of the most interesting points on the way, the vehicle comes closer to the bottom; stops, if necessary; lands on the bottom; and fulfills complete program of the study, sampling, selective photographing, etc., inclusive. Herewith, navigational accuracy is continuously complied with, and all data are recorded to computer. Samples are coupled to relief peculiarities: top of hydrothermal buildup, slope, foot, vertical wall, etc. Usually these descriptions are made by the observer. For the sampling, manipulators are used (two on each vehicle) with seven degrees of freedom. Hard geological samples are taken directly by closing manipulator wrists. Sediments are sampled with special tubes taken by the manipulator's hand and pushed into sediment layer, and then 30–40 cm of sediment upper layer is sampled. For animals, sampling dip nets are used, which are also taken in a manipulator, and upon animal sampling, the net with the sample is twisted to preserve an animal till surface. There are also dip nets, which are closed with spring trigger. To sample small animals (shrimps, crabs, fish, eels etc.), a slurp-gun suction device is used, which with a special pump sucks animals in a long armored hose, through which animals are transported to sleeves of 2 L volume. Slurp gun has five replaceable sleeves, which are moved under suction hose with remotely controlled device. Thus, during one dive, five sleeves can be filled by animal suction in various points of the hydrothermal field. Another method of animal collecting is meshed trap with a bait inside. The vehicles usually leave such traps in the region of the hydrothermal field and collect them in several days. Sometimes traps are delivered to the ship almost full of various animals, which sometimes eat each other (fish skeletons and other animal remainders were found). Practice shows that such sampling method is rather effective. Water sampling is made with Niskin bottle of 20 L volume. Each vehicle is equipped with one such bottle, which is closing by a pilot usually near a smoker. Usually there are many suspensions and animals in water. Besides vehicles are equipped with titanium bottle of 0.7–1 L volume intended for hot fluid pressure sampling directly from smokers. Fluid sampling needs a well-trained pilot as fluid sampling is made with vehicle suspension in water column and accurate positioning of the bottles in the hot fluid stream is

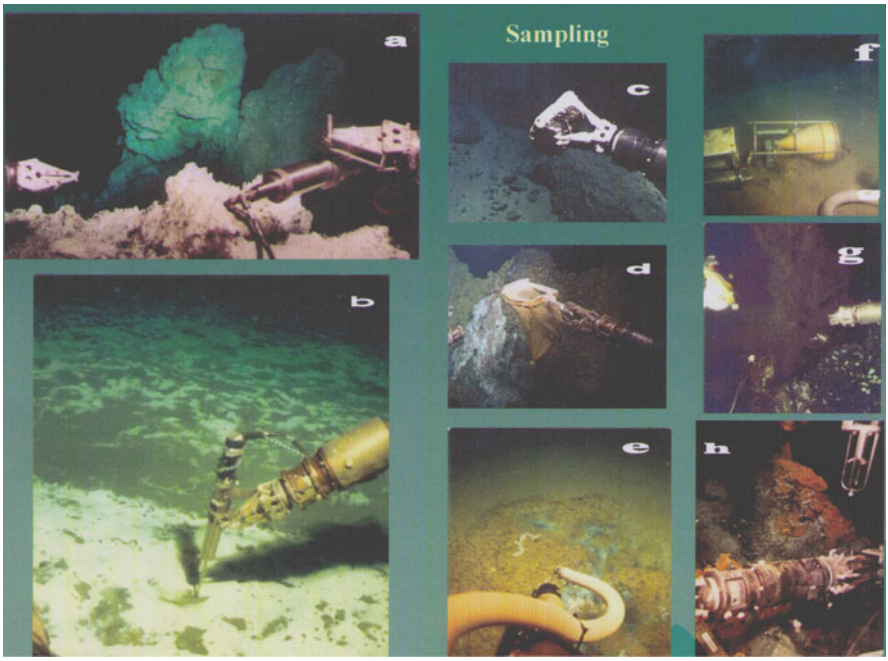

Fig. 9 Sampling devices of the Mir submersibles: (**a**) titanium bottle for the sampling of hydrothermal fluid under pressure; (**b**) heat flow sensor; (**c**) manipulator. The rock is in the wrist; (**d**) biological net; (**e**) slurp gun – sucking sampler; (**f**) sedimentary trap; (**g**) hydrothermal fluid is taken by titanium bottle from the smoker; (**h**) manipulator and 3D current meter (*upper right corner*)

needed. This really precise operation is rather complicated for remotely operated vehicles.

One should note that Mir DMS high maneuvering ability allows sampling in complicated situations: from smoker prominent peaks at the height of tens of meters over the bottom, from vertical walls, from small shoulders not making it possible to land the vehicle on bottom, and even from negative-angle walls overhanging the vehicle. All these operations are made in vehicle hovering mode and its precise maneuvering in water column near the studied subject.

Figure 9a–h demonstrates various samplers used by pilots while operating Mir DMS.

Tables 4 and 5 specify data on Mir DMS scientific equipment measurement sensors, detachable equipment, sampling devices inclusive.

Mir vehicles are equipped with self-contained data acquisition system, which during the entire process of submergence continuously registers navigational data, measurement results, and other parameters. Upon submergence, it is rather easy to recover vehicle routing, on-route sampling points, measurement data coupled to certain point, etc.

The deep manned submersibles Mir contributed much to the study of hydrothermal fields on bottom of the World Ocean. Conducted studies demonstrated high efficiency of manned vehicle use for that purpose.

Such great contribution of the Mirs to scientific research of the ocean and particularly of hydrothermal fields on the bottom wouldn't be possible without great scientists of IO RAS and other organizations, which provided scientific programs of the expeditions and the dives.

In practically all expeditions participated very high qualified group of scientists, who developed scientific programs of the expeditions and provided visual observations during the dives personally. There were academicians A. P. Lisitsyn, M. E. Vinogradov, N. S. Bortnikov, Professor L. P. Zonenshain, Yu. A. Bogdanov, A. Yu. Lein, S. V. Galkin, A.V. Vereshchaka, A.V. Gebruk, L. I. Moskalev, and others.

On the basis of the results, obtained by the Mirs over 20 books and over 1,000 articles in Russian and international journals were published.

Big volume of data obtained by the Mirs is still undeveloped and awaits the processing and publication.

References

1. Sagalevich AM (1987) Oceanology and manned submersibles. Nauka, Moscow, 256 pp
2. Ballard RD, Grassle JF (1979) Return to oases of the deep. Natl Geogr 156(5):587–705
3. Beebe W (1934) Half mile down. Harcourt, Brace, New York, 94 pp
4. Busby FR (1976) Manned submersibles. off. Oceanography NAVY, Washington D.C., 764 pp
5. Piccard J, Dietz RS (1961) Seven miles down. Putman's, New York, 178 pp
6. Riffaud C, Pichon X (1976) La expedition FAMOUS. P. Michel, 219 pp
7. Keach DL (1964) Down "Thresher" by bathyscaphe. Natl Geogr 125(6):34–51
8. Bogdanov Yu A, Sagalevich AM (1984) New data on the structure of the Reykjanes Ridge. Vestnik AN SSSR 4:127–131
9. Sagalevitch AM (2009) The deep. Voyages to Titanic and beyond. Botanical Press, Redondo Beach, California, 295 pp
10. Sagalevitch AM (1996) MIR submersibles in science and technology. Mar Technol Soc J 30 (1):7–12
11. Bogdanov Yu A, Lisitsyn AP, Sagalevitch AM, Gurvich EG (2006) Hydrothermal ore-formation process of the oceanic bottom. Nauka Publisher, Moscow (in Russian)
12. Lisitsyn AP, Sagalevich AM, Bogdanov YuA et al (1989) The first geological expedition to the deep manned vehicles "Mir". Bull Acad Sci USSR 1:86–94
13. Galkin SV, Sagalevich AM (2012) Hydrothermal vent ecosystems of the World Ocean. M GEOS 144 pp
14. Gebruk AV (ed) (2002) Biology of hydrothermal systems. KMK, Moscow. 543 pp. (in Russian)
15. Lein AY, Ivanov MV (2009) Biochemical cycle of methane in the ocean. Nauka Publisher, Moscow (in Russian)

Conclusions

Liudmila L. Demina and Sergey V. Galkin

Abstract The recent 10 years are characterized by a marked success in our knowledge of the marine trace metal biogeochemistry, resulted from the International GEOTRACES Program (http://www.geotraces.org) ocean basin transects, including the areas of the mid-ocean ridges. Meanwhile, it is the authors' opinion that now it's time to summarize available data on trace metal biogeochemistry in the deep ocean hydrothermal vent ecosystems. In this book we aimed to outline some features that control processes of metal input from the deep-sea hydrothermal vents followed by their transport, dispersion in the ambient seawater, and biological accumulation. An important contribution in the biogeochemical research is associated with knowledge of the biological structure of bottom fauna inhabiting vent areas, as well as with deep biosphere of the subseafloor igneous crust. Some outlooks for the future research are proposed.

Keywords Bioaccumulation, Bottom fauna, Deep-sea hydrothermal systems, Subseafloor biosphere, Trace metals

Content

Today, about 40 years after the discovery of hot springs on the Galapagos Spreading Centre scientific community have learnt about the influence of hydrothermal input of some trace metals on the global ocean. Recent researches focused on the

L.L. Demina (✉) and S.V. Galkin
P.P. Shirshov Institute of Oceanology, Russian Academy of Sciences, 36, Nakhimovsky Pr., Moscow 117997, Russia
e-mail: l_demina@mail.ru; galkin@ocean.ru

L.L. Demina, S.V. Galkin (eds.), *Trace Metal Biogeochemistry and Ecology of Deep-Sea Hydrothermal Vent Systems*, Hdb Env Chem (2016) 50: 195–206,
DOI 10.1007/698_2016_8,
Published online: 18 May 2016

biogeochemically important element iron have shown the responsibility of hydrothermal venting for much of the dissolved iron flux into the deep ocean [1]. The International GEOTRACES ocean basin transects and other studies [2–9] have demonstrated unexpected magnitude of the hydrothermal dissolved Fe and Mn inputs in the deep ocean. For instance, the lateral transport of hydrothermal Fe, Mn, and Al is extending up to 4000 km west of the southern East Pacific Ridge, therefore crossing a significant part of the deep Pacific Ocean; the dissolved Fe behaves conservatively, the resulting flux is more than four times what was assumed before [10]. Hydrothermal vents in the North Atlantic can serve as a source of isotopically light iron, which travels thousands of kilometers from vent sites, potentially influencing surface productivity. Dissolved stable iron isotope ratios (δ^{56}Fe) revealed that hydrothermal venting contributed about 2–6% of dissolved Fe along a transect in the North Atlantic Ocean [11]. In the Pacific Ocean, the basin scale plume lateral distribution of the soluble, colloidal, and particulate forms of Fe from the East Pacific Rise was revealed; while the character of Mn distribution differs from that of Fe [9].

Organic complexation of trace metals results in stabilizing of dissolved forms, while the microbial uptake of iron, as well as nanoparticles and the formation of iron containing particulate organic matter, may play the key role in the global ocean transport of metals from deep-sea hydrothermal vents [12, 13].

An understanding of some metal export from the hydrothermal vents resulted from studies is focused now mainly on the deep-sea vent fields at the mid-ocean ridges. Enlargement of biogeochemical investigations related to the hydrothermal systems, to the shallow island arc vent in different parts of the world ocean, will contribute to assessment the impact of environmental parameters, firstly water depth and pressure, the global ocean biogeochemical cycling of trace metals [1].

As it is known, hydrothermal vent areas exhibit a wide range of environmental conditions, including great variation in depth, associated physical parameters, different geologic setting, and underlying rocks. The MAR is a slow-spreading ridge (spreading rate <6 cm/year), and the EPR is a fast-spreading ridge (>6 cm/year). All these factors are reflected in different maximum fluid temperatures, pH, and concentration levels of reduced compounds and metals.

Faunal communities of studied areas also vary greatly in taxonomic composition and spatial structure. Communities of the Pacific and Atlantic Oceans vent areas exhibit particularly pronounced differences in taxonomic composition. Between these two regions there are practically no shared species. The shallowest Atlantic area Menez Gwen has a lot of differences from deeper areas of the MAR. Herewith the depth was suggested as the main factor determining the differences between MAR hydrothermal vent communities [14]. A type of substratum, morphology of hydrothermal edifices, etc. are also important factors determining microdistribution of animals.

Along with all the variety of hydrothermal manifestations, in the spatial structure of communities a number of general patterns can be revealed. Thus, the high-temperature zone directly adjacent to black and white smokers is occupied in the Atlantic by the assemblage of shrimps *Rimicaris exoculata,* while in the Pacific – by

the assemblage of alvinellid polychaetes (*Alvinella pompejana* and *A. caudata*). The bathymodiolin mussels reside in the zone of warm diffuse outflows at temperatures from 2°C to 20°C. Siboglinids (vestimentiferans) may occur together with mytilids, but more often they settle closer to hydrothermal vent emissions and live at temperatures exceeding 20°C. On the contrary, vesicomyid clams are confined to weak outflows and practically never were recorded in shimmering water. Mobile predators and scavengers (mostly crustaceans, large gastropods) are distributed all over the field. Filter-feeders using advective water currents are characteristic for the periphery of the fields. Their distribution is largely determined by the availability of suitable substratum [15]. For further analysis of bioaccumulation function of vent organisms the habitat conditions and characteristics of spatial structure of communities should be taken into account.

Deep-sea hydrothermal vent environments represent wide range of chemical and physical conditions that include the extremes in temperature and concentrations of reduced gases (H_2S, H_2, and CH_4) and heavy metal that limits areas where life can exist. On the other hand, deep-sea hydrothermal vent biotopes are an example of complicated biogeochemical systems due to both processes of trace elements' supply and removal by the different components of ecosystem.

In water of the vent biotopes the trace metal concentrations decrease sharply while fluids mixing with seawater. Along with a conservative dilution of fluids with seawater, various physical–chemical processes take place such as precipitation of Fe, Mn, Zn, and Cu mineral phases (sulfides and hydroxides), followed by their partial dissolution. The abundant life surrounding submarine hydrothermal vents induces the biogeochemical processes, first of all biological uptake of trace metals, followed by their efflux. The latter as well as physical–chemical processes result in transformation of chemical composition of the fluids.

The concentrations of the typical hydrothermal metals in the fluids (Fe, Mn, Zn, and Cu) decreased sharply (up to four orders of magnitude) in water above the fauna settlements, that was attributed to sulfides' and oxy-hydroxides' precipitation, as well as by metal accumulation in different organs of the vent taxa. The concentrations of other metals in the biotope water are 3–50 times lower than in the initial fluids of the MAR, EPR, and Guaymas Basin fields as compared to the reference deep ocean water. However, in all cases the trace metal levels in water of the deep-sea hydrothermal biotope are 1–3 orders of magnitude higher than that in the ocean [16–18].

The inter-site comparison has revealed the differences in some trace metal levels between water of biotope of the low- and high-temperature vent sites, namely: enrichment of the latter in Fe, Mn, Zn, Cu, Cr, Ag, As, and Pb relatively the low-temperature Menez Gwen and Lost City. The scale of enrichment is different for different metals, and on the average it reaches tenfold for Fe, Mn, Zn, Cu, and only 2–3-fold for the rest of metals. Thus, despite the metal concentrations differ strongly in end-member fluids of the high- and low-temperature vent fields, differences in metal levels in the biotope water become smooth [18].

The further research efforts should be focused on recognition of the distinctive chemical interactions between and in surrounding environment. We should try to

estimate the trace metal interchange with organisms of vent assemblages based on both field observation and modeling.

Deep-sea hydrothermal vent communities are characterized by complicated taxonomic, trophic, and spatial structure. Different groups of animals consume chemosynthetic bacterial production by different ways. According to their ecological requirements, vent animal populations occupy different zones within the vent field. This fact be reflected in the existence of microscale faunal zonation of vent communities. A "typical" hydrothermal field provides several main microhabitats each of which has its own suite of potentially dominant megafaunal types. This "landscape determining" species usually dominate corresponding assemblages and could be used as indicator taxa. In disjunct biogeographical regions, established zones are marked by vicariating taxa and assemblages. The boundaries of different vent fauna assemblages could be rather sharp or feebly marked appearing to be defined by gradients of water chemistry as well as the hydrodynamic regime within the vent field. The idealistic scheme is complicated by the influence of various local factors. Complexity is also added by many mobile animals not restricted to certain assemblages and "background" deep-sea fauna which may enter the hydrothermal community to feed. As a whole, the different habitats within a vent zone are more or less distinguishable. The influence of different factors determining the spatial structure of vent communities remains not clear. Although we suggest to ensure the correct analyses of bioconcentration function of vent organisms, such factors as taxonomic position of animals, trophic specialization, patterns of nutrition physiology, the stages of ontogenesis, and microdistribution patterns of animal populations should be taken into consideration [19].

The accumulation pathways of some trace metals in the hydrothermal most abundant taxon *Bathymodiolus* mussel are understood now [20]. The direct uptake of metals both in dissolved species and in form of mineral particles precipitating in the fluid-seawater mixing zone is a main route of metal accumulation in mussel tissues. At the same time, chemical transformation and detoxification of metals are important processes that control metal accumulation by the mussels. An important contribution to regulating chalcophilic metals such as Zn, Cd, and Cu belongs to metallothioneins which are strongly metal-binding proteins with functional groups containing sulfur. In addition to this, the essential earth alkaline metals, and possibly Mn, are also biologically regulated by the organisms [21].

However, there are some unsolved questions on the respective role of fluids and particles in metal uptake by mussels and for the site of metal storage. Besides, since nanoparticles and metal-bearing colloids were registered in the vent environments [6], their contribution to metal accumulation is of importance for future research of the hydrothermal systems.

The abundant settlements of animals and their capacity for metal accumulation are undoubtedly influenced by environmental conditions. Amongst them the basic one is the trace metal levels in the biotope water, which reflects trace metal composition of the fluids. On the other hand, such biological factors as ontogeny and trophic specialization also can determine patterns of bioaccumulation of some trace metals. As a whole bioaccumulation of trace metals by hydrothermal

organisms is defined by the sum of a number of abiotic and biological parameters of the environment, which may interact and influence each other.

The influence of the trace metal level in water of different hydrothermal biotope one can reveal while comparing trace metal content in the same organs of the same genus. The relevant candidate for this is *Bathymodiolus spp.* mussels, which are most abundant in habitats of five geochemically different hydrothermal vent fields of the MAR (Menez Gwen, Rainbow, Broken Spur, and Snake Pit), as well as of the EPR (9°50' N). Inter-site comparison of the Fe, Mn, Zn (principle metals in fluids) partitioning in gills of the *Bathymodiolus* mussels, that host bacterial endosymbionts, as well as shells, resulted in a significant difference only between the high-temperature vent areas (Rainbow, Broken Spur), on the one hand, and the shallow low-temperature Menez Gwen, on the other hand. Enrichment of the Rainbow fluids in Ni and Co, due to serpentinization of ultramafic-hosted basement of this area, is reflected on their elevated contents (up to 10 times relatively other metals) in *Bathymodiolus* shells.

Concentrations of some metals in the tissues correlate directly with the metal load in the environment and reflect the high variability of metal concentrations in the fluids and particles they are exposed to. This fact was evidenced by a registering of the highest trace metal concentrations in bodies of the most thermophile organisms – polychaete *Alvinella pompejana,* which occupy biotope with the maximal metal load, of the vent chimneys on the 9°50'N field at the EPR [22]. One more evidence is a detection of the hydrothermal sulfide minerals (pyrite FeS_2 and wurtzite ZnS) in digestive glands tracts and gills of *Bathymodiolus* mussels sampled at the Rainbow [23] and Snake Pit vent sites [24]. Research results require special and more detailed studies concerning the accumulation mechanisms of heavy metals in *Alvinella pompejana*, as well as *Riftia pachiptila*, inhabiting the hottest places at thevent fields.

Despite Mn in fluids displays a level close to Fe, Mn values in tissues of *Bathymodiolus* mussels are much lower than that of Fe, and are similar to such metals as Pb, Cd, Cr, Co, Cr, and Mo [24, 25]. Unlike Fe, data for Mn speciation in water of habitats are lacking, so this issue should be deeper investigated to better understand reasons of such alteration of Fe and Mn in their biogeochemical behavior in the hydrothermal vent ecosystems.

Among the biological factors which can influence metal accumulation we have considered the stage of ontogeny and trophic level specific variations. Size dependent differences reflect the metabolism intensity, on the one hand, and time of exposure to metal rich biotope water, on the other hand. So to study the ontogeny influence, we have sampled specimens at one and the same mussel cluster, i.e., they grew under the equal environmental conditions of proximity of methane, hydrogen sulfide, and heavy metal sources. Our research results for *Bathymodiolus azoricus* mussels (shell length varied from 24 to 116 mm) sampled from the same mussel bed at Rainbow vent area have shown a noticeable ontogeny effect in micronutrients such as Fe, Mn, Ni, and Cu, namely 3–50-fold higher contents in shells of younger mussels relatively older ones [26]. Meanwhile in the mussel gills a 2–5-fold decrease of content with the mussel growth was detected for both the essential

metals Zn, Ni, Co, Se, and nonessential Sb [24]. Significant size dependence of metal accumulation in gills was detected only for Hg: an eightfold decrease with a mussel growth within the limits of shell length from 3 to 12 cm; higher Hg contents in juveniles being attributed to their reduced lipid amounts compared to adults [27].

From our data, a weak tendency of age dependence was recorded for the Vestimentiferan tube worm *Riftia pachyptila* – a dominant vent taxon at the Guaymas Basin. The younger individuals (tube length 14 cm on average) accumulate somewhat less Fe and Zn compared to older (tube length 128 cm on average) specimens. The rest of metals did not show a defined pattern of metal accumulation versus age [22]. The growth of Cd and Fe contents in vestimentum of *Riftia pachyptila* from the Guaymas Basin in accordance with size of specimens was observed by [28].

Chemolithoautotrophic bacteria are known to be a chemosynthetic primary producers, which feed hydrothermal organisms. Consumers of the first trophic level involve those organisms that depend on chemosynthesis, but in a different way utilizing its products. (1) Endosymbiotrophers – Vestimentiferans and Bivalve molluscs (mussels and clams), in the gills and trophosome of which intracellular bacteria function. (2) Ectosymbiotrophers – shrimps, using bacterial organic matter by use of external organs – maxillipeds. (3) Bacteriophages – grazers (polychaetes Alvinellidae) and the filter-feeders (polychaetes Serpulidae), feeding on bacterial mats and filtering bacteria from the water column. Consumers of the second trophic level are carnivores – predators and scavengers: mainly crustaceans and some species of gastropods [19]. This knowledge allows us to hypothesize patterns of metal trophic transfer in further research.

Biological interactions such as host-symbiont and host-parasite associations for *Bathymodiolus* mussel inhabiting the Azores triple junction (MAR) vent fields were examined by [29]. These authors have displayed a general trend of increased accumulation of Cu, Fe, and Zn from primary producers (endosymbiont bacteria) to primary consumers (symbiont reliant species and filter-feeders) and to secondary consumers (predators and scavengers). Biomagnification of Hg due to organic Hg, as well as of Zn and possibly Cu, caused by accumulation from prey to predator through trophic links was revealed in the crustacean link, but not in the mussel path [23]. There is a need for the future more detailed investigation on the food chains with a special attention to both essential and toxic metals like Hg.

From the very beginning of hydrothermal investigations it was revealed the abnormal abundance of the hydrothermal organisms inhabiting the near-vent area. In Table 1 one can see some values of abundance and biomass (wet soft tissues) of dominant hydrothermal communities. The maximal biomass was recorded at the Logachev vent field (MAR) for the *Bathymodiolus* mussels and *Abyssogena* clams settlements which reach to the soft tissues to 19–20 kg/m^2 [30], while combined with shells – up to 60 kg/m^2 [31]. It should be noted that at the Menez Gwen area the soft tissues biomass of mussels varied from 10 to 15 kg/m^2. Biomass of dominant taxa at the Galapagos Rift and Juan de Fuca Ridge – Vestimentiferan *Riftia and Ridgeia* relatively varied in limits of 0.1–15 kg/m^2 [32, 33]. Contribution of polychaetes *Alvinella* in total biomass is much less and doesn't exceed 2.4 kg/m^2

Table 1 Abundance and biomass of the dominant bottom organisms inhabiting some deep-sea hydrothermal areas of the ocean

Taxon	Area	Abundance, indiv. m^{-2}	Biomass wet, soft tissues, m^{-2}	References
Mussels *Bathymodiolus*	MAR: Logachev Menez Gwen	21,000 500	17–19 10–15	Gebruk et al. [30] Colaco et al. [43]
Clams *Abyssogena*	MAR: Logachev	140	20	Gebruk et al. [30]
Vestimentiferan *Riftia* *Ridgeia*	Galapogos Rift Juan de Fuca	200 50,000	8–15 0.1–11	Hessler and Smithey [32] Sarrazin and Juniper [33]
Polychaete *Alvinella*	EPR	30–1000	2.4	Desbruyéres and Laubier [34]

[34]. Note that in background areas of the abyssal ocean areas, the average biomass of benthic animals usually is below 2 g/m^2, i.e., about 3 orders of magnitude less.

For the comparison and role estimation of the living organisms in the trace metal bioaccumulation, a term the Bioaccumulation Potential (BP) accounting for the integral amounts of trace metal in the dominant communities' biomass (BP) was proposed. The BP characterizes the intensity of the trace metal biological uptake, it is calculated from two parameters: (1) the total mass of trace metals (M bio, 10^6 t) taken up by the whole bodies of the dominant communities, and (2) the biomass of these organisms (per unit area). We have examined data on the two geochemically different areas that are known to be highly productive: shelves and deep-sea hydrothermal vent fields, based on the integrated median average content of metals in the whole bodies and average biomass of the dominated organisms (Table 2). A comparison showed that the BP of metals by mussels in the vent biotope was 5–25-fold higher relatively shelf areas [35, 36]. BP of trace metals gives the following sequences:

shelf areas: Fe > Zn > Mn > Cu > Pb > Ni > Co > Cr > As, Cd > Ag, Se, Sb > Hg;
hydrothermal vent areas at the MAR: Fe > Zn > Cu > As > Ni > Pb > Mn > Co > Cr > Cd > Se > Ag > Sb > Hg.

One can notice a certain similarity in the order of BP values' decreasing in the two areas: the highest BP was recorded for Fe and Zn, and the lowest one for Se, Sb, and Hg. Iron is followed by Mn and Cu in the first sequence, whereas in the third (hydrothermal) sequence, Mn is shifted from Fe and Zn toward metals with lower BP; i.e., Fe and Mn may have a different pattern of bioaccumulation. The reasons for this should be studied more deeply.

The deep-sea hydrothermal vent biota of the Mid-Atlantic Ridge acts as a powerful deep-water biological pump. However, the fact that the area inhabited by vent animals constitutes a small portion of the total area of the ocean floor, allows us to conclude that the hydrothermal biological pump has a rather local character. The separate problem is the exploration of the deep biosphere of the

Table 2 Trace metal bioaccumulation potential ($mg \cdot m^{-2}$ of the biotope floor) of the dominant communities in the coastal areas and some deep-sea hydrothermal vents [36]

Metal	Coastal areas' mussels	MAR hydrothermal vent fields' mussels
Mn	470	894
Fe	9128	63,060
Co	19.4	258
Ni	78.5	1092
Cu	102	4272
Zn	656	17,100
As	7.8	2142
Cd	7.1	142
Pb	87	1013

subseafloor basement. The last 2 decades have involved a change in view of the ocean crust and its potential to harbor life, and today the subseafloor biosphere is considered to be widespread at both ocean ridges and off-axis [37–39]. Hydrothermal vents are considered as windows into a potential but not yet confirmed subseafloor biosphere [40]. Still, our knowledge of the deep biosphere of the subseafloor crust is limited with respect to abundance, diversity, and ecology and is a research frontier in geological, biological, and oceanological sciences. Subseafloor basalts also play an important role as habitats for life throughout Earths geological history, started from ~3.5 Ga up until today [41]. At the moment we are limited by issues involved in sampling, and there is an urgent need for development of new drilling methods and sampling techniques. With, hopefully, emergent techniques in the future that allow contaminant-free studies of the subseafloor biosphere fundamental questions await to be answered. We don't know yet how deep and how diversified and abundant is the deep subseafloor biosphere and whether does it vary with depth. Important question is what are the accessible energy sources and the metabolic pathways of the microorganisms. We should answer how temperature, pressure, and pH dependent/resistant are the microorganisms of the subseafloor biosphere. The open question is still the geological age of the deep biosphere. All these questions should be answered to estimate the ecological role of deep biosphere in global deep ocean balance [42].

Acknowledgements We are grateful to Russian Scientific Foundation (Project No 14-50-00095 "World Ocean in XXI century: climate, ecosystems, mineral resources and disasters") for partial support of this work.

References

1. Sander SG, Koschinsky A (2016) The export of iron and other trace metals from hydrothermalvents and the impact on their marine biogeochemical cycle. Hdb Env Chem. doi:10.1007/698_2016_4

2. Hawkes JA, Connelly DP, Gledhill M, Achterberg EP (2013) The stabilisation and transportation of dissolved iron from high temperature hydrothermal vent systems. Earth Planet Sci Lett 375:280–290
3. Tagliabue A, Bopp L, Dutay JC, Bowie AR, Chever F, Jean-Babtiste P, Bucciarelli E, Lannuzel D, Remenyi T, Sarthou G, Aumont O, Gehlen M, Jeandel C (2010) Hydrothermal contribution to the oceanic dissolved iron inventory. Nat Geosci 3:252–256. doi:10.1038/NGEO818
4. Wu JF, Roshan S, Chen G (2014) The distribution of dissolved manganese in the tropical-subtropical North Atlantic during US GEOTRACES 2010 and 2011 cruises. Mar Chem 166:9–24. doi:10.1016/j.marchem.2014.08.007
5. Bennett SA, Achterberg EP, Connelly DP, Statharn PJ, Fones GR, German CR (2008) The distribution and stabilisation of dissolved Fe in deep-sea hydrothermal plumes. Earth Planet Sci Lett 270(3-4):157–167. doi:10.1016/j.epsl.2008.01.048
6. Yucel M, Gartman A, Chan CS, Luther GW (2011) Hydrothermal vents as a kinetically stable source of iron-sulphide-bearing nanoparticles to the ocean. Nat Geosci 4(6):367–371. http://www.nature.com/ngeo/journal/v4/n6/abs/ngeo1148.html#supplementary-information
7. Nishioka J, Obata H, Tsumune D (2013) Evidence of an extensive spread of hydrothermal dissolved iron in the Indian Ocean. Earth Planet Sci Lett 361:26–33. doi:10.1016/j.epsl.2012.11.040
8. Schlitzer R (2004) Ocean data view. http://odv.awi-bremerhaven.de,
9. Fitzsimmons JN, Boyle EA, Jenkins WJ (2014) Distal transport of dissolved hydrothermal iron in the deep South Pacific Ocean. Proc Natl Acad Sci 111(47):16654–16661. doi:10.1073/pnas.1418778111
10. Resing JA, Sedwick PN, German CR, Jenkins WJ, Moffett JW, Sohst BM, Tagliabue A (2015) Basin-scale transport of hydrothermal dissolved metals across the South Pacific Ocean. Nature 523(7559):200-U140. doi:10.1038/nature14577
11. Conway TM, John SG (2014) Quantification of dissolved iron sources to the North Atlantic Ocean. Nature 511(7508):212–215. doi:10.1038/nature13482
12. Sander SG, Koschinsky A, Massoth GJ, Stott M, Hunter KA (2007) Organic complexation of copper in deep-sea hydrothermal vent systems. Environ Chem 4:81–89. doi:10.1071/EN06086
13. Li M, Toner BM, Baker BJ, Breier JA, Sheik CS, Dick GJ (2014) Microbial iron uptake as a mechanism for dispersing iron from deep-sea hydrothermal vents. Nat Commun 5. doi:10.1038/ncomms4192
14. Rybakova (Goroslavskaya) E, Galkin S (2015) Hydrothermal assemblages associated with different foundation species on the East Pacific Rise and Mid-Atlantic Ridge, with a special focus on mytilids. Mar Ecol 36:45–61
15. Galkin SV, Demina LL (2016) Geologic-geochemical and ecological characteristics of selected hydrothermal areas. Hdb Env Chem. doi:10.1007/698_2016_3
16. Kádár E, Costa V, Martins I, Santos RS, Powell JJ (2005) Enrichment in trace metals (Al, Mn, Co, Cu, Mo, Cd, Fe, Zn, Pb and Hg) of the macro-invertebrate habitats at hydrothermal vents along the Mid-Atlantic Ridge. Hydrobiology 548:191–205
17. Demina LL, Holm NG, Galkin SV, Lein AY (2013) Some features of the trace metal biogeochemistry in the deep-sea hydrothermal vent fields (Menez Gwen, Rainbow, Broken Spur at the MAR and 9o50'N at the EPR): a synthesis. J Mar Syst 126:94–105
18. Demina LL (2016) Trace metals in water of the hydrothermal biotopes. Hdb Env Chem. doi:10.1007/698_2016_1
19. Galkin SV (2016) Structure of hydrothermal vent communities. Hdb Env Chem. doi:10.1007/698_2015_5018
20. Koschinsky A, Kausch M, Borowski C (2014) Metal concentrations in the tissues of the hydrothermal vent mussel *Bathymodiolus*: reflection of different metal sources. Mar Environ Res 95:62–73
21. Koschinsky A (2016) Sources and forms of trace metals taken up by hydrothermal vent mussels, and possible adaption and mitigation strategies. Hdb Env Chem. doi:10.1007/698_2016_2

22. Demina LL, Galkin SV (2016) Factors controlling the trace metal distribution in hydrothermal vent organisms. Hdb Env Chem. doi:10.1007/698_2016_5
23. Colaço A, Bustamante P, Fouquet Y, Sarradin PM, Serrão-Santos R (2006) Bioaccumulation of Hg, Cu, and Zn in the Azores triple junction hydrothermal vent fields food web. Chemosphere 65:2260–226722
24. Demina LL, Galkin SV (2008) On the role of abiogenic factors in the bioaccumulation of heavy metals by the hydrothermal fauna of the Mid-Atlantic Ridge. Oceanology 48:784–797
25. Cosson RP, Thiebaut E, Company R, Castrec-Rouelle M, Colaco A, Martins I, Sarradin P-M, Bebianno MJ (2008) Spatial variation of metal bioaccumulation in the hydrothermal vent mussel *Bathymodiolus azoricus*. Mar Environ Res 65:405–415
26. Demina LL, Galkin SV, Dara OM (2012) Trace metal bioaccumulation in the shells of mussels and clams at deep-sea hydrothermal vent fields. Geochem Int 50(2):133–147
27. Kádár E, Santos RS, Powell JJ (2006) Biological factors influencing tissue compartmentalization of trace metals in the deep-sea hydrothermal vent bivalve *Bathymodiolus azoricus* at geochemically distinct vent sites of the Mid-Atlantic Ridge. Environ Res 101:221–229
28. Ruelas-Inzunza J, Páez-Osuna F, Soto LA (2005) Bioaccumulation of Cd, Co, Cr, Cu, Fe, Hg, Mn, Ni, Pb and Zn in trophosome and vestimentum of the tube worm *Riftia pachyptila* from Guaymas basin. Gulf Calif Deep-Sea Res I 52:1319–1323
29. Kádár E, Costa V, Segonzac M (2007) Trophic influences of metal accumulation in natural pollution laboratories at deep-sea hydrothermal vents of the Mid-Atlantic Ridge. Sci Total Environ 373:464–472
30. Gebruk AV, Chevaldonné P, Shank T, Lutz RA, Vrienhoek RC (2000) Deep-sea hydrothermal vent communities of the Logatchev area (14°45'N, Mid-Atlantic Ridge): diverse biotope and high biomass. J Mar Biol Assoc U K 80:383–394
31. Demina LL, Galkin SV (2010) Polychaete *Alvinella pompejana* – extrathermophile and metal "champion". Priroda 8:14–21 (in Russian)
32. Hessler PR, Smithey WMJ (1983) The distribution and community structure of megafauna at the Galapagos Rift hydrothermal vents. Hydrothermal processes at seafloor spreading centers. In: Rona P (ed) NATO conference in marine sciences. 12 (IV). N.-Y. Plenum Press, pp 735–770
33. Sarrazin J, Juniper SK (1999) Biological characteristics of a hydrothermal edifice mosaic community. Mar Ecol Prog Ser 185:1–19
34. Desbruyères D, Laubier L (1991) Systematics, phylogeny, ecology and distrubution of the *Alvinellidae* (Polychaeta) from deep-sea hydrothermal vents. Ophelia 5:31–45
35. Demina LL (2013) Comparative estimation of trace metal bioaccumulation in the geochemically different zones of the ocean (the marginal filter, euphotic zone and deep-sea hydrothermal vent fields). In: Abstract of GOLDSCHMIDT-2013, Florence, Italy. 25–31 August 971. www.minersoc.org. doi:10.1180/minmag.2013.077.5.4
36. Demina LL (2015) Quantification of the role of organisms in the geochemical migration of trace metals in the ocean. Geochem Int 53(3):224–240. doi:10.1134/S0016702915030040
37. Edwards KJ, Bach W, McCollom T (2005) Geomicrobiology in oceanography: microbe-mineral interactions at and below the seafloor. TRENDS Microbiol 13:449–456
38. Schrenk MO, Huber JA, Edwards KJ (2009) Microbial provinces in the subseafloor. Ann Rev Mar Sci 2:279–304
39. Orcutt BN, Sylvan JB, Knab NJ, Edwards KJ (2011) Microbial ecology of the dark ocean above, at, and below the sea-floor. Microbiol Mol Biol Rev 75:361–422
40. Deming JW, Baross JA (1993) Deep-sea smokers – windows to a subsurface biosphere. Geochim Cosmochim Acta 57:3219–3230
41. Furnes H, McLoughlin N, Muehlenbachs K, Banerjee N, Staudigel H, Dilek Y, de Wit M, Van Kranendonk M, Schiffman P (2008) Oceanic pillow lavas and hyaloclastites as habitats for microbial life through time-A review. In: Dilek Y, Furnes H, Muehlenbachs K (eds) Links between geological processes, microbial activities and evolution of life. Springer, New York, pp 1–68

42. Ivarsson M, Holm NG, Neubeck A (2016) The deep biosphere of the subseafloor igneous crust. Hdb Env Chem. doi:10.1007/698_2015_5014
43. Colaso A, Desbruyères D, Comtet T, Alayse AM (1998) Ecology of the Menez Gwen hydrothermal vent field (Mid-Atlantic Ridge/Azores Triple Junction). Cah Biol Mar 39:237–240

Index

L.L. Demina, S.V. Galkin (eds.), *Trace Metal Biogeochemistry and Ecology of Deep-Sea Hydrothermal Vent Systems*, Hdb Env Chem (2016) 50: 207–210,
DOI 10.1007/978-3-319-41340-2,